eman ta zabal zazu

Universidad del País Vasco

Euskal Herriko Unibertsitatea

Pharmacometric analysis of the in vitro activity of echinocandins, amphotericin B and isavuconazole against *Candida auris*

Doctoral Thesis

Unai Caballero Cuenca

Leioa, 2021

INDEX

I. INTRODUCTION

1. Invasive candidiasis

Invasive candidiasis is the most common fungal disease and *Candida* spp is the third or fourth cause of nosocomial infection in ICU patients after *Staphylococcus aureus* and *Pseudomonas aeruginosa* (Quindós, 2015). Despite the medical advances over the last decades, it is still a prominent cause of morbidity and shows mortality rates up to 40% (Kullberg and Arendrup, 2015) and even 70% in case of sepsis (Pappas et al., 2018). The term invasive candidiasis may refer to bloodstream infection (candidaemia) or to the deep infection of other organs, such as liver, kidney and spleen, with or without candidaemia (Pappas et al., 2018).

Invasive candidiasis is caused by yeasts within the genus *Candida.* Some *Candida* species are part of the human microbiome. *Candida albicans* is found, for example, in oral and gut microbiota in up to 50% of the population or in the vaginal microbiota of 10-50% of women. Presence of *Candida* has been also described in urinary and respiratory tracts and less likely on the skin (Quindós, 2015). When there is a rupture in the intestinal barriers caused by abdominal surgery, an imbalance in the microbiome due to the administration of antimicrobials, or an impairment of the immune system, *Candida* may disseminate through the bloodstream and colonize other organs, causing an invasive fungal infection (Figure 1). In fact, major risk factors for invasive candidaemia are abdominal surgery, hematologic malignant disease, solid-organ transplantations or treatment with broad-spectrum antibiotics, among others (Kullberg and Arendrup, 2015).

Candida albicans remains as the main aetiological agent, but in the last decades, there has been an epidemiological swift and the incidence of non-*C. albicans* candidaemia has grown, accounting for half of total cases worldwide (Giacobbe et al., 2020). Species distribution varies geographically, with *Candida glabrata* being second to *C. albicans* in Northern Europe or the United States, whereas in Latin America and Southern Europe *Candida parapsilosis* is the second species most frequently isolated, and *Candida tropicalis* in India and East Asia (Quindós et al., 2018). In the last decade, a new species has emerged and has become a serious threat to healthcare systems: *Candida auris.*

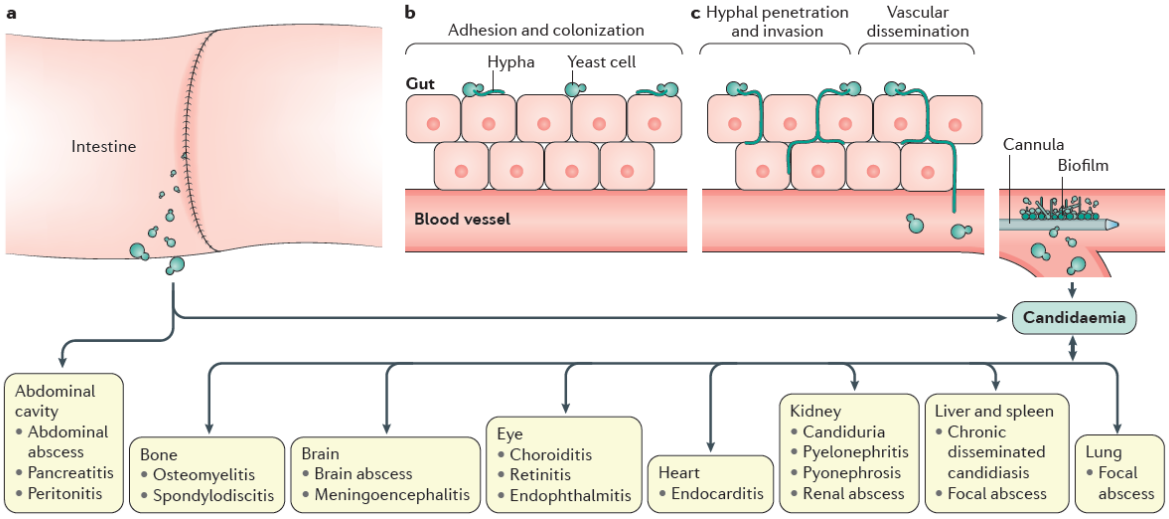

Figure 1. Pathogenesis of invasive candidiasis. a) Rupture of the abdominal barrier b) *Candida* as part of the human microbiome c) factors like immunosuppression can lead to growth and dissemination of *Candida*. Infection may also originate from the insertion of external objects like a cannula. Taken from Pappas et al. 2018.

2. *Candida auris*

Candida auris was first described in Japan in 2009 (Satoh et al., 2009), it was isolated from the external ear canal of a patient (hence the name "auris"). By October 2019, there had been reported more than 4733 cases across the five continents (Chen et al., 2020), causing notable outbreaks in countries such as Spain, India or the United States (Figure 2). The high persistence in the hospital environment, the difficulties for a proper identification and its multi-drug resistant profile make *C. auris* a challenging pathogen to control and treat. Organisms like the United States Center for Disease Control and Prevention (CDC) or the World Health Organization (WHO) have classified *C. auris* as an "urgent threat" and a pathogen of global public health interest (CDC, 2019; WHO, 2020).

Separate clonal populations of *C. auris* emerged simultaneously and independently on different geographic locations, rather than from a single source, as revealed by the whole-genome sequencing of global clinical isolates (Lockhart et al., 2017). Molecular sequencing also demonstrated that *C. auris* is part of the *Metschnikowiaceae* family. The phylogenetically closest species are part of the *Candida haemulonii* clade, and *Candida (Clavispora) lusitaniae* is a sister clade (Cuomo et al., 2018). Both of these species have shown to be multi-drug

resistant or less susceptible to treatment (Kim et al., 2009; Cantón et al., 2013). Up to now, five phylogenetically distinct clades have been identified and reported (Du et al., 2020): Clade I (South Asian), Clade II (East Asian), Clade III (South African), Clade IV (South American) and Clade V (Iran).

Additionally, this pathogen is associated with high rates of mortality due to invasive infections among patients in intensive care units (Osei Sekyere, 2018). Chen et al. recently conducted a meta-analysis that included all clinical cases reported in literature up to October 2019 (Chen et al., 2020). Their research concluded that the overall pooled mortality for *C. auris* candidemia was 45%, which is a little bit higher than the caused by other species of *Candida* and similar to bloodstream infections caused by drug-resistant bacteria. The study did not find significant differences in mortality between clades, but most available cases were englobed within clade I. Conversely, Forgács et al. analysed the infections caused by strains of each clade in a neutropenic murine model and found differences in mortality. Clade IV showed the highest mortality at day 21 (96%), followed by clade I (80%), clade III (45%) and clade II (44%) (Forgács et al., 2020).

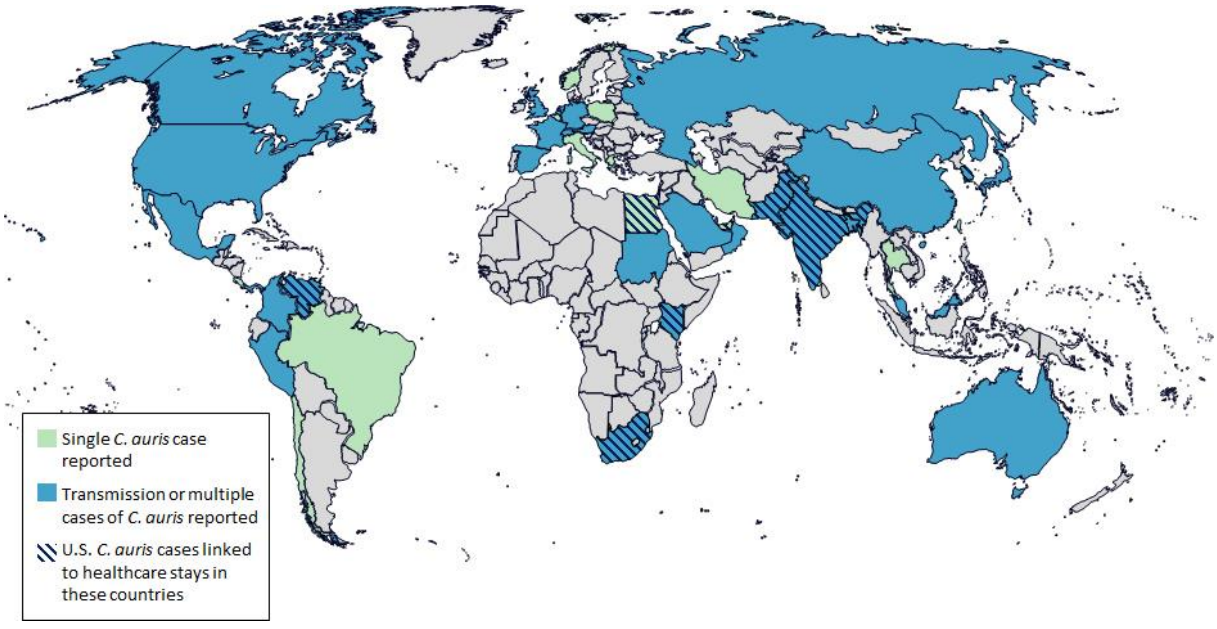

Figure 2. Global distribution of *C. auris* cases as of January 21st, 2021. Taken from https://www.cdc.gov/fungal/candida-auris/tracking-c-auris.html#world

2.1. Susceptibility of *C. auris* to antifungal drugs

Antifungal drug resistance is said to be the exception rather than the norm in *Candida* spp. (Lockhart, 2019), except for the *Metschnikowiaceae* family, of which *C. auris* is a member. Although the first reported strain of *C. auris* was susceptible to all antifungal drugs (Satoh et al., 2009), subsequent isolates from multiple outbreaks and clinical cases have shown an intrinsic resistance to fluconazole, with most strains showing minimum inhibitory concentrations (MICs) >32 mg/L (Arendrup et al., 2017b; Morales-Lopez et al., 2017; Adams et al., 2018; Chowdary et al., 2018; Ruiz-Gaitán et al., 2019; Taori et al., 2019). It is important to highlight that antimicrobial susceptibility breakpoints are species-specific and are established based on extensive research of preclinical and clinical data. However, that is not the case yet for *C. auris.* Up to now, there are not antifungal clinical breakpoints reported for *C. auris*. Alternatively, tentative breakpoints have been established by the CDC, which should be interpreted following CLSI testing methodology. These breakpoints, based on reported modal distribution of MICs from different geographical locations, are as follows: fluconazole ≥ 32 mg/L; amphotericin B ≥ 2 mg/L; anidulafungin ≥ 4 mg/L; micafungin ≥ 4 mg/L and caspofungin ≥ 2 mg/L. Isolates with a MIC equal or higher than the reported should be considered resistant. Thus, the "resistance" rates reported from different studies usually take these breakpoints as reference. However, information from these tentative breakpoints for *C. auris* should be regarded as a general guide, considering that a correlation between breakpoints and clinical outcomes has not been established yet (CDC, 2020).

Resistance varies between geographical regions (Ong et al., 2019). In a study by Chowdary et al. with 350 *C. auris* isolates from India, fluconazole resistant strains were 90% of the total, amphotericin B 8%, and anidulafungin and micafungin 2% (Chowdary et al., 2018). Additionally, 25% of the isolates were multidrug-resistant (MDR); the most common drug-resistant combination was azole and 5-fluorocytosine, followed by azole and amphotericin B. Similar results were reported in New York (Adams et al., 2018), with resistance rates of 98% to fluconazole and 25% to both fluconazole and amphotericin B. Conversely, isolates from Spain and London were not resistant to amphotericin B or echinocandins, but they showed azole resistance (Ruiz-Gaitán et al., 2019; Taori et al., 2019). In the aforementioned meta-analysis by Chen et al., it was concluded that the overall resistance rates of *C. auris* to fluconazole, amphotericin B, caspofungin, micafungin and anidulafungin were 91, 12, 12.1, 0.8 and 1.1%,

respectively (Chen et al., 2020). Those resistance patterns and number of MDR isolates are rarely seen in other species of *Candida* (Chowdary et al., 2018).

Few works have studied antifungal susceptibility beyond MIC determination. Based on the results obtained in a murine model, Lepak and collaborators (Lepak et al., 2017) suggested susceptibility breakpoints of 16 mg/L for fluconazole, 4 mg/L for micafungin and 1 mg/L for amphotericin B. On the other hand, Dudiuk et al., investigated antifungal activity by time-kill methodology and concluded that *C. auris* was "tolerant" to echinocandins and noted that the concentrations of amphotericin B needed for fungicidal action were "extremely high" (Dudiuk et al., 2019).

Current guidelines recommend echinocandins as initial and empirical treatment for adults and children older than 2 months of age. If the patient is clinically unresponsive or fungaemia persists for more than five days, liposomal amphotericin B is the alternative. For children younger than 2 months of age and neonates amphotericin B deoxycholate is the first choice (CDC, 2020).

3. Pharmacological treatment of invasive candidiasis

The treatment of invasive candidiasis is based on different clinical, microbiological and pharmacological criteria, such as the immune status of the patient, the specific characteristics of the mycosis (aetiological agent, location of infection, antifungal susceptibility, etc.) or the pharmacokinetic and pharmacodynamic properties of the drug (Quindós, 2015).

Unlike antibacterial drugs, the arsenal to combat invasive fungal infections consists of only four classes of compounds: polyenes (amphotericin B), azoles (fluconazole, itraconazole, posaconazole, voriconazole and isavuconazole), echinocandins (anidulafungin, caspofungin and micafungin) and flucytosine. Polyenes and azoles disrupt the cell membrane while echinocandins inhibit the synthesis of a key component of the fungal wall. On the other hand, flucytosine or 5-fluorocytosine impairs DNA syntesis (Figure 3) (Quindós, 2015).

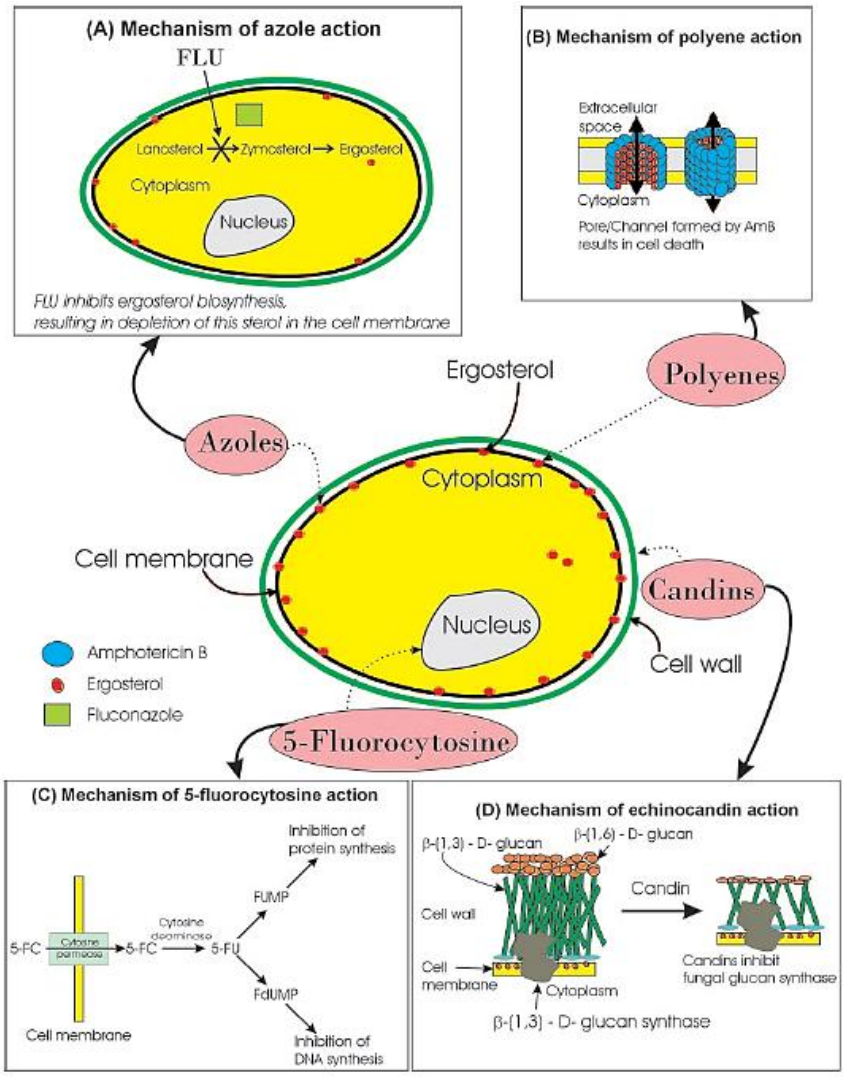

Figure 3. Mechanism of action of antifungal drugs. Taken from Mukherjee et al., 2005.

3.1. Polyenes: Amphotericin B

Amphotericin B was the first antifungal agent labelled to treat invasive mycoses and almost the only available drug for decades until the irruption of the azoles and the echinocandins during the 1990s and the 2000. It is an amphoteric molecule, a hydrophobic polyene macrolide with a carboxylate and a mycosamine appendage (Soo Hoo, 2017) (Figure 4). Amphotericin B binds with high affinity to ergosterol, the main sterol in fungal cell membrane that regulates fluidity. This drug forms pores in the lipidic bilayer and disrupts the cell membrane, which leads to fungal death (Quindós, 2015). It has been widely accepted that the main mechanism responsible for the fungicidal activity is pore formation, although some works have concluded that just the binding to ergosterol is enough, while pore formation has a secondary role in cell death (Palacios et al., 2007; Gray et al., 2012). Amphotericin B exhibits a broad-spectrum; it is active

against *Candida, Aspergillus, Mucor, Paracoccidioides* and *Cryptococcus neoformans*, among others. Currently, it is an alternative treatment for most cases of invasive candidiasis, since therapeutic options with better safety profiles are available (Pappas et al., 2016). Amphotericin B remains as the first choice for *Candida* induced endocarditis or meningoencephalitis and in urinary tract infections caused by fluconazole-resistant *Candida* (Pappas et al., 2016).

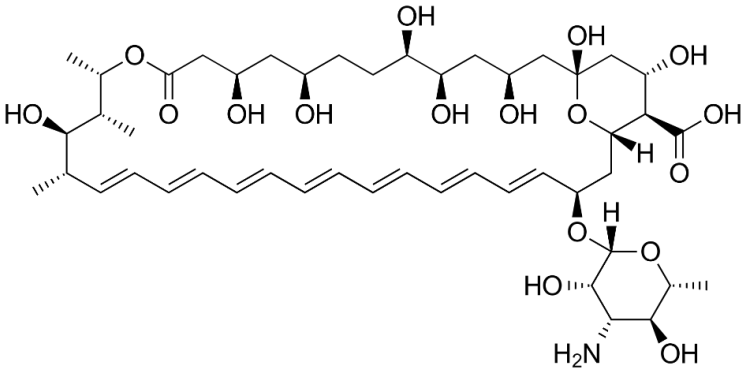

Figure 4. Chemical structure of amphotericin B.

Amphotericin B deoxycholate is the "conventional" pharmaceutical formulation; it can only be administered intravenously, as a 4-6 hour infusion. Common dosage for adult patients is 0.6-1.0 mg/kg/day, although 1.5 mg/kg/day is still tolerated and might be considered if necessary (Bellmann and Smuszkiewicz, 2017). Plasma concentrations follow a three-compartment pharmacokinetic profile, with a rapid elimination first and a long terminal half-life ($t_{1/2}$) of 127 hours. It does not go through any apparent metabolic process, as most is excreted unchanged in urine and faeces (Bekersky et al., 2002a). Amphotericin B is highly bound to plasma proteins (mainly albumin and α_1-acid glycoprotein) in a rather unusual concentration-dependent manner, probably due to its amphoteric nature. Nevertheless, protein binding is around 95.5-96% at clinically achievable plasma concentrations (Bekersky et al., 2002b).

Administration of amphotericin B is limited due to the adverse effects it causes, which can be divided into immediate side effects due to infusion (infusion-related adverse events or IRAE) and side effects caused by prolonged use (Mediavilla et al., 2014). Half of the patients will experiment IRAE, which encompasses chills, rigors, fever, hypotension or hypertension, hypoxia, nausea, vomiting, and hypokalaemia (Bellmann and Smuszkiewicz, 2017).

Nephrotoxicity is the main adverse effect of prolonged treatment with amphotericin B; it can cause hypomagnesemia, hypokalaemia, polyuria, acidaemia and renal insufficiency. Although usually considered to be reversible, chronic renal failure can occur in patients that have been administered > 4 g of cumulative dose (Laniado-Laborín and Cabrales-Vargas, 2009).

To avoid IRAE and nephrotoxicity, continuous infusion of amphotericin B deoxycholate was proposed (Chabot et al., 1989). Some studies reported lower adverse effects and mortality in the patients treated with continuous infusion (Eriksson et al., 2001; Peleg and Woods, 2004), whereas Maharom and Thamilktikul observed quite the contrary; a significantly higher mortality in patients that had the drug administered by continuous infusion compared to those who had the intermittent infusion regime (Maharom and Thamilktikul, 2006). The basis for the discrepancy may lay in the fact that the pharmacokinetic/pharmacodynamic (PK/PD) index for amphotericin B is maximum drug concentrations over MIC ratio (C_{max}/MIC) (Andes et al., 2001) and thus, antifungal efficacy would be linked to total drug exposure.

The development of special pharmaceutical formulations has been a successful strategy for reducing the serious adverse effects of amphotericin B treatment. Liposomal amphotericin B (marketed as AmBisome®) has demonstrated a better security profile than the conventional deoxycholate formulation (Walsh et al., 1999) and the same efficacy as micafungin (Kuse et al., 2007). In fact, liposomal amphotericin B has substituted the conventional formulation in those countries with resourceful health systems.

Despite decades of use, resistance to amphotericin B is still rare in *Candida* (Pfaller, 2012; Lockhart, 2019). Mutations in the genes involved in the ergosterol biosynthesis pathway such as *ERG11*, *ERG2* and *ERG6* are key factors in resistance development (Ahmad et al., 2019).

3.2. Azoles

The azoles constitute one of the most important therapeutic groups to fight fungal infections. They are synthetic heterocyclic compounds that are divided into imidazoles (2 nitrogen atoms in the azolic ring) and triazoles (3 nitrogen atoms in the azolic ring). Only the latter are used in the treatment of invasive candidiasis. Azoles exert their antifungal activity by inhibiting lanosterol 14-α-demethylase, a fungal cytochrome P450-dependent enzyme that is essential for the ergosterol biosynthesis pathway (Quindós, 2015). The lack of ergosterol in the fungal cell membrane enhances permeability and inhibits cell growth and proliferation. The antifungal

action is fungistatic against *Candida* and *Cryptococcus* and fungicidal against *Aspergillus* (Quindós, 2015). Azoles are an alternative to echinocandins for the treatment of invasive candidiasis and the preferred agents for prophylaxis and step-down therapy (Pappas et al., 2016).

Triazoles (fluconazole, itraconazole, posaconazole, voriconazole and isavuconazole) can be administered both orally and intravenously. They are one of the safest antifungal groups, as most common side effects are minor gastrointestinal symptoms, although hepatotoxicity and QT interval prolongation have also been reported (Bellmann and Smuszkiewicz, 2017). Rather than possible side effects, what drives precaution when administering azoles is the capacity to inhibit the cytochrome P450 (CYP) family, leading to relevant drug-drug interactions. The most prominent mechanism of resistance to azoles are mutations in the gene that encodes the target enzyme, *ERG11*, and the overexpression of efflux pumps encoded by *MDR* or *CDR* genes (Pfaller, 2012).

-Isavuconazole

Isavuconazole is the latest addition to the therapeutic group. It is currently approved for the treatment of invasive aspergillosis and mucormycosis. It has shown anti-*Candida* activity in vitro and in vivo (Guinea et al., 2008, Lepak et al., 2013), although a clinical trial could not demonstrate the non-inferiority of isavuconazole to caspofungin in the treatment of invasive candidiasis (Kullberg et al., 2019). Like the other triazoles, isavuconazole may be administered both orally and intravenously. As it displays a high oral bioavailability of 98%, doses are equal for both administration routes. The treatment starts with a loading dose of 200 mg every 8 hours for the first 48 hours, followed by a maintenance dose of 200 mg daily. Isavuconazole displays a high protein binding of 98-99%, a large volume of distribution (V_d) of 300-500 L and a long $t_{1/2}$ of 100 hours (Schmitt-Hoffmann et al., 2006). A recent population pharmacokinetic study in solid-organ transplant recipients found that intravenous isavuconazole showed a two-compartment pharmacokinetics, with sex and body mass index as covariates on clearance (Cl) and peripheral volume of distribution (V_p) respectively (Wu et al., 2020).

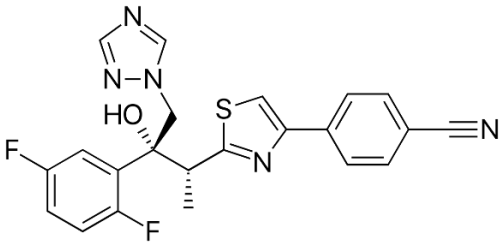

Figure 5. Chemical structure of isavuconazole.

Isavuconazole is a moderate inhibitor of CYP3A4; it enhances the plasma concentrations area under the curve ($AUC_{0-\infty}$) of immunosuppressant drugs like sirolimus and tacrolimus by 84% and 125%, respectively (Groll et al., 2016). $AUC_{0-\infty}$ of midazolam increases up to 106%, whereas coadministration with rifampicin decreases that of isavuconazole by 90% (Townsend et al., 2017). Thus, close monitoring is strongly advised when immunosuppressant agents or benzodiazepines are coadministered with isavuconazole (Bellmann and Smuszkiewicz, 2017). Similar to the rest of triazoles, adverse effects are usually mild (Ellsworth and Ostrosky-Zeichner, 2020).

3.3. Echinocandins

Echinocandins (anidulafungin, caspofungin and micafungin) are the last class added to the therapeutic arsenal and have become the first choice for the treatment of invasive candidiasis (Pappas et al., 2016). Resistance cases to triazole antifungal drugs and amphotericin B has led to the recommendation for the use of echinocandins as first-choice treatment of systemic candidiasis due to *C. auris*.

Echinocandins are semisynthetic cyclic hexa-lipopetides with an N-aryl side chain. Due to their chemical structure and large molecular weight, oral bioavailability is poor, and they are only available for intravenous administration. The mechanism of action of these drugs is the non-competitive inhibition of β-(1, 3)-D-glucan synthase, an enzyme involved in the biosynthesis of β-(1, 3)-D-glucan in the fungal cell wall. Lack of β-(1, 3)-D-glucan in the cell wall causes abnormal shapes and swelling of the cells, ultimately leading to fungal death (Perlin, 2011). Echinocandins are considered fungicidal against most *Candida* species, and fungistatic against *Aspergillus.* The lack of glucan in mammalian cells may explain the few side effects of this class and unlike azoles, drug-drug interactions are rare. Resistance to echinocandins is usually

linked to mutations in the *FKS1* and *FKS2* genes that encode the catalytic subunit of the target enzyme (Katiyar et al., 2012).

-Anidulafungin

Anidulafungin has an alkoxytriphenyl side chain and a molecular weight of 1140 Da (Figure 6). The advised dosing regimen consists of a loading dose of 200 mg on day 1 followed by 100 mg daily for the rest of the treatment. Anidulafungin follows a two-compartment pharmacokinetics, with a steady-state volume of distribution (V_{SS}) of 0.54 L/kg, a plasma Cl of 15 mL/h/kg and a mean $t_{1/2}$ of 25.6 hours (Dowell et al., 2004). Protein binding is as high as 99%. It is not metabolized by the liver, but rather undergoes a spontaneous degradation in plasma and the inactive products are eliminated via biliary excretion. Although it is not recommended the administration of anidulafungin to infants, some studies point out that an exposure similar to that of adults can be achieved safely (Xie et al., 2020). Adverse events include hyperglycaemia, headache, nausea or an increase of hepatic aminotransferases.

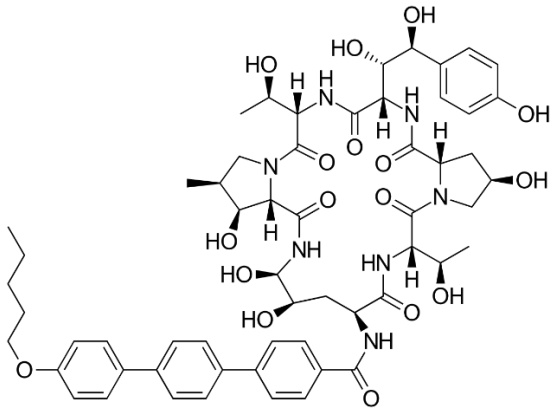

Figure 6. Chemical structure of anidulafungin

-Caspofungin

Caspofungin has a fatty acid side chain and a molecular weight of 1093 Da (Figure 7). The treatment starts with a loading dose of 70 mg followed by 50 mg once daily (70 mg if body weight is higher than 80 kg). Caspofungin has a V_d that goes from 0.03 L/kg at the start of the treatment to 0.3-2 L/kg after a few days, a Cl of 10 mL/h/kg, a $t_{1/2}$ of 8 hours and a protein binding around 95% (Stone et al., 2002a and 2002b). It is metabolized in the liver by hydrolysis and N-acetylation, independent from the CYP system, and it is excreted through urine and faeces (Balani et al., 2000). Although some interactions have been reported, they are not

considered of clinical importance. As well as with anidulafungin, adverse effects are not very frequent and include gastrointestinal symptoms, hypokalaemia or the reversible increase of the hepatic aminotransferases.

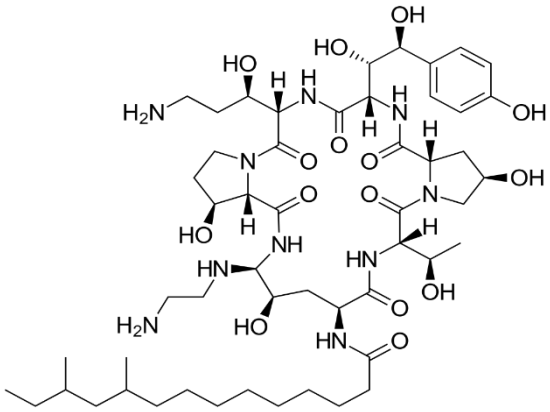

Figure 7. Chemical structure of caspofungin.

-*Micafungin*

Micafungin has a complex aromatic side chain and a molecular weight of 1292 Da (Figure 8). Recommended dosing regime is a daily dose is of 100 mg for invasive candidiasis, 150 mg for oesophageal candidiasis and 50 mg for prophylaxis; no loading dose is required. After a week of a daily dosage of 100 mg, mean parameter values are 17.3 L for V_{SS}, 1.1 L/h for Cl and 12 hours for $t_{1/2}$ (Hiemenz et al., 2005). Protein binding is 99.8 %, it undergoes hepatic metabolism through catechol-o-methyl transferase and the metabolites are eliminated via biliary excretion. Most common adverse effects are leukopenia, neutropenia, anaemia and gastrointestinal symptoms.

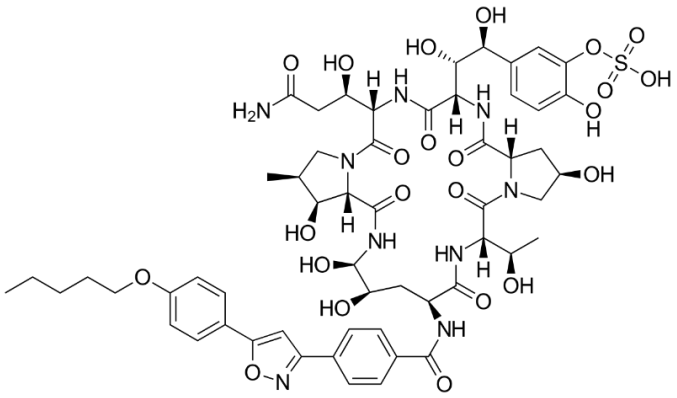

Figure 8. Chemical structure of micafungin

3.4. Alternative approaches: new antifungal drugs, combination therapy and drug repurposing

Due to the relative scarce options to treat invasive fungal infections and the emergence of resistant strains and new species like *C. auris*, there is an urgent need to enhance the therapeutic arsenal. The discovery of new antifungal drugs is insufficient, which leads to the need of other strategies to overcome this problem, like the use of combination therapy or drug repurposing.

-New antifungal drugs in development

Fosmanogepix is the first molecule of a new antifungal class and is currently in Phase 2 clinical trials. It is the prodrug of manogepix, an inhibitor of the Gwt1 enzyme, an essential molecule in the trafficking and anchoring of mannoproteins to the fungal cell membrane and wall (Shaw and Ibrahim, 2020). It has shown in vitro and in vivo activity against *Candida*, including *C. auris* (Berkow and Lockhart, 2018; Pfaller et al., 2019; Arendrup et al., 2020a).

Ibrexafungerp is a novel inhibitor of the β-(1, 3)-D-glucan synthase. As a triterpenoid, its chemical structure is simpler than that of the echinocandins, which allows the oral administration of the drug (Ghannoun et al., 2020). Ibrexafungerp has in vitro fungicidal activity against *Candida* (Scorneaux et al., 2016) and in vivo efficacy in murine models of disseminated candidiasis (Wiederhold et al., 2018). It is currently in Phase 2 and Phase 3 clinical studies (Ghannoun et al., 2020). In a recent study, the in vitro activity of ibrexafungerp against *C. auris* was investigated and it was reported promising activity against this species, including isolates resistant to echinocandins and other drugs (Arendrup et al., 2020c). In the same line, Larkin et al. also concluded that this agent displays potent in vitro antifungal and anti-biofilm activity against *C. auris* (Larkin et al., 2017).

Rezafungin is considered the first next-generation echinocandin, with distinctive pharmacokinetic features. It has a chemical structure analogue to anidulafungin, but it has a long $t_{1/2}$ (> 130 hours) that allows for once-weekly intravenous administration (Sandison et al., 2017). Similar to the other three echinocandins, rezafungin is highly protein bound, with a free fraction of 0.2-3% (Ong et al., 2016). The in vitro and in vivo antifungal activity of rezafungin is similar to that of the rest of the three approved echinocandins (Lepak et al., 2018; García-Effron, 2020; Pfaller et al., 2020). STRIVE, a Phase 2 study, showed that rezafungin is as effective as caspofungin in the treatment of invasive candidiasis (Thompson et al., 2020).

Interestingly, unlike previous studies for non- auris species of *Candida*, rezafungin has recently shown the same or greater in vitro killing activity against *C. auris* compared to the three echinocandins (Kovács et al., 2021).

-*Combination therapy*

Identifying new compounds is one potent strategy, but not the only one. Antifungal combination therapy is of increasing interest, especially as an approach to overcome antimicrobial resistance and fight difficult to treat organisms (Novak et al., 2020). It is expected that when drugs with different mechanisms of action are combined, synergism will occur and the antimicrobial spectrum and efficacy will be broaden (Brill et al., 2018). The combinations of different antifungal groups have been studied with in vitro and in vivo models of invasive candidiasis.

The combination of azoles and echinocandins have shown variable results depending on the studied species, drugs and methods employed. Overall, synergism has been reported for the newer azoles and echinocandins (Baltch et al., 2008; Chen et al., 2013; Katragkou et al., 2017). Similar successful results have been described for the combination of amphotericin B with echinocandins for the treatment of invasive candidiasis or in some cases of refractory candidaemia (Hossain et al., 2003; Olson et al., 2005; Ostrosky-Zeichner et al., 2005; Serena et al., 2008). Conversely, azoles and amphotericin B display in vitro antagonism (Lewis et al., 1998; Lignell et al., 2007), which may be because both drug classes act on the same target (Baddley and Pappas, 2005). Nevertheless, a clinical trial did not find antagonism when these two drug classes were coadministered, but a trend towards improved success (Rex et al., 2003). Nowadays, the only approved clinical recommendation regarding antifungal combination therapy in invasive candidiasis is the concomitant treatment of amphotericin B and flucytosine for the following indications: native valve endocarditis, *Candida* CNS infection, azole-resistant *C. glabrata*, ascending pyelonephritis and fluconazole-resistant *Candida* endophthalmitis (Pappas et al., 2016).

Regarding antifungal drug combination studies against *C. auris*, there is still very little research on the subject. Recent works have evaluated the in vitro interactions of antifungal drugs against *C. auris* (Fakhim et al., 2017; Bidaud et al., 2019; O´Brien et al., 2020; Pfaller et al., 2021) or the combination of antifungal drugs with other antimicrobial agents (Eldesouki et al., 2018; Bidaud et al., 2020; Schwarz et al., 2020; Wu et al., 2020).

-Drug repurposing

Antifungal drug repurposing has been defined as the new utility of various types of marketed, non-antifungal drugs that are repositioned as novel antifungal agents. This approach has been proposed as an alternative to the scarce discovery of new therapeutic agents and to the emerging resistance to the limited currently available antifungal drugs (Kim et al., 2020). Based on this strategy, recent studies have identified several candidate compounds with activity against *C. auris* (Wall et al., 2018; de Oliveira et al., 2019). Some of these compounds have also shown synergic antifungal activity in combination with approved antifungal drugs (de Oliveira et al., 2019).

4. In vitro methods for the study of antifungal activity

In vitro methods, such as MIC determination or time-kill curves, are attractive and widely used approaches to study antimicrobial susceptibility. These methods are usually standardized and reproducible, and allow obtaining information about the direct interaction between drug and microorganism. On the other hand, complex in vivo factors are overlooked and therefore, the information obtained by these methods often does not allow for direct translation to the clinical setting.

4.1. MIC determination

The MIC of a drug is defined as the lowest concentration needed to inhibit the visible growth of a microorganism to a predefined degree (50%, 90% or complete inhibition) after a period of incubation (EUCAST, 2020b). Its determination is a well-established method, routinely used in clinical microbiology laboratories (Mueller et al., 2004; Quindós, 2015). Moreover, American (CLSI) and European (EUCAST) committees have standardized the obtaining of MICs by broth microdilution techniques. There are also commercial kits available based on microdilution and colorimetric techniques, as well as on agar diffusion assays such as the E-test.

Even though the MIC provides initial information on the susceptibility of the microorganism against the drug, this value should be interpreted with caution. In fact, the use of MIC values as the main descriptor of the efficacy of an antimicrobial agent can be misleading, as the clinical outcome depends on complex interactions between the three elements of the antimicrobial

therapy: the host, the microorganism, and the drug. However, once there have been established specific PK/PD indices through proper preclinical, clinical and epidemiological investigation, species-specific sensitivity breakpoints may be defined (Asín-Prieto et al., 2015). When MIC values for a drug are higher than the sensitivity breakpoint, the studied microorganism will be considered resistant to that drug, and therapeutic failure will be very likely to occur.

Despite its usefulness, especially in the clinical setting, there are some important drawbacks to this approach. MIC values are interpreted as "all or nothing" effect and all concentrations below or above it are treated equally, without considering the dynamic concentration-response profiles, which does not reflect the in vivo situation. In fact, the MIC, usually determined at a fixed concentration of the antimicrobial agent, does not provide information on the killing kinetics of the drug, whether fungicidal endpoint is achieved or if increasing drug concentrations changes the rate of antimicrobial activity (Mueller et al., 2004).

4.2. Time-kill curves

In vitro time-kill experiments overcome some of the drawbacks of MIC determination, as they can provide more information about the activity of the drug. Subsequent sampling of microbial counts in vitro can be used to provide a time course of antimicrobial action (time-kill curve) (Schmidt et al., 2007). By analysing the results from time-kill curves, it can be determined if the activity of an antimicrobial drug is concentration, time or species-dependent, whether the drug is fungistatic or fungicidal, the rate of the killing or growing, as well as detecting regrowth phenomena (Cantón and Pemán, 1999; Nielsen and Friberg, 2013). There are two different types of in vitro time-kill experiments: static time-kill curves and dynamic time-kill curves. The experimental setting of static time-kill curves, where the microorganisms are exposed to constant concentrations of the drug, is very similar to that of the standardized broth microdilution techniques for MIC. Samples are taken from the wells containing the cell cultures at different time points and plated onto growth agar for subsequent counting of the colony forming units (CFU). Finally, the change in CFU/mL over time for each drug concentration (and growth control) is graphically represented (Figure 9).

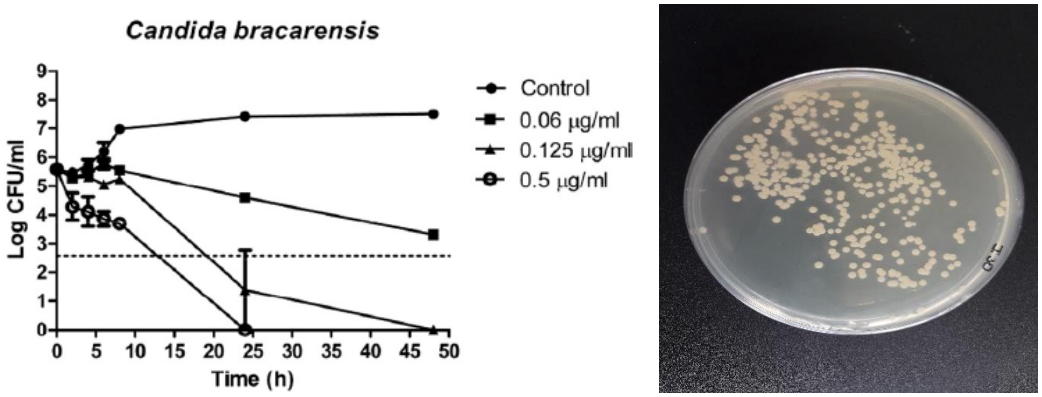

Figure 9. Left: Example of a graphical representation of in vitro static time-kill curves. Taken from Gil-Alonso et al., 2015a. Right: *C. auris* colony forming units in Sabouraud growth agar.

In dynamic time-kill curve experiments, the pathogens are exposed to changing concentrations of the antimicrobial agent, and sampling and viable counts are performed as in the mentioned static experiments. This experimental setting allows to simulate in vivo pharmacokinetics of total or unbound drug and thus, the exposure-response profile is closer to the clinical situation (Elefanti et al., 2014). On the other hand, dynamic models are much more complex to work with than the static ones (Mueller et al., 2004; Nielsen and Friberg, 2013). Nevertheless, both modalities are laborious and their implementation in the clinical setting is often not feasible.

In vitro time-kill methodology can also be used for the study of the postantifungal effect (PAFE). PAFE refers to the sustained killing of fungus when it is exposed briefly to an antifungal agent and is a drug and species dependent effect (Gil-Alonso et al., 2015b). The interest in studying the PAFE of antifungal drugs is focused on the design of dosing regimens, as drugs with a prolonged PAFE may require less frequent administrations than drugs with short or no PAFE at all. In this line, some studies investigated the PAFE of the main therapeutic groups; amphotericin B and echinocandins display a prolonged PAFE against various species of *Candida*, whereas fluconazole does not (Ernst et al., 2000; Nguyen et al., 2009; Smith et al., 2011; Gil-Alonso et al., 2015b).

4.3. In vitro methods for the study of combination therapy

Considering the growing demand of combination therapy, there is a need for reliable methods for evaluating joint effects of antifungal drugs. In a similar manner to the study of monotherapy, in vitro techniques to test the interaction of antifungal agents can be divided into MIC-based or time-kill based approaches.

4.3.1. Checkerboard method

The checkerboard method is one of the most common techniques to study antimicrobial drug-drug interactions. An array of concentrations are tested in a 2-dimensional layout, in microtitre plates (hence the name of the method), usually following a modified version of standardized broth microdilution methods (Otto et al., 2019). Thus, the inhibition of the fungal cell growth by each drug alone and in combination is analysed.

-Analysis of checkerboard data

Once the data from checkerboard experiments has been collected, a proper analysis is needed in order to determine the nature of the drug-drug interaction. Synergism can be defined as the combined effect of two or more drugs that is greater than the additive sum of each drug effect when acting alone (Greco et al., 1996). To conclude whether two antifungal agents exert a synergistic effect or not, the empirical results are often analysed with two main theories: Loewe´s additivity and Bliss independence (Meletiadis et al., 2005).

Loewe´s additivity is based on the hypothesis that a drug cannot interact with itself. The result of that "sham mixture" is additivity, whereas drug combinations that exert a bigger effect than that additivity are synergistic and those that exert a lower effect are antagonistic (Roell et al., 2017). The fractional inhibitory concentration index (FICI) is derived from this theory and is one of the most popular and widely used methods for screening synergic combinations with antifungals. To obtain the index, the MIC of the compounds alone and in combination are compared and the value of the index will determine the nature of the interaction (Odds, 2003). The analysis of the results is quite simple, but it also ignores all the concentration-effect data that do not correspond to the MICs, and variable results can be obtained depending on the chosen endpoints (Meletiadis et al., 2005). The response surface analysis approaches overcome these drawbacks, as all the generated data is analysed through statistical methods, providing more robust interpretations. On the other hand, it is a more complex procedure, and there can be variability in the results depending on the mathematical model and statistical method that are chosen for the analysis (Roell et al., 2017). The universal response surface approach (URSA) of Greco and colleagues is an example of this kind of approach (Greco et al., 1995).

Bliss Independence is based on the assumption that the drugs act independently of each other. Similar as Loewe´s additivity, if the combined effect of the drugs is higher than the model

prediction, then, synergy is declared and if not, antagonism is claimed. One of the most criticised facts of this theory is the assumption that drugs act completely independent and do not interact at all (Roell et al., 2017). However, it is still widely accepted, and contrary to Loewe based methods, Bliss is mostly tested by response surface approach, whether the method is non-parametric (Prichard et al., 1993) or parametric (Di Veroli et al., 2016).

4.3.2. Time-kill curves

Despite the usefulness of the checkerboard method, as it is based on the observation of fungal growth inhibition (similar to MIC determination for single agents), it does not provide further information on the killing kinetics of the drug. Whether the synergic activity is fungistatic or fungicidal, or if the interaction is concentration-dependent and increasing concentration of both drugs (or just one) increases the effect are overlooked. To check all this information, time-kill curve experiments may be carried out and interactions are assessed by comparing the activity of the drugs in monotherapy and in combination (Mukherjee et al., 2005) (Figure 10).

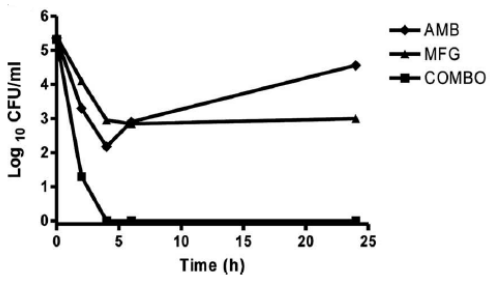

Figure 10. Example of in vitro time-kill curves of two antifungal drugs in monotherapy and in combination against *Candida* spp. AMB: amphotericin B; MFG: micafungin; COMBO: combination. Taken from Serena et al., 2008.

5. Pharmacokinetic/pharmacodynamic modelling and simulation of antifungal activity

The dosage of a drug given to a patient is related to the effect through two major processes, pharmacokinetics (PK) and pharmacodynamics (PD). Pharmacokinetics links the dosage of a drug (and/or its metabolites) with the concentration it reaches in plasma or tissues. Pharmacodynamics, on the other hand, links those concentrations with the pharmacological effect. Thus, PK/PD modelling describes and quantifies the relationship between dose, concentration and effect of a drug and afterwards, predicts the effect-time course resulting from dosing schedules (Nielsen and Friberg, 2013) (Figure 11).

By the integration of PK and PD models, a framework of the dose-exposure-response relationship is provided. The application of models can be descriptive or predictive. Descrptive models characterise existing data while predictive models simulate untested scenarios (Owen and Fiedler-Kelly, 2014). PK/PD modelling and simulation is an important and useful tool to design adequate and safe dosing regimens and is a pivotal part of modern drug development.

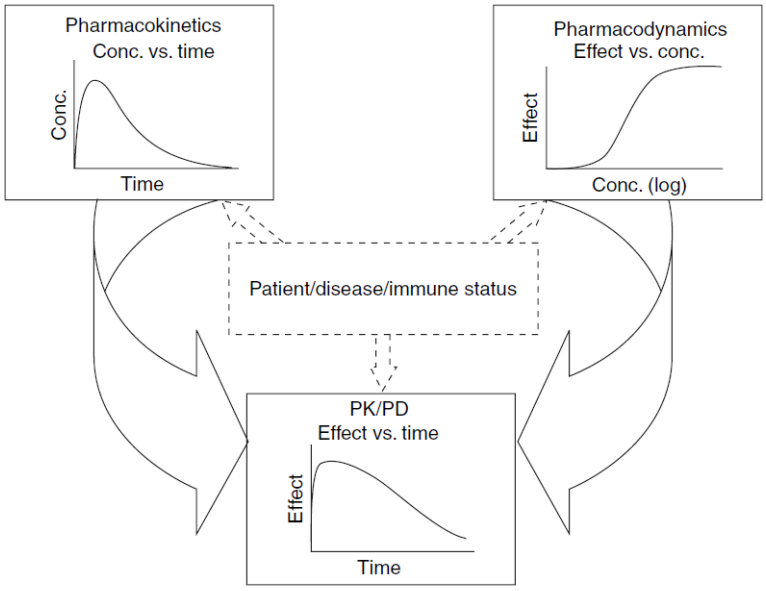

Figure 11. Integration of pharmacokinetics and pharmacodynamics. Taken from Schmidt et al., 2009.

5.1. PK/PD indices

PK/PD indices establish a quantitative relationship between a PK parameter (reflects drug exposure) and a microbiologic/pharmacodynamic parameter (the MIC) and are used to predict antimicrobial efficacy (Asín-Pietro et al., 2015). The three PK/PD indices are the time during which drug concentrations are above the MIC (T>MIC), maximum drug concentrations over MIC ratio (C_{max}/MIC) and area under 24 h concentration time curve over MIC ratio (AUC_{24}/MIC) (Figure 12). Since only free, unbound drug is able to interact with the microorganisms, the PK exposure is also expressed as the free fraction (f) (Schmidt et al., 2007). Among the three major patterns of antimicrobial activity, the first mentioned index suits antimicrobials that display time-dependent behaviour and no or very short persistent effects, while the other two best describe the activity of drugs that show prolonged persistent effects on the microbial population, whether they are concentration-dependent or not.

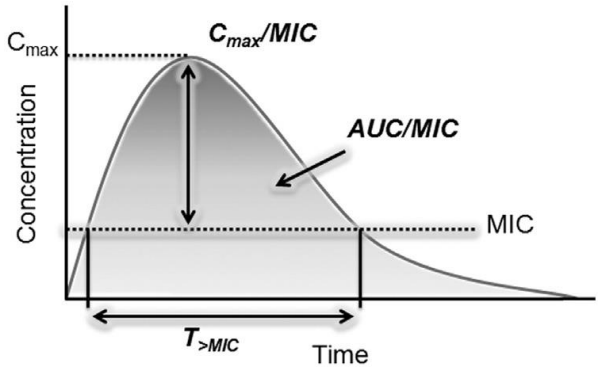

Figure 12. The three main PK/PD indices. Taken from Asín-Prieto et al., 2015.

When establishing which PK/PD index and pharmacodynamic target is associated with the success of therapy, both in vitro and in vivo studies are performed. A treatment target, such as 1-log kill, is selected and the PK/PD index that best correlates with the efficacy data is then chosen (Andes et al., 2008; Lepak et al., 2013; Lepak et al., 2018).

The PK/PD index associated with the efficacy of both triazoles and echinocandins is AUC_{24}/MIC, and C_{max}/MIC for amphotericin B, although only fluconazole´s index has been properly linked to clinical success (Pea, 2020). The PK/PD summary endpoints mentioned above are useful, but they are not exempt from limitations (Nielsen et al., 2011). These indices involve the uncertainty inherent in MICs, as detailed information about the time course of the PK and PD processes is overlooked, and the dynamic changes that may occur in the sensitivity over a treatment period cannot be characterised (Nielsen and Friberg, 2013).

Once the adequate index has been identified, the antimicrobial drug and the optimal dosing regimen can be selected in order to maximize the probability to attain the targeted exposure. Monte Carlo simulation is a statistical modelling strategy that, considering the PK and PD variability for the determinations of the PK/PD index, expands the sample size in order to predict the likely outcome of different therapeutic scenarios or the attainment of a therapeutic target. The clinical outcome can be estimated with the probability of target attainment (PTA), which is defined as the probability that a specific value of the PK/PD index is achieved at a certain MIC (Mouton et al., 2005). The PTA can also be described as the percentage of simulated patients with an estimated PK/PD index equal to or higher than the value linked to the efficacy of the drug against a pathogen with a certain MIC (Asín-Prieto et al., 2015).

5.2. Pharmacometrics. PK/PD modelling and simulation based on time-kill data

Pharmacometrics is the science of interpreting and describing pharmacology in a quantitative fashion. It is fed from pharmacokinetic models, pharmacodynamic models, pharmacodynamic–biomarker-outcomes link models, statistics, stochastic simulation, data visualization, and computer programming (Ette and Williams, 2007). The usefulness of pharmacometrics has been widely recognized by regulatory agencies, academia and pharmaceutical companies. In this regard, modelling and simulation techniques have emerged as a powerful tool to integrate preclinical and clinical data and to provide a scientific approach for rational dosage regimen design and treatment optimization (Schmidt et al., 2008; Trivedi et al., 2013).

In vitro infection models provide a framework for understanding the PK/PD relationships of antimicrobial drugs. In particular, time-kill experiment results can be described with precision by mathematical PK/PD models. Moreover, available clinical PK data can be used with these models to simulate different dosing scenarios and clinical settings. In consequence, PK/PD modelling has been recognised as a valuable tool to help define strategies for antimicrobial treatment. Time-kill based PK/PD models allow to: i) describe actual data; ii) better understand the interaction between drug and microorganism; iii) obtain predictions of untested scenarios; iv) design new studies (Nielsen and Friberg, 2013).

The mathematical models built to explain the time-kill data might vary in complexity, but they all share the same basic components: i) microorganism submodel, which characterises the growth rate and natural death rate of the microbial population over time. Parameters such as k_g (growth rate) or N_{max} (maximum microbial density due to saturation of the system) are part of this submodel; ii) PK model, which characterises drug concentrations over time. In a static experimental setting, concentrations are constant, while in a dynamic setting concentrations usually change set to a first-order elimination constant; iii) full PK/PD model, which merges the two submodels (microorganism model and pharmacokinetic model) to fully characterise the effect of the antimicrobial over the microorganism. Usually, the effect is concentration-dependent in a non-linear way and one of the most used models to describe it is the E_{max} sigmoidal model. The main PD parameters that describe that effect are the E_{max} (maximum effect reached by the drug) and the EC_{50} (the drug concentration needed to reach half the maximum effect) (Nielsen and Friberg, 2013). Furthermore, these mathematical models may

also provide a useful tool to describe antimicrobial resistance or reduced drug sensitivity. In this line, different modelling strategies for describing reduced drug sensitivity have been reported in literature, on the basis of the previous knowledge of the microorganism system, the experimental setting, and the observed data, like regrowth phenomena in the time-kill curves experiments (Schmidt et al., 2009; Grégoire et al., 2010; Khan et al, 2016; Sy et al., 2017).

Regarding antifungal drugs and *Candida*, there are few PK/PD models developed from in vitro kinetic data: caspofungin and fluconazole against *Candida albicans* (Venisse et al., 2008); voriconazole against *Candida spp.* (Li et al., 2009); and more recently, anidulafungin against *Candida spp.* (Gil-Alonso et al., 2016b). However, despite the relevance of *C. auris*, PK/PD modeling of antifungal drugs for this emergent species is still lacking.

Model building and parameter estimation may be achieved by means of non-linear mixed effects modelling.

5.2.1. Non-linear mixed effects modelling

One of the major milestones in pharmacometrics has been the application of population methods to assess the PK/PD relationships. Population approaches provide estimates of typical values for PK or PD parameters and the variability between and within individuals in the population can be quantified. Additionally, covariates or factors that can explain the variability can be studied.

Non-linear mixed effects (NLME) modelling is the foundation of pharmacometrics and population PK/PD analysis. The term 'mixed' refers to the fact that fixed effects (structural parameters) and random effects (variability) are modelled simultaneously (Owen and Fiedler-Kelly, 2014). Variability, in turn, comprises two layers: a first layer of residual variability, while the second handles the variability between individuals.

The population model for the observed *y* dependent variable (log CFU/mL for example) for the *i*th subject at the *j*th time point can be expressed as follows:

$$y_{ij} = f(\theta_i, t_{ij}) + \varepsilon_{ij} \qquad \varepsilon = N(0, \sigma^2) \qquad \text{(Eq. 1)}$$

Where f is the function that represents the structural PK/PD model, θ_i represents the model parameters and ε_{ij} is the residual error, that is, the deviation from observed and predicted data.

It is assumed that the residual variability follows a normal distribution with mean zero and variance σ^2.

At the same time, structural parameters will usually exhibit interindividual variability defined as follows:

$\theta_i = \theta + \eta \qquad \eta = N(0, \omega^2)$ (Eq. 2)

The interindividual error (η) represents the variability in the parameter values within a population, between the different individuals/subjects. It is assumed to follow a normal distribution with mean zero and a variance ω^2.

Additionally, if some variability rises between observation periods, interoccasion variability may be defined (κ), which follows normal distribution with mean zero and a variance π^2 (Karlsson and Sheiner, 1993).

Moreover, it is also possible to calculate the standard error of estimates (SEE) associated with the fixed and random parameters, which gives an idea of the validity and precision of the model.

In summary, the whole model can be defined as follows:

$y_i = f(\chi_i, g(\theta, \eta_i, \kappa_{1,i}\, \kappa_{2,i} \dots, \kappa_{m,i})) + h(\chi_i, g(\theta, \eta_i, \kappa_{1,i}\, \kappa_{2,i} \dots, \kappa_{m,i}), \varepsilon_i)$ (Eq. 3)

where $g()$ is the vector function describing the parameters for the ith individual defined by the typical population parameter θ, the individual deviations vector η_i and the m occasion deviation vectors $\kappa_{x,i}$. $f()$ describes the structural model dependent on the individual variable vector χ_i (observation times, design variables, covariates…), and $h()$ is the error model dependent on the residual error deviation vector ε.

-Selection of the residual error model

Residual (also called intraindividual) error can be modelled in different ways:

- Additive (homoscedastic) error model

  The value of the residual error is independent on the observation magnitude; variance is constant across the whole observation range.

  $y_i = f + \varepsilon_i$ (Eq. 4)

- Proportional (heteroscedastic)

  The value for the residual error is dependent on the observation; variance is not constant throughout the whole observation range.

  $y_i = f\,(1+ \varepsilon_i)$ (Eq. 5)

- Combined model

  In some cases it may be helpful to model the error as a combination of additive and proportional.

  $y_i = f\,(1+ \varepsilon_i) + \varepsilon_2$ (Eq. 6)

- Exponential model

  A less common way to describe the residual error is through an exponential model.

  $y_i = f \times e^{\varepsilon_i}$ (Eq. 7)

-*Selection of the interindividual error model*

Interindividual variability can be expressed with similar models as those for the intraindividual variability

- Additive model

  η is added to the typical population parameter value and the variance remains constant.

  $\theta_i = \theta + \eta_i$ (Eq. 8)

- Proportional model

  The variance for the individual structural parameter increases with increasing values

  $\theta_i = \theta\,(1+ \eta_i)$ (Eq. 9)

- Exponential model

  More commonly used that the intraindividual counterpart

  $\theta_i = \theta \times e^{\eta_i}$ (Eq. 10)

-Estimation methods

In NLME modelling software like NONMEM, parameters are obtained by maximum likelihood (ML) estimation. The aim is to reduce the value of an objective function (OFV), which quantifies the fit of the model to the data (Owen and Fiedler-Kelly, 2014). The minimization search is divided into stages called iterations, each of which results into a different parameter estimate. It is assumed that the parameter values estimated in the last iteration, when the difference between observations and predictions is minimal, corresponds to the best fit. Under the assumption of a normal distribution for the parameters, the OFV equals to minus two times the natural logarithm of the likelihood (-2LL), which is reported when the regression converges (Bauer, 2019a).

In NLME modelling, there is no closed form solution for the integral that defines the MLE, and a linearization is needed (Thai et al., 2014). One of the most common estimation methods in pharmacometrics is the first-order conditional estimation method (FOCE), where the η are included in the estimation process, providing not only the population parameters, but also the individual (posterior Bayes estimates) parameters for every subject within the studied population in a single step (Owen and Fiedler-Kelly, 2014; Bauer, 2019b).

-Validation of the model

Evaluation of the predictive performace of the model is important, especially if it is intended for simulation purposes. There are several ways to check model performance and choose the correct model. First, the estimated parameters should have reasonable values. That is, they should make physiological sense or match accordingly to the experimental data that has been analysed. Another key element in model assessment is the visual examination of the goodness-of-fit (GOF) plots, such as model-predicted vs observed dependent variable graphs or analysis of the residuals vs time. Finally, once there are few candidate models to choose from for the final model, simulation based visual predictive checks (VPC) or bootstrapping can be applied

to make a final decision (GOF plots, VPC and bootstrapping are further explained in Materials and Methods section).

-*Simulations*

Once the final PK/PD model has been selected or constructed, it can be used to make predictions and study different therapeutic scenarios, such as diverse dosing regimens or the therapeutic/toxic effect of a drug on a specific population (children, obese patients, the elderly…). Oftentimes, one of the main goals of model building is focused on performing simulations, which have a key role in clinical trials or regulatory decision-making (Owen and Fiedler-Kelly, 2014). Simulation-based approaches that combine in vitro *Candida* spp time-kill data with pharmacokinetic data collected in vivo have been scarcely used for antifungal drugs (Venisse et al., 2008; Li et al., 2009; Gil-Alonso et al., 2016b).

II. HYPOTHESIS AND OBJECTIVES

C. auris is a multidrug-resistant fungal pathogen that has recently emerged globally as a cause of life-threatening invasive infections. In addition, isolates are included into five distinct clades representing different geographical regions, with growing evidence of different drug susceptibility patterns.

This species is intrinsically resistant to fluconazole and shows reduced susceptibility to other triazoles including the newest isavuconazole. Amphotericin B is usually reserved for non-responders to standard treatments, depending on MIC results. However, a wide range of MIC values for this drug have been reported and amphotericin B susceptibility cannot be currently anticipated. Although echinocandins are nowadays considered as first line therapy for the treatment of *C. auris* infections, resistance to these drugs along with therapeutic failures have been reported.

Despite the increasing concern on the reduced treatment options of *C. auris* infections, very few studies have investigated the in vitro time-kill activity of antifungal drugs against this species. Furthermore, PK/PD models, valuable tools to better characterise the activity of antimicrobial agents, are still lacking for this species.

Because of the limited available therapeutic options and the risk of treatment failure, alternative strategies, such as combination therapies need to be studied in deep. Amphotericin B, isavuconazole and echinocandins have different cell targets, and the study of their combinations might be useful. In this line, recent studies investigated the combinations of azoles, echinocandins, amphotericin B and flucytosine, with disparate results of indifference or synergy, depending on the combined drugs and tested isolates of *C. auris.*

Combining isavuconazole and echinocandins may be an interesting approach to be further investigated, considering among others that, echinocandins are nowadays the first-line treatment for infections caused by *C. auris* and that isavuconazole is the newest addition to the triazole group. Although isavuconazole is labelled for the treatment of aspergillosis and mucormycosis, the reported anti-*Candida* activity together with its biopharmaceutical and pharmacokinetic properties make it a promising candidate for combination therapy.

On the other hand, the combination of amphotericin B with echinocandins, although not recommended in official guidelines yet, is an empirical approach in the clinical setting when dealing with candidaemia resistant to monotherapy treatments. Thus, given the susceptibility

profile of *C. auris* to currently available drugs, the study of amphotericin B plus echinocandin combination should be taken into consideration. To our knowledge, the combination of amphotericin B with echinocandins against *C. auris* has not been investigated through time-kill curve methodology.

Additionally, PK/PD model-based simulation is an approach that bridges in vitro results to the clinical setting, helping in the design of studies and therapeutic decision making. Thus, the implementation of this strategy should be considered, especially for multi-resistant emerging species.

The overall aim of this Doctoral Thesis was to evaluate the in vitro activity of antifungal drugs belonging to the three main classes against *C. auris*, in monotherapy and in combinations, and to develop pharmacometric models for describing and predicting the activity of the drugs.

The specific objectives of the present study were:

I. To describe and compare the in vitro activity of amphotericin B, isavuconazole, anidulafungin, caspofungin and micafungin in monotherapy against *C. auris* clinical isolates.

   In order to fulfil the first objective, the following experiments were conducted:

   1. Determination of the MIC.
   2. Time-kill assays for all drugs.
   3. PAFE assays for drugs that exerted significant antifungal activity.

II. To study the antifungal activity of different drug combinations against *C. auris* clinical isolates.

   In order to fulfil the second objective, the following procedures were performed:

   1. Time-kill assays for the combinations of amphotericin B with anidulafungin or caspofungin.
   2. Checkerboard assays for the combinations of isavuconazole with anidulafungin, caspofungin or micafungin and subsequent data analysis through parametric and non-parametric approaches.
   3. Time-kill assays for the combinations of isavuconazole with anidulafungin, caspofungin or micafungin.

III. To perform pharmacometric analysis, through modelling and simulation, in order to characterise the activity of antifungals and help in decision making.

In order to meet the third objective, the following procedures were carried out:

1. Development of PK/PD models for amphotericin B in monotherapy and for the combinations of isavuconazole with echinocandins.

2. Model-based simulations of standard and alternative dosing regimens to predict treatment outcomes.

III. MATERIALS AND METHODS

1. Materials

1.1. Laboratory materials and equipment

- Petri dishes (Corning, USA)
- 96-well flat-bottom microtitre plates (Sarsted, Germany)
- T-shaped spreader (Corning, USA)
- Laminar air flow cabinet (Faster Two 30, Italy)
- Incubator (Memmert, Spain)
- Centrifuge Biofuge pico (Heraeus, Spain)
- Autoclave (P Selecta, Spain)
- pH meter basic 20 (Crison, Spain)
- Densitometer Densimat (Biomériaux, France)
- Image analyser ChemiDoc Imaging system (Bio-Rad, USA)
- Spectrophotometer Infinite F50 (Tecan, Switzerland)

1.1. Culture media and reagents

- RPMI 1640 medium (Sigma-Aldrich, USA)
- Sabouraud dextrose agar (Scharlab, Spain)
- Suspension medium (Biomériaux, France)
- Phosphate buffer saline (Sigma-Aldrich, USA)
- Dimethyl sulfoxide (Sigma-Aldrich, USA)

1.2. Software

- NONMEM v. 7.4.3 (Icon, USA)
- PsN v. 4.9.0 (University of Uppsala, Sweden)
- R v. 3.6.0 and RStudio v.1.2.1335 (RProject)
- Pirana v. 2.9.6 (Certara, USA)
- S-PLUS v. 6.2 (Insightful Corporation, USA)
- ADAPT-5 (University of Southern California, USA)
- Mathematica v. 12.1 (Wolfram Research Inc., USA)
- Combenefit v. 2.021 (University of Cambridge, UK)

- GraphPad Prism v. 5.01 (GraphPad Software, USA)
- Microsoft Excel 2016 (Microsoft, USA)

2. Microorganisms

Six *C. auris* clinical blood isolates (UPV/EHU 17-257, UPV/EHU 17-259, UPV/EHU 17-261, UPV/EHU 17-263, UPV/EHU 17-265 and UPV/EHU 17-267) from an outbreak in Hospital Universitario y Politécnico La Fe (Valencia, Spain) (Ruiz-Gaitán et al., 2018) were studied in the present Doctoral Thesis. Fungal strains were stored in vials with sterile distilled water at room temperature for up to 1 year, while commercially prepared cryogenic Microbank vials (Pro-Lab diagnostics, USA) maintained at -70ºC were used for prolonged storage.

3. Antifungal drugs

Amphotericin B, isavuconazole, anidulafungin, caspofungin and micafungin were the drugs used in this study (Table 1). The antifungal compounds were obtained in powder form and were prepared and preserved according to their respective manufacturer´s recommendations. Drugs were dissolved in dimethyl sulfoxide (DMSO) to obtain stock solutions of 3200 mg/L and stored at -80ºC until use.

Table 1. Antifungal drugs.

Antifungal drugs	Group	Manufacturer	Purity
Amphotericin B	Polyene	Sigma-Aldrich	82%
Isavuconazole	Azole	Basilea Pharmaceutica	99%
Anidulafungin	Echinocandin	Pfizer SLU	82.4%
Caspofungin	Echinocandin	Merck Sharp & Dome	91.2%
Micafungin	Echinocandin	Astellas Pharma	93.7%

4. In vitro methods for the study of antifungal activity in monotherapy

4.1. MIC determination

MIC for each drug and fungal strain was obtained by the standardized broth microdilution technique described by EUCAST (EUCAST, 2020b). According to the obtained drug MIC results and following the proposed epidemiological cut-off values (ECOFF), *C. auris* isolates were defined as wild-type (WT) or non-wild-type (NWT) (Arendrup et al., 2017b).

4.2. Time-kill experiments

Static time-kill curve experiments were carried out on flat-bottom microtitre plates in RPMI medium, with a final volume of 200 µL per well at 37 ºC for 48 h. *C. auris* blood isolates were grown at 37 ºC for 24 h prior to the start of each experiment to obtain fungal cultures in early logarithmic phase growth. Cells were suspended in RPMI medium to achieve a starting inoculum size of 1-5 x 10^5 CFU/mL and added to the microtitre plate containing different concentrations of the antifungal agent of study (Table 2). Growth control was also measured by adding the inoculum to wells containing RPMI medium without drug. Samples for viable counts were taken at 0, 2, 4, 6, 8, 24 and 48 h, plated in triplicate onto Sabouraud dextrose agar (SDA) and incubated for 24-48 h at 37 ºC. Depending on the drug concentration, samples were either first diluted in PBS or plated directly. When it was expected a sterilizing activity, the whole well was sampled onto a SDA plate (Figure 13). Experiments were conducted in duplicate for each isolate on different days. The lower limit of detection was 5 CFU/mL. Fungistatic activity was defined when the drug exerted a < 3 log CFU/mL reduction compared to the starting inoculum and fungicidal when the reduction was ≥ 3 log CFU/mL (Gil-Alonso et al., 2015a).

Table 2. Drug concentrations used in monotherapy studies.

Antifungal drugs	Concentrations (mg/L)
Amphotericin B	0.25, 0.5, 1, 2, 4
Isavuconazole	0.06, 0.125, 0.25, 0.5, 1, 2, 4
Anidulafungin	0.125, 0.25, 0.5, 1, 2, 4
Caspofungin	0.25, 0.5, 1, 2, 4
Micafungin	0.125, 0.25, 0.5, 1, 2, 4

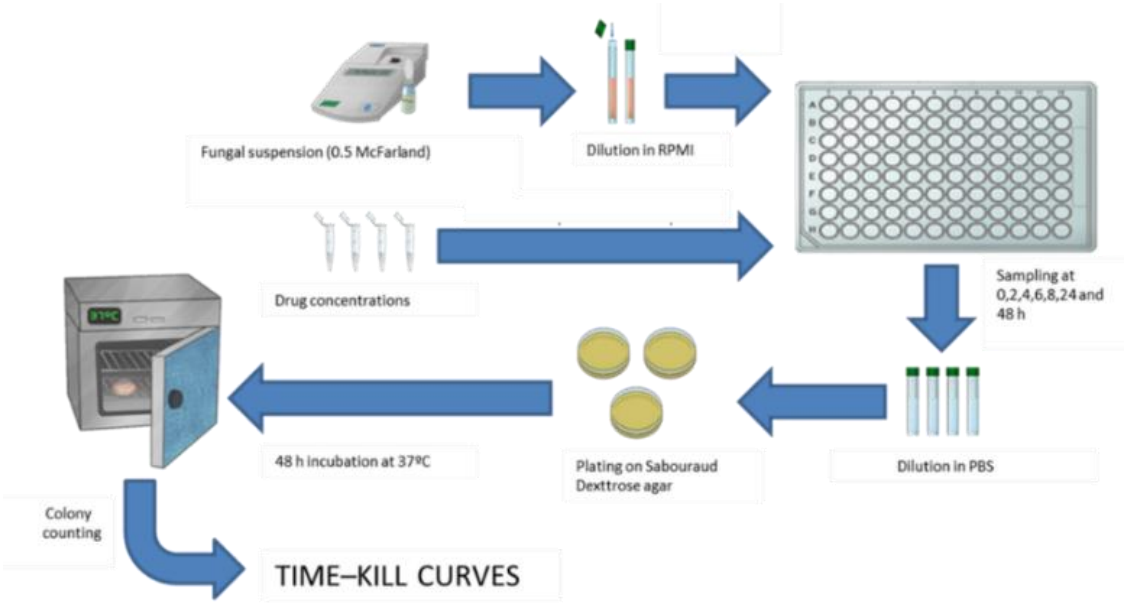

Figure 13. Graphic summary of time-kill curve experimental procedure.

4.3. Determination of PAFE

PAFE experiments were conducted parallel to time-kill curves, testing the same concentrations (Table 2) and following a similar procedure, with slight modifications. Cells were suspended in RPMI medium to achieve a starting inoculum size of 1-5 x 10^5 CFU/mL and added to the microtitre plate. After an incubation of 1 hour at 37ºC, drug was removed from the media by three centrifugation cycles (2000 rpm, 10 minutes each). Cell pellets were re-suspended in RPMI and added back to the microtitre plates. Control cultures were also subjected to the same procedure. Sample for viable counts were taken at 0, 2, 4, 6, 8, 24 and 48 h after re-suspension, plated in triplicate onto SDA and incubated for 24-48 h at 37 ºC. Experiments were performed in duplicate for each isolate on different days. PAFE was calculated as follows:

$$PAFE = T - C \quad \text{(Eq. 11)}$$

where "T" is the time needed by the treated fungal cultures to growth 1 log after drug removal and "C" is the time needed by the control group to growth 1 log after last washout. For the experiments where the 1 log growth of the treated culture was reached between 8 h and 24 h, a non-lineal regression of the data was performed in order to extrapolate "T". Additionally, maximum log reductions of time-kill and PAFE experiments were compared and used to

calculate a PAFE/time-kill index in order to determine the percentage of cell killing that could be attributed to the PAFE (Gil-Alonso et al., 2015b).

5. In vitro methods for the study of antifungal drug combinations

5.1. Checkerboard method

An 8x12-design checkerboard microdilution method, in 96-well flat-bottom microtitre plates, with RPMI 1640 medium, following EUCAST guidelines and modified for drug combinations (Bidaud et al., 2020) was used to study isavuconazole-echinocandin interactions. Isavuconazole was added to columns 2 to 11, at concentrations that ranged from 0.0075 to 4 mg/L. Aliquots of anidulafungin, caspofungin or micafungin were added to rows A-G, and covered a range of 0.03-2 mg/L. Thus, concentrations of the drug combinations ranged from 0.0075 mg/L of isavuconazole plus 0.03 mg/L of echinocandin to 4 mg/L of isavuconazole plus 2 mg/L of echinocandin. Wells from column 12 were left for growth control and H1 and H12 wells were used as sterility control (Figure 14). On the day of the experiment, fungal isolates, previously incubated at 37 ºC overnight, were suspended in distilled water to obtain a starting inoculum of 0.5-2.5 x 10^5 CFU/mL and were added to the microtitre plates. Plates were then incubated at 37 ºC for 48 h and the absorbance of each well was measured on a spectrophotometer Infinite F50 (Tecan, Switzerland), at a wavelength of 450 nm. *Candida parapsilosis* ATCC 22019 and *Candida krusei* ATCC 6258 were used as quality controls. Experiments were conducted by triplicate on different days.

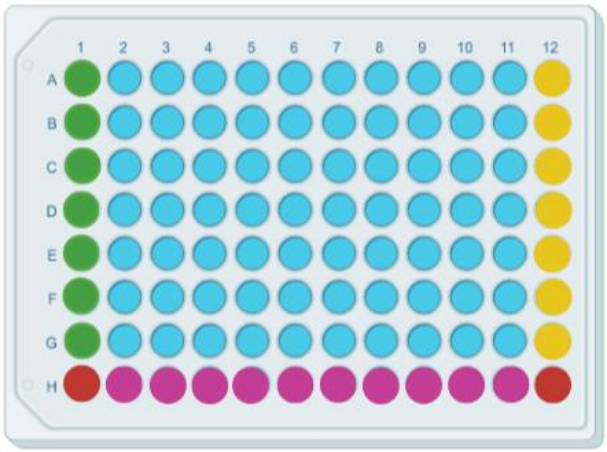

Figure 14. Distribution of elements of an 8x12 checkerboard. Green wells: Echinocandins alone. Purple wells: isavuconazole alone. Blue wells: Isavuconazole and echinocandins in combination. Yellow wells: Growth control. Red wells: Sterility control.

5.1.2. Checkerboard data analysis

Absorbance data obtained from checkerboard experiments were transformed into percentages, with the mean value of the growth control absorbance set to 100%. The data were analysed by FICI (Odds, 2003) and surface response models: Loewe´s additivity based Greco model and Bliss Independence (Greco et al., 1995; Meletiadis et al., 2005).

-FICI

The determination of the FICI of a drug combination is based on Loewe´s additivity and is calculated as follows:

$$\mathrm{FICI} = \frac{\mathrm{MIC_{A+B}}}{\mathrm{MIC_A}} + \frac{\mathrm{MIC_{A+B}}}{\mathrm{MIC_B}} \qquad \text{(Eq. 12)}$$

where MIC_{A+B} is the MIC of the drugs A and B in combination, MIC_A the MIC of drug A alone and MIC_B is the MIC of drug B alone. Drug interactions where defined as synergistic if FICI ≤ 0.5, no interaction if 0.5 <FICI ≤ 4 and antagonistic if FICI > 4 (Odds, 2003).

-Greco model

The parametric surface approach described in the Greco model is defined by the following equation:

$$1 = \frac{\mathrm{Drug_A}}{\mathrm{IC_{50,A}}\mathrm{x}(\frac{\mathrm{E}}{\mathrm{E_{con}-E}})^{(\frac{1}{\mathrm{mA}})}} + \frac{\mathrm{Drug_B}}{\mathrm{IC_{50,B}}\mathrm{x}(\frac{\mathrm{E}}{\mathrm{E_{con}-E}})^{(\frac{1}{\mathrm{mB}})}} + \frac{\alpha\ \mathrm{x\ Drug_A x\ Drug_B}}{\mathrm{IC_{50,A}x\ IC_{50,B}x}\ (\frac{\mathrm{E}}{\mathrm{E_{con}-E}})^{(\frac{1}{2\mathrm{mA}}+\frac{1}{2\mathrm{mB}})}} \qquad \text{(Eq. 13)}$$

where $Drug_A$ and $Drug_B$ are the concentrations of isavuconazole and echinocandin respectively, $IC_{50,A}$ and $IC_{50,B}$ are the concentrations of each drug that achieve 50% of the maximum activity, mA and Mb are the slopes of the concentration-effect curves or Hill´s coefficient, E_{con} is the effect in the absence of drug, E is the fractional effect and α is the interaction parameter that describes the nature of the interaction. When the value of α was positive and its 95% confidence interval (CI) was also positive, the interaction was defined as synergistic. A positive α with 95% CI including zero described an additive interaction. When α was negative without its 95% CI overlapping zero, an antagonistic interaction was claimed. The analysis was run in ADAPT-5 (D'Argenio et al., 2009); parameter estimation was achieved by the weighted least squared (WLS) method:

$$O_{WLS}(\theta) = \sum_{i=1}^{l}\sum_{j=1}^{m} w_{ij}\left(z_i(t_j) - y_i(\theta, t_j)\right)^2 \qquad \text{(Eq. 14)}$$

The weighted least square estimate is the value of θ that minimizes $O_{WLS}(\theta)$. $y_i(\theta,t_j)$ represents the solution of the i^{th} model equation at time t_j. The weights for each observation, w_{ij}, were initially set to 1.

Additionally, observation versus model prediction three-dimensional plots were generated by Mathematica v. 12.1, whereas standardized residuals versus model prediction two-dimensional plots were provided by GraphPad Prism 5.01.

Finally, the parameters obtained for the different combinations were then compared by 1-way ANOVA and Tukey´s multiple comparison test using GraphPad Prism 5.01.

-Bliss Independence model

Bliss Independence model, which assumes that the relative effect of a drug at a particular concentration is independent on the other drug, is defined by the following equation:

$E_{ind}=E_A \times E_B$ (Eq. 15)

where E_{ind} is the predicted percentage of growth and E_A and E_B are the observed percentage of growth in the presence of drug A and drug B, respectively.

Interactions were defined by the following equation:

$\Delta E = E_{ind}-E_{obs}$ (Eq. 16)

where ΔE is the difference between the model predicted percentage of fungal growth (E_{ind}) and the observed percentage of growth (E_{obs}).

When the ΔE of each specific combination of *x* mg/L of isavuconazole and *y* mg/L of echinocandin was positive and its 95 % CI did not include zero, the interaction was defined as synergistic. When the ΔE was negative and its 95 % CI did not include zero, the interaction was defined as antagonistic. Any other case was considered indifferent. The sum of all statistically significant synergistic and antagonistic interactions (ΣSYN_ANT) was the main parameter that summarized the whole interaction surface for the studied drug-drug combinations (Katragkou

et al., 2017; Otto et al., 2019). Additionally, when the ΣSYN_ANT value obtained for each checkerboard analysis was below 100%, weak interaction was defined; values between 100% and 200% were defined as moderate and those higher than 200% were considered strong (Meletiadis et al., 2005).

Combenefit was the software used to perform the Bliss analysis by means of parametric determination (Di Veroli et al., 2016). Combenefit creates a reference surface based on Bliss independence that is evaluated from the dose-response curves of each of the two combined agents. These dose-response curves were generated via fitting to a Hill equation with varying maximum effect:

$$Hill(X = x) = 1 + \frac{E_{c\infty} - 1}{1 + (IC_{50}/x)^H} \qquad \text{(Eq. 17)}$$

The parameters IC_{50}, H and $E_{c\infty}$ characterise the concentration where half of the effect is obtained, the slope of the dose-response curve, and the plateau effect (i.e. asymptote value), respectively. The following equation was minimized by maximum likelihood:

$$F(E_{c\infty}, IC_{50}, H) = \sum_{i=1}^{n} \sum_{j=1}^{p} \left(\frac{E_i(c_j) - HILL(c_j, E_{c\infty}, IC_{50}, H)}{\sigma_j} \right)^2 \qquad \text{(Eq. 18)}$$

where c_j corresponds to the jth concentration value for agent A or B (p concentrations), $E_i(c_j)$ corresponds to the measured effect for concentration level c_j and replicate i (n replicates), and σ_j is the standard deviation obtained for all the measures at concentration c_j.

The resulting dose-response curves were used to generate the dose-response surface for the reference model. The software compared the experimental surface to the modelled one and attributed a percentage score. In the matrix display, if more than one replicate was provided, the software coloured each synergy level only if the result was significant following a one-sample t-test (* p <0.05; ** p <0.001, *** p <10^{-4}).

5.2. Time-kill experiments of the drug combinations

Time-kill curve experiments for combinations of amphotericin B plus anidulafungin/caspofungin and isavuconazole plus anidulafungin/caspofungin/micafungin were carried out similarly to as described in section 4.1. for the monotherapies. The concentrations assayed for each combination are summarized in Table 3 and Table 4. The concentrations of drugs studied in combinations were chosen based on the results of the checkerboard and monotherapy time-kill curves. To assess the interaction between drugs correctly, the concentrations assayed in the combinations were also studied in monotherapy simultaneously. Synergism was declared when the difference in fungal count reduction between the drug with highest effect in monotherapy and its corresponding combination was > 2 log CFU/mL (Mukherjee et al., 2005) (Figure 15). Experiments were carried out in duplicate on different days. Time-kill curves were analysed by fitting the observations to the following exponential equation, as previously described (Cantón et al., 2013; Gil-Alonso et al., 2015a):

$N_t = N_0 \times e^{kt}$ (Eq. 19)

where N_t is the number of CFU/mL at time t, N_0 is the starting cell inoculum, k is the growing or killing rate constant and t is the incubation time. This equation was linearized by applying natural logarithms. Positive k values show fungal growth and negative values indicate killing. GOF for each combination was assessed by the r^2 value (>0.8). Significant differences in killing kinetics among combinations and concentrations were assessed by ANOVA followed by Bonferroni´s post hoc test in GraphPad Prism 5.01. A *p* value <0.05 was considered significant.

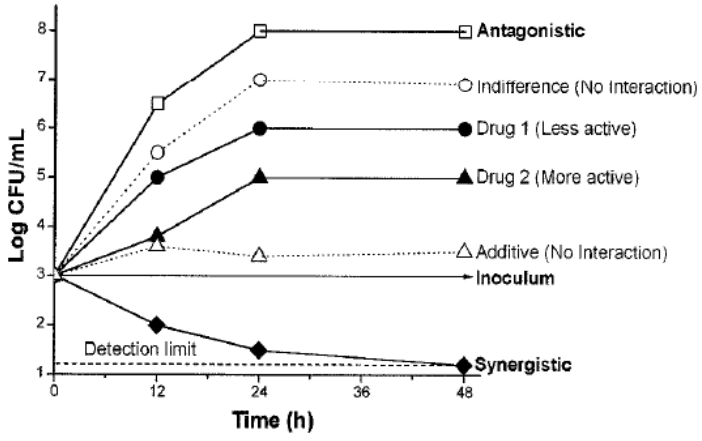

Figure 15. Interpretation of antifungal interactions in time-kill methodology. Taken from Mukherjee et al., 2005.

Table 3. Studied combinations of amphotericin B + anidulafungin/caspofungin.

Amphotericin B (mg/L)	Anidulafungin/Caspofungin (mg/L)
0.5	0.5/1/2
1	0.25/0.5/1

Table 4. Studied combinations of isavuconazole + echinocandins.

Isavuconazole (mg/L)	Echinocandin (mg/L)
0.06	0.125
0.125	4
0.25	0.5/1
2	2
4	4

6. PK/PD modelling and simulation of time-kill curves

PK/PD modelling and simulation was conducted for all drugs in monotherapy and the combinations of isavuconazole with the echinocandins. A schematic description of the workflow of the model building and simulation process in this work is shown in Figure 16.

First, a bibliographical search was done to check published structural models that could fit our time-kill data. Simultaneously, time-kill data were explored to assist in the choosing of the structural models and the initial estimates of model parameters. Once candidate models were built and/or chosen, tentative first runs of the base models (with interindividual variability set to zero) were carried out. After checking parameter estimates, the SEE and the GOF plots for a first model discrimination, candidate models were re-run checking interindividual (IIV) and interoccasion variability (IOV), along with different error models. A second evaluation and model discrimination was then conducted based on improvement of objective function (ΔOFV), GOF plots and SEE. With the remaining best-fit models, VPCs were employed for final model

validation and decision. Finally, non-parametric bootstrap was performed with the chosen model to confirm whether it was appropriate.

The final PD model from the previous step was combined with PK models of the antifungal drugs from literature to predict the fungal killing for the drugs and combinations, for different dosing regimen scenarios. The first simulated scenarios were the effects of standard dosing on the studied isolates. Secondly, the effect of different dosing regimens were simulated. The effect of both standard treatments and alternative ones were also simulated for different MIC scenarios and finally conclusions were drawn from the simulation results.

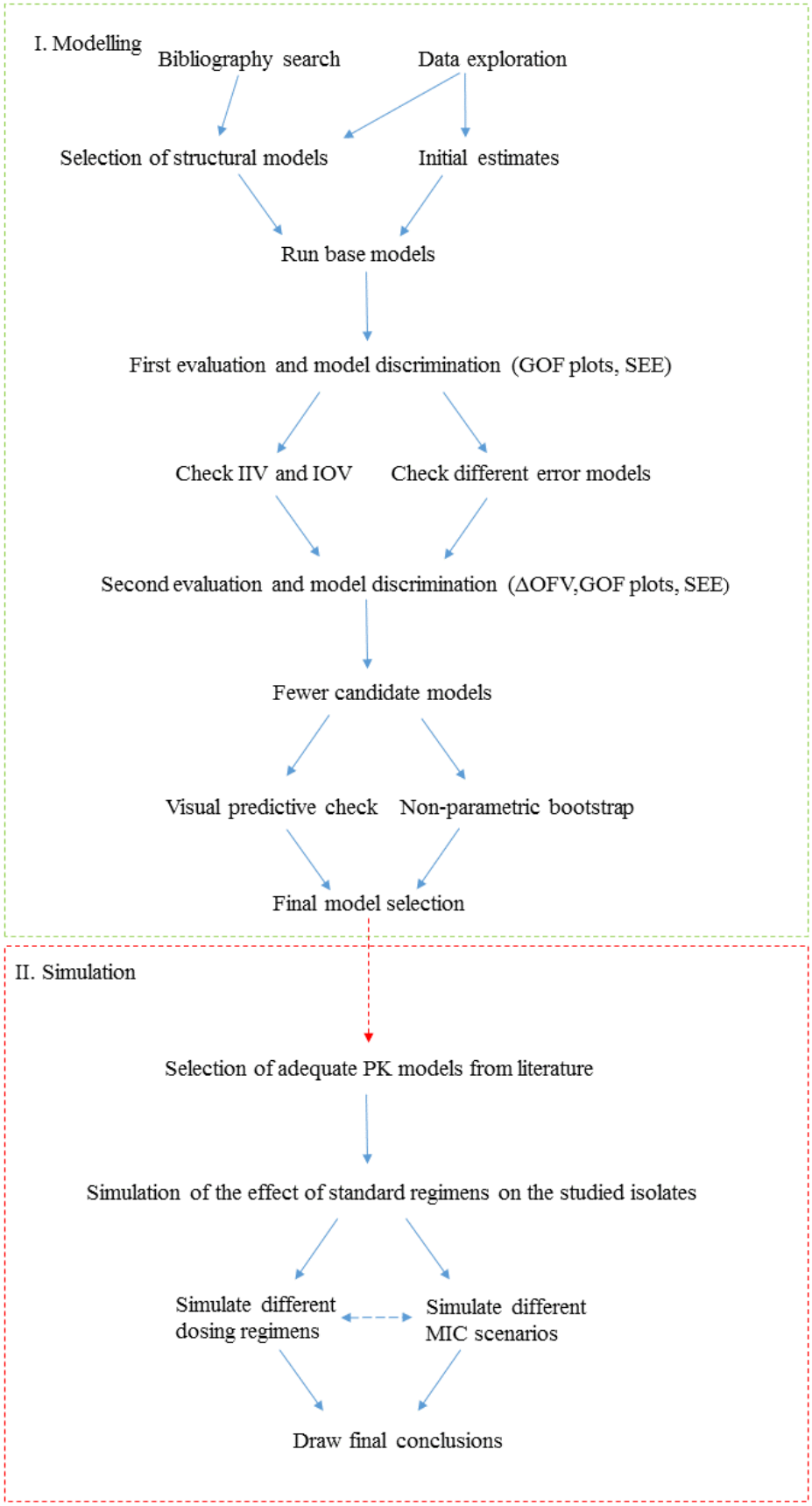

Figure 16. Schematic description of the workflow of the PK/PD modelling and simulation process.

6.1. Model building

6.1.1. Structural models

-Models for monotherapy

The following model was used to describe the evolution of the fungal culture over time in the absence of drug:

$$\frac{dN}{dt} = \left[k_{growth}\left(1-\frac{N}{N_{max}}\right)x\,(1-e^{-\alpha t})\right]\times N \qquad \text{(Eq. 20)}$$

where dN/dt is the change in the number of *Candida* cells as a function of time, k_{growth} is the growth rate constant (h^{-1}) of *Candida* in the absence of drug, N is the number of viable cells (log CFU/mL), N_{max} is the maximum total density of fungal population in the stationary phase (log CFU/mL) and α accounts for the delay in growth observed due to experimental settings.

The effect of an antifungal drug was incorporated into this model as a direct effect, as follows:

$$\frac{dN}{dt} = \left[k_{growth}\left(1-\frac{N}{N_{max}}\right)x\,(1-e^{-\alpha t}) - \text{"drug effect"}\right]\times N \qquad \text{(Eq. 21)}$$

The most common model for drug effect is the sigmoid E_{max} model or Hill equation:

$$\text{Effect} = \frac{E_{max}\,x\,C^{h}}{EC_{50}^{h}+C^{h}} \qquad \text{(Eq. 22)}$$

where E_{max} is a model estimated parameter that accounts for the maximum killing rate constant (h^{-1}), C is drug concentration at any time t (mg/L), EC_{50} is the concentration of the drug necessary to achieve half the maximum effect (mg/L) and *h* is the Hill factor or sigmoidicity factor, which modifies the steepness of the slope and smoothens the concentration-effect curve. When the Hill factor equals to 1, the model is called ordinary E_{max} model or E_{max} model.

A parameterisation of the E_{max} model was also checked:

$$\text{Effect} = \text{Slope}\ x\ C^{h} \qquad \text{(Eq. 23)}$$

where Slope equals to $E_{max}/(EC_{50})^{h}$.

The mechanism of action of drugs can drive the model development process. For instance, an indirect response model was investigated for isavuconazole. This drug, as an azole, exhibits a fungistatic effect and an inhibition of the k_{growth} was modelled (Venisse et al., 2009):

$$\frac{dN}{dt} = \left[k_{growth}\left(1-\frac{N}{N_{max}}\right) x\,(1-e^{-\alpha t}) \; x \left(1-\frac{E_{max} \; x \; C^h}{EC_{50}^h + C^h}\right)\right] \times N \qquad \text{(Eq. 24)}$$

Moreover, a semi-mechanistic model that included two fungal stages, consisting of a drug-susceptible fungal subpopulation (S) and a drug-resistant subpopulation (R) was also tested (Nielsen and Friberg, 2013). A schematic representation of the model is depicted in Figure 17. This two-subpopulation model accounted for the biphasic killing behaviour observed in the time-kill assays with amphotericin B.

First-rate order constants that may define both populations were the natural growth rate (k_{growth}), natural death rate (k_{death}) and the transfer constant from S into R (k_{SR}). The equation that described the S subpopulation in the absence of drug was as follows:

$$dS/dt = k_{growthS} \; x \; S \; x \; (1-e^{-\alpha t}) - k_{deathS} \; x \; S - k_{SR} \; x \; S \qquad \text{(Eq. 25)}$$

where dS/dt is the change in the number of the S subpopulation as a function of time and $k_{growthS}$ is the growth rate of the S subpopulation.

In the case of the resistant or less susceptible subpopulation R, different models have been proposed to define it. A non-growing, drug insensitive microbial subpopulation was described by the following equation:

$$dR/dt = k_{SR} \; x \; S - R \; x \; k_{death} \qquad \text{(Eq. 26)}$$

It was also described as a subpopulation with its own growth rate ($k_{growthR}$) and death rate (k_{deathR}) constants, different from the S subpopulation:

$$dR/dt = k_{SR} \; x \; S + R \; x \; k_{growthR} - R \; x \; k_{deathR} \qquad \text{(Eq. 27)}$$

As previously mentioned, k_{SR} is the parameter that described the transfer of fungal cells from a susceptible state into a more resistant one. It was either estimated as a structural parameter or defined as follows:

$$k_{SR} = \frac{(k_{growthS}-k_{deathS}) \text{ x } (S+R)}{N_{max}} \qquad \text{(Eq. 28)}$$

where S and R are the compartments with susceptible and resistant fungal populations, respectively, and N_{max} is the maximum total density of fungal population in the stationary phase (log CFU/mL).

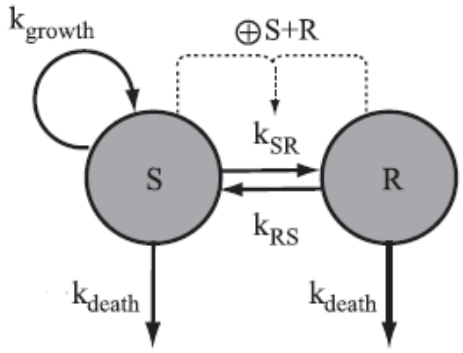

Figure 17. PD model with two-subpopulation compartments. In this case, R is a non-growing subpopulation, insensitive to drug treatment and with the same k_{death} as the S subpopulation. k_{RS} is the transfer-rate constant from R to S. Taken from Nielsen et al., 2007.

-Models for combination therapy

The combinations of isavuconazole and echinocandins were modelled in a similar way to that described in equation 21:

$$\frac{dN}{dt} = \left[k_{growth}\left(1-\frac{N}{N_{max}}\right) \text{x } (1-e^{-\alpha t}) - \text{"}combined\ effect\text{"}\right] \times N \qquad \text{(Eq. 29)}$$

where the combined effect refers to the drug effect driven by the combination of isavuconazole with anidulafungin, caspofungin or micafungin, expressed as an additive effect as follows:

$$\text{Combined effect} = (EFF_{ISV} + EFF_{CANDIN}) \text{ x Int} \qquad \text{(Eq. 30)}$$

$$\text{Combined effect} = (EFF_{ISV} + EFF_{CANDIN})^{Int} \qquad \text{(Eq. 31)}$$

where EFF_{ISV} and EFF_{CANDIN} are the effects exerted by isavuconazole and an echinocandin, respectively (described by equation 22 or 23) and *Int* is the parameter that describes the interaction. If *Int* has a negative value, the interaction is described as antagonistic; if the value

is $0 < x \leq 1$, then the interaction is additive and if it is estimated to be bigger than 1 then the interaction is synergistic (the total effect is bigger than the additive sum of the parts).

The following equation built by Mohamed and colaborators also described the total killing of the microbial population as dependent on the additive effects of both drugs. Aditionally, the interaction was evaluated using an empirical interaction function to test for statistically significant differences from additivity:

$$\text{Combined effect} = \text{EFF}_{\text{ISV}} \text{x} \left(1 + \frac{\text{EFF}_{\text{CANDIN}}}{\text{EFF}_{\text{CANDIN}}+\text{EFF}_{\text{ISV}}}\right)^{\text{Int}} + \text{EFF}_{\text{CANDIN}} \text{x} \left(1 + \frac{\text{EFF}_{\text{ISV}}}{\text{EFF}_{\text{ISV}}+\text{EFF}_{\text{CANDIN}}}\right)^{\text{Int}} \quad \text{(Eq. 32)}$$

A positive value of *Int* reflects synergism and a negative value defines indifference or antagonism (Mohamed et al., 2016).

Data analysis and modelling was performed with NONMEM v. 7.4.3, with FOCE as estimation method and ADVAN13 subroutine. Perl-speaks-NONMEM (PsN) was used as run manager and Pirana as workbench.

6.1.2. Model discrimination and validation

Model performance and discrimination were assessed following several procedures. First, the coherence of the estimated parameters was checked. That is, whether those parameter values were reasonable and had physiological sense or matched accordingly to the experimental data. Additionally, it was verified that the SEE of the parameters expressed as the CV were below 30%.

Model performance and discrimination between candidate models were based on the following criteria:

-*Changes in OFV*

Nested models were compared with each other analysing the changes in the OFV (ΔOFV). In NONMEM, the OFV equals to -2 times the log of the likelihood (-2LL) and therefore, the difference between two models follows an asymptotical Chi square distribution (χ^2) with as many degrees of freedom as the number of added parameters. The significance corresponding to different –2LL is shown in Table 5.

Table 5. Reduction of the –2LL value and corresponding statistical significance.

Increase in the number of parameters	Reduction in the -2 LL	*p* value
1	3.84	<0.05
1	7.88	<0.005
1	10.83	<0.001
2	5.99	<0.05
2	10.6	<0.005
2	13.82	<0.001

-Goodness-of-fit plots

Visual inspection of the so-called GOF plots allows detecting systematic deviations generated by misspecifications in the structural or statistical model and give an idea of the fit of the model to the empirical data (Ette and Williams, 2007). GOF plots were generated by R Studio using the Xpose library.

Graphical representation of the observations (also called dependent variables, DV) versus population predictions (PRED) or individual predictions (IPRED) are shown in Figure 18. If the plots are evenly distributed around the identity line, the structural model is adequate. Observations versus IPRED graphics should show better fit as it incorporates the individual fits by including the interindividual variability into the model.

Graphical representation of the residuals versus time also offer information about model misspecifications. Residuals are the difference between the observed and model predicted dependent variables. Weighted residuals (WRES) are calculated by taking into account the residual variability model and normalizing the residuals, so they are expected to follow a normal distribution with a mean of 0 and a variance of 1 (Owen and Fiedler-Kelly, 2014).

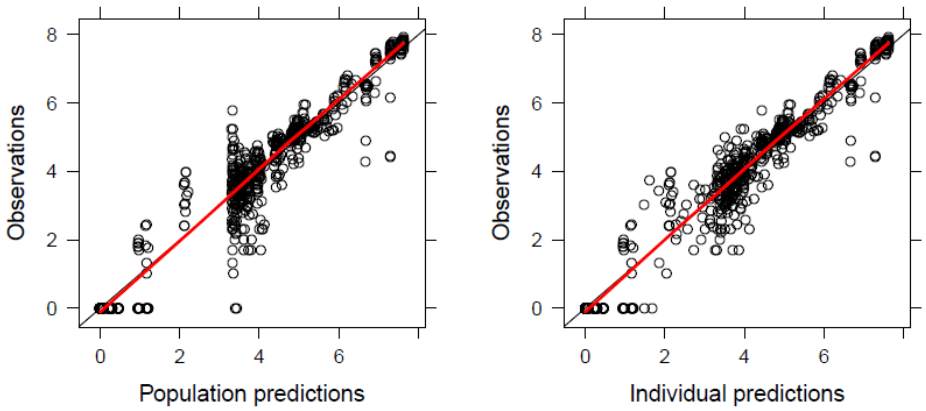

Figure 18. Observations vs population (left) and individual (right) predictions. The black line is the identity line and the solid red line shows the trend of the data.

Hooker and collaborators demonstrated that NONMEM calculates WRES with the first order (FO) method regardless of the estimation method employed, so they introduced the conditional weighted residuals (CWRES), which are more appropriate in the context of FOCE estimation (Hooker et al., 2007). Plots of CWRES against time and plots of CWRES versus predictions should be evenly centred around zero line, without systematic bias and most values within -2 to +2 SD (Figure 19).

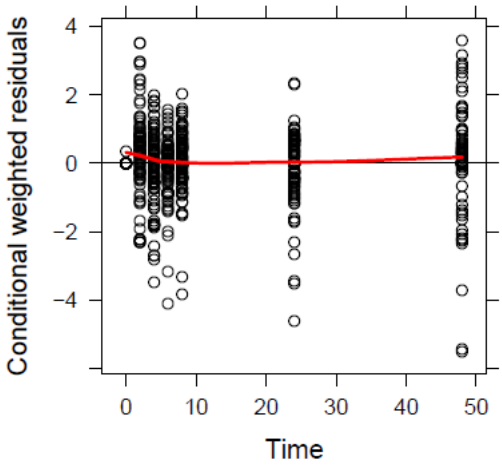

Figure 19. Conditional weighted residuals (CWRES) vs Time (h). The black line marks the 0 value for CWRES and the red line shows the trend of the CWRES.

-Visual predictive checks

The VPC is a simulation-based internal validation technique. The basis of this procedure considers that if a model is correct, the simulated data originated by the model should follow the same characteristics as the original data. A VPC shows model adequateness when most observed data lay within the simulation interval (Karlsson and Savic, 2007). In this Thesis, models were evaluated through VPC by simulating 1000 individuals with the $SIMULATION command in NONMEM. The mean value of the simulations and its 95% CI were calculated and graphically represented with S-Plus (Figure 20).

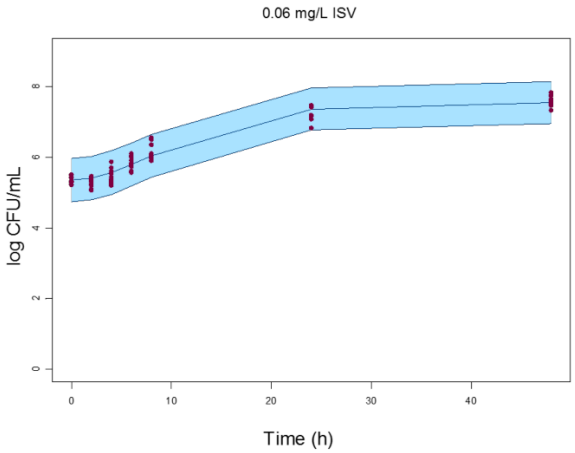

Figure 20. Example of a visual predictive check (VPC) generated for our simulations with isavuconazole. Observed data (full circles), the mean prediction (solid line) and 95% model prediction interval (shaded area) of the simulations.

-Bootstrap

Bootstrapping is a widely used statistical method based on resampling that provides another internal evaluation technique for PK/PD modelling. In the present work, the non-parametric bootstrap was performed using PsN. Specifically, *n* number of datasets (500 for amphotericin B and 1000 for the combinations of isavuconazole and echinocandins) were built by resampling from the original dataset, and the final model was run with each generated dataset to obtain the corresponding parameter estimates (Ette and Williams, 2007). The median value of each parameter and its 95% CI interval generated by bootstrapping were compared to the parameter values of the final model. The model was considered stable if the final parameter estimates laid within the 95% CI of the bootstrap. Additionally, a relative bias (%) was calculated as follows (Thai et al., 2014):

Relative bias (%) = (bootstrap median - final model estimate)/final model estimate x 100 (Eq. 33)

The bootstrap parameter estimates were defined as unbiased when relative bias was within ±10 % (Thai et al., 2014).

6.2. PK/PD simulations

Once final PK/PD models were developed and validated, the next step was to perform simulations of different scenarios that could help to draw conclusions about the susceptibility of *C. auris* to antifungal treatments.

First, a PK model developed for each drug was extracted from literature. A summary description of the PK model characteristics is provided in Table 6.

Table 6. Summary description of the PK models used for simulations of PK profiles.

Drug	Model description	Covariates	Subjects (n)	Source
Amphotericin B	Tricompartmental	No (not a population analysis)	Healthy subjects (5)	Bekersky et al., 2002a
Isavuconazole	Bicompartmental	Sex on Cl BMI on V_p	SOT recipients (79)	Wu et al., 2020
Anidulafungin	Bicompartmental	SOFA score on Cl BMI on V_c	ICU patients (13)	Kapralos et al., 2020
Caspofungin	Bicompartmental	No	ICU patients (21)	Martial et al., 2016
Micafungin	Bicompartmental	No	ICU patients (20)	Martial et al., 2017

Cl: Clearance. V_c: Central volume of distribution. V_p: Peripheral volume of distribution. BMI: Body Mass Index. SOFA: Sepsis-related Organ Failure assessment. SOT: Solid Organ Transplant. ICU: Intensive Care Unit.

PK/PD simulations were conducted sequentially. First, the PK profiles of 1000 individuals were simulated and the total plasma concentrations were corrected for the free, unbound drug, considering the protein binding reported in literature for each drug. Next, databases were created with the mean free concentrations to serve as the input for the PK part of the developed PK/PD models. Finally, the effect on fungal burden after 1-week treatment for 1000 individuals was simulated by applying the final PK/PD models. As with the PK/PD model development and VPC, simulations were performed with NONMEM, using $SIMULATION command. The

mean value of the simulations and its 95% CI were calculated and graphically represented with S-Plus.

The first scenario tested aimed to examine the drug efficacy, expressed as either fungal burden reduction or suppression of growth, after different dosing schedules. Other dosage alternatives were proposed in case of failure. Recommended standard dosages and alternative dosing regimens tested by simulations are shown in Table 7. For the combination therapy of isavuconazole and echinocandins, 4 different dose schedules were tested: I) standard treatment of both isavuconazole and the echinocandin. II) standard dosing schedule of isavuconazole plus alternative treatment of echinocandin. III) alternative treatment of isavuconazole plus standard dosing of echinocandin. IV) alternative treatment of both isavuconazole and echinocandin. Alternative doses were based on proposals from other works and/or clinical guides (Martial et al., 2016; Pappas et al., 2016; Martial et al., 2017; Kapralos et al., 2020).

Moreover, since all isolates in the present study had the same MIC for all studied drugs, different MIC scenarios were tested following an equation that relates the EC_{50} of a drug with the MIC (Schmidt et al., 2009):

$$MIC = \left(\frac{d}{E_{max} - d}\right)^{1/h} \times EC_{50} \qquad \text{(Eq. 33)}$$

where *d* is a drug-independent constant and *h* is the Hill factor. The EC_{50} value for each MIC scenario was then included in the PK/PD model and simulations were performed similarly.

Table 7. Standard and alternative dosing-schedules.

Drug	Standard treatment	Alternative Dosing-schedules
Amphotericin B	0.6-1 mg/kg/day	1.5 mg/kg/day
Isavuconazole	200 mg every 8 h, first 48 h + 200 mg/day after	400 mg every 8 h, first 48 h + 200 mg/day after
Anidulafungin	200 mg L.D + 100 mg/day	200 mg L.D + 200 mg/day
Caspofungin	70 mg first day + 50 mg/day	100 mg/day
Micafungin	100 mg/day	600 mg/day

L.D: Loading dose

IV.RESULTS

1. In vitro activity of antifungal drugs in monotherapy

1. 1. MIC determination

MICs of each drug were equal for all *C. auris* clinical isolates and are listed in Table 8. According to the currently proposed ECOFFs, isolates were considered WT for amphotericin B, isavuconazole, anidulafungin and micafungin. There are not published ECOFFs for caspofungin.

Table 8. Minimum inhibitory concentrations (MIC) for each drug.

Drug	MIC (mg/L)
Amphotericin B	1
Isavuconazole	0.06
Anidulafungin	0.125
Caspofungin	0.25
Micafungin	0.125

1.2. Time-kill curves

-Amphotericin B

Graphical representation of mean time-kill curves for every isolate and replicates is shown in Figure 21. Amphotericin B exhibited concentration-dependent fungicidal activity. Fungicidal effect (3 log reduction compared to initial inoculum) was rapidly achieved, at 2 and 4 h, for concentrations of 4 mg/L and 2 mg/L, respectively. The fungicidal effect was very similar for all the isolates. At concentrations of 1 mg/mL (equal to MIC), the effect was fungistatic overall, with a biphasic killing kinetic trend with fungal regrowth by the end of the experiment for all clinical isolates except *C. auris* 17-259. A similar biphasic trend was also observed at 0.5 mg/L

in isolates 17-257 and 17-263. Nevertheless, neither 0.5 mg/L nor 0.25 mg/L resulted in an antifungal effect of interest.

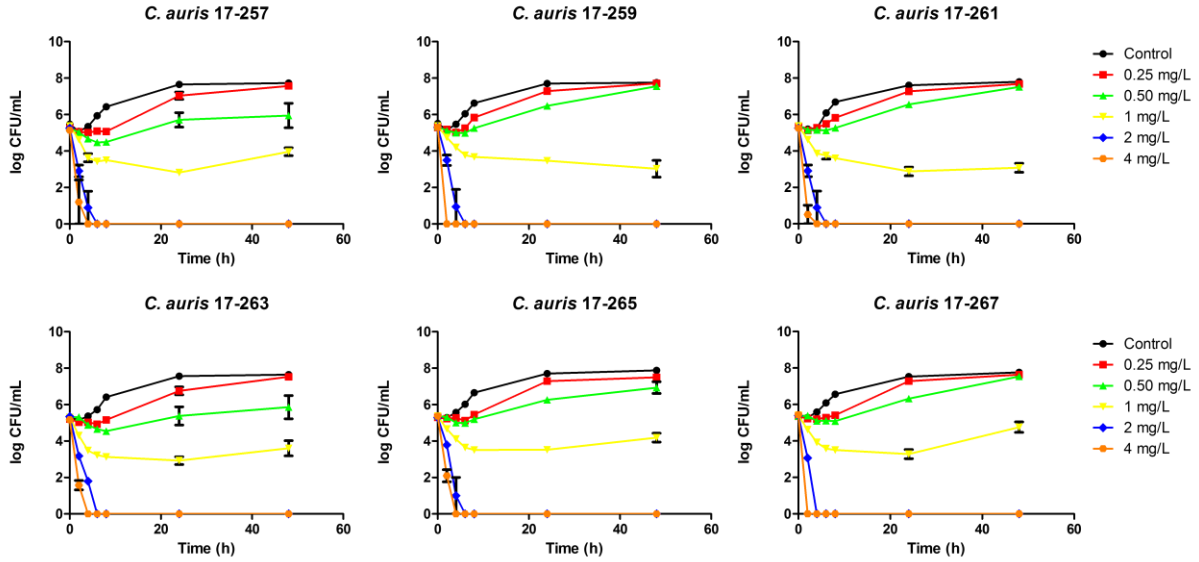

Figure 21. Mean time-kill curves for amphotericin B against *C. auris*. Each data point represents the mean result ± standard deviation (error bars) of all replicates.

-Isavuconazole

Isavuconazole did not exhibit fungicidal nor fungistatic effect against *C. auris.* A small killing activity was exerted at concentrations of 2 and 4 mg/L (32 and 64 times the MIC respectively) the first 4 hours, but the fungal cultures rapidly recovered and started growing again (Figure 22).

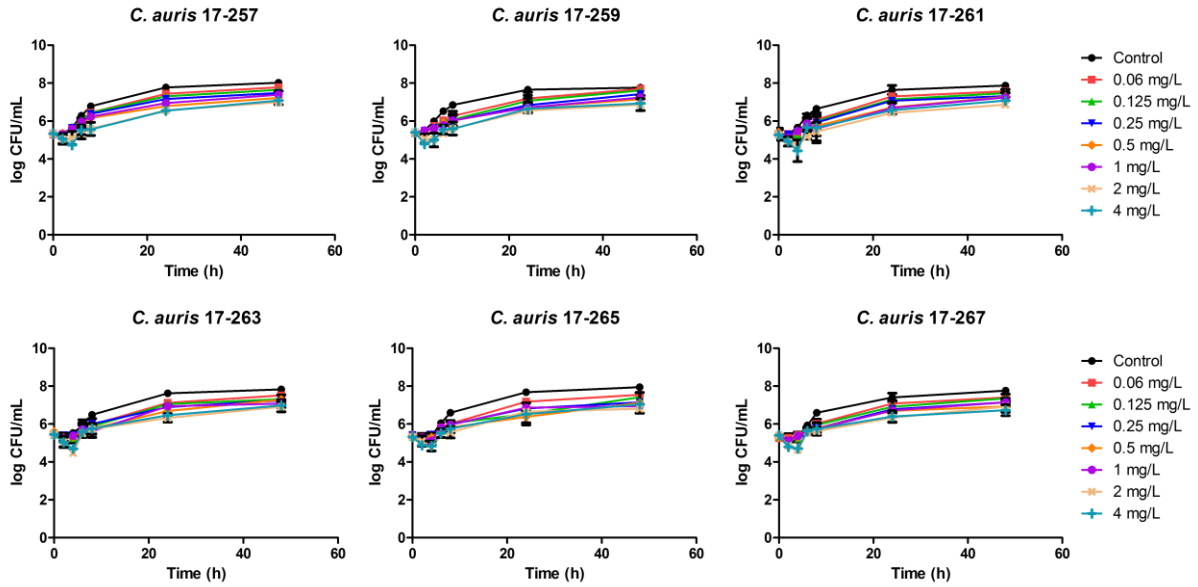

Figure 22. Mean time-kill curves for isavuconazole against *C. auris*. Each data point represents the mean result ± standard deviation (error bars) of all replicates.

-Echinocandins

Echinocandins did not exert fungistatic nor fungicidal effect. Anidulafungin and micafungin had a similar time-kill profile as isavuconazole, with a slight killing activity at concentrations of 2 and 4 mg/L (16 and 32 times the MIC) the first hours and a fast recovery afterwards. On the other hand, caspofungin showed even less antifungal activity (Figures 23-25).

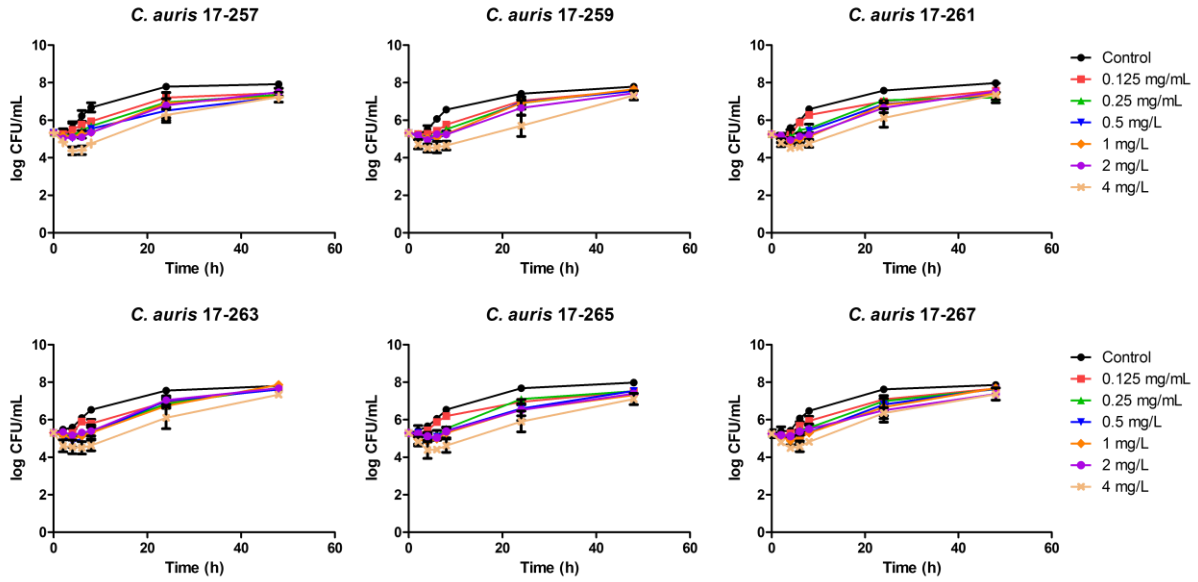

Figure 23. Mean time-kill curves for anidulafungin against *C. auris*. Each data point represents the mean result ± standard deviation (error bars) of all replicates.

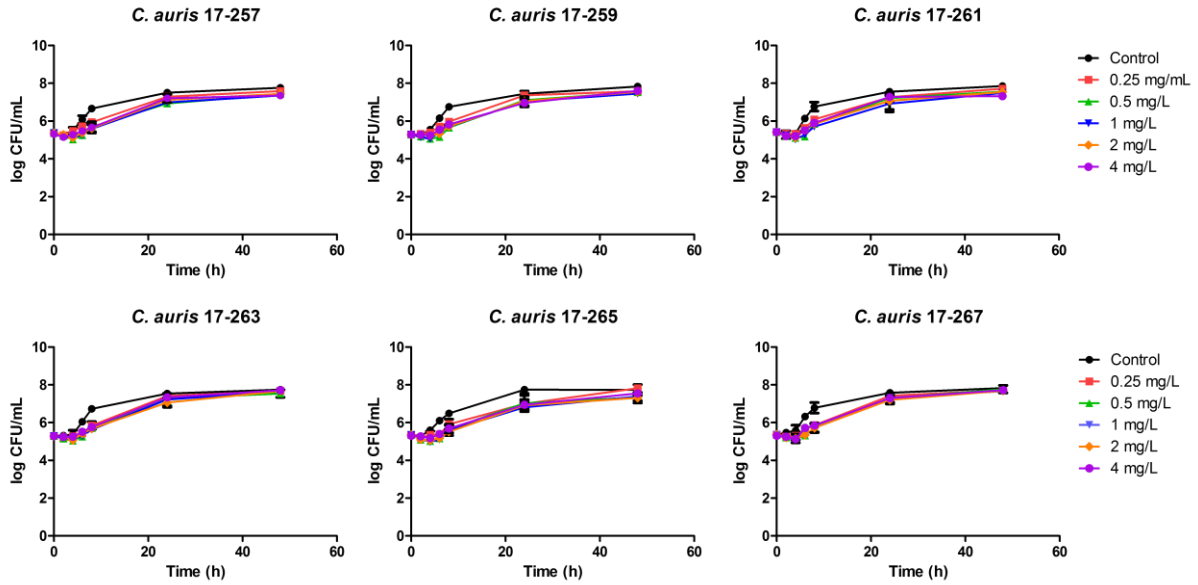

Figure 24. Mean time-kill curves for caspofungin against *C. auris*. Each data point represents the mean result ± standard deviation (error bars) of all replicates.

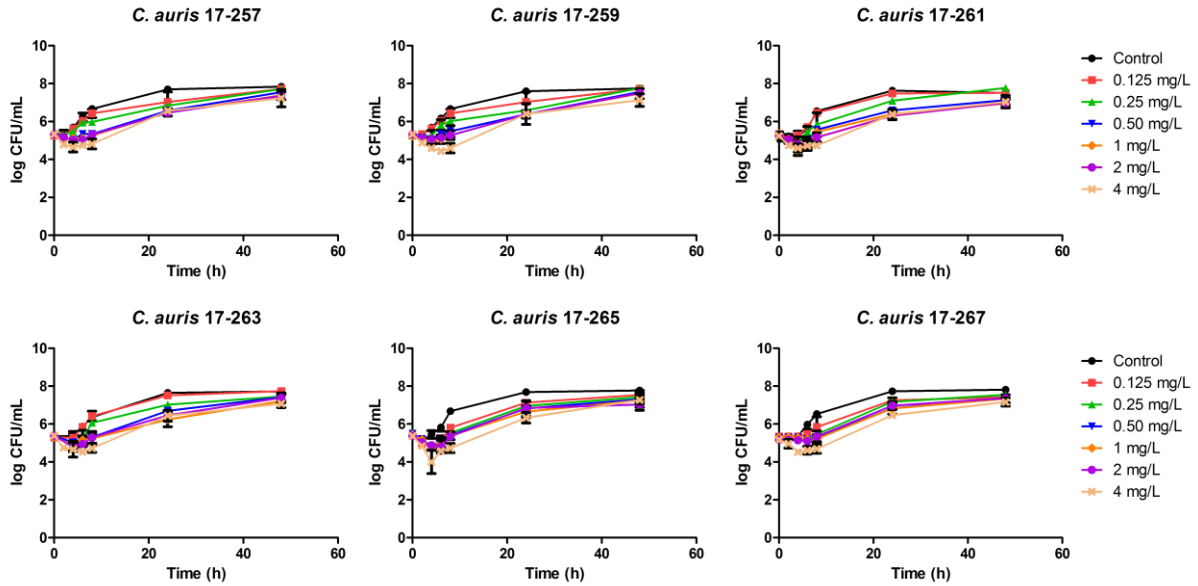

Figure 25. Mean time-kill curves for caspofungin against *C. auris*. Each data point represents the mean result ± standard deviation (error bars) of all replicates.

1.3. PAFE determination and analysis

PAFE was studied and determined for amphotericin B, as it was the only drug with a remarkable antifungal activity. Results of PAFE experiments are summarized in Table 9. Short PAFEs were achieved with the concentrations of 2 and 4 mg/L of amphotericin B, with median values of 4.6 h and 3.5 h, respectively. The longest PAFE was about 6.5 h, at the concentration of 2

mg/L against *C. auris* 17-259. PAFE was higher for the concentration of 2 mg/L than for the concentration of 4 mg/L due to differences in growth rate. As it is pointed out in Figure 26, fungal killing was not observed during PAFE experiments, therefore, it could be concluded that PAFE had no role in the fungicidal activity of amphotericin B (expressed as PAFE/TK).

Table 9. PAFE results for amphotericin B against *C. auris*.

C. auris isolate	Amphotericin B (mg/L)	Time-kill (log CFU/mL)	PAFE killing (log CFU/mL)	PAFE/TK	PAFE (h)
17-257	2	5.41	0	0	4.5
	4	5.41	0	0	2.6
17-259	2	5.51	0	0	6.5
	4	5.51	0	0	4.24
17-261	2	5.42	0	0	4.61
	4	5.42	0	0	3.78
17-263	2	5.28	0	0	3.55
	4	5.28	0	0	2.7
17-265	2	5.29	0	0	4.5
	4	5.29	0	0	3.2
17-267	2	5.37	0	0	5.5
	4	5.37	0	0	4.8

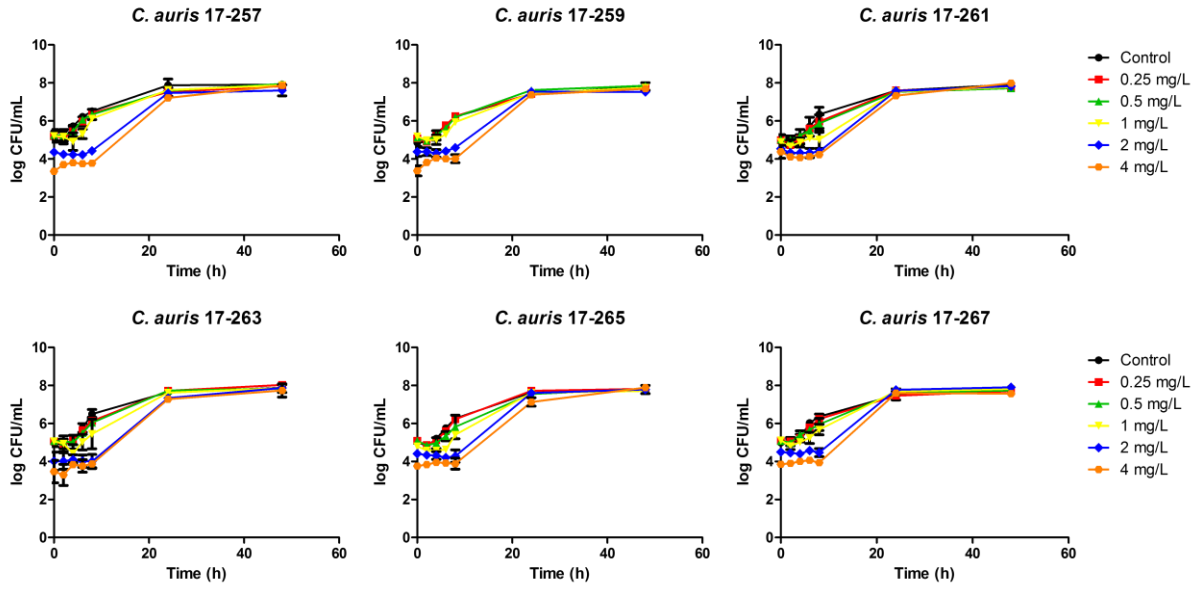

Figure 26. Mean PAFE curves for amphotericin B against *C. auris*. Each data point represents the mean result ± standard deviation (error bars) of all replicates.

2. In vitro activity of combination therapies against *Candida auris*

2.1. Amphotericin B plus anidulafungin or caspofungin

Mean time-kill curves for all isolates and combinations are shown in Figure 27. Fungal counts at 8, 24 and 48 h for each isolate and combination are depicted in Table 10. As previously reported, the antifungal activity of amphotericin B alone at the concentration of 0.5 mg/L was limited against the six isolates of *C. auris*, as no fungicidal nor fungistatic effect was achieved. Similarly, echinocandins alone had a negligible effect even at the highest tested concentrations. In contrast to the poor results of the monotherapies, the combination of 0.5 mg/L of amphotericin B with anidulafungin or caspofungin led to a sustained fungistatic effect, and the fungicidal endpoint was reached against some isolates. The interactions were synergistic from 24 h onwards for all isolates and concentrations. Conversely, 1 mg/L of amphotericin B showed fungistatic activity, and the combinations with the echinocandins were mostly additive. Regardless of the additivity detected, when ≥ 0.5 mg/L of echinocandin was combined with 1 mg/L of amphotericin B, fungicidal effect was achieved against all isolates.

Interestingly, a quarter of all combination time-kill experiments showed regrowth phenomena. The regrowth was observed specially for the combinations of 0.5 mg/L of amphotericin B with 2 mg/L of echinocandin, which resulted, in the case of caspofungin, in a lower mean effect compared to the combination that included 1 mg/L of caspofungin (Figure 27). Mean time-kill curves for each isolate are shown in Annex I.

When the killing-rate constants were analysed, positive k values, non-different from control curves were obtained for all the drugs and concentrations in monotherapy ($k= 0.055\ h^{-1}$), except for amphotericin B at 1 mg/L, with a negative mean k value ($k= -0.031\ h^{-1}$), indicating fungal killing, even though fungicidal threshold was not reached (Table 10). In contrast to the positive k values for echinocandins alone and for 0.5 mg/L of amphotericin B, the time-kill curves patterns shifted for the combinations, all killing-rate constants were negative and significantly different from monotherapy. That was also the case for the combinations of anidulafungin with 1 mg/L of amphotericin B. Conversely, only the k of the combination of 1mg/L amphotericin B plus 1 mg/L of caspofungin was significantly different from amphotericin B monotherapy. The reason may be due to the higher variability observed in the activity of caspofungin in contrast to anidulafungin. Mean killing rate constants for each drug combination are graphically represented in Figure 28.

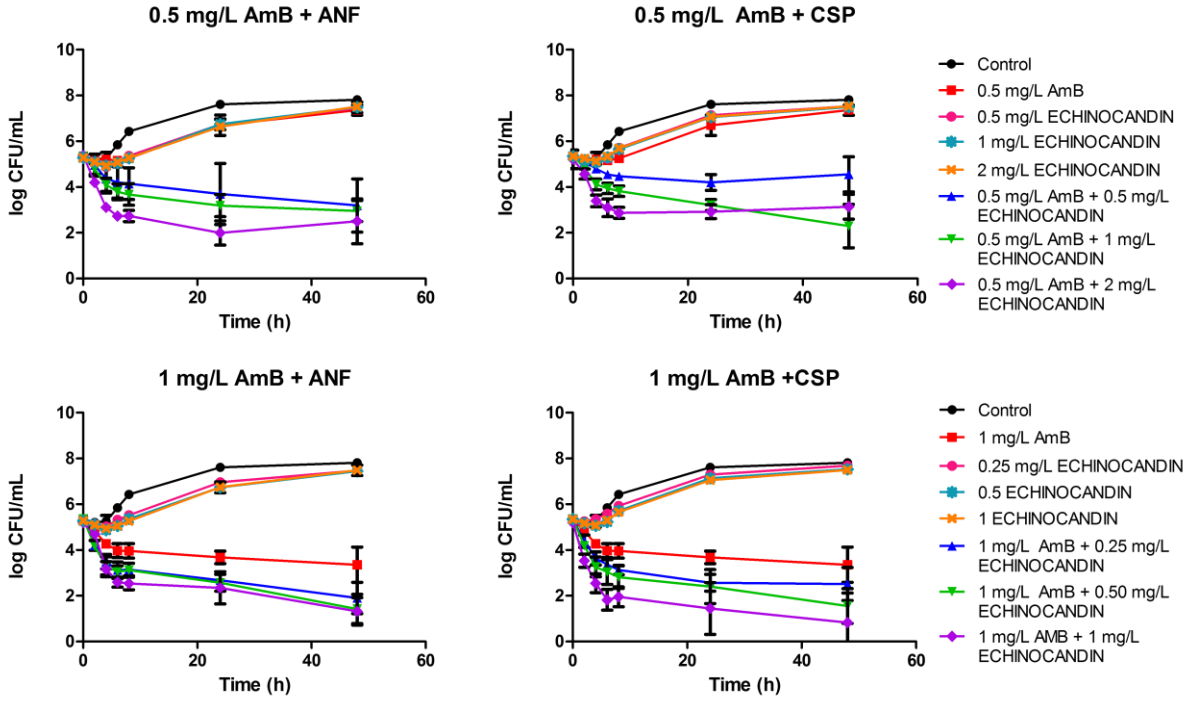

Figure 27. Mean time-kill curves for the combinations of amphotericin B + anidulafungin (top and bottom left) or caspofungin (top and bottom right) against *C. auris*. Each data point represents the mean result ± standard deviation (error bars) of all isolates and replicates.

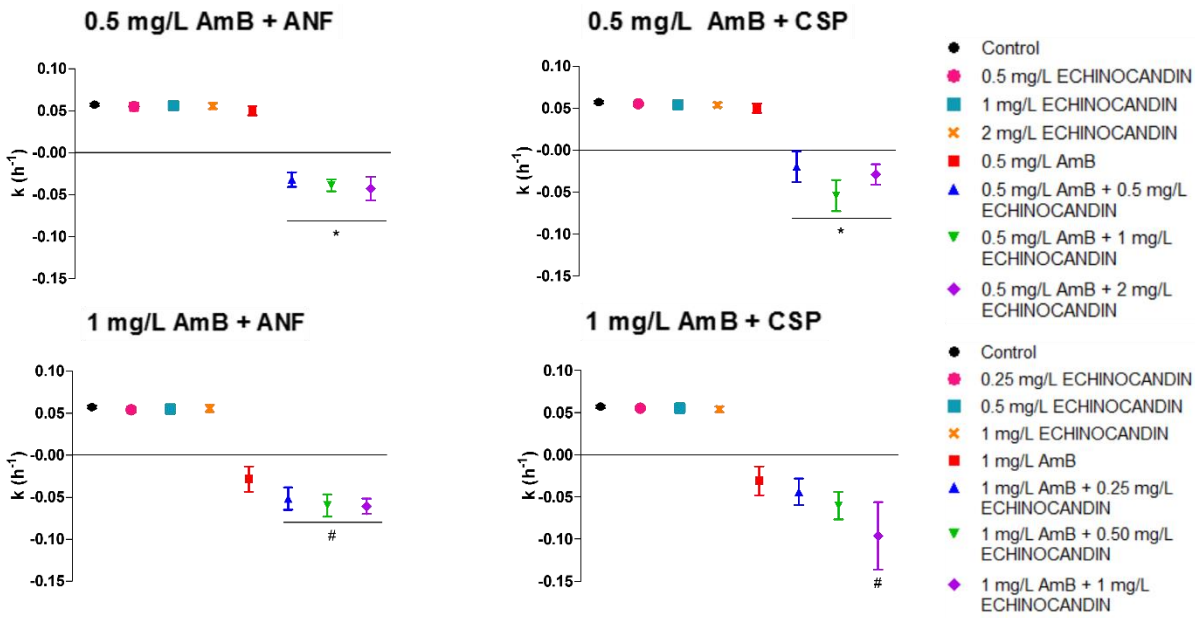

Figure 28. Mean killing-rate constant values for the combinations of amphotericin B + anidulafungin (top and bottom left) or caspofungin (top and bottom right) against *C. auris*. Each data point represents the mean result ± standard deviation (error bars) of all isolates and replicates. **p*<0.05 vs. 0.5 mg/L AmB; # *p*<0.05 vs. 1 mg/L AmB (One-way ANOVA followed by Bonferroni´s post hoc test).

Table 10. Fungal counts at 8, 24 and 48 h and interaction classification: Synergy is marked in bold and fungicidal effects are underlined.

		Fungal count (log CFU/mL) (SD)					
	AmB+ECH	AmB+ANF			AmB+CSP		
	(mg/L)	8h	24h	48h	8h	24h	48h
17-257	Control	6.68 (0.26)	7.65 (0.08)	7.83 (0.10)	6.68 (0.26)	7.65 (0.10)	7.83 (0.10)
	0.5 AmB	5.14 (0.29)	6.58 (0.43)	7.37 (0.14)	5.14 (0.29)	6.58 (0.43)	7.37 (0.14)
	0.5+0.5	4.52 (0.26)	**3.91 (0.05)**	**3.62 (0.58)**	4.62 (0.07)	**4.36 (0.40)**	**5.26 (0.10)**
	0.5+1	3.73 (0.31)	**3.72 (0.31)**	**2.86 (0.66)**	4.10 (0.00)	**3.22 (0.25)**	**3.96 (0.51)**
	0.5+2	**2.92 (0.16)**	**1.10 (1.55)**	**1.07 (1.51)**	**2.98 (0.30)**	**3.21 (0.45)**	**3.20 (0.08)**
	1 AmB	4.03 (0.23)	3.40 (0.21)	2.52 (0.06)	4.03 (0.23)	3.40 (0.20)	2.52 (0.06)
	1+0.25	3.15 (0.49)	2.90 (0.71)	1.35 (0.21)	3.12 (0.17)	2.37 (0.11)	2.68 (0.19)
	1+0.5	3.13 (0.18)	2.21 (0.17)	0.84 (1.19)	3.07 (0.10)	2.60 (0.69)	1.71 (1.39)
	1+1	2.87 (0.03)	2.66 (0.04)	1.71 (0.56)	2.50 (0.14)	2.09 (0.84)	2.62 (0.12)
17-259	Control	6.20 (0.00)	7.62 (0.06)	7.71 (0.3)	6.20 (0.00)	7.63 (0.06)	7.71 (0.30)
	0.5 AmB	5.23 (0.05)	6.81 (0.04)	7.32 (0.00)	5.23 (0.05)	6.81 (0.04)	7.32 (0.00)
	0.5+0.5	4.67 (0.00)	**4.21 (0.02)**	**3.54 (0.18)**	4.65 (0.02)	**4.29 (0.66)**	**4.08 (0.36)**
	0.5+1	3.65 (0.07)	**3.32 (0.04)**	**2.77 (0.54)**	3.98 (0.02)	**3.47 (0.16)**	**2.52 (0.11)**
	0.5+2	**3.08 (0.39)**	**2.49 (0.86)**	**2.44 (2.39)**	3.31 (0.25)	**3.20 (0.29)**	**3.40 (0.22)**
	1 AmB	4.42 (0.32)	4.16 (1.03)	3.20 (0.69)	4.43 (0.32)	4.17 (1.00)	3.20 (0.69)
	1+0.25	3.68 (0.25)	2.72 (0.22)	2.63(1.99)	3.52 (0.17)	3.07 (0.04)	2.48 (0.70)
	1+0.5	3.30 (0.00)	3.28 (0.47)	**0.50 (0.70)**	3.45 (0.21)	2.44 (0.22)	1.76 (1.00)
	1+1	2.83 (0.14)	2.87 (1.37)	2.09 (0.84)	**2.17 (0.17)**	2.43 (0.21)	2.37 (3.35)
17-261	Control	6.38 (0.02)	7.54 (0.01)	7.95 (0.09)	6.38 (0.02)	7.54 (0.01)	7.95 (0.08)
	0.5 AmB	5.20 (0.05)	6.40 (0.40)	7.50 (0.16)	5.23 (0.05)	6.4 (0.43)	7.48 (0.16)
	0.5+0.5	4.42 (0.20)	**3.79 (0.39)**	**3.55 (0.14)**	4.38 (0.16)	**3.96 (0.22)**	**5.08 (1.17)**
	0.5+1	3.35 (0.02)	**3.03 (0.37)**	**3.00 (1.00)**	3.55 (0.44)	**3.22 (0.49)**	**1.85 (0.21)**
	0.5+2	**2.86 (0.05)**	**3.23 (0.78)**	**3.39 (1.12)**	**2.73 (0.05)**	**2.48 (0.05)**	**3.52 (1.03)**
	1 AmB	3.85 (0.07)	3.61 (0.48)	3.77 (0.46)	3.85 (0.07)	3.61 (0.48)	3.77 (0.46)
	1+0.25	3.13 (0.28)	2.55 (0.40)	1.79 (0.49)	2.95 (0.12)	2.57 (0.13)	3.60 (0.73)
	1+0.5	3.06 (0.09)	2.39 (0.80)	1.79 (1.40)	3.00 (0.01)	3.31 (0.59)	**1.00 (0.01)**
	1+1	2.26 (0.15)	3.22 (2.00)	**0.60 (0.84)**	**1.3 (0.42)**	1.97 (2.78)	**0.00 (0.00)**
17-263	Control	6.88 (0.44)	7.54 (0.04)	7.93 (0.09)	6.88 (0.44)	7.54 (0.04)	7.93 (0.09)
	0.5 AmB	5.30 (0.37)	7.05 (0.10)	7.54 (0.01)	5.30 (0.37)	7.05 (0.11)	7.54 (0.01)
	0.5+0.5	4.68 (0.20)	**4.68 (0.60)**	**3.28 (1.16)**	4.70 (0.14)	**3.94 (0.17)**	**3.19 (0.84)**
	0.5+1	3.88 (0.16)	**2.68 (0.27)**	**3.11 (0.87)**	3.75 (0.11)	**2.84 (0.42)**	**1.68 (0.01)**
	0.5+2	**2.58 (0.16)**	**1.7 (0.49)**	**2.40 (0.80)**	**2.66 (0.23)**	**2.69 (1.68)**	**3.40 (2.35)**
	1 AmB	3.88 (0.26)	2.99 (0.43)	4.93 (0.42)	3.88 (0.25)	2.99 (0.43)	4.94 (0.41)
	1+0.25	2.90 (0.59)	2.23 (1.12)	**1.77 (1.96)**	3.10 (0.47)	1.99 (1.33)	**1.43 (0.98)**
	1+0.5	2.90 (0.47)	2.29 (1.76)	**1.91 (1.65)**	2.38 (0.54)	2.06 (0.06)	**1.90 (1.63)**
	1+1	2.25 (0.35)	2.23 (0.24)	**0.95 (1.34)**	2.25 (0.49)	2.19 (0.15)	**0.00 (0.00)**
17-265	Control	6.43 (0.33)	7.7 (0.19)	7.81 (012)	6.43 (0.33)	7.70 (0.20)	7.80 (0.12)
	0.5 AmB	5.50 (0.47)	7.28 (0.06)	7.49 (0.04)	5.50 (0.47)	7.28 (0.06)	7.49 (0.04)
	0.5+0.5	4.55 (0.35)	**4.72 (0.2)**	**4.32 (1.43)**	4.55 (0.26)	**4.78 (0.03)**	**3.26 (0.14)**
	0.5+1	3.02 (0.96)	**2.65 (0.91)**	**2.29 (0.40)**	3.82 (0.68)	**2.75 (0.43)**	**1.42 (0.98)**
	0.5+2	**2.66 (0.53)**	**2.25 (0.23)**	**1.74 (0.55)**	**2.70 (0.00)**	**2.93 (0.08)**	**2.09 (0.74)**
	1 AmB	4.17 (0.19)	3.34 (0.49)	3.10 (0.00)	4.16 (0.18)	3.34 (0.49)	3.10 (0.00)
	1+0.25	2.96 (1.36)	2.38 (1.33)	**1.07 (1.52)**	3.02 (0.74)	2.67 (0.49)	2.10 (0.18)
	1+0.5	3.20 (0.98)	2.45 (0.51)	2.1 (0.72)	2.88 (0.82)	**1.23 (1.74)**	**0.53 (0.74)**
	1+1	2.61 (0.11)	1.37 (1.59)	1.73 (1.41)	**1.80 (0.00)**	**0.00 (0.00)**	**0.00 (0.00)**
17-267	Control	6.52 (0.16)	7.59 (0.15)	7.59 (0.23)	6.52 (0.16)	7.59 (0.15)	7.6 0(0.24)
	0.5 AmB	5.11 (0.21)	6.06 (0.12)	6.94 (0.57)	5.11 (0.21)	6.06 (0.13)	6.94 (0.57)
	0.5+0.5	4.46 (0.18)	**4.04 (0.40)**	**4.01 (0.15)**	4.25 (0.16)	**3.86 (0.16)**	**4.58 (0.48)**
	0.5+1	4.40 (0.14)	**3.73 (0.09)**	**3.69 (0.43)**	3.91 (0.02)	**3.36 (0.01)**	**2.39 (0.00)**
	0.5+2	**2.65 (0.35)**	**2.00 (0.25)**	**3.52 (0.00)**	**2.70 (0.14)**	**2.62 (0.52)**	**3.06 (0.00)**
	1 AmB	3.80 (0.14)	3.82 (0.44)	4.04 (0.19)	3.80 (0.14)	3.82 (0.43)	4.04 (0.18)
	1+0.25	3.05 (0.44)	2.73 (0.36)	2.79 (1.14)	2.94 (0.27)	3.56 (0.51)	3.31 (0.00)
	1+0.5	3.22 (0.40)	2.52 (0.84)	**1.39 (0.52)**	2.21 (0.50)	2.92 (1.10)	2.88 (0.10)
	1+1	2.39 (0.06)	**1.74 (1.02)**	**0.84 (1.18)**	**1.70 (0.70)**	**0.00 (0.00)**	**0.00 (0.00)**

AmB: amphotericin B; ECH: echinocandin; ANF: anidulafungin; CSP: caspofungin.

2.2. Isavuconazole plus echinocandins

2.2.1. Checkerboard assays and analysis

Checkerboard experiments showed that neither isavuconazole nor the echinocandins monotherapy at the concentrations tested were able to stop completely fungal growth, expressed as an absorbance value close to 0%. Isavuconazole had a higher potency than echinocandins, as it reached a 50% reduction in the absorbance value at concentrations 0.06-0.125 mg/L, whereas echinocandins needed the highest concentrations tested (1-2 mg/L) to reach that threshold. Conversely, absorbance values close to 0% were reached with combinations that included ≥ 0.125 mg/L of isavuconazole plus ≥ 0.5 mg/L of echinocandins.

FICI results and the interaction parameters obtained from Greco and Bliss analysis for all *C. auris* isolates and drug combinations are summarized in Table 11. The determination of the FICI showed synergism for the three isavuconazole-echinocandin combinations against all isolates.

On the other hand, synergistic interactions were found by the Greco model in 5 out of 6 clinical isolates for the combination of isavuconazole and micafungin, in 3 out of 6 for the combination of isavuconazole and anidulafungin and in 2 out of 6 for the combination of isavuconazole and caspofungin. For the remaining isolates, the tested combinations were classified as additive, with a clear trend towards synergism, as shown by the 95% CI. GOF plots shown in Figure 29 for a representative isolate, revealed the concentrations for which the model-predicted effect (% absorbance) deviated from the experimental data. In general, the fitted response surface followed the same pattern as the experimental data and no systematic deviation of the model was detected in the residual plots. However, the model deviated from the data at higher absorbance values, which corresponded to either echinocandin monotherapy or combinations with low concentrations of both drugs. GOF plots for the rest of isolates are shown in Annex II.

As depicted in Figure 30, the IC_{50} obtained when fitting the Greco model to the experimental data was significantly higher for caspofungin than for anidulafungin or micafungin (p<0.001).

Table 11. Fractional Inhibitory Concentration Index (FICI) and interaction parameters determined by Greco model (α) and Bliss model (ΣSYN_ANT). Synergic interactions according to FICI and Greco model are underlined.

C. auris	ISV + ANF			ISV + CSP			ISV + MCF		
	FICI Median (Range)	Greco α (95 % CI)	Bliss ΣSYN_ANT (ΣSYN; ΣANT)	FICI Median (Range)	Greco α (95 % CI)	Bliss ΣSYN_ANT (ΣSYN; ΣANT)	FICI Median (Range)	Greco α (95 % CI)	Bliss ΣSYN_ANT (ΣSYN; ΣANT)
17-257	0.27 (0.24-0.30)	151 (16.53-285.5)	86.91 (87.22; -0.31)	0.26 (0.25-0.52)	38.59 (-8.106-85.28)	36.56 (41.22; -4.66)	0.24 (0.15-0.38)	112.8 (22.70-202.9)	66.01 (66.79; -0.78)
17-259	0.36 (0.25-0.49)	21.7 (5.105-38.38)	29.24 (30.27; -1.03)	0.37 (0.36-1.25)	22.23 (1.016-43.44)	11.44 (20.75; -8.56)	0.15 (0.13-0.25)	216.7 (11.37-422.0)	57.59 (59.49; -1.90)
17-261	0.19 (0.015-0.19)	102.1 (4.056-200.1)	57.38 (57.73; -0.35)	0.25 (0.08-0.5)	42.64 (-14.72-100.00)	40.67 (45.46; -4.79)	0.37 (0.15-0.49)	57.88 (0.85-114.9)	50.88 (53.70; -2.82)
17-263	0.18 (0.09-0.18)	186.9 (-3.962-377.8)	73.23 (73.32; -0.09)	0.25 (0.18-0.37)	114.4 (-1.911-230.6)	75.71 (75.89; -0.18)	0.16 (0.08-0.38)	674.4 (-138.3-1487)	111.56 (112.09; -0.53)
17-265	0.18 (0.15-0.37)	48.71 (-15.71-113.1)	72.8 (75.17; -2.37)	0.38 (0.25-0.49)	37.12 (2.344-71.90)	60.31 (60.64; -0.33)	0.14 (0.12-0.15)	175.1 (14.32-335.8)	80.14 (80.37; -0.23)
17-267	0.25 (0.14-0.36)	204.1 (-5.106-413.9)	69.61 (69.63; -0.02)	0.36 (0.25-0.38)	41.85 (-1.016-84.71)	46.37 (48.08; -1.71)	0.25 (0.13-0.49)	95.66 (24.84-166.5)	71.35 (71.72; -0.37)
Median	0.22	-	71.205	0.31	-	43.52	0.2	-	68.68

ΣSYN_ANT: total sum of synergic and antagonistic interactions. ΣSYN: sum of synergic interactions. ΣANT: sum of antagonistic interactions. ISV: isavuconazole. ANF: anidulafungin. CSP: caspofungin. MCF: micafungin.

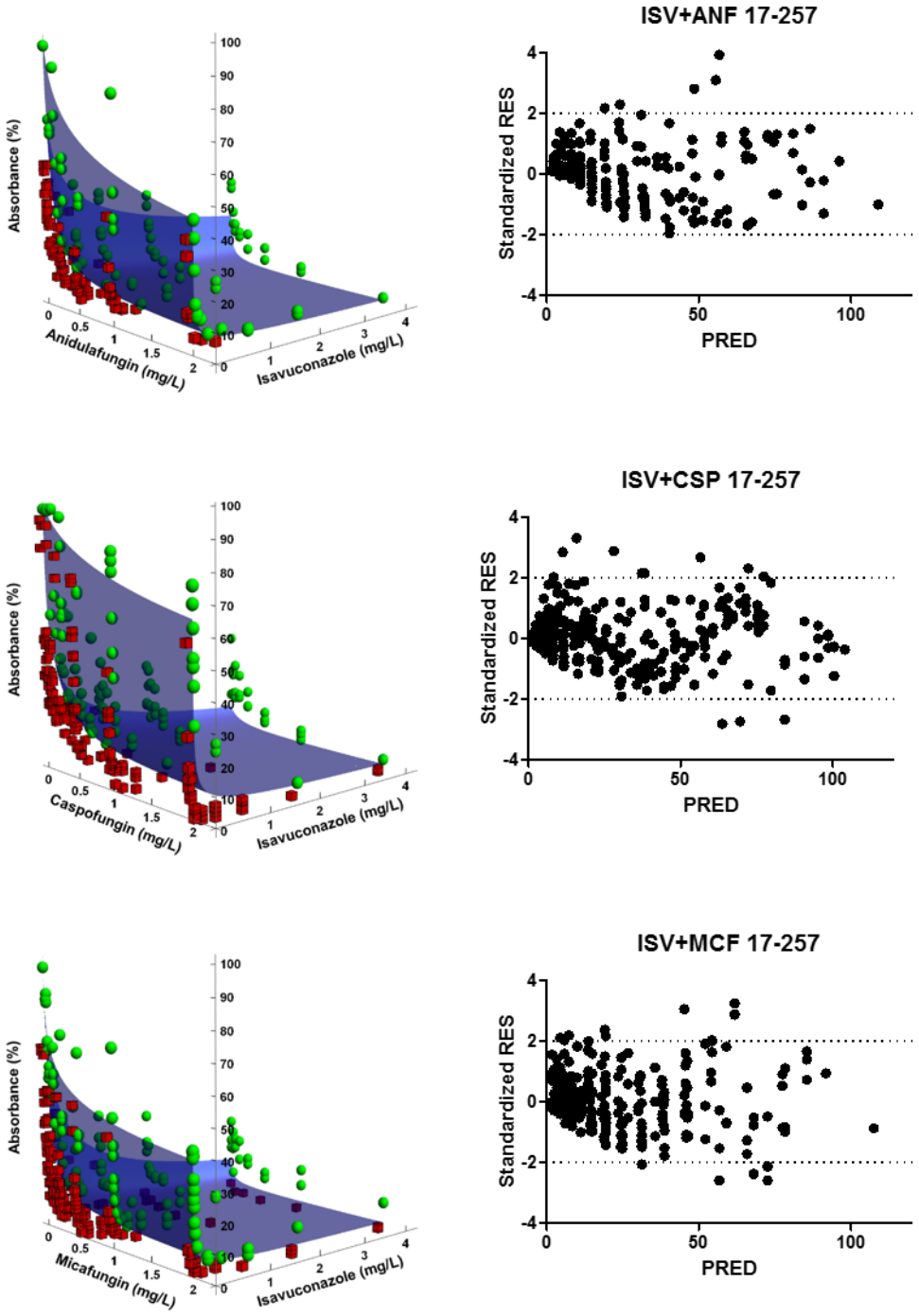

Figure 29. Goodness-of-fit plots of the Greco model for the combination of isavuconazole and anidulafungin, caspofungin or micafungin against *C. auris* 17-257. Left: The blue surface represents model predictions, the green spheres represent observations above the fitted surface and the red spheres represent observations below the fitted surface. Right: Standardized residuals (Standardized RES) versus predictions (PRED). ISV: isavuconazole. ANF: anidulafungin. CSP: caspofungin. MCF: micafungin.

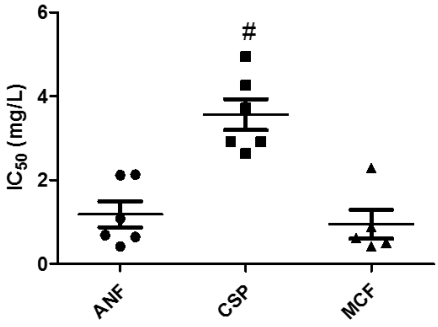

Figure 30. IC_{50} values determined by Greco model for each clinical strain. Mean and standard errors are plotted (#p<0.001 compared to ANF and MCF). ANF: anidulafungin. CSP: caspofungin. MCF: micafungin.

The summary parameter values of the Bliss independence based model, ΣSYN_ANT, showed weak synergistic interactions (values below 100%) for all combinations and isolates, except for isavuconazole and micafungin against *C. auris* 17-265 (Table 11). Both response surface methods, Greco and Bliss, were in concordance. An exception was isolate 17-259, as the combination of isavuconazole with anidulafungin or caspofungin was classified as synergistic with Greco model, but ΣSYN_ANT values were low (29.44 and 11.44 %, respectively) and the distribution matrix showed a scarce number of synergic combinations. The median ΣSYN_ANT for combinations with caspofungin was lower than the ones for anidulafungin and micafungin (Table 11), but the difference was not statistically significant. Checkerboard results and Bliss analysis also revealed that both synergy and a low absorbance value effect were achieved with the combination consisting of low isavuconazole concentration (0.125 mg/L) and higher of echinocandins (≥ 0.5 mg/L). The surface response according to Bliss method of a representative isolate for each drug combination in an 8x12-checkerboard design is depicted in Figure 31. A synergistic distribution and the degree of synergism are represented by the coloured area. Surface response graphs and matrix for the rest of the isolates are provided in Annex II.

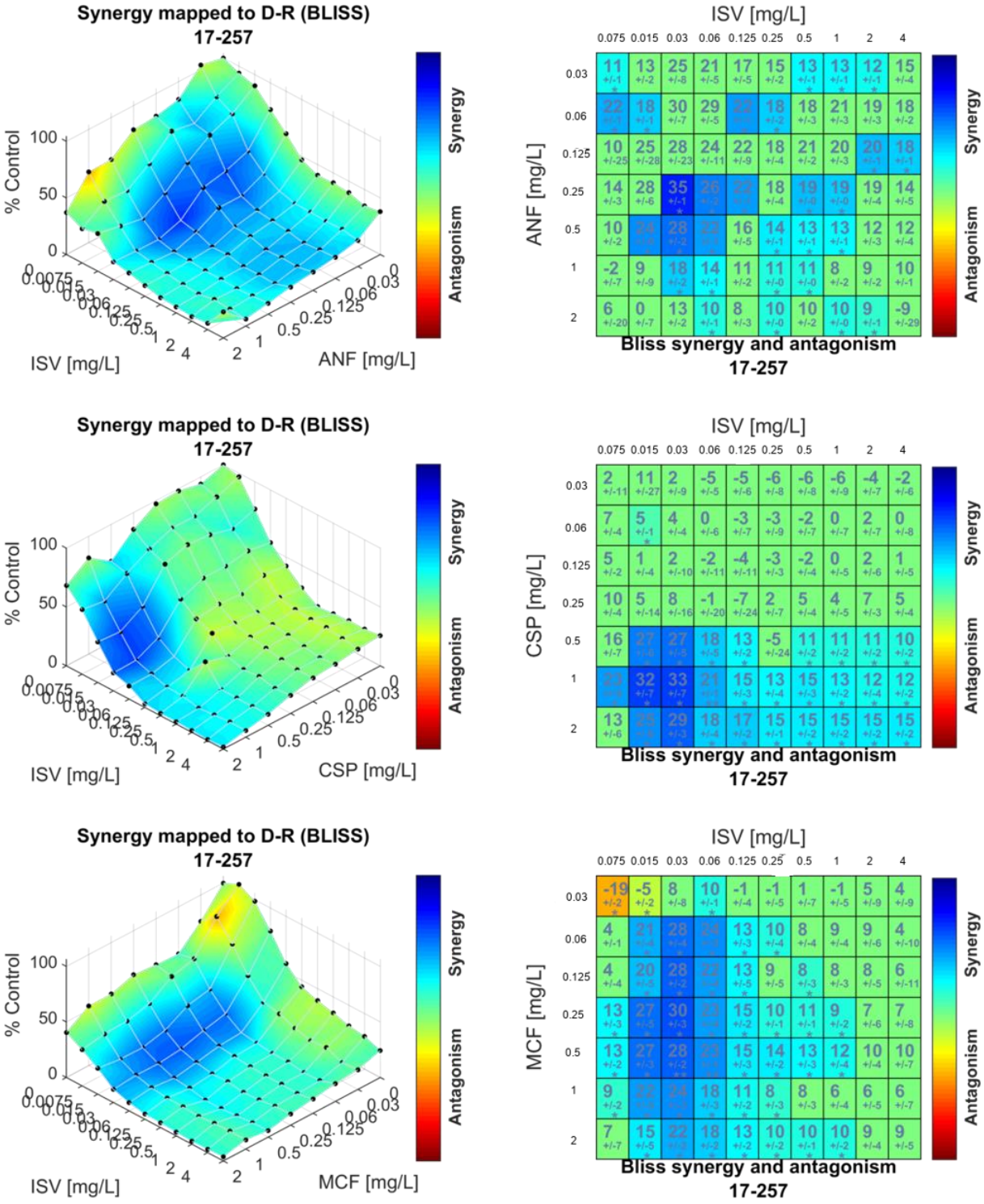

Figure 31. Synergy distribution determined by Bliss interaction model for the combination of isavuconazole (ISV) and anidulafungin (ANF), caspofungin (CSP) or micafungin (MCF) against *C. auris* 17-257. Left: Synergy distribution mapped to dose-response surface. Right: Matrix synergy plot with synergy scores for each combination.

2.2.2. Time-kill procedures

Mean time-kill curves for isavuconazole and echinocandins, alone and in combination, are provided in Figure 32. Drug monotherapies did not achieve significant antifungal activity, as observed in the plots and demonstrated by the positive k values (0.01-0.05 h^{-1}). Conversely, synergism and fungistatic activity were achieved with combinations that included concentrations of isavuconazole ≥ 0.125 mg/L and echinocandin ≥ 1 mg/L, showing similar profiles of antifungal activity over time for all three azole-echinocandin combinations.

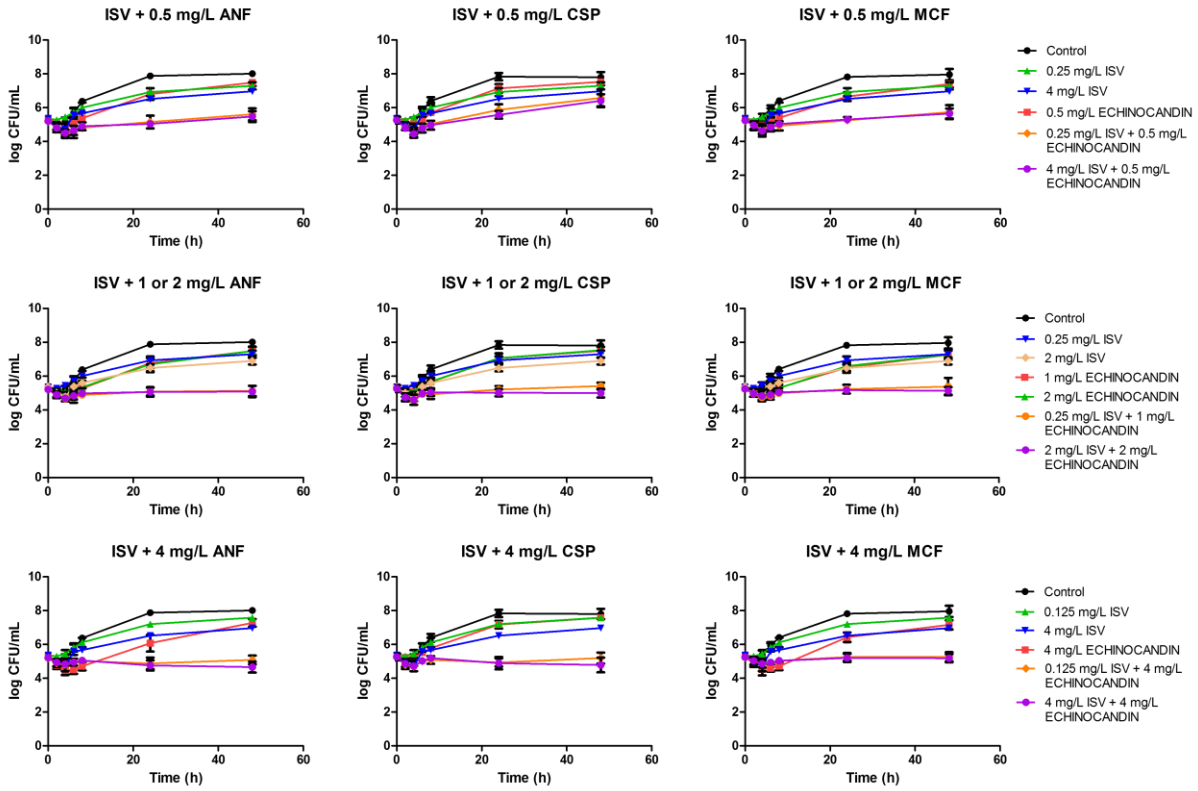

Figure 32. Mean time-kill curves for isavuconazole (ISV) in combination with anidulafungin (ANF), caspofungin (CSP) or micafungin (MCF) against *C. auris*. Each data point represents the mean result ± standard deviation (error bars) of the six isolates and replicates.

Although the activity of isavuconazole plus 0.5 mg/L of anidulafungin or micafungin was not fungistatic according to the established definition, the regression analysis of the curves revealed that the killing-rate constant of those drug combinations was not significantly different from a zero slope, indicating a lack of fungal growth through 48 h. That was not the case for the combinations with 0.5 mg/L of caspofungin, as it did not result in a significant reduction in

fungal growth (positive k value of 0.02 h^{-1}). This result correlates with the aforementioned Greco analysis that pointed out a lower potency for this echinocandin. Combinations that included concentrations of echinocandin ≥ 1 mg/L also yielded curves with a killing rate constant non-different from zero, indicating that, once the fungistatic effect was achieved, increasing drug concentrations for both agents did not result in a significant reduction in fungal count over time.

3. PK/PD modelling and simulation of antifungal activity

3.1. PK/PD modelling and simulation of the in vitro activity of amphotericin B

3.1.1. Final PK/PD model results

The developed model was able to describe successfully the effect of amphotericin B against the studied *C. auris* clinical isolates. This model could characterise the initial and higher killing rate at the higher amphotericin B concentrations, 2 and 4 mg/L, as well as the biphasic trend or regrowth observed in most experiments with the concentration of 1 mg/L.

The final model consisted in a semi-mechanistic model that included two fungal stages, a drug-susceptible fungal subpopulation (S) and a drug-resistant subpopulation (R), with a transfer rate constant from S to R (Figure 33). The differential equations that defined both subpopulations were as follows:

$$dS/dt = k_{growthS} \times S \times (1-e^{-\alpha t}) - \text{Drug effect} \times S - k_{deathS} \times S - k_{SR} \times S \quad \text{(Eq. 35)}$$

$$dR/dt = k_{growthR} \times R + k_{SR} \times S \quad \text{(Eq. 36)}$$

It was not possible a simultaneous estimation of both $k_{growthS}$ and k_{deathS} in this experimental setting. Hence, in an initial fit, $k_{growthS}$ was estimated by fitting both the single-stage model (Eq. 20) and the two-stage model (Eq. 35 and 36) to the control data. $k_{growthS}$ estimation was similar in both models (0.118 and 0.186 h^{-1}) and k_{deathS} was then fixed to a value 10 times lower (0.01 h^{-1}) for final parameter estimation. A specific k_{growth} was calculated for the R subpopulation ($k_{growthR}$) to account for the regrowth observed at certain concentrations between 24 to 48 h. A k_{deathR} parameter 10 times lower than the $k_{growthR}$ was considered negligible.

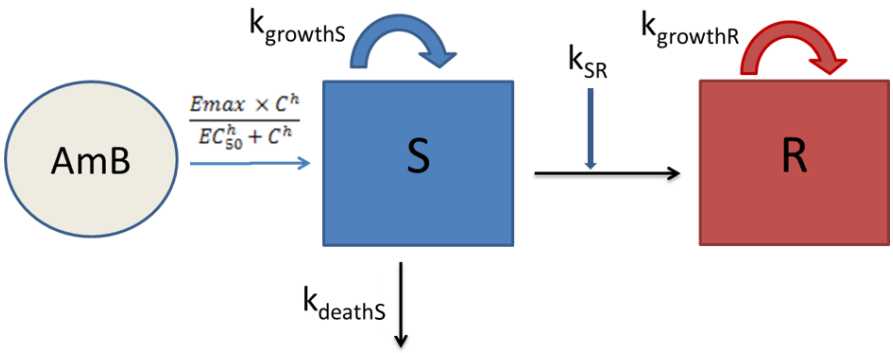

Figure 33. Schematic representation of the final PK/PD model for amphotericin B against *C. auris*. The total fungal population consists of two different subpopulations (S+R), with a first-rate order constant (k_{SR}) that describes the transfer of fungal cells from a susceptible state (S) to a resistant one (R). Amphotericin B (AmB) exerts its effect on the susceptible subpopulation. $k_{growthS}$: growth rate of susceptible subpopulation; $k_{growthR}$: growth rate of resistant subpopulation. k_{deathS}: death-rate constant of the susceptible subpopulation.

Final model parameters and the standard error of the estimates, alongside bootstrap estimations are presented in Table 12. Considering the standard errors and the bootstrap results, the parameters of the model were properly estimated. *Candida* related parameters were $k_{growthS}$ and k_{deathS} for S subpopulation (0.111 h^{-1} and 0.01 h^{-1}, respectively) and $k_{growthR}$ for R subpopulation (0.01 h^{-1}). k_{deathS} an $k_{growthR}$ were fixed whereas $k_{growthS}$ was allowed to be estimated. When the model incorporated different values of α (delay in growth) for the absence or presence of the drug, a better fit was achieved. A modified E_{max} sigmoidal model best described the effect of the drug; E_{max} was equal to 0.784 h^{-1} and EC_{50} was equal to 1.88 mg/L (1.88 times higher than the MIC). Hill factor was fixed to allow the model to correctly estimate the PD parameters. Variability in the response was best captured by IOV on EC_{50} rather than IIV, where each occasion was defined as each prepared batch of microtitre plates (4 in total). GOF plots and VPCs that show adequate model fit are shown in Figures 34, 35 and 36.

Table 12. Parameter estimates (typical values and standard error –SEE– as CV %), bootstrap estimates (mean and 95% CI) and relative bias (%) of the PK/PD model.

Parameter	Description	Model estimate and SEE (CV %)	Bootstrap median estimate (95% CI)	Relative bias (%)
$k_{growthS}$ (h^{-1})	Fungal growth rate constant of the S subpopulation	0.111 (3%)	0.111 (0.101-0.116)	0
$k_{growthR}$ (h^{-1})	Fungal growth rate constant of the R subpopulation	0.01 (fixed)	-	-
k_{death} (h^{-1})	Fungal death rate constant	0.01 (fixed)	-	-
E_{max} (h^{-1})	Maximum kill rate constant of amphotericin B	0.784 (12%)	0.795 (0.635-1.04)	1.4
EC_{50} (mg/L)	Concentration of amphotericin B at which 50% of the E_{max} is achieved	1.88 (3%)	1.89 (1.78-2.05)	0.53
h	Hill factor that that modifies the steepness of the slope and smoothens the curve	4 (fixed)	-	-
α (control)	Delay in fungal growth in the absence of drug	0.748 (3%)	0.754 (0.664-0.882)	0.8
α (drug)	Delay in fungal growth in the presence of drug	0.231 (10%)	0.233 (0.193-0.274)	0.74
N_{max} (log CFU/mL)	Maximum fungal density	7.66 (1%)	7.67 (7.49-7.85)	0.13
σ (log CFU/mL)	Residual error	0.271 (14%)	0.261 (0.189-0.329)	-3.69
π_1 (%CV)	Occasion 1	0 (fixed)	-	-
π_2 (%CV)	Occasion 2	9.5 (35%)	9.46 (2.52-15.98)	-0.42
π_3 (%CV)	Occasion 3	18.4 (24%)	18.36 (9.92-28.12)	-0.22
π_4 (%CV)	Occasion 4	7.5 (37%)	7.03 (2.68-12.28)	-6.27

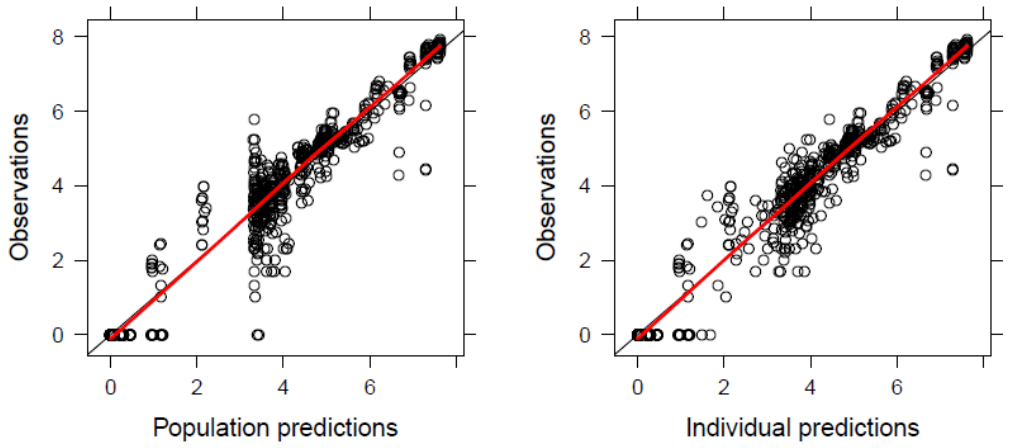

Figure 34. Observed fungal counts (log CFU/mL) versus population predictions (left) or individual predictions (right). The red lines are the trend in the observations

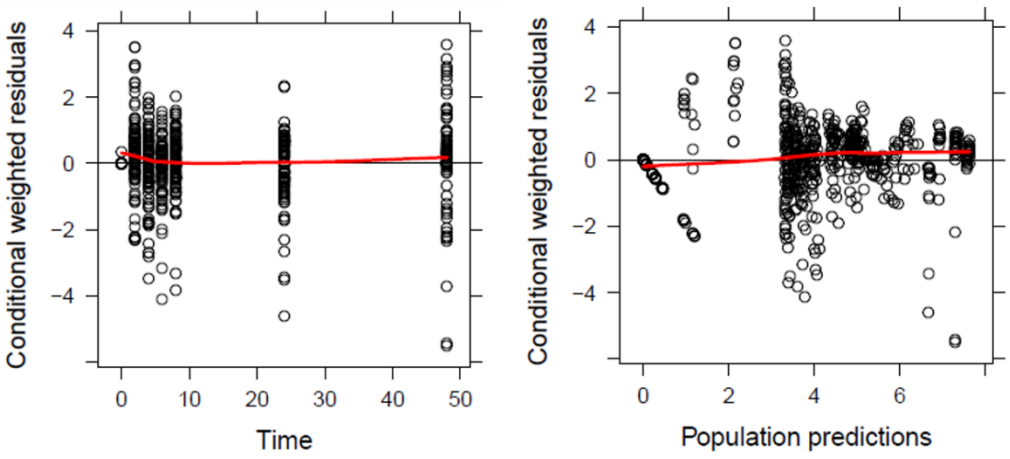

Figure 35. Conditional weighted residuals (CWRES) against time (h) (left) or population predictions (right). The red lines are the trend in the observations.

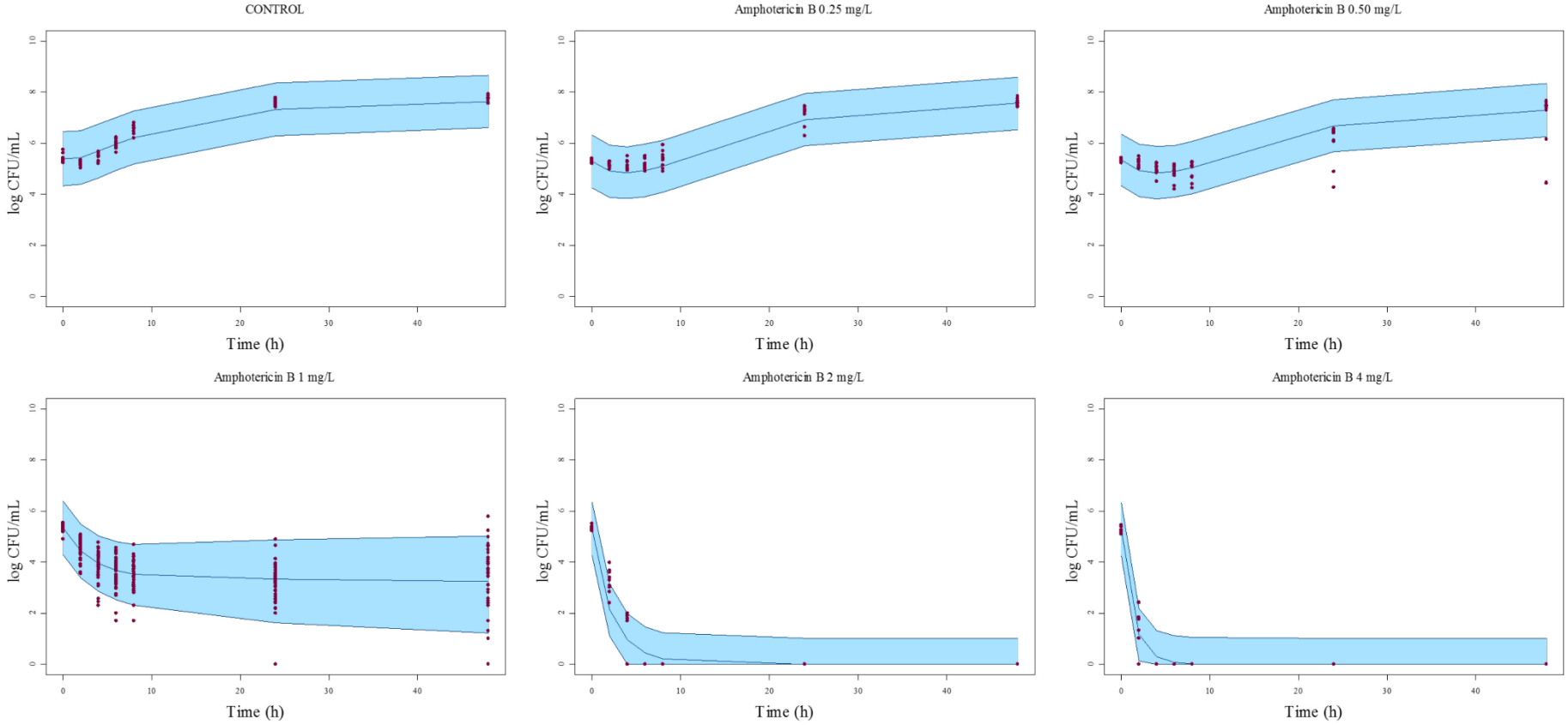

Figure 36. Visual predictive check (VPC) for the final model, with the observed fungal counts (full circles), the mean prediction (solid line) and 95% model prediction interval (shaded area) of the simulations

3.1.2. PK/PD simulations of amphotericin B treatment

The expected time-kill curves for different doses of amphotericin B were simulated by using using the human PK parameters and accounting for protein binding. The simulated total and unbound concentrations of amphotericin B for standard intravenous dosing regimens of 0.6 and 1 mg/kg/day and the alternative 1.5 mg/kg/day and their expected activity on *C. auris* over a one-week treatment are shown in Figure 37. None of the simulated standard dosing scenarios showed successful activity against *C. auris*.

Additional simulations with MIC scenarios ranging from 0.06 to 0.5 mg/L were performed for a 1-week period (Figure 38). Simulations with the lowest dose, 0.6 mg/kg/day, showed that a fungistatic activity would be achieved at the 5th day of treatment for MIC values of amphotericin B of 0.06 mg/L. The next simulated dose, 1 mg/kg/day, resulted in fungicidal activity from the second day onwards, and fungistatic with the first administration. Finally, the highest dose of 1.5 mg/kg/day led to a fungicidal endpoint achievement immediately after the first administration. Furthermore, for a MIC of 0.125 mg/L, a fungistatic effect would be reached at the 3rd day, and fungicidal at the 5th day at this highest dose level.

.

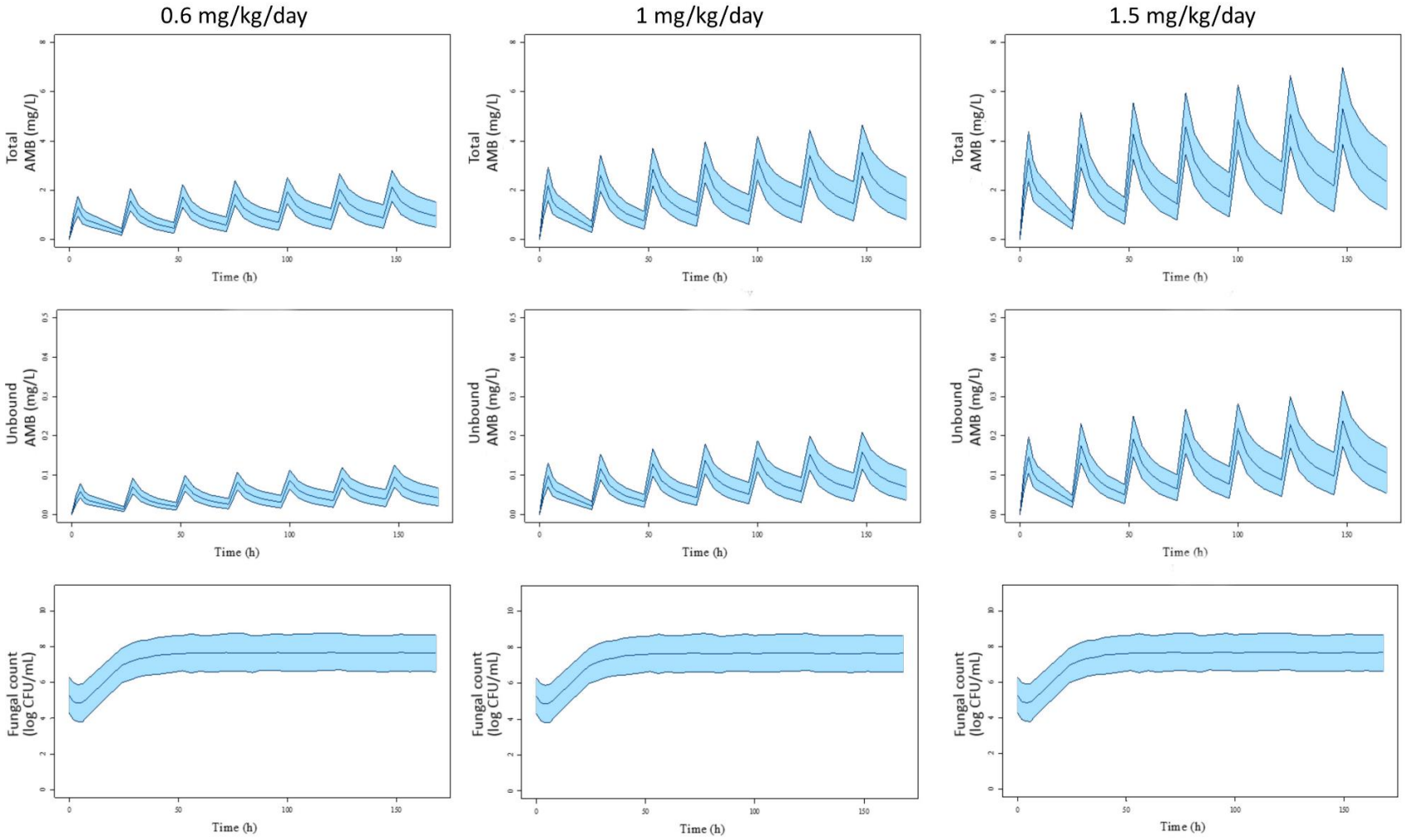

Figure 37. Predicted total (top row) and unbound (mid row) plasma concentrations of amphotericin B (AMB) and the effect on fungal burden (bottom row) for each treatment (columns). The mean (solid line) and 95% prediction interval (coloured space) are represented.

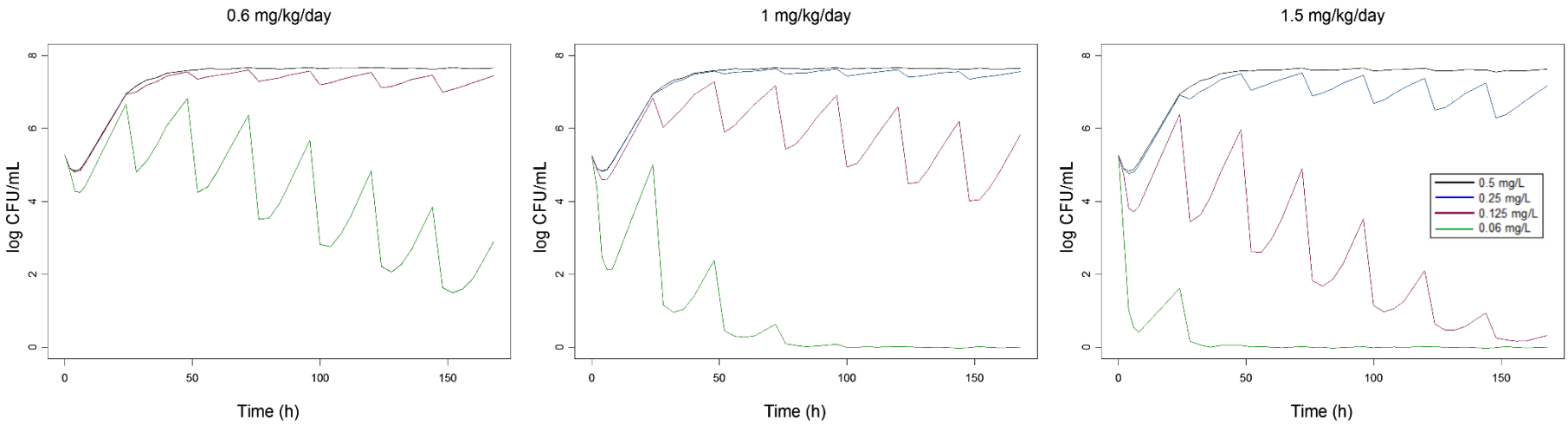

Figure 38. Simulations of the effect of amphotericin B on fungal burden by MIC and dosing regimen. Black line: MIC of 0.5 mg/L; blue line: MIC of 0.25 mg/L; purple line: MIC of 0.125 mg/L; green line: MIC of 0.06 mg/L.

3.2. PK/PD modelling and simulation of the in vitro activity of the combinations of isavuconazole with echinocandins

3.2.1. Final PK/PD model results

-Additional time-kill curves

In order to obtain enough information about the concentration-effect relationship for model building, additional time-kill curve experiments were conducted. Based on previous results, the combinations of 0.06 mg/L of isavuconazole plus 0.125 mg/L of anidulafungin/caspofungin were examined. The results are summarized and compared to the control and the rest of combinations in Figure 39. The incorporation of this additional dose combination to the analysis allowed a better estimation of the EC_{50} parameter, as the E_{max} was fairly enough determined from the remaining combinations.

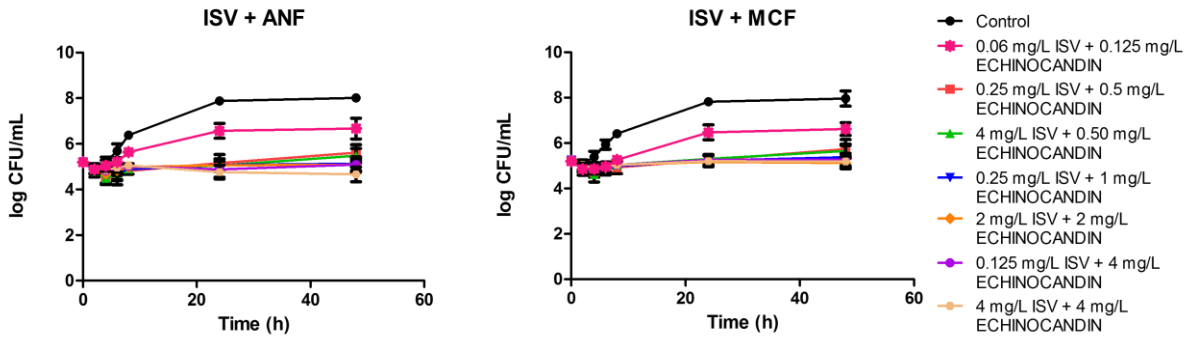

Figure 39. Mean time-kill curves for isavuconazole (ISV) in combination with anidulafungin (ANF) or micafungin (MCF) against *C. auris*. Each data point represents the mean result ± standard deviation (error bars) of the six isolates and replicates.

-Monotherapy modelling

As a previous step to the modelling of combination therapy, each drug in monotherapy was modelled first, obtaining information regarding the best structural model and initial parameter estimates. A single-population model defined by the following equation best captured the activity of isavuconazole and the echinocandins alone:

$$\frac{dN}{dt} = \left[k_{growth}\left(1-\frac{N}{N_{max}}\right)x\,(1-e^{-\alpha t}) - \frac{E_{max}xC^h}{EC_{50}^h+C^h}\right]\times N \qquad \text{(Eq. 37)}$$

where dN/dt is the change in the number of *Candida* cells as a function of time, k_{growth} is the growth rate constant (h^{-1}) of *Candida*, N is the number of viable cells (log CFU/mL), N_{max} is the maximum total density of fungal population in the stationary phase (log CFU/mL) and α accounts for the delay in growth observed due to experimental settings. E_{max} is the maximum effect produced by the drug (h^{-1}), C is drug concentration at time t (mg/L), EC_{50} is the concentration of the drug necessary to achieve half the maximum effect (mg/L) and h is the Hill factor, which modifies the steepness of the slope and smoothens the concentration-effect curve. Final model parameters and the standard error of the estimates are presented in Table 12. As expected from the experimental data, E_{max} values were low for all drugs. Hill factor had to be fixed for the echinocandins for a proper estimation of the PD parameters. A better fit was obtained for anidulafungin and micafungin if different α values were estimated for the absence or presence of drug. Conversely, inclusion of IIV or IOV did not improve model fit. GOF plots that show adequate model fit are provided in Figure 40. A slight trend to overestimate the effect of caspofungin at 8 h could be observed (Figure 40 c). Nevertheless, an overall adequate model fit was concluded from the GOF plots. VPCs for each drug are shown in Annex III.

Table 13. Parameter estimates for each drug: typical values and standard errors (as CV %).

Parameter	Description	ISV	ANF	CSP	MCF
k_{growth} (h^{-1})	Fungal growth rate constant	0.129 (fixed)	0.126 (fixed)	0.117 (fixed)	0.126 (fixed)
E_{max} (h^{-1})	Maximum kill rate constant of the drug	0.027 (1%)	0.0156 (8%)	0.0099 (9%)	0.0177 (7%)
EC_{50} (mg/L)	Concentration of drug at which 50% of the E_{max} is achieved	0.364 (14%)	0.435 (20%)	0.221 (4%)	0.242 (35%)
h	Hill factor that that modifies the steepness of the slope and smoothens the curve	0.468 (10%)	1 (fixed)	5 (fixed)	1 (fixed)
α (control)	Delay in fungal growth in the absence of drug	0.214[a] (9%)	0.232 (6%)	0.127[a] (3%)	0.161 (17%)
α (drug)	Delay in fungal growth in the presence of drug	-[a]	0.0596 (13%)	-[a]	0.0671 (8%)
N_{max} (log CFU/mL)	Maximum fungal density	8.04 (0%)	8.03 (0%)	8.19 (0%)	8.18 (1%)
σ (log CFU/mL)	Residual error	0.0584 (3%)	0.0791 (3%)	0.0491 (6%)	0.0938 (14%)

ISV: isavuconazole. ANF: anidulafungin. CSP: caspofungin. MCF: micafungin. [a]Single α parameter for both control and drug data.

a)

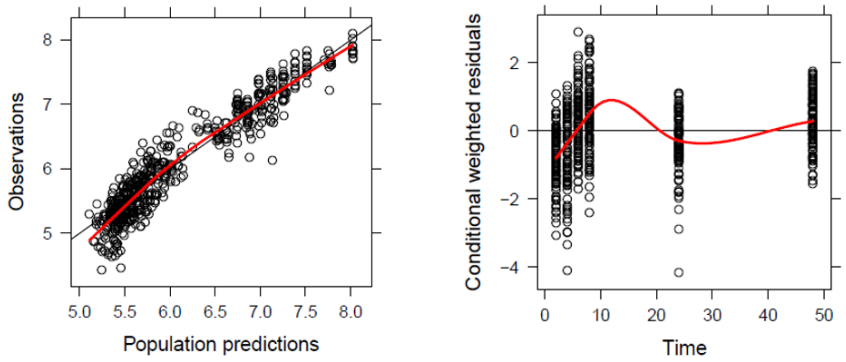

b)

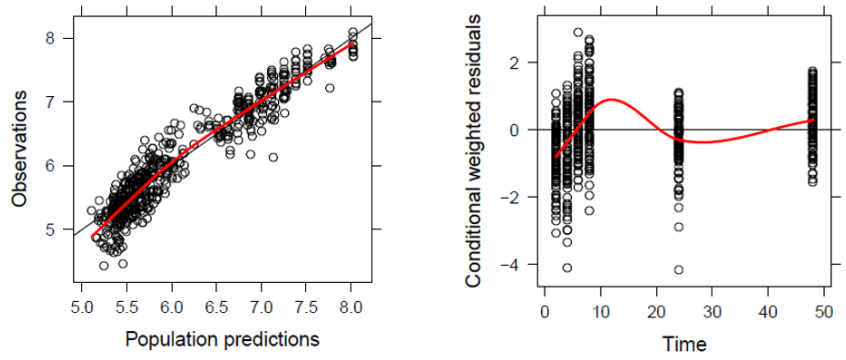

c)

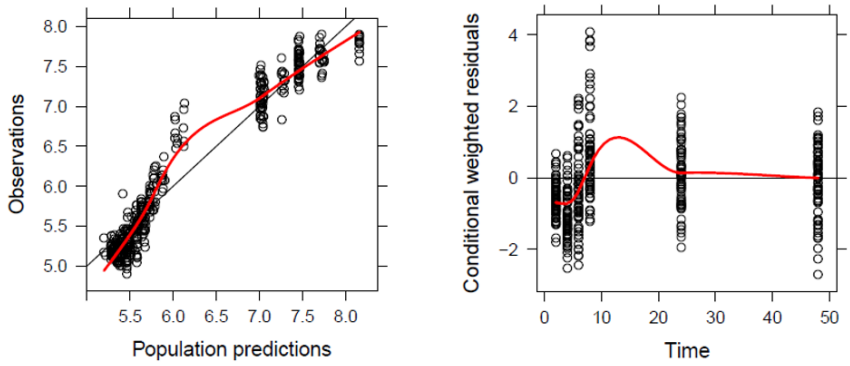

d)

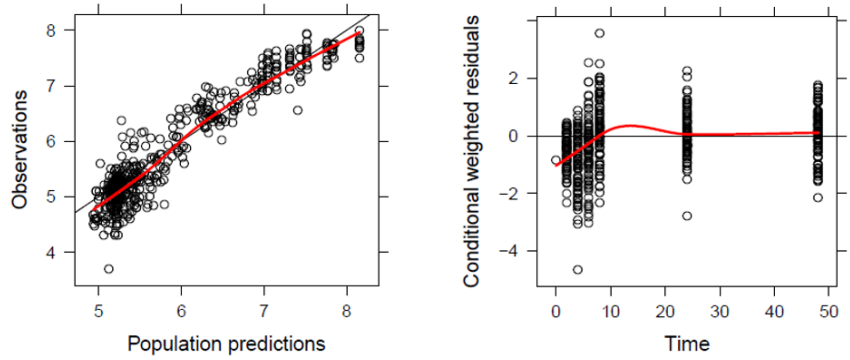

Figure 40. Observed fungal counts (log CFU/mL) vs population predictions (left) and conditional weighted residuals (CWRES) over time (right) plots for a) isavuconazole, b) anidulafungin, c) caspofungin and d) micafungin. The red lines are smooth lines showing the trend in the observations.

-PK/PD model for combination therapy

The best structural model that fitted all isavuconazole plus echinocandin combinations was defined by Equation 29 (already described in Materials and Methods section):

$$\frac{dN}{dt} = \left[k_{growth}\left(1-\frac{N}{N_{max}}\right) x\,(1-e^{-\alpha t}) - "combined\ effect"\right] \times N \qquad \text{(Eq. 29)}$$

Candida related parameters (k_{growth}, N_{max}, α) have already been discussed in the previous monotherapy subsection, whereas Equation 32 defined the "combined effect":

$$\text{Combined effect} = EFF_{ISV}\, x\left(1+\frac{EFF_{CANDIN}}{EFF_{CANDIN}+EFF_{ISV}}\right)^{Int} + EFF_{CANDIN}\, x\left(1+\frac{EFF_{ISV}}{EFF_{ISV}+EFF_{CANDIN}}\right)^{Int} \qquad \text{(Eq. 32)}$$

where EFF_{ISV} and EFF_{CANDIN} are the effect exerted by isavuconazole and the echinocandins, respectively, defined as an E_{max} sigmoidal effect (Equation 21) and *Int* is the parameter that reflects the drug-drug interaction.

Final model parameters and the standard error of the estimates, alongside bootstrap estimations for every combination are presented in Table 14, 15 and 16. Model parameters in the three combinations were estimated with RSE <20% and with relative bias under 2%, indicating model stability and a proper estimation of parameters. The EC_{50} of isavuconazole was similar in the three combinations (0.0683, 0.0554 and 0.0584 mg/L for the combinations of isavuconazole with anidulafungin, caspofungin and micafungin, respectively). The EC_{50} of anidulafungin and micafungin were also similar (0.176 and 0.171 mg/L) whereas caspofungin EC_{50} was almost 3 times higher (0.452 mg/L). These parameter estimates mirror quite reasonably the empirical data; giving yet another prove of correct modelling. The interaction parameter *Int* was positive in every combination, which alongside a positive 95% CI allowed to classify the drug interactions as synergistic. As expected, this modelling outcome is consistent with the synergism described for the combinations of isavuconazole and echinocandins from checkerboard and time-kill data analysis (Results Section 2.2). A single α was defined in each combination, as the estimation of different values for the absence or presence of drug did not improve the model fit. Additionally, similar to the analysis of single-agent activity, neither the inclusion of IIV nor IOV improved the model fit, hence, those variabilities were absent from the final model. Thus, variability was solely defined by the

residual model, which was additive. GOF plots and VPCs that show adequate model fit are provided in Figures 41 to 44.

Table 14. Parameter estimates (typical values and standard error –SEE– as CV %), bootstrap estimates (mean and 95% CI) and relative bias (%) of the PK/PD model of isavuconazole + anidulafungin.

		ISV + ANF	
Parameter	**Description**	**Model estimate and SEE (CV %)**	**Bootstrap estimate median (95% CI) and relative bias [%]**
k_{growth} (h^{-1})	Fungal growth rate constant	0.158 (fixed)	-
E_{maxISV} (h^{-1})	Maximum kill rate constant of isavuconazole	0.0198 (0%)	0.0199 (0.0182-0.0210) [0.5%]
EC_{50ISV} (mg/L)	Concentration of isavuconazole at which 50% of the E_{maxISV} is achieved	0.0683 (5%)	0.0683 (0.0580-0.0799) [0%]
h_{ISV}	Hill factor for isavuconazole	1.58 (3%)	1.60 (1.15-2.05) [1.26%]
E_{maxANF} (h^{-1})	Maximum kill rate constant of anidulafungin	0.0272 (3%)	0.0270 (0.0250-0.0290) [-0.73%]
EC_{50ANF} (mg/L)	Concentration of anidulafungin at which 50% of the E_{maxANF} is achieved	0.176 (9%)	0.174 (0.148-0.215) [-1.36%]
h_{ANF}	Hill factor for anidulafungin	1 (fixed)	-
α	Delay in fungal growth	0.162 (4%)	0.162 (0.152-0.174) [0%]
N_{max} (log CFU/mL)	Maximum fungal density	8 (fixed)	-
Int	Interaction parameter	0.55 (13%)	0.56 (0.42-0.67) [1.81%]
σ (log CFU/mL)	Residual error	0.0906 (2%)	0.0897 (0.0849-0.0938) [-0.99%]

Table 15. Parameter estimates (typical values and standard error –SEE– as CV %), bootstrap estimates (mean and 95% CI) and relative bias (%) of the PK/PD model of isavuconazole + caspofungin.

		ISV + CSP	
Parameter	**Description**	**Model estimate and SEE (CV %)**	**Bootstrap estimate median (95% CI) and relative bias [%]**
k_{growth} (h^{-1})	Fungal growth rate constant	0.140 (fixed)	-
E_{maxISV} (h^{-1})	Maximum kill rate constant of isavuconazole	0.0168 (3%)	0.0168 (0.0160-0.0177) [0%]
EC_{50ISV} (mg/L)	Concentration of isavuconazole at which 50% of the E_{maxISV} is achieved	0.0554 (9%)	0.0558 (0.0469-0.0658) [0.72%]
h_{ISV}	Hill factor for isavuconazole	1.16 (11%)	1.16 (0.94-1.41) [0%]
E_{maxCSP} (h^{-1})	Maximum kill rate constant of caspofungin	0.0157 (6%)	0.0157 (0.0137-0.0174) [0%]
EC_{50CSP}(mg/L)	Concentration of caspofungin at which 50% of the E_{maxCSP} is achieved	0.452 (9%)	0.447 (0.376-0.534) [-1.11%]
h_{CSP}	Hill factor for caspofungin	1.37 (8%)	1.38 (1.23-1.63) [0.73 %]
α	Delay in fungal growth	0.161 (4%)	0.161 (0.148-0.178) [0%]
N_{max} (log CFU/mL)	Maximum fungal density	8 (fixed)	-
Int	Interaction parameter	1.14 (10%)	1.14 (0.93-1.39) [0%]
σ (log CFU/mL)	Residual error	0.0815 (3%)	0.0806 (0.0753-0.0855) [-1.10%]

Table 16. Parameter estimates (typical values and standard error –SEE– as CV %), bootstrap estimates (mean and 95% CI) and relative bias (%) of the PK/PD model of isavuconazole + micafungin.

		ISV + MCF	
Parameter	**Description**	**Model estimate and SEE (CV %)**	**Bootstrap estimate median (95% CI) and relative bias [%]**
k_{growth} (h^{-1})	Fungal growth rate constant	0.145 (fixed)	-
E_{maxISV} (h^{-1})	Maximum kill rate constant of isavuconazole	0.0176 (3%)	0.0176 (0.0164-0.0186) [0%]
EC_{50ISV} (mg/L)	Concentration of isavuconazole at which 50% of the E_{maxISV} is achieved	0.0511 (3%)	0.0515 (0.0476-543) [0.78%]
h_{ISV}	Hill factor for isavuconazole	1.12 (6%)	1.13 (0.95-1.33) [0.89%]
E_{maxMCF} (h^{-1})	Maximum kill rate constant of micafungin	0.025 (4%)	0.025 (0.023-0.027) [0%]
EC_{50MCF} (mg/L)	Concentration of micafungin at which 50% of the E_{maxMCF} is achieved	0.171 (9%)	0.171 (0.142-0.199) [0%]
h_{MCF}	Hill factor for micafungin	1 (fixed)	-
α	Delay in fungal growth	0.158 (4%)	0.158 (0.145-0.171) [0%]
N_{max} (log CFU/mL)	Maximum fungal density	8 (fixed)	-
Int	Interaction parameter	0.41 (18%)	0.41 (0.28-0.56) [0%]
σ (log CFU/mL)	Residual error	0.0828 (6%)	0.0819 (0.0720-0.0915) [-1.09%]

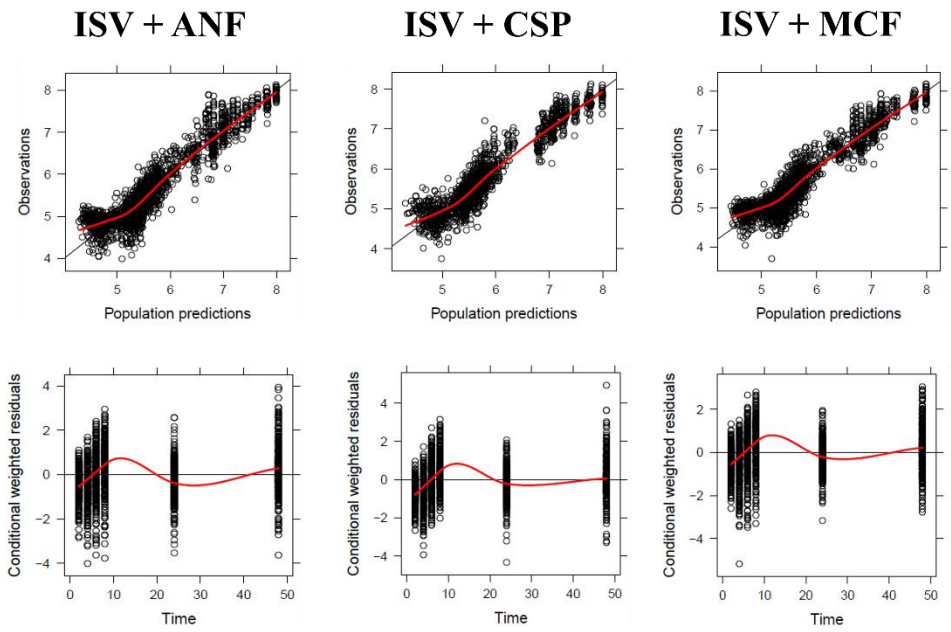

Figure 41. Observed fungal counts (log CFU/mL) vs population predictions (top) and conditional weighted residual (CWRES) over time (bottom) plots for isavuconazole + anidulafungin (ISV + ANF), isavuconazole + caspofungin (ISV + CSP) and isavuconazole + micafungin (ISV + MCF). The red lines are smooth lines showing the trend in the observations.

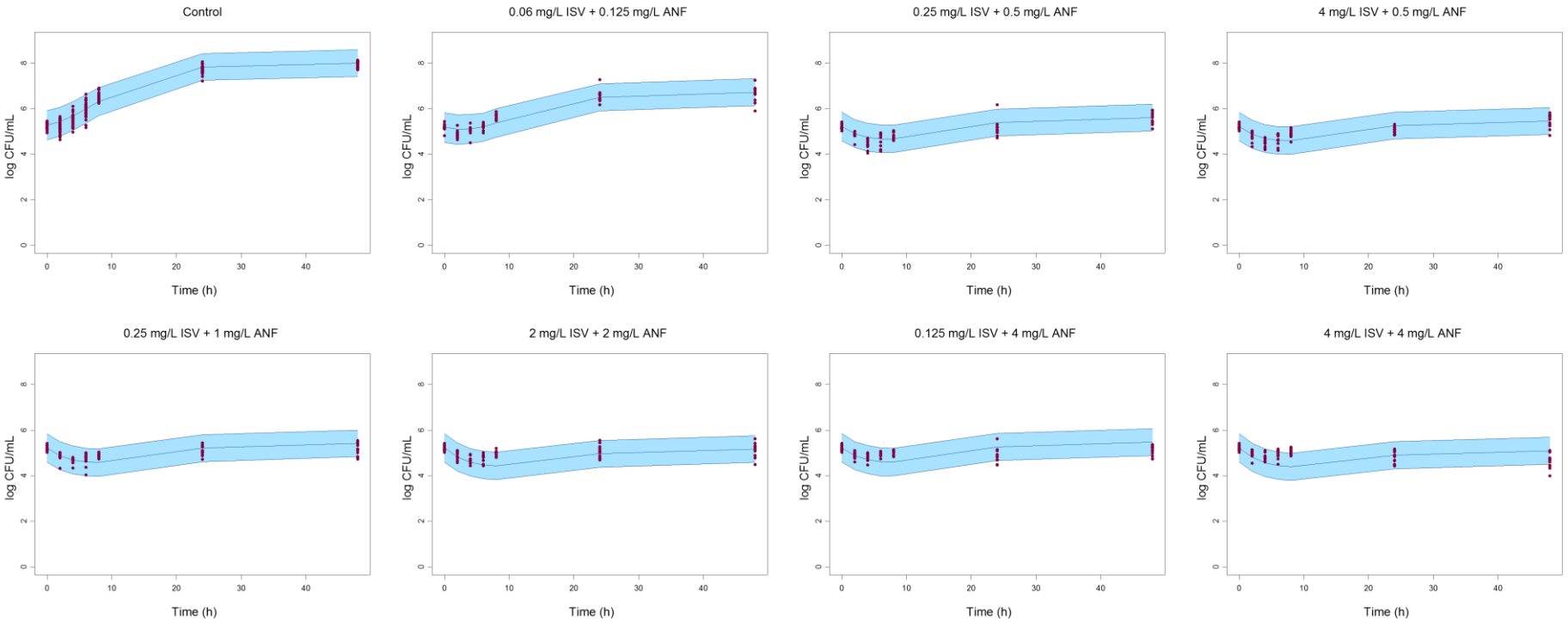

Figure 42. Visual predictive check (VPC) for the final model of isavuconazole + anidulafungin, with the observed fungal counts (full circles), the mean prediction (solid line) and 95% model prediction interval (shaded area) of the simulations.

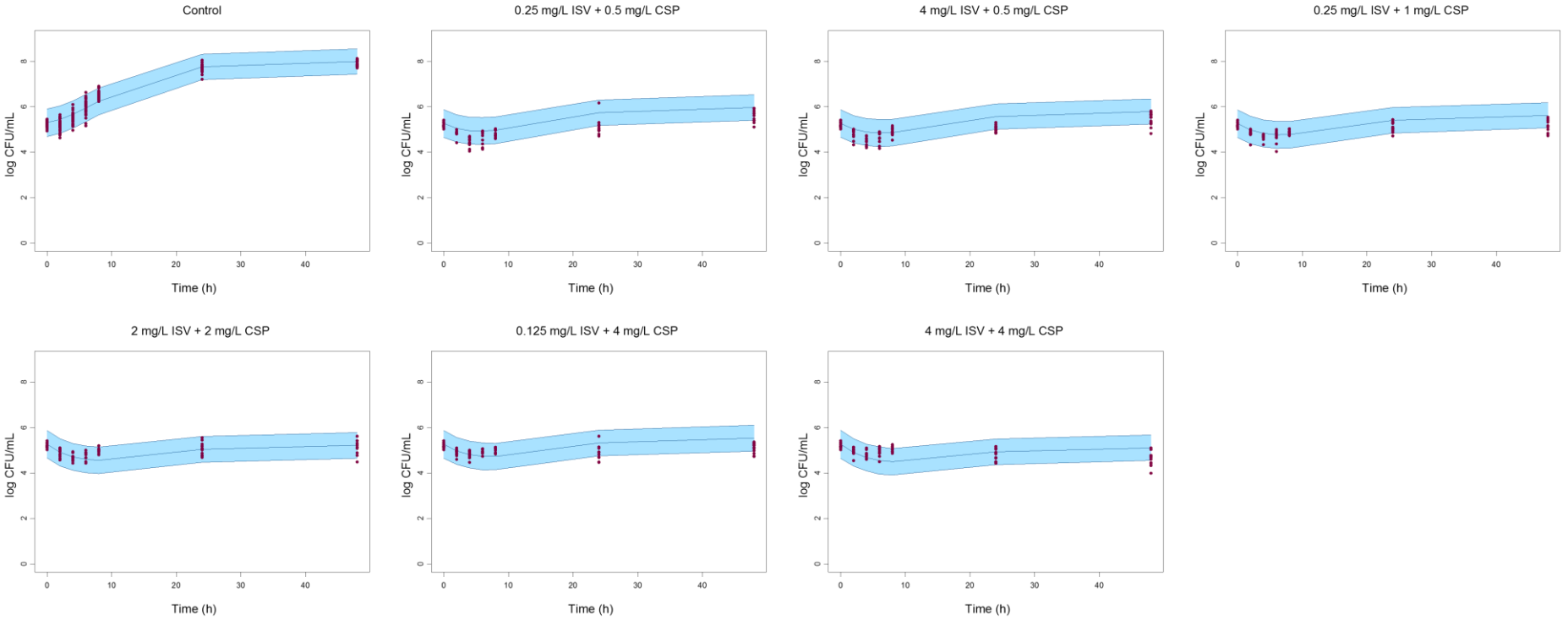

Figure 43. Visual predictive check (VPC) for the final model of isavuconazole + caspofungin, with the observed fungal counts (full circles), the mean prediction (solid line) and 95% model prediction interval (shaded area) of the simulations.

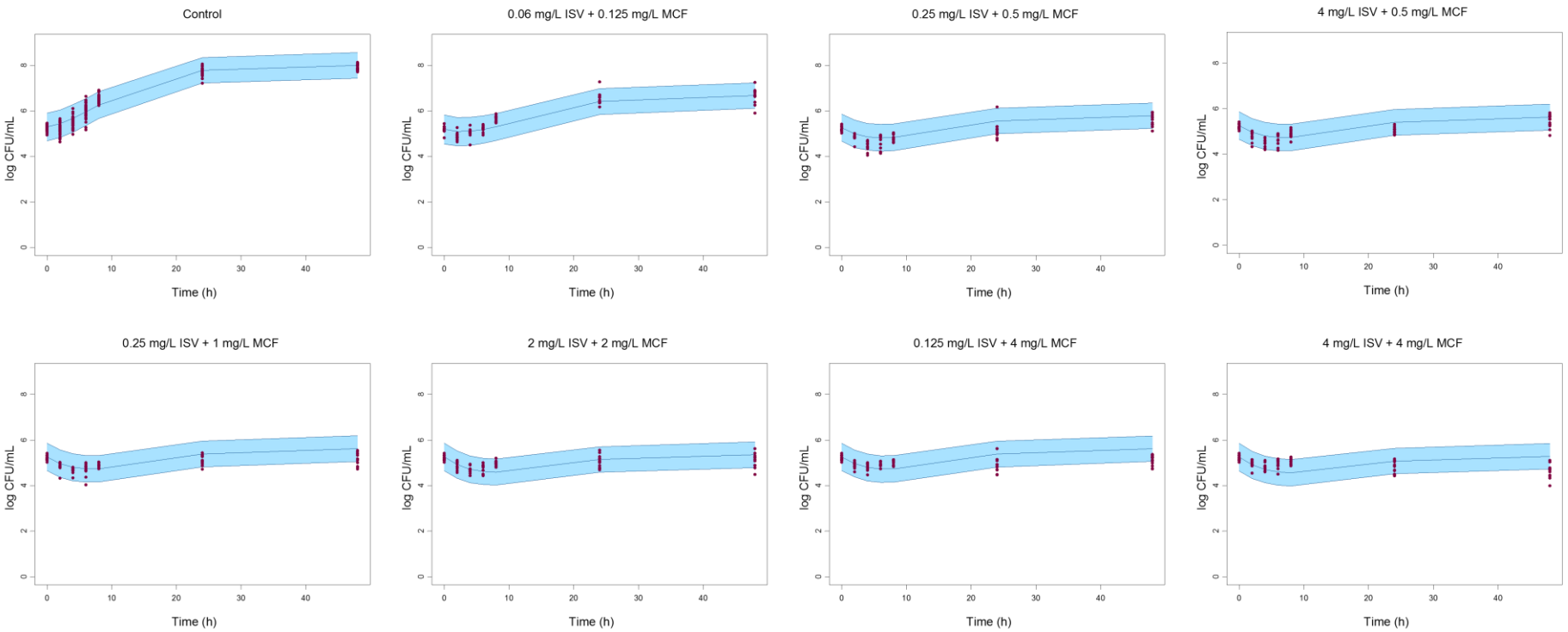

Figure 44. Visual predictive check (VPC) for the final model of isavuconazole + micafungin, with the observed fungal counts (full circles), the mean prediction (solid line) and 95% model prediction interval (shaded area) of the simulations.

3.2.2. PK/PD simulations of isavuconazole plus echinocandin treatments

Pharmacometric simulations were performed using the developed model (Eq. 29 and 32) along with PK models selected from literature (Table 6). Total and unbound concentration-time profiles of each drug after standard and alternative intravenous infusion dosing regimens were simulated for one thousand virtual patients (men and women, with a BMI of 25) over a week (Figure 45 and Figure 46). As depicted in Figure 47, none of the simulated dosing scenarios for any combination showed successful activity against the studied *C. auris* isolates, as the simulated responses did not result in a decrease in fungal density.

Additional simulations were performed over a 1-week period for various MIC scenarios ranging from 0.015 to 0.06 mg/L for isavuconazole, from 0.015 to 0.125 mg/L for anidulafungin and micafungin and from 0.015 to 0.25 mg/L for caspofungin. The simulation outcomes revealed that combinations of isavuconazole with anidulafungin or caspofungin were able to inhibit fungal growth in the first 24 h and stop fungal growth from 24 h onwards. The fungal growth inhibition was attained, depending on the dosing regimens tested, for the following MIC scenarios: 1) 0.015 mg/L for isavuconazole and 0.015 mg/L for echinocandin; 2) 0.015 mg/L for isavuconazole and 0.03 mg/L for echinocandin; 3) 0.03 mg/L for isavuconazole and 0.015 mg/L for echinocandin; 4) 0.03 mg/L for isavuconazole and 0.03 mg/L for echinocandin; 5) 0.015 mg/L for isavuconazole and 0.06 mg/L for echinocandin; 6) 0.03 mg/L of isavuconazole and 0.06 mg/L of echinocandin. There were no differences in treatment outcomes between men and women. Conversely, the combination of isavuconazole and micafungin was not successful for the evaluated doses and MIC scenarios. The combined dosing schedules and MIC scenarios that inhibited fungal growth are provided in Table 17. The drug combination and doses that would lead to higher antifungal coverage (all the six MIC scenarios) was the use of alternative dosages of both isavuconazole (400 mg every 8 h, first 48 h followed by 200 mg daily) plus caspofungin (100 mg daily) (Figure 48).

As expected, all alternative doses in drug combinations attained a higher antifungal coverage compared to the standard combination dosing schedules. In fact, combinations with currently used standard doses of isavuconazole and anidulafungin would only inhibit fungal growth if MIC $\leq$ 0.015 mg/L for both drugs. In the case of the combination with caspofungin, standard

doses would only inhibit fungal growth if MIC ≤ 0.015 mg/L for isavuconazole and MIC ≤ 0.03 mg/L for caspofungin.

Table 17. Summary of different dosing regimens for the combination of isavuconazole with anidulafungin or caspofungin and MIC scenarios (numbered 1 to 6) for which fungal growth was inhibited.

	Standard ISV	Alternative ISV
Standard ANF	1	1-3
Alternative ANF	1-3	1-5
Standard CSP	1,2	1-4
Alternative CSP	1-5	1-6

Standard ISV/ANF/CSP: standard dosing-regimen of isavuconazole, anidulafungin or caspofungin. Alternative ISV/ANF/CSP: alternative dosing-regimen of isavuconazole, anidulafungin or caspofungin.

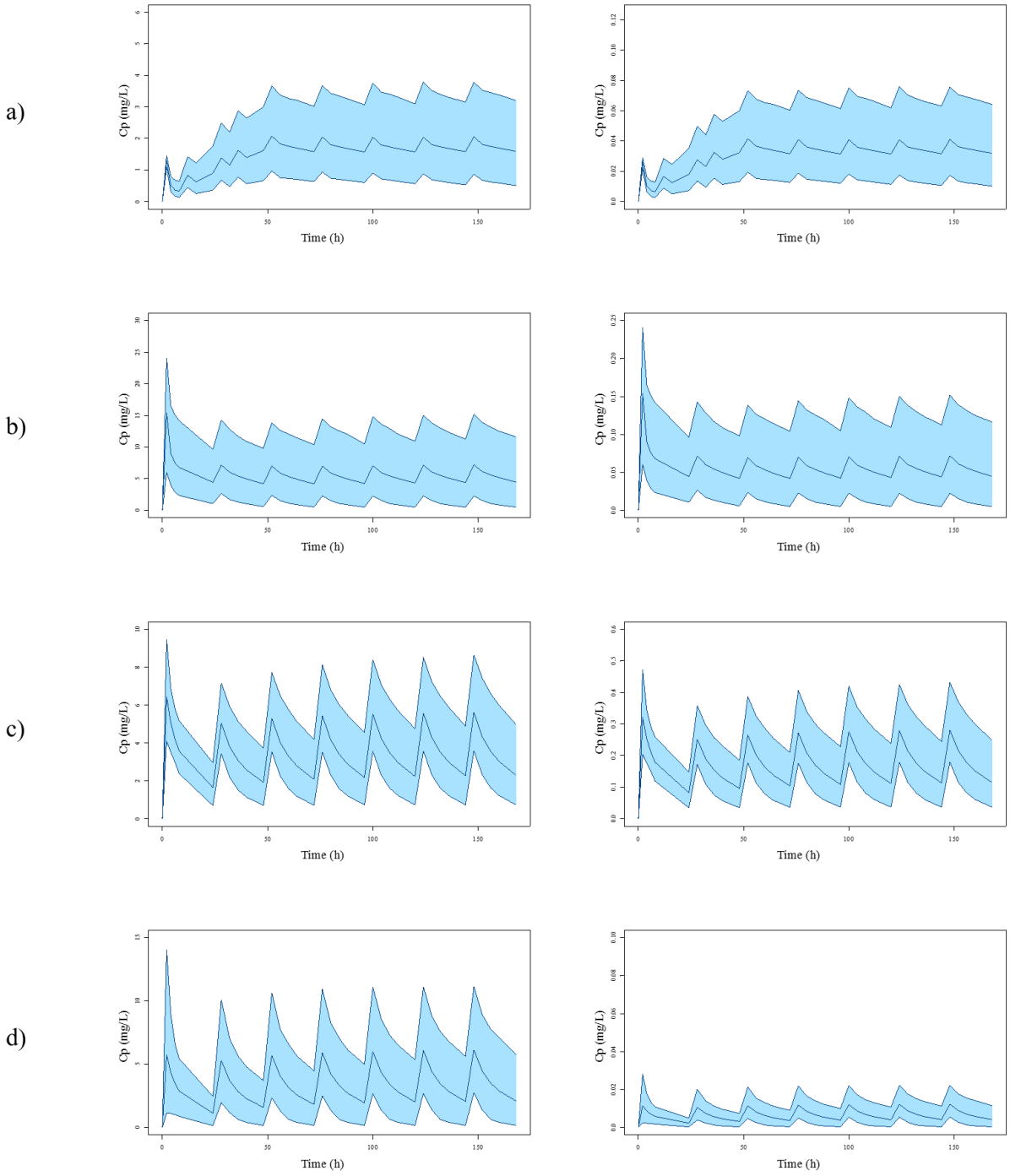

Figure 45. Simulated total plasma concentrations (left) and unbound concentrations (right) over 1 week after standard treatment of a) isavuconazole, b) anidulafungin, c) caspofungin and d) micafungin. The mean (solid line) and 95% prediction interval (coloured space) are represented.

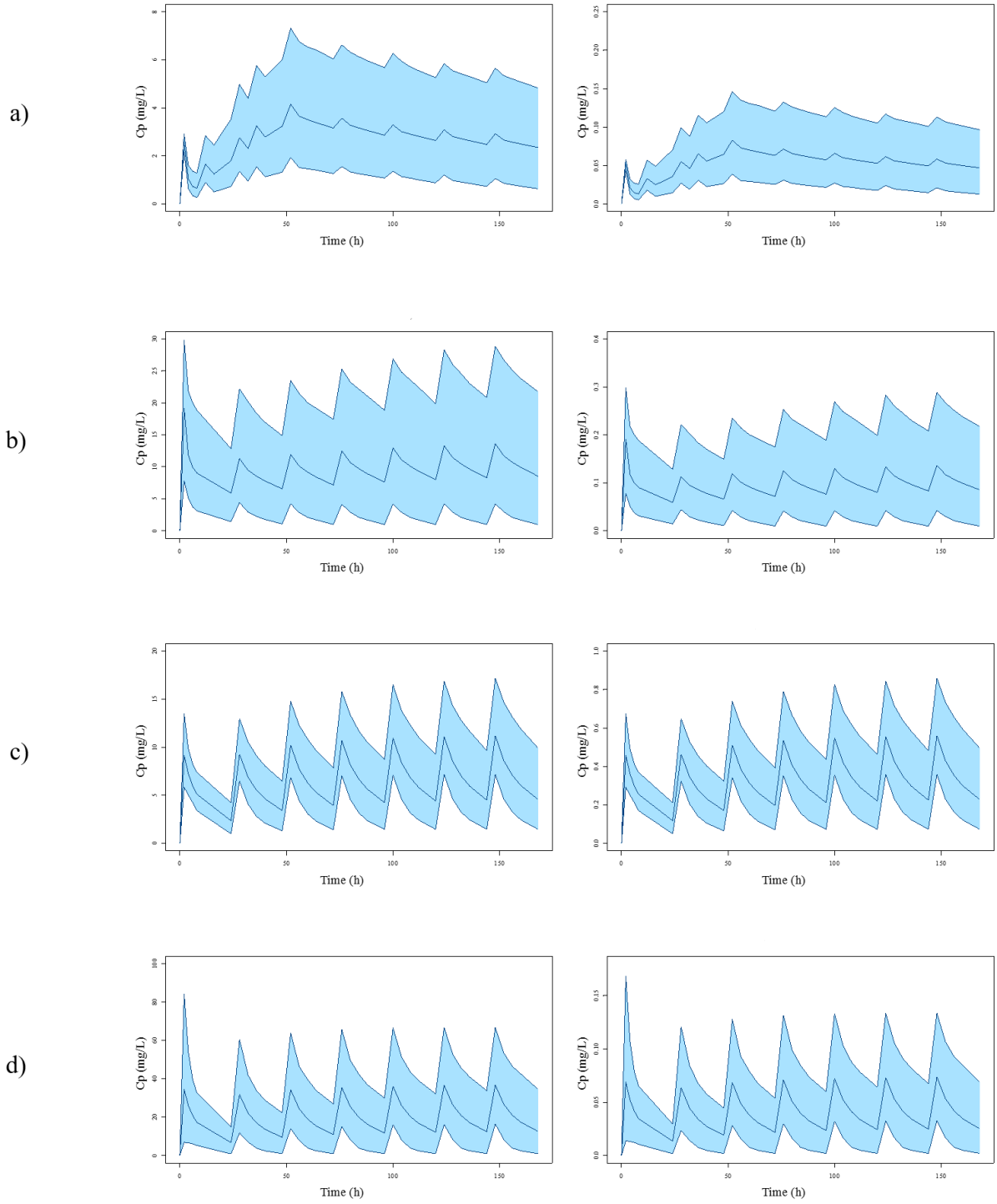

Figure 46. Simulated total plasma concentrations (left) and unbound concentrations (right) over 1 week after standard treatment of a) isavuconazole, b) anidulafungin, c) caspofungin and d) micafungin. The mean (solid line) and 95% prediction interval (coloured space) are represented.

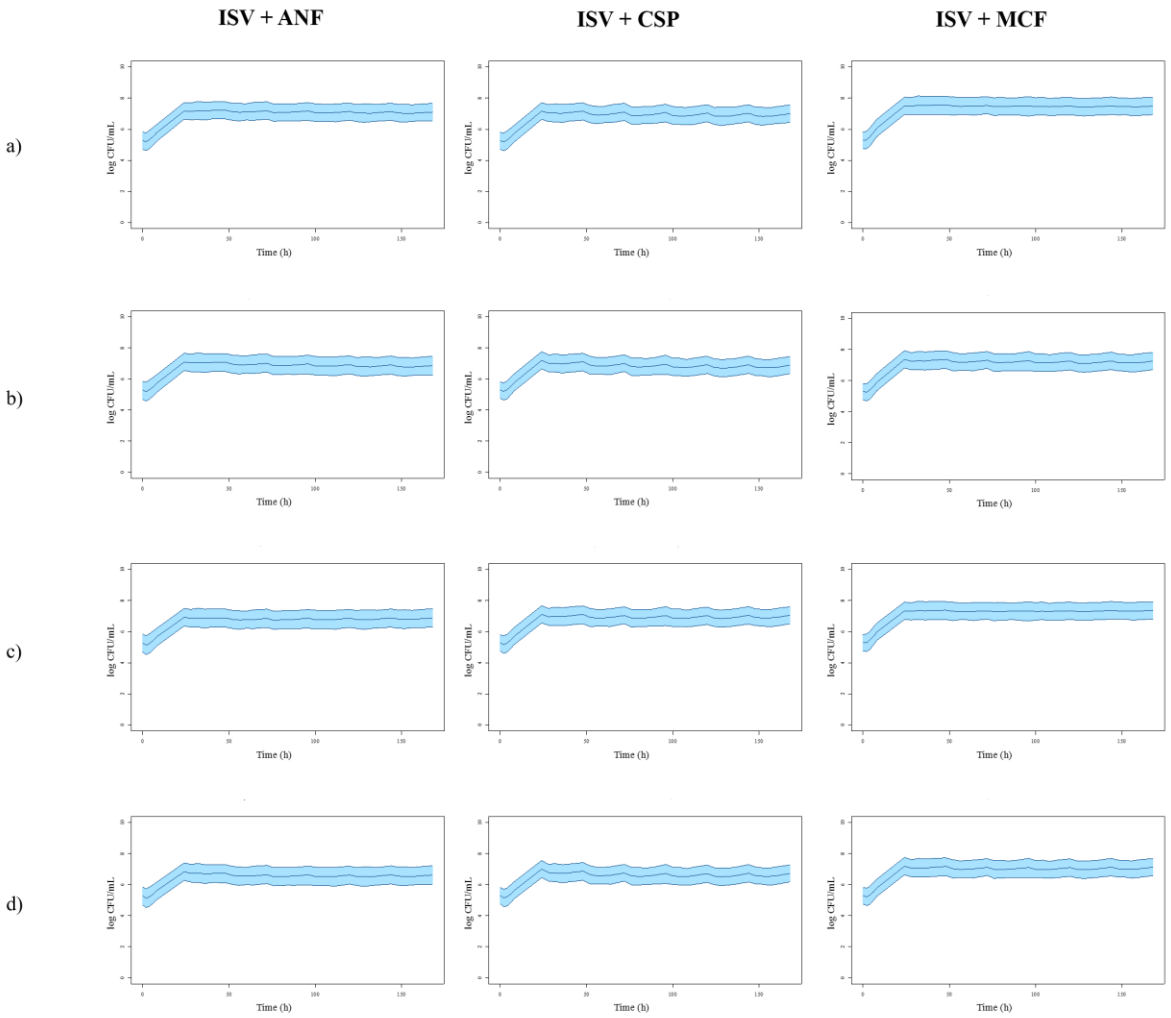

Figure 47. Effect on fungal burden of different dosing-regimens (a-d) of isavuconazole + anidulafungin (ISV + ANF), isavuconazole + caspofungin (ISV + CSP) and isavuconazole + micafungin (ISV + MCF). a) standard dosing of both isavuconazole and echinocandins, b) standard dosing of isavuconazole + alternative dosing of echinocandins, c) alternative dosing of isavuconazole + standard dosing of echinocandin, d) alternative dosing of both isavuconazole and echinocandins. The mean (solid line) and 95% prediction interval (coloured space) are represented.

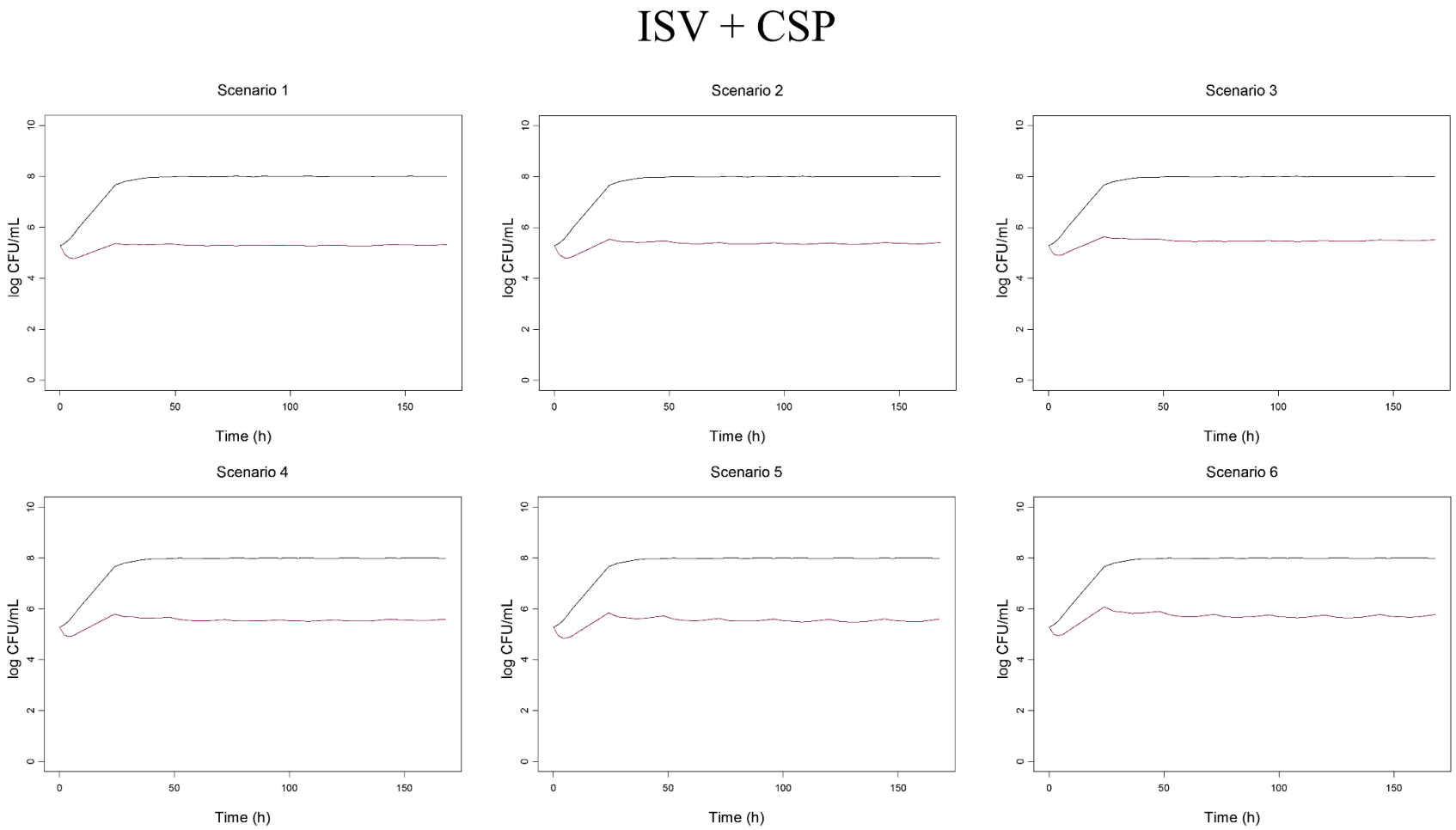

Figure 48. Effect on the fungal burden by the combination of proposed alternative dosages of isavuconazole and caspofungin (ISV +CSP). Black line represents growth control (no treatment) and the magenta line represents the mean outcome of the treatment arm. Scenario 1: MIC of 0.015 mg/L for ISV and 0015 mg/L for CSP. Scenario 2: MIC of 0.015 mg/L for ISV and 0.03 mg/L for CSP. Scenario 3: MIC of 0.03 mg/L for ISV and 0.015 mg/L for CSP. Scenario 4: MIC of 0.03 mg/L for ISV and 0.03 mg/L for CSP. Scenario 5: MIC of 0.015 mg/L for ISV and 0.06 mg/L of CSP. Scenario 6: MIC of 0.03 mg/L for ISV and 0.06 mg/L for CSP.

V. DISCUSSION

1. In vitro activity of echinocandins, amphotericin B and isavuconazole

C. auris is a multi-drug resistant yeast pathogen responsible for numerous cases of fungaemia globally since 2009 (Bidaud et al., 2018). This fungus spreads rapidly in hospitals and nursing homes, and it has been classified as an "urgent threat" pathogen according to the United States Centers for Disease Control and Prevention's (CDC) 2019 Antibiotic Resistance Threats Report (CDC, 2019).

According to the First Meeting of the WHO Antifungal Expert Group on Identifying Priority Fungal Pathogens, there is an overall consensus that *C. auris* is a pathogen of global public health interest and should be evaluated based on the limited existing therapeutic options due to resistance or other treatment issues (WHO, 2020).

Up to date, most susceptibility studies on *C. auris* have focused on the determination of the MIC. The MIC is the standard PD parameter used as a marker of fungal susceptibility and antimicrobial efficacy, yet it possesses some limitations. The antimicrobial activity of drugs is a dynamic process, while MIC is a threshold value. Concentrations below or above the MIC are ignored and thus, a more precise and quantitative information about the concentration-effect profile of the drug is often missing. It is also noteworthy that even for the same microbial species, same MIC values among different isolates can result in different killing kinetics (Mueller et al., 2004). Thus, studies that characterise the antimicrobial activity beyond the measurement of MIC are needed. In vitro time-kill curves allow obtaining more information about the effect of different drug concentrations on microbial population over a time period.

Despite the relevance of *C. auris*, information about how antifungal drugs act against this species is limited. In the first part of the Doctoral Thesis, the killing kinetics of echinocandins, amphotericin B and isavuconazole was established by time-kill methodology.

1.1. In vitro activity of antifungal drugs in monotherapy: MIC and time-kill curves

The first finding of the Thesis was the lack of in vitro antifungal activity of the three currently approved echinocandins against the clinical isolates of *C. auris* studied in time-kill curves. However, echinocandins are the first-choice treatment for invasive candidiasis, including those caused by *C. auris* and animal models have also suggested that echinocandins are the most

active drug class against this pathogen (Lepak et al., 2017). This discrepancy between our in vitro results and the consideration of echinocandins as a drug of choice is striking. The killing kinetic patterns observed in our studies for echinocandins against *C. auris* resemble the killing profile shown for this antifungal class against species of *Candida* with reduced intrinsic susceptibility like *C. guilliermondii* (Canton et al., 2006) and interestingly also with the taxonomically close species *C. lusitaniae* (Canton et al., 2013). However, the MIC values of echinocandins in our study are in agreement with the MIC values reported by other authors against *C. auris* (Arendrup et al., 2017b; Dudiuk et al., 2019). Caspofungin MIC was higher than the other two echinocandins MICs, in concordance with other reports (Dudiuk et al., 2019; Kovács et al., 2021). Based on the proposed tentative ECOFFs for *C. auris* (Arendrup et al., 2017b), the isolates in our study are considered WT for anidulafungin and micafungin. There are no published ECOFFs for caspofungin, since a high interlaboratory variability in modal MICs is widely acknowledged for this drug (Espinel-Ingroff et al., 2013). In this line, the in vitro results of caspofungin should be cautiously interpreted. As no breakpoints are available for *C .auris*, we used the proposed tentative ECOFFs to classify the isolates as WT, instead of using the CDC approach of considering the breakpoints for closely related *Candida* species. Other authors previously used the ECOFF criteria, as susceptibility breakpoints are species- and method-dependent (Ruiz-Gaitán et al., 2019). Nevertheless, it should be highlighted that ECOFF values, unlike breakpoints, do not classify isolates in susceptible or resistant, as this endpoint does not account for the pharmacology of the drug nor the outcomes from clinical studies (Espinel-Ingroff and Turnidge, 2016).

As expected, our MIC results are within the range of those reported by Ruiz-Gaitán et al. for *C. auris* isolates from a Spanish outbreak. It has been proposed that the Spanish isolates belong to a genotipically distinct clade from the reported in India, the UK, Oman and Venezuela, and are probably related to the South African clade (Ruiz-Gaitán et al., 2018).

On the other hand, the killing kinetics evaluation demonstrated the lack of antifungal activity of the three echinocandins in monotherapy, more remarkable for caspofungin. So far, there are only two works that have evaluated the activity of echinocandins against *C. auris* with time-kill curve approach. In those studies, the first in vitro evidence of the lack of fungicidal effect of the echinocandins was provided (Dudiuk et al., 2019; Kovács et al., 2021). Dudiuk et al. studied Colombian isolates from the South American clade and the average k values for caspofungin and anidulafungin were close to zero. Our results are similar, especially for

caspofungin at 48 h, although the activity of anidulafungin in their study was higher, since they reported a fungistatic effect at 24 and 48 h (Dudiuk et al., 2019). Kovács et al. investigated the killing activities of the three echinocandins against isolates from each clade. Their results were mostly in agreement with Dudiuk et al. and with the present Thesis. They found fungistatic activity against the isolates the isolates from all clades, but those from South African clade were the least susceptible (Kovács et al. 2021).

Isavuconazole is a novel triazole with PK and PD advantages compared to the other azoles. However, its in vitro activity profile, especially with regard to *C. auris*, is unknown and warrants further investigation. To our knowledge, this is the first study that has analysed the activity of this new triazole against *C. auris* with this methodology. Similar to echinocandins, isavuconazole, with lower MIC and also classified as WT, did not show significant activity against this yeast in time-kill assays. Katragkou et al. reported a similar low activity of isavuconazole against *C. albicans*, whereas concentrations ≥ 0.06 mg/L were fungistatic against *C. parapsilosis* (Katragkou et al., 2017).

The in vitro activity of echinocandins and isavuconazole observed in this work could be considered as "trailing effect". Trailing is defined as an in vitro phenomenon in which fungal growth is reduced but still visible above MIC (Marcos-Zambrano et al., 2016; Binder et al., 2019). It has usually been described for azoles, although it has also been reported for echinocandins (Varga et al., 2008). This low-susceptibility pattern has been linked to molecular adaptative responses to stress (Rosenberg et al., 2018), but whether it is directly translated to therapeutic failure or not remains unclear (Astvad et al., 2018; Rosenberg et al., 2018; Binder et al., 2019).

In contrast to the absence of activity of the echinocandins and isavuconazole, amphotericin B exerted a rapid and concentration-dependent fungicidal activity. It should be noted that this rapid killing activity and fungicidal endpoint achievement are important for infection eradication, and both features were captured by time-kill methodology. Killing activity against *C. auris* began at 2 mg/L. While with 1 mg/L (equal to the MIC value) killing was also observed, fungicidal endpoint was not achieved and a regrowth behaviour was evidenced, resembling the killing-kinetic pattern of the study of Dudiuk et al. and close to the profile described for amphotericin B-resistant species like *C. guilliermondii* or *C. lusitaniae* (Di Bonaventura et al., 2004; Cantón et al., 2006; Dudiuk et al., 2019).

It should be highlighted that, the concentration-dependent regrowth observed in the static time-kill assays laid the foundation for the subsequent semi-mechanistic modelling of amphotericin B, as it will be convened shortly.

1.2. PAFE of amphotericin B

PAFE was studied and determined for amphotericin B, as it was the only drug with a remarkable antifungal activity. PAFE data, together with time-kill information of drugs, may be clinically useful in the study of the dosage regimens to manage candidiasis. Whereas antifungal drugs that have long PAFE may be given less frequently, the antifungal drugs with short PAFE may require a frequent administration (Oz et al., 2013). The existence of PAFE, defined as the continuation of suppression of fungal growth after the drug is removed from the fungal suspension, depends on both the fungal species and the class of the antifungal drug. An overall prolonged PAFE of the three echinocandins has been reported against *C. albicans*, *C. glabrata*, *C. parapsilosis* and *C. krusei* (Smith et al., 2011; Ernst et al., 2000; Nguyen et al., 2009; Gil-Alonso et al., 2016a). Azoles, on the other hand, display a negligible or no PAFE against *C. albicans* (Manavathu et al., 2004), against *C. krusei* (Oz et al., 2013), or against *C. guilliermondii* and *C. lusitaniae* (Di Bonaventura et al., 2004).

According to previous findings, amphotericin B produced prolonged and dose-dependent PAFE against *C. albicans* (Ernst et al, 2000; Manavathu et al., 2004), also against more infrequent clinical isolates of *C. guilliermondii* and *C. lusitaniae* (Di Bonaventura et al., 2004), and a significant dose-dependent PAFE was also reported against *C. krusei* (Oz et al., 2013). A short PAFE was detected for other polyene, nystatin, against *Candida dubliniensis* isolates. Ellepola studied the PAFE of amphotericin B against oral isolates of different *Candida* species and reported significant PAFE variations amongst species, with the lowest for *C. albicans* (5.9 h) and the longest for *C. parapsilosis* (12.7 h) (Ellepola , 2012). In the light of these previous reports, we aimed to evaluate the PAFE of this drug against *C. auris*. Thus, in parallel with the time-kill experiments, PAFE studies were carried out. Amphotericin B displayed a short PAFE at ≥ 2 mg/L against *C. auris*, with range values from 3.5 to 6.5 h. Fungal killing was not achieved during PAFE experiments, therefore, it could be concluded that PAFE had no role in the fungicidal activity of amphotericin B. It seems evident that PAFE depends strongly on *Candida* species, as some of them, like *C. auris* in our study, recovers sooner from drug exposure than others.

The lack of PAFE studies with any drug against *C. auris* precluded comparisons. However, the short PAFE of amphotericin B against *C. auris* is consistent with the resistant nature of this species, even though this drug remains the likely drug of choice in patients with echinocandin-resistant *C. auris* (Arendrup et al., 2017a).

To conclude this first section, it is important to point out that the results of this part, in addition to providing descriptive information on the activity of the drugs studied in monotherapy, allowed us to obtain relevant information that has been applied in the subsequent experimental designs and pharmacometric analyses. Drug combinations and concentrations studied were, to a large extent, selected based on the results of the monotherapies. The time-kill curves also helped in the selection of the structural models that were tested for data fitting.

2. In vitro activity of combination therapies

On the background of growing evidence of reduced susceptibility of *C. auris* to available drugs, there is a need of increasing antifungal options and further studying treatment alternatives. In this line, the approach of combining drugs with different mechanisms of antifungal action has been proposed to optimize the therapeutic management of invasive mycoses. The motivations for studying the activity of drug combinations include: i) to assess the potential synergistic interaction; ii) to reduce the risk of further resistance development during treatment; iii) to reduce the dose of drugs with recognized toxicity like amphotericin B. However, few works have analysed the interaction between first-line agents against this emerging yeast. To our knowledge, this is the first work that has studied the combination of amphotericin B or isavuconazole with echinocandins against *C. auris* through in vitro time-kill curves.

2.1. Amphotericin B plus anidulafungin/caspofungin

Although echinocandins are the first-choice treatment for invasive candidiasis, the present study found that anidulafungin and caspofungin in monotherapy had no activity against any of the six *C. auris* isolates studied, while amphotericin B did, although in monotherapy only at concentrations ≥1 μg/ml. The lack of fungicidal activity found in vitro for echinocandins against *C. auris*, along with the high concentrations of amphotericin B required to reach the fungicidal endpoint, support the interest to examine the combinations with the two classes of antifungal agents.

The main results that should be highlighted in the current study are, on one hand, that synergy was rapidly achieved (8h) with the combinations of amphotericin B at 0.5 mg/L and the highest concentration of anidulafungin or caspofungin (2 mg/L). Once achieved, the synergy was sustained over 48 h. Moreover, the combinations of amphotericin B at 1 mg/L and anidulafungin or caspofungin, resulted in a fungicidal activity. The achievement of this fungicidal activity and the earlier arrival to this point was related to higher concentrations of echinocandins. The findings of synergy and in some cases fungicidal activity of the present study are promising, especially if the lack of activity of the drugs alone (except for amphotericin B at the high concentration) is considered.

To our knowledge, this is the first work that has studied the combination of amphotericin B with echinocandins against *C. auris* through in vitro time-kill curves. Very few studies have

examined the effect of antifungal drug combinations against this pathogen and most of them have assessed the interactions solely with checkerboard data and FICI determination. O'Brien et al. studied *C. auris* isolates from a New York outbreak, and found synergism for the combination of flucytosine and echinocandins or amphotericin B, but not for the combination of amphotericin B with echinocandins (O´Brien et al., 2020). The New York strains that they evaluated were related to the South Asian clade, while our isolates from the Valencia outbreak are related to the South African clade, which could explain the lack of concordance between studies. The combination of amphotericin B with flucytosine tested against *C. auris* isolates with fractional inhibitory concentration index resulted in indifferent interaction (Bidaud et al., 2019).

Combination therapy with amphotericin B and echinocandins has been studied for other species of *Candida*, with variable results. Kiraz et al. reported that amphotericin B plus caspofungin showed synergism in 46% of the tested *C. glabrata* isolates with time-kill assays (Kiraz et al., 2009). Another study found a similar degree of synergism with anidulafungin against various species of *Candida* (Teixeira-Santos et al., 2012). Conversely, other studies with *C. glabrata* demonstrated a lack of synergy with the combinations of amphotericin B and echinocandins (Denardi et al., 2017). Serena et al. studied the combination of amphotericin B with micafungin. Although most interactions were deemed indifferent by the checkerboard method, those strains that showed synergism were further analysed by time-kill methodology and the combination demonstrated a fast killing activity (Serena et al., 2008).

Regarding in vivo studies, Olson et al. tested the combinations of amphotericin B and caspofungin or micafungin in immunosuppressed mice infected with *C. glabrata* and found that both combinations, administered either concomitantly or sequentially, reduced significantly the fungal burden in tissues compared to any of the drugs in monotherapy (Olson et al., 2005). Hossain et al. also reported a significant fungal reduction with the co-administration of amphotericin B and caspofungin against azole-resistant *C. albicans*. However, when mice survival was checked, the difference between combination therapy and monotherapy with amphotericin B was not significant, even though the survival was higher in the drug combination group (Hossain et al., 2003).

Clinical evidence regarding the combination of amphotericin B with echinocandins for invasive candidiasis is scarce and mostly published as case reports. Mpakosi et al. reported the successful treatment with liposomal amphotericin B and micafungin of a preterm infant with *Candida*

(Metschnikowia) pulcherrima fungaemia (Mpakosi et al., 2016). This rare species is also part of the Metschnikowiaceae family. Another report from Japan described the eradication of *C. guillermondii* infection in an oncology patient using the same combination (Saitoh et al., 2008). Roberts et al. reported a case of a patient suffering from *C. auris* intra-articular infection successfully treated with amphotericin-impregnated spacer in addition to systemic fluconazole or micafungin (Roberts et al., 2019). Apart from these case reports, there is limited evidence on this issue, and the combined therapy of echinocandins with amphotericin B has been used mostly in the treatment of invasive aspergillosis. Yilmaz et al. observed that the combination of amphotericin B and caspofungin was safe and effective in the treatment of invasive fungal infections of children with haematological malignancy, refractory to amphotericin B, and caused by *Aspergillus* or *Candida* (Yilmaz et al., 2011). The multicentre observational ProCAS study evaluated the effectiveness and safety of caspofungin in monotherapy and in combination with amphotericin B or voriconazole in adult haematological patients with invasive candidiasis. Favourable results were reported for *C. krusei* fungemia treated with amphotericin B plus caspofungin (Jarque et al., 2013).

Published works suggest that there might be differences in antifungal susceptibility among *C. auris* clades (Bidaud et al., 2019; Kovács et al., 2021). Therefore, the synergism and antifungal activity shown by the combinations of amphotericin B and anidulafungin or caspofungin in our study may not replicate in isolates belonging to other clades.

In conclusion, the combinations of amphotericin B with echinocandins provided greater killing with a lower dose requirement of amphotericin B against all isolates of *C. auris*. These findings could support a new therapeutic approach by combining two first-line antifungal drugs in those cases where invasive candidiasis does no respond to current treatment. However, further in vivo studies are needed to better assess possible clinical relevance, considering criteria of effectiveness and safety.

2.2. Isavuconazole plus anidulafungin, caspofungin or micafungin

Isavuconazole is the latest addition to the triazole group and its pharmacological properties make it an interesting choice to study for antifungal combinations. It can be administered both orally and intravenously, has a large volume of distribution and high protein binding, the inhibitory effect on CYP34A is lower than that of posaconazole or voriconazole (Ellsworth and Ostrosky-Zeichner, 2020) and the pharmacokinetic variability is lower than the observed for

voriconazole (Mangal et al., 2018; Wu et al., 2020). On the other hand, echinocandins are nowadays first-line options for the treatment of invasive candidiasis, having similar pharmacokinetic and pharmacodynamic properties (Bellman and Smuszkiewicz, 2017).

In the present study, isavuconazole and echinocandin combinations showed promising results, as they were deemed mainly synergistic by two different analysis methods and were able to halt fungal growth for 48 h in time-kill experiments. Furthermore, the synergism resulted from the combination therapy is particularly relevant if we consider the lack of efficacy shown by the studied drugs in monotherapy in our study. The in vitro evidence of non-fungicidal activity of the drugs in monotherapy supports the interest of studying drug combinations. Up to now, there are only seven published studies that have evaluated the in vitro activity of antifungal drug combinations against *C. auris*. In a recent study, Pfaller et al. examined the in vitro activity of voriconazole or isavuconazole in combination with anidulafungin against *C. auris* isolates by using the checkerboard method and the FICI analysis. They observed synergism or partial synergism against most isolates, greater for the combinations of isavuconazole plus anidulafungin compared with voriconazole plus anidulafungin (Pfaller et al., 2021). In a previous study, Fakhim et al. reported that voriconazole and micafungin exhibited synergism against *C. auris* determined by the FICI, whereas the combinations of voriconazole with caspofungin or echinocandins with fluconazole resulted indifferent (Fakhim et al., 2017). Therefore, the synergy results of our study are consistent with these two reports of combinations of azoles and anidulafungin or micafungin against *C. auris*. Furthermore, we validated the checkerboard results with time-kill experiments. O'Brian et al. studied *C. auris* isolates from a New York outbreak, and found synergism for the combination of flucytosine with the rest of antifungal classes, but not for the combination of azoles with echinocandins (O´Brian et al., 2020). Conversely, flucytosine showed no interaction with other antifungal drugs against Indian *C. auris* isolates (Bidaud et al., 2019). This highlights the fact that the antimicrobial activity of drug-drug interactions may be not only species-specific but also strain-specific. Other works have focused on the combination of antifungal drugs with non-antifungal agents, such as colistin, miltefosine or sulfamethoxazole, as an approach to enhance the therapeutic arsenal against *C. auris* (Eldesouky et al., 2017; Bidaud et al., 2020; Wu et al., 2020). To date, the only published in vivo combination study, a model of *Caenorhabditis elegans* infected with *C. auris*, supported the combination of sulfamethoxazole and voriconazole (Eldesouky et al., 2017). However, there is not in vivo or clinical evidence regarding the combination of echinocandins plus azoles against *C. auris*.

The combination of azoles and echinocandins was studied in other species of *Candida* as well, with variable results depending on the drug, the species and the employed methods. In a recent work, the in vitro combination of fluconazole with anidulafungin or micafungin was synergistic against *C. parapsilosis* complex according to the FICI (Ahmadi et al., 2020). Conversely, another in vitro study that also used the FICI reported that the combination of fluconazole and micafungin was indifferent against *C. parapsilosis* and other species of *Candida* (Rodríguez et al., 2007). Indifferent interactions were also obtained in time-kill experiments when fluconazole was combined with caspofungin against *C. glabrata* (Kiraz et al., 2010) or with anidulafungin or caspofungin against *C. albicans*, *C. krusei* and *C. tropicalis* (Roling et al., 2002). Murine models also showed no interaction when fluconazole was the azolic agent of the combination (Graybill et al., 2003; Marine et al., 2006). When it comes to combinations with the newest azoles, variable interactions are found in literature. Synergism was observed in a checkerboard analysis between posaconazole or voriconazole and the three echinocandins against multi-drug resistant *C. glabrata* (Denardi et al., 2017); another study with *C. glabrata* showed that the interaction of voriconazole and caspofungin was synergic in time-kill curve experiments (Baltch et al., 2008); posaconazole and caspofungin exerted synergistic activity against *C. albicans* both in vitro and in a murine model (Chen et al., 2013). On the other hand, Kiraz et al. analysed azole-caspofungin combinations against *C. glabrata* and observed mostly indifferent interactions (Kiraz et al., 2010). Voriconazole and anidulafungin did not show activity against biofilm formation in five different *Candida* species (Valentin et al., 2016). Regarding the combination of isavuconazole with other antifungal agents for non-auris *Candida*, Katragkou et al. detected synergistic interaction with the combination of isavuconazole and micafungin against *C. albicans* and *C. parapsilosis*, determined by Bliss analysis and time-kill curves (Katragkou et al., 2017). Apart from *Candida* species, isavuconazole-echinocandin combination therapy has given rise to different results against filamentous fungi such as *Aspergillus*, with synergic outcomes in some studies (Katragkou et al., 2014; Petraitis et al., 2017; Buil et al., 2020) and indifferent isavuconazole-echinocandin interaction determined by FICI in another study (Raffetin et al., 2018).

Synergism applied to drug-drug combinations can be defined in a simple way as the interaction between two or more compounds that exerts a greater effect than the additive sum of the effects of each drug when acting alone (Greco et al., 1996). Nevertheless, determination of synergism or antagonism is far from simple. There are many factors that have to be considered, such as the experimental setting to obtain the empirical data or the mathematical methods chosen for

the analysis (Chou, 2006). When analysing checkerboard data of antimicrobial drugs, Loewe´s additivity is usually determined by the non-parametric approach of the FICI, obtained by comparing the MIC of the compounds alone and in combination (Odds et al., 2003). On one hand, FICI method is well established and straightforward, on the other, it ignores all the concentration-response data that do not correspond to MICs and variable results and interpretations may be expected depending on the MIC endpoints (Meletiadis et al., 2005). Parametric approaches, such as the Greco universal response surface approach (URSA) and the Bliss interaction model, overcome this drawback, as the whole drug-concentration range is analysed (Greco et al., 1995). It also allows the estimation of parameters (such as IC_{50}) and the associated confidence intervals based on more robust mathematical and statistical methods (de Miranda Silva et al., 2018). One limitation of Loewe´s additivity based models is that it requires the dose-response curves to be accurately estimated for each drug alone (Roell et al., 2017). In the current work, that was not possible for micafungin against *C. auris* 17-265, and thus, the value of α was high and its CI wide. Nevertheless, the results obtained with the parametric and non-parametric approaches, showed synergistic interactions for the isavuconazole-echinocandins combinations. Furthermore, this agreement between approaches and the sensitivity of the models in detecting even weak interactions is concordant with other reports that have compared different drug interaction models (Meletiadis et al., 2005; Otto et al., 2019; Bidaud et al., 2020).

It is important to take into consideration that lack of synergism of a drug combination does not necessarily mean that the effectiveness of the combination is negligible. After all, when antimicrobial agents are combined, the goal is to reduce the microbial density, regardless of the nature of the interaction. Additionally, in the interpretation of a synergism result, it should be considered whether it has been observed under clinically relevant conditions; whether the observed synergism is obtained at concentrations that are clinically achievable and the extent of the effect. Bliss independence model-based surface analysis allowed identifying the concentration range of each combined drug where synergism was claimed. In summary, synergism was detected with the combination of low concentrations (<0.125 mg/L) both of isavuconazole and echinocandins. Antifungal effect was further examined by time-kill experiments, in which we tested the concentrations that showed zero absorbance value in the checkerboard assays, as that reflects an antifungal effect of interest. It was observed that fungal growth was reduced thorough 48 h by all the isavuconazole-echinocandin combinations tested, but none of them achieved fungicidal activity. Furthermore, the time-kill curve analysis

revealed that once the fungistatic effect and synergism were achieved with the echinocandin-azole combinations, higher concentrations did not result in a higher reduction in fungal burden. These threshold concentrations were isavuconazole ≥ 0.125 mg/L and echinocandin ≥ 1 mg/L. Time-kill curve experiments also supported that an additive effect can also be of interest, as none of the drugs in monotherapy had fungistatic activity and the interaction of all combinations at 24 h was additive but fungistatic too. To our knowledge, this is the first study that has determined the in vitro interactions of a triazole with echinocandins against *C. auris* by use of both checkerboard assays and time-kill analysis.

It is worth to note that the antifungal effect and the synergy observed with the studied combinations were observed at clinically achievable and safe drug concentrations related to standard dosing. Nevertheless, any in vitro system, no matter how sophisticated, is a simplification of the much more complex in vivo situation and proper in vitro-in vivo correlations have not been established for azole-echinocandin combinations. In fact, in vivo or clinical studies on antifungal combination therapy in *C. auris* infections are lacking.

In conclusion, in the present in vitro study, the combinations of isavuconazole with anidulafungin, caspofungin or micafungin against *C. auris* were mostly synergistic and fungistatic, providing evidence that combination therapy is a promising approach to be further investigated, especially when the drugs alone show reduced activity.

3. PK/PD modelling and simulation of antifungal activity

Once time-kill curve experiments have been performed, PK/PD model building that describes the data is an interesting tool to predict and simulate untested scenarios that may help in decision-making and design of further studies. Therefore, this part of the Thesis is based upon the potential of PK/PD modelling to characterise in vitro time-kill data and supports the use of these models to make predictions of different scenarios.

3.1. PK/PD modelling and simulation of the in vitro activity of amphotericin B

Few PK/PD models have been developed for antifungal agents (Li et al., 2008; Venisse et al., 2008; Gil-Alonso et al., 2016b). To the best of our knowledge, the present study is the first work that has used a semi-mechanistic approach to model the antifungal activity of amphotericin B against *C. auris*. Even though previous studies based on PK/PD animal models have suggested that echinocandins are the most effective drugs to treat *C. auris* infections (Lepak et al., 2017), in vitro time-kill studies have observed that amphotericin B is more active than echinocandins (Dudiuk et al., 2019). Our studies have also provided evidence of the scarce activity of the echinocandins in monotherapy against the studies isolates, even at concentrations higher than the MICs and ECOFF values, along with a remarkably higher activity of amphotericin B. In fact, amphotericin B was the only fungicidal agent, confirming the results obtained by Dudiuk et al. with other strains. Based on this background regarding the high in vitro activity of amphotericin B against *C. auris*, the aim of this part of the Thesis was to develop a PK/PD model to capture the relationship between fungal burden and amphotericin B concentrations and go beyond the typically descriptive information on PD provided by the time-kill curves. The static time-kill experiments performed showed fungal regrowth or a biphasic trend, and therefore, a semi-mechanistic model that included two fungal subpopulations with different susceptibility to the drug was developed to capture this behaviour. This kind of approach has been extensively applied to model antibiotic activity successfully (Nielsen and Friberg 2013; Brill et al., 2018). The model successfully characterised the rapid initial killing after amphotericin B exposure followed by regrowth. In the model of the present study, the emergence of resistance is triggered by a high microbial burden, with the susceptible population switching to a resistant one, a process described by a first-order rate constant that also accounted for the self-limiting growth rate (Nielsen et al., 2007). The model best fitted the data when a

different growth rate constant for the resistant subpopulation was defined ($k_{growthR}$); this parameter was estimated to be 10 times lower than the growth rate constant for the susceptible subpopulation ($k_{growthS}$), which is in agreement with the 'fitness cost' observed in some species of *Candida* when they develop resistance mechanisms (Sasse et al., 2012). Moreover, phenotypic switching during treatment with amphotericin B has been described for *C. lusitaniae* (Asner et al., 2015), a closely related species of *C. auris*. Nevertheless, the main goal of model building was to accurately describe the antimicrobial activity and perform simulations rather than to provide insight into resistance mechanisms, for which specific microbiological and molecular procedures would be needed. On the other hand, the lack of similar PK/PD models reports for *C. auris* or amphotericin B in the literature has precluded comparisons.

The developed model was then used to simulate expected time-kill curves for typical amphotericin B dosing regimens. This approach provided expected *C. auris* kill curves at clinically attainable concentrations. A three-compartment model for amphotericin B deoxycholate (Bekersky et al., 2002a) was implemented for the simulation of plasma concentrations of the drug in human patients for dosing regimens of 0.6, 1 and 1.5 mg/kg/day. The latter dose is more commonly used for the treatment of invasive aspergillosis rather than for candidaemia (EUCAST, 2020a), but we also considered this dosing schedule for simulation purposes due to the low susceptibility profile of *C. auris* and the concentration-dependent PD of amphotericin B shown in our study, in concordance with other in vitro and in vivo results (Lepak et al., 2017; Dudiuk et al., 2019). Higher doses were not considered due to the toxicity of the drug. Amphotericin B, as many antifungal agents, is highly bound to plasma proteins, around 95% at clinically achievable concentrations (Bekersky et al., 2002b), and this feature was taken into account in the PK/PD simulations.

Regarding the different pharmaceutical formulations available, liposomal amphotericin B (L-AMB) is the current first choice due to its improved safety profile and comparable efficacy to conventional amphotericin B deoxycholate. However, the cost of lipidic formulations can be too high for healthcare systems in developing countries, which makes the conventional formulation still relevant and listed as essential drug (WHO, 2020). In addition, it is still not clear which fraction of the total plasma concentration of L-AMB is active, as protein binding is not applicable for this formulation (Groll et al., 2019), which makes the bridging between in vitro experiments and in vivo simulations harder to perform. Therefore, the simulations in our study were carried out for the deoxycholate formulation. Nevertheless, studies in animal models

of invasive candidiasis and clinical trials have shown similar efficacy for both formulations (Groll et al., 2019). This may reflect a comparable exposition of the fungal population to free drug and therefore conclusions driven by PK/PD simulations may be also applicable for L-AMB. In fact, EUCAST susceptibility breakpoints are based on adult standard dosages of both formulations (Arendrup et al., 2020b).

As previously mentioned, an approach solely based on the MIC of antimicrobials provides limited information. Conversely, PD parameters derived from the analysis of time-kill curves, such as E_{max} and $EC_{50,}$ give more detailed information on the activity of the drug. However, obtaining these data in the clinical setting is time-consuming, laborious, and usually not feasible. By employing mathematical relationship between the MIC and EC_{50}, as it has been carried out in the present study, this drawback can be overcome, since it is possible to link the results of the PK/PD modelling and simulation of time-kill curves with the drug MIC (Schmidt et al., 2007).

Simulations of different dosages pointed out that the treatment with amphotericin B deoxycholate would not be effective. Additionally, other possible treatment outcomes were tested by simulating different susceptibility scenarios, with MICs below 1 mg/L. Standard treatments of 0.6 and 1 mg/kg/day would only be effective against *C. auris* isolates for a MIC of 0.06 mg/L. However, a higher dosage of 1.5 mg/kg/day would also be effective for a MIC up to 0.125 mg/L. Therefore, contrary to expectations (Lockhart et al., 2019), the susceptibility breakpoint of amphotericin B for *C. auris* might be lower than 1 mg/L. Similar threshold values for amphotericin B have been reported for other species of *Candida* and filamentous fungi, such as *Aspergillus*. In a murine model of invasive candidiasis caused by *C. krusei*, a daily dose of 1 mg/kg of amphotericin B was effective in reducing the kidney fungal burden when the MIC of the drug was of 0.125 mg/L, but ineffective when MIC was of 0.5 mg/L (Kardos et al., 2018). In another murine model study, doses of 1.5 mg/kg/day of amphotericin B resulted in a 15 day survival percentage of >50% for *C. glabrata*, and <25 % for *C. tropicalis*, the MIC being 1 mg/L for both species (Marine et al., 2009). In an in vitro dynamic system that mimicked human PK of unbound amphotericin B against *Aspergillus*, those species considered resistant to amphotericin B had a PTA of 0% when the MIC was 1 mg/L; for a PTA of 80% a MIC of 0.25 mg/L was needed (Elefanti et al., 2014). On the other hand, a work that analysed the effect of antifungal drugs against *C. auris* infection in a murine model of invasive candidiasis concluded that the MIC cut-off for amphotericin B was 1.5 mg/L (Lepak et al., 2017). However,

variability between strains was high and the 50% effective dose (ED_{50}) was as high as 5 mg/kg/day, a dose that can be lethal (Mohr et al., 2005). These variable results highlight some uncertainty in analysing susceptibility and cut-off points for this pathogen.

The results obtained in this study from in vitro experiments should be cautiously interpreted, as previous reports of amphotericin B in vivo efficacy correlation with in vitro studies against *C. auris*, either with MIC or time-kill curves, are lacking. Even though time-kill curve methodology is a more complex technique that provides further information than MIC determination, it is still an in vitro approximation to the much more complex in vivo reality. Factors such as host immunity status and drug tissue distribution are overlooked, whereas fungal burden may be overestimated, as growth rate is much faster in the rich environment of the microbiological broth culture than in the human infection sites (de la Peña et al., 2004).

In conclusion, the developed PK/PD model was able to characterise properly the antifungal activity of amphotericin B against *C. auris.* The simulations pointed out that amphotericin B, regardless of dosing adjustments, would be unlikely to provide therapeutic exposures to treat infections caused by *C. auris* with a MIC of 1 mg/L. In other words, isolates with MIC values of 1 mg/L would be linked to treatment failure and in consequence, amphotericin B resistance rate in this fungal species may be higher than previously reported (Chowdary et al., 2017). Our results may be extrapolated to *C. auris* clinical isolates with similar EC_{50}/MIC ratio. Nevertheless, further studies are needed to fully characterise the susceptibility profile of *C. auris* to amphotericin B and optimize antifungal therapy.

3.2. PK/PD modelling and simulation of the in vitro activity of the combinations of isavuconazole with echinocandins

There are several works published with PK/PD models for antibiotic combinations (Brill et al., 2018; Kristoffersson et al., 2020; Zhao et al., 2020). To our knowledge, this is the first study in which in vitro data based PK/PD modelling and simulation has been applied for antifungal drug combinations.

First, monotherapy time-kill curves were analysed to obtain information regarding the structural model and initial parameter estimates for the subsequent combination data modelling. A single-drug population model was able to reasonably characterise the antifungal activity of each drug. This activity was limited and similar for all drugs, although caspofungin had the lowest

E_{max}. Lower in vitro efficacy and/or potency of caspofungin compared to the rest of the echinocandins has also been reported for other species of *Candida* (Espinel-Ingroff and Cantón, 2010; Gil-Alonso et al., 2015a and 2015b). The discrepancy between the EC_{50} estimation by the Greco model and the present approach may seem striking, but it has to be taken into account that both the mathematical models and the PD endpoints were different. Greco model was used to analyse absorbance data at one specific time-point (48 h), whereas the PK/PD model was applied to time-kill data (log CFU/mL) gathered over a full 48-hour period. Thus, discrepancies in parameter estimates between both approaches may be warranted. Nevertheless, each model proved to be adequate for the characterization of the respective data.

The antifungal activity of the combinations of isavuconazole plus echinocandins in our study was successfully characterised by a previously proposed empirical interaction function for antibacterial combinations (Mohammed et al., 2016). Moreover, the positive value of the interaction parameter *Int* obtained for each isavuconazole-echinocandin combination indicated synergistic interactions, in agreement with the conclusions of the checkerboard and time-kill assays. The EC_{50} and E_{max} estimated for isavuconazole were similar in the three combinations, indicating that the effects of each echinocandin on the PD of isavuconazole were equivalent. Furthermore, there was a remarkable 6-fold decrease on the EC_{50} of isavuconazole when combined with echinocandins. This aligned with the main hypothesis explaining the molecular basis for azole-echinocandin synergism. Echinocandins disrupt cell wall synthesis by inhibiting 1,3-β-D-glucan synthase, which apart from the antifungal activity caused by the disruption itself, could also help to enhance the azole activity by increasing the access to the cell membrane, where these drugs inhibit the biosynthesis of ergosterol (Mukherjee et al., 2005; Katragkou et al., 2017). Additionally, the EC_{50} of anidulafungin and micafungin were also lower compared to monotherapy and were about the same for both drugs, whereas the EC_{50} of caspofungin in combination was almost three times higher than those of anidulafungin and micafungin, correctly pointing out the lower potency detected by time-kill curves.

Since infections caused by resistant or monotherapy poor-responding *Candida* have been quite infrequent until the irruption of *C. auris,* there is little clinical evidence regarding combination therapy and in consequence, there are no official recommendations addressing it, beyond amphotericin B plus flucytosine combination for some specific invasive mycoses (Pappas et al., 2016). In our study, the alternative dosages used for simulations were based on proposals from other authors´ works, in which they concluded through Monte Carlo simulations that

higher echinocandin dosing would be needed when the MICs of anidulafungin and caspofungin were above 0.06 mg/L and above 0.03 mg/L for micafungin (Martial et al., 2016; Bader et al., 2018; Wasmann et al., 2019). It was also considered the recommended high dosing for echinocandins (Pappas et al., 2016) and the information provided by clinicians that deal with such infections. For isavuconazole, the therapeutic window has not been established yet, although a recent work identified 4.87 mg/L and 5.13 mg/L in serum to be the threshold for toxicity (Furfaro et al., 2019). The simulated mean concentrations in our study were below those values and even though a fraction of the population exceeded them, the main toxicity reported was gastrointestinal and not severe.

Despite the synergism found in vitro for the combination of isavuconazole with echinocandins, when the PK/PD simulations were conducted to generate expected kill curves for virtual patients, it was revealed that none of the combinations at standard or higher dosages would be effective against these isolates of *C. auris*. Simulation outcomes for lower MICs showed that the combination of isavuconazole and micafungin was not successful for the evaluated doses and MIC scenarios. Conversely, combinations of isavuconazole with anidulafungin or caspofungin were able to inhibit fungal growth, depending on the dosing regimens tested for MICs up to 0.03 mg/L for isavuconazole and 0.06 mg/L for echinocandins. These MIC thresholds for high-dosing combination therapy were similar to the susceptibility-breakpoints for anidulafungin and micafungin established by EUCAST for *C. albicans* and *C. glabrata* (Arendrup et al., 2020b). In a recent study by Bader et al., echinocandin exposure values were generated with Monte Carlo simulations and PTA analysis was conducted in order to evaluate approved doses and higher ones for the treatment of *C. glabrata* infections. Interestingly, anidulafungin at standard dosages (200 mg followed by 100 mg daily) was unlikely to attain therapeutic exposures relative to MIC_{90} in most simulated patients. Moreover, dose increases to 300 mg followed by 200 mg daily, did not achieve a significant improvement. In contrast, micafungin and caspofungin achieved therapeutic exposures at standard approved dosages and relative to MIC_{90} values. However, when these two echinocandins were evaluated one dilution above the MIC_{90} for *C. glabrata*, micafungin did not result in favourable PTA while caspofungin did. To sum up, this study suggested that regardless of dosing increases of anidulafungin and micafungin, these two drugs are unlikely to provide therapeutic exposures against isolates with elevated MICs (one dilution above the MIC_{90}) (Bader et al., 2018). Our simulation results, despite conducted with another modelling and simulation approach, are in agreement with Bader et al., since the standard or alternative dosing regimens of echinocandins,

even combined with isavuconazole in our studies, would not provide successful outcomes when dealing with *C. auris* isolates with elevated MIC values. In view of these results, testing other regimes such as extended-interval dosing regimens was ruled out, although it might initially seem interesting because of the long half-life of anidulafungin, caspofungin and isavuconazole, together with the concentration-dependent activity of the antifungal drugs. In this regard, despite promising results have been reported with extended-interval dosing in murine models of candidiasis (Gumbo et al., 2007; Lepak et al., 2016), clinical studies evaluating such regimens are lacking.

While there are not susceptibility-breakpoints for isavuconazole yet, the threshold of 0.03 mg/L in combination therapy also resembles the conclusions of Wu et al. driven by Monte Carlo simulations and the PTA with standard treatment against *Candida* (Wu et al., 2020). Overall, this highlights the importance of bridging the in vitro results to an in vivo scenario, as the conclusions may change drastically. However, that bridging is also challenging and there are some important considerations that need to be addressed, as it will be discussed below.

Drugs are bound to proteins in plasma, most prominently to albumin and α-1-glycoprotein acid. Only the unbound fraction of the drug will be able to exert its effect on the microorganism (Gonzalez et al., 2013). To account for this widely acknowledged fact, when a PK/PD model is used for simulating clinical outcomes, the total plasma concentrations of the drug measured or predicted are corrected for the unbound fraction reported in literature (Nielsen and Friberg, 2013). Although it is an accepted approach, it may be simplistic, especially for highly protein-bound (>90%) compounds like antifungal drugs. Anidulafungin and micafungin are bound to plasma proteins up to 99 and 99.8% respectively. When the total plasma concentrations after standard treatments of both drugs are corrected by the unbound fraction, the free drug concentrations are suboptimal, and simulation outcomes point erroneously to therapeutic failures (Gil-Alonso et al., 2016b). In vitro experiments have shown that serum indeed affects the activity of antifungal drugs compared to protein-free mediums, but the increase in MIC or fungicidal concentrations in those works were not as high as predicted by the unbound-fraction (Odabasi et al., 2007; Ishikawa et al., 2009; Cafini et al., 2012; Elefanti et al., 2013). Ishikawa et al. investigated and compared the activity of micafungin in RPMI medium and in serum from patients and evidenced an antifungal activity in serum much higher than the anticipated by a free fraction of 0.02% (Ishikawa et al., 2009). They suggested that the binding of micafungin might be weak and reversible, and that in the presence of *Candida*, it releases from the protein

and binds to the fungal target. Elefanti et al. also used a similar reasoning to explain the activity of anidulafungin, amphotericin B and voriconazole in serum against *Aspergillus*. Nevertheless, they theorized that the shift from bound to unbound drug might be not so prominent in vivo, since the total volume of drug distribution is much bigger than the volume of infection, which is the opposite of the in vitro environment (Elefanti et al., 2013). Cafini et al. reported that not only anidulafungin and voriconazole were active in serum against *Aspergillus*, but also that the drug activity was higher in serum that in media supplemented with albumin (Cafini et al., 2012). This could reflect an influence of the rest of plasma proteins and components in the drug-fungus interaction. Interestingly, Kovács et al. recently found that echinocandins were more active in serum-supplemented RPMI than in standard RPMI against *C. auris*. In this case, the authors stated that high concentrations of echinocandin might stimulate chitin synthesis as a compensatory mechanism; lower free drug concentrations in serum-supplemented media would not trigger that biosynthesis, thus paradoxically leading to a higher killing activity (Kovács et al., 2021).

Besides the complex interaction that might happen between the drug, the pharmacological target and plasma proteins (Peletier et al., 2009), there are also some clinical scenarios that might change the drug free fraction, such as hypoalbuminaemia. Hypoalbuminaemia refers to low levels of serum albumin, which increases unbound drug concentrations. Since hypoalbuminaemia is a common state in critically ill patients, free drug concentrations of highly bound antimicrobials will be higher in those patients (Ulldemolins et al., 2011). A study found that teicoplanin unbound fraction ranged from 71 to 97%, with higher unbound levels correlating with lower albumin levels (Roberts et al., 2014). Increased free drug concentrations subsequently lead to higher volume of distribution and an augmented clearance, which would be problematic for time-dependant antimicrobials, whereas concentration-dependant drugs like antifungals would probably benefit from the high free levels, especially for the first hours in the dosing interval (Roberts et al., 2013). In this line, Martial et al. argued that the PTA values calculated for micafungin in ICU patients in their work might be underestimated, as they did not have information regarding free micafungin concentrations (Martial et al., 2017).

Another complex in vivo factor not accounted for in simulations is tissue distribution. When the infection site is located in organs and tissues outside plasma, the drug must reach those locations in order to exert an antimicrobial effect. Thus, the PD of anti-infective drugs would be more related to tissue concentrations rather than plasma concentrations (González et al.,

2013). Echinocandins are rapidly and widely distributed into organs affected by invasive candidiasis such as the kidneys, lungs, liver and spleen, achieving higher concentrations than in plasma (Bellman and Smuszkiewicz, 2017). Louie et al. observed in a murine model of systemic candidiasis that whereas the concentration of caspofungin in plasma was below the MIC, the concentration in kidney tissue was much higher and thus, better explained the antifungal activity (Louie et al., 2005). Anidulafungin also remains longer in these tissues than in plasma, achieving tissue concentrations ten times that of plasma, as seen in animal models (Gumbo et al., 2006; Damle et al., 2008). Gumbo et al. stated that the tissue concentrations of anidulafungin in rats are in the order of the estimated EC_{50}, and therefore, more closely related to the observed effect in clinical practice (Gumbo et al., 2006). On the other hand, micafungin tissue concentrations are more similar to the plasmatic ones, but the antifungal effect is persistent even when tissue concentrations are below the MIC (Gumbo et al., 2007). To date, there are not available studies on specific tissue distribution of echinocandins in humans. With regard to isavuconazole, studies in both animals and humans have shown that it is well distributed into tissue, including hard to access ones like the brain, and that those concentrations are high enough to exert an effect (Warn et al., 2009; Ervens et al., 2014; Wiederhold et al., 2016; Schmitt-Hoffmann et al., 2017; Lee et al., 2019).

In conclusion, the developed PK/PD model was able to characterise properly the antifungal activity of isavuconazole in combination with echinocandins against *C. auris*. Model-based simulations predicted that the combinations of isavuconazole with anidulafungin or caspofungin would be effective for MICs up to 0.03 and 0.06 mg/L respectively, whereas the combination with micafungin would lead to treatment failure. Further studies are needed to better understand the interaction between drugs and fungal targets in vivo and thus, to strengthen simulation-based decision-making.

4. Limitations of the study and future steps

There are certain limitations in this Thesis that need to be addressed. Some of these limitations were directly related to methodological aspects of this work, while other limitations were inherent to the novel and emerging nature of this pathogen.

The main limitation of the present study was the limited number of isolates tested. Of note, our study only included bloodstream isolates of *C. auris*, collected from the main outbreak in a Spanish hospital, first detected in 2016. When the experimental part of the Thesis was launched in 2017, the outbreak of *C. auris* in Spain had just started, with a significant focus on Hospital Universitario y Politécnico La Fe, in Valencia, that kindly provided the six isolates for this project. However, this Thesis work does not fall within the framework of large-scale studies on the screening of antifungal activity against this newly emerged pathogen, but responds to the need to shed more light on the activity of the main groups of drugs available, both first line and alternative, by using pharmacometric tools. In this line, one of the advantages of PK/PD modelling and simulation applied to antimicrobial compounds, is that this approach allows a proper characterisation of in vitro data gathered from few strains. Nevertheless, the incorporation of more isolates, especially from different clades, would have broadened the knowledge and applicability of the results of this work.

As it has been previously stated, in vitro time-kill curves have certain limitations. Complex in vivo factors such as immune response and drug distribution are overlooked. Additonally, the medium in which the time-kill experiments have been/are carried out is also another factor to take into consideration. On one hand, fungal burden may be overestimated, as growth rate is much faster in the rich environment of the microbiological broth culture than in the human infection sites (de la Peña et al., 2004). On the other, as it is a protein-free medium, concentration-effect relationships have to be corrected for the protein binding accounted in literature, which may also be an oversimplification (Peletier et al., 2009; Elefanti et al., 2013). Studies that investigate tissue distribution in humans and free drug concentrations at infection sites are needed, as it would improve model-based simulations and predictions. Nevertheless, given the limitations, in vitro results should be supported by further in vivo studies in animal models of invasive candidiasis.

Very few studies have characterised the activity of different antifungal drugs with time-kill methods (Dudiuk et al., 2019; Kovács et al., 2021) and the PK/PD modelling and simulation

approaches for *C. auris* infection are still lacking, precluding comparison of our results in some aspects. So far, regarding *C. auris* antifungal susceptibility testing and interpretation reports are mostly based on MIC.

The absence of clinical guidelines that include antifungal combination therapy recommendations was another noteworthy limitation. We are aware that although there are no clinical guidelines to support it, the use of combinations of antifungal drugs, in particular amphotericin B together with echinocandins concomitantly and at full doses, has been shown to be effective and is often used. In the absence of recommendations for combinations in clinical guidelines, the selection of scenarios to simulate the dosing regimens of combination therapies was based on clinical experience as suggested by clinicians.

VI. CONCLUSIONS

1. The MICs of amphotericin B, isavuconazole, anidulafungin, caspofungin and micafungin were below the proposed tentative susceptibility breakpoints for *C. auris*.

2. Amphotericin B showed concentration-dependent fungicidal activity against *C. auris* in time-kill assays. Conversely, neither isavuconazole nor the echinocandins showed fungicidal or fungistatic against *C. auris*.

3. The PAFE exerted by amphotericin B was very short and had no role in the fungicidal activity of the drug.

4. The combination of amphotericin B with anidulafungin or caspofungin significantly enhanced the activity of the drugs compared to monotherapy at the concentrations tested in time-kill curves.

5. There was an overall agreement between the parametric and non-parametric methods in the interpretation of the checkerboard data.

6. There was concordance between the checkerboard method and time-kill curve methodology for the evaluation of drug-drug interactions.

7. The interaction of isavuconazole and anidulafungin, caspofungin or micafungin was deemed synergistic by the checkerboard method and time-kill assays. In addition, the antifungal activity determined in time-kill curve experiments was concentration-dependent and fungistatic.

8. A semi-mechanistic PK/PD model consisting of fungal subpopulations with different drug-susceptibilities was able to characterise the activity of amphotericin B in time-kill curves.

9. Pharmacometric simulations predicted that the studied *C. auris* isolates would be resistant to amphotericin B treatment.

10. Simulations performed with different MIC scenarios suggested a susceptibility breakpoint of amphotericin B for *C. auris* lower than the currently proposed one.

11. A PK/PD model adapted for drug combinations successfully characterised both the activity and the nature of the interaction for the combinations of isavuconazole with anidulafungin, caspofungin or micafungin.

12. PK/PD modelling-based simulations predicted that the studied *C. auris* isolates would be resistant to isavuconazole and echinocandin combination treatment.

13. Simulations conducted with different MIC scenarios and alternative dosing schedules predicted the highest activity for the combination of isavuconazole and caspofungin, followed by the combination of isavuconazole and anidulafungin. Isavuconazole plus micafungin did not show any activity.

VII. REFERENCES

Adams, E., Quinn, M., Tsay, S., Poirot, E., Chaturvedi, S., Southwick, K. et al. (2018). *Candida auris* in healthcare facilities, New York, USA, 2013-2017. *Emerg. Infect. Dis.* 10, 1816-1824. doi:10.3201/eid2410.180649 [doi]

Ahmad, S., Joseph, L., Parker, J. E., Asadzadeh, M., Kelly, S. L., Meis, J. F. and Khan, Z. (2019). *ERG6* and *ERG2* are major targets conferring reduced susceptibility to amphotericin B in clinical *Candida glabrata* isolates in Kuwait. *Antimicrob. Agents Chemother.* 2, 10.1128/AAC.01900-18. Print 2019 Feb. doi:e01900-18 [pii]

Ahmadi, A., Mahmoudi, S., Rezaie, S., Hashemi, S. J., Dannaoui, E., Badali, H. et al. (2020). In vitro synergy of echinocandins with triazoles against fluconazole-resistant *Candida parapsilosis* complex isolates. *J. Glob. Antimicrob. Resist.*, 331-334. doi:S2213-7165(19)30295-4 [pii]

Andes, D., Diekema, D. J., Pfaller, M. A., Prince, R. A., Marchillo, K., Ashbeck, J. and Hou, J. (2008). In vivo pharmacodynamic characterization of anidulafungin in a neutropenic murine candidiasis model. *Antimicrob. Agents Chemother.* 2, 539-550. doi:AAC.01061-07 [pii]

Andes, D., Stamsted, T. and Conklin, R. (2001). Pharmacodynamics of amphotericin B in a neutropenic-mouse disseminated-candidiasis model. *Antimicrob.Agents Chemother.* 3, 922-926. doi:10.1128/AAC.45.3.922-926.2001 [doi]

Arendrup, M. C., Chowdhary, A., Jorgensen, K. M. and Meletiadis, J. (2020a). Manogepix (APX001A) in vitro activity against *Candida auris*: Head-to-head comparison of EUCAST and CLSI MICs. *Antimicrob. Agents Chemother.* 10, 10.1128/AAC.00656-20. Print 2020 Sep 21. doi:e00656-20 [pii]

Arendrup, M. C., Friberg, N., Mares, M., Kahlmeter, G., Meletiadis, J., Guinea, J. and Subcommittee on Antifungal Susceptibility Testing (AFST) of the ESCMID European Committee for Antimicrobial Susceptibility Testing (EUCAST). (2020b). How to interpret MICs of antifungal compounds according to the revised clinical breakpoints v. 10.0. *Clin. Microbiol.Infect.* 11, 1464-1472. doi:S1198-743X(20)30347-5 [pii]

Arendrup, M. C., Jorgensen, K. M., Hare, R. K. and Chowdhary, A. (2020c). In vitro activity of ibrexafungerp (SCY-078) against *Candida auris* isolates as determined by EUCAST methodology and comparison with activity against *C. albicans* and *C. glabrata* and with the activities of six comparator agents. *Antimicrob.Agents Chemother.* 3, 10.1128/AAC.02136-19. Print 2020 Feb 21. doi:e02136-19 [pii]

Arendrup, M. C. and Patterson, T. F. (2017a). Multidrug-resistant *Candida*: Epidemiology, molecular mechanisms, and treatment. *J.Infect.Dis.* suppl_3, S445-S451. doi:10.1093/infdis/jix131 [doi]

Arendrup, M. C., Prakash, A., Meletiadis, J., Sharma, C. and Chowdhary, A. (2017b). Comparison of EUCAST and CLSI reference microdilution MICs of eight antifungal compounds for *Candida auris* and associated tentative epidemiological cutoff values. *Antimicrob. Agents Chemother.* 6, 10.1128/AAC.00485-17. Print 2017 Jun. doi:e00485-17 [pii]

Asín-Prieto, E., Rodriguez-Gascon, A. and Isla, A. (2015). Applications of the pharmacokinetic/pharmacodynamic (PK/PD) analysis of antimicrobial agents. *J. Infect. Chemother.* 5, 319-329. doi:10.1016/j.jiac.2015.02.001 [doi]

Asner, S. A., Giulieri, S., Diezi, M., Marchetti, O. and Sanglard, D. (2015). Acquired multidrug antifungal resistance in *Candida lusitaniae* during therapy. *Antimicrob. Agents Chemother.* 12, 7715-7722. doi:10.1128/AAC.02204-15 [doi]

Astvad, K. M. T., Sanglard, D., Delarze, E., Hare, R. K. and Arendrup, M. C. (2018). Implications of the EUCAST trailing phenomenon in *Candida tropicalis* for the in vivo susceptibility in invertebrate and murine models. *Antimicrob. Agents Chemother.* 12, 10.1128/AAC.01624-18. Print 2018 Dec. doi:e01624-18 [pii]

Baddley, J. W. and Pappas, P. G. (2005). Antifungal combination therapy: Clinical potential. *Drugs.* 11, 1461-1480. doi:65112 [pii]

Balani, S. K., Xu, X., Arison, B. H., Silva, M. V., Gries, A., DeLuna, F. A. et al. (2000). Metabolites of caspofungin acetate, a potent antifungal agent, in human plasma and urine. *Drug Metab. Dispos.* 11, 1274-1278.

Baltch, A. L., Bopp, L. H., Smith, R. P., Ritz, W. J. and Michelsen, P. B. (2008). Anticandidal effects of voriconazole and caspofungin, singly and in combination, against *Candida glabrata*, extracellularly and intracellularly in granulocyte-macrophage colony stimulating factor (GM-CSF)-activated human monocytes. *J. Antimicrob. Chemother.* 6, 1285-1290. doi:10.1093/jac/dkn361 [doi]

Bauer, R. J. (2019a). NONMEM tutorial part I: Description of commands and options, with simple examples of population analysis. *CPT Pharmacometrics Syst. Pharmacol.* doi:10.1002/psp4.12404 [doi]

Bauer, R. J. (2019b). NONMEM tutorial part II: Estimation methods and advanced examples. *CPT Pharmacometrics Syst. Pharmacol.* doi:10.1002/psp4.12422 [doi]

Bekersky, I., Fielding, R. M., Dressler, D. E., Lee, J. W., Buell, D. N. and Walsh, T. J. (2002a). Pharmacokinetics, excretion, and mass balance of liposomal amphotericin B (AmBisome) and amphotericin B deoxycholate in humans. *Antimicrob. Agents Chemother.* 3, 828-833. doi:10.1128/aac.46.3.828-833.2002 [doi]

Bekersky, I., Fielding, R. M., Dressler, D. E., Lee, J. W., Buell, D. N. and Walsh, T. J. (2002b). Plasma protein binding of amphotericin B and pharmacokinetics of bound versus unbound amphotericin B after administration of intravenous liposomal amphotericin B (AmBisome) and amphotericin B deoxycholate. *Antimicrob. Agents Chemother.* 3, 834-840. doi:10.1128/aac.46.3.834-840.2002 [doi]

Bellmann, R. and Smuszkiewicz, P. (2017). Pharmacokinetics of antifungal drugs: Practical implications for optimized treatment of patients. *Infection.* 6, 737-779. doi:10.1007/s15010-017-1042-z [doi]

Bidaud, A. L., Botterel, F., Chowdhary, A. and Dannaoui, E. (2019). In vitro antifungal combination of flucytosine with amphotericin B, voriconazole, or micafungin against *Candida auris* shows no antagonism. *Antimicrob. Agents Chemother.* doi:AAC.01393-19 [pii]

Bidaud, A. L., Djenontin, E., Botterel, F., Chowdhary, A. and Dannaoui, E. (2020). Colistin interacts synergistically with echinocandins against *Candida auris. Int. J. Antimicrob. Agents.* 3, 105901. doi:S0924-8579(20)30040-6 [pii]

Binder, U., Aigner, M., Risslegger, B., Hortnagl, C., Lass-Florl, C. and Lackner, M. (2019). Minimal inhibitory concentration (MIC)-phenomena in *Candida albicans* and their impact on the diagnosis of antifungal resistance. *J. Fungi (Basel).* 3, 10.3390/jof5030083. doi:E83 [pii]

Brill, M. J. E., Kristoffersson, A. N., Zhao, C., Nielsen, E. I. and Friberg, L. E. (2018). Semi-mechanistic pharmacokinetic-pharmacodynamic modelling of antibiotic drug combinations. *Clin. Microbiol. Infect.* 7, 697-706. doi:S1198-743X(17)30670-5 [pii]

Buil, J. B., Bruggemann, R. J. M., Bedin Denardi, L., Melchers, W. J. G. and Verweij, P. E. (2020). In vitro interaction of isavuconazole and anidulafungin against azole-susceptible and azole-resistant *Aspergillus fumigatus* isolates. *J. Antimicrob. Chemother.* 9, 2582-2586. doi:10.1093/jac/dkaa185 [doi]

Cafini, F., Sevillano, D., Alou, L., Gomez-Aguado, F., Corcuera, M. T., Gonzalez, N. et al. (2012). Effect of protein binding on the activity of voriconazole alone or combined with anidulafungin against *Aspergillus* spp. using a time-kill methodology. *Rev. Esp. Quimioter.* 1, 47-55. doi:cafini [pii]

Cantón, E. and Pemán, J. (1999). Antifungal time-kill curves. *Rev. Iberoam. Micol.* 2, 82-85. doi:19991682 [pii]

Cantón, E., Pemán, J., Hervás, D. and Espinel-Ingroff, A. (2013). Examination of the in vitro fungicidal activity of echinocandins against *Candida lusitaniae* by time-killing methods. *J. Antimicrob. Chemother.* 4, 864-868. doi:10.1093/jac/dks489 [doi]

Cantón, E., Pemán, J., Sastre, M., Romero, M. and Espinel-Ingroff, A. (2006). Killing kinetics of caspofungin, micafungin, and amphotericin B against *Candida guilliermondii*. *Antimicrob. Agents Chemother.* 8, 2829-2832. doi:50/8/2829 [pii]

CDC. (2019). Antibiotic Resistance Threats in the United States, 2019. U.S. Department of Health and Human Services, CDC. https://stacks.cdc.gov/view/cdc/82532

CDC. (2020) . *C .auris* antifungal susceptibility testing and breakpoints. https://www.cdc.gov/fungal/candida-auris/c-auris-antifungal.html

Chabot, G. G., Pazdur, R., Valeriote, F. A. and Baker, L. H. (1989). Pharmacokinetics and toxicity of continuous infusion amphotericin B in cancer patients. *J. Pharm. Sci.* 4, 307-310. doi:S0022-3549(15)47938-9 [pii]

Chen, J., Tian, S., Han, X., Chu, Y., Wang, Q., Zhou, B. and Shang, H. (2020). Is the superbug fungus really so scary? A systematic review and meta-analysis of global epidemiology and mortality of *Candida auris*. *BMC Infect. Dis.* 1, 827-020-05543-0. doi:10.1186/s12879-020-05543-0 [doi]

Chen, Y. L., Lehman, V. N., Averette, A. F., Perfect, J. R. and Heitman, J. (2013). Posaconazole exhibits in vitro and in vivo synergistic antifungal activity with caspofungin or FK506 against *Candida albicans. PLoS One.* 3, e57672. doi:10.1371/journal.pone.0057672 [doi]

Chou, T. C. (2006). Theoretical basis, experimental design, and computerized simulation of synergism and antagonism in drug combination studies. *Pharmacol. Rev.* 3, 621-681. doi:58/3/621 [pii]

Chowdhary, A., Prakash, A., Sharma, C., Kordalewska, M., Kumar, A., Sarma, S. et al. (2018). A multicentre study of antifungal susceptibility patterns among 350 *Candida auris* isolates (2009-17) in india: Role of the *ERG11* and *FKS1* genes in azole and echinocandin resistance. *J. Antimicrob. Chemother.* 4, 891-899. doi:10.1093/jac/dkx480 [doi]

D'Argenio DZ, Schumitzky A, Wang X. (2009). ADAPT 5 user's guide: Pharmacokinetic/pharmacodynamic systems analysis software. Biomedical Simulations Resource.

Damle, B., Stogniew, M. and Dowell, J. (2008). Pharmacokinetics and tissue distribution of anidulafungin in rats. *Antimicrob. Agents Chemother.* 7, 2673-2676. doi:10.1128/AAC.01596-07 [doi]

de la Peña, A., Grabe, A., Rand, K. H., Rehak, E., Gross, J., Thyroff-Friesinger, U. et al. (2004). PK-PD modelling of the effect of cefaclor on four different bacterial strains. *Int. J. Antimicrob. Agents.* 3, 218-225. doi:10.1016/j.ijantimicag.2003.07.009 [doi]

de Oliveira, H. C., Monteiro, M. C., Rossi, S. A., Peman, J., Ruiz-Gaitan, A., Mendes-Giannini, M. J. S. et al. (2019). Identification of off-patent compounds that present antifungal activity

against the emerging fungal pathogen *Candida auris. Front. Cell. Infect. Microbiol.*, 83. doi:10.3389/fcimb.2019.00083 [doi]

Denardi, L. B., Keller, J. T., Oliveira, V., Mario, D. A. N., Santurio, J. M. and Alves, S. H. (2017). Activity of combined antifungal agents against multidrug-resistant *Candida glabrata* strains. *Mycopathologia.* 9-10, 819-828. doi:10.1007/s11046-017-0141-9 [doi]

Di Bonaventura, G., Spedicato, I., Picciani, C., D'Antonio, D. and Piccolomini, R. (2004). In vitro pharmacodynamic characteristics of amphotericin B, caspofungin, fluconazole, and voriconazole against bloodstream isolates of infrequent *Candida* species from patients with hematologic malignancies. *Antimicrob. Agents Chemother.* 11, 4453-4456. doi:48/11/4453 [pii]

Di Veroli, G. Y., Fornari, C., Wang, D., Mollard, S., Bramhall, J. L., Richards, F. M. and Jodrell, D. I. (2016). Combenefit: An interactive platform for the analysis and visualization of drug combinations. *Bioinformatics.* 18, 2866-2868. doi:10.1093/bioinformatics/btw230 [doi]

Dowell, J. A., Knebel, W., Ludden, T., Stogniew, M., Krause, D. and Henkel, T. (2004). Population pharmacokinetic analysis of anidulafungin, an echinocandin antifungal. *J. Clin .Pharmacol.* 6, 590-598. doi:10.1177/0091270004265644 [doi]

Du, H., Bing, J., Hu, T., Ennis, C. L., Nobile, C. J. and Huang, G. (2020). *Candida auris*: Epidemiology, biology, antifungal resistance, and virulence. *PLoS Pathog.* 10, e1008921. doi:10.1371/journal.ppat.1008921 [doi]

Dudiuk, C., Berrio, I., Leonardelli, F., Morales-Lopez, S., Theill, L., Macedo, D. et al. (2019). Antifungal activity and killing kinetics of anidulafungin, caspofungin and amphotericin B against *Candida auris*. *J. Antimicrob. Chemother.* 8, 2295-2302. doi:10.1093/jac/dkz178 [doi]

Eldesouky, H. E., Li, X., Abutaleb, N. S., Mohammad, H. and Seleem, M. N. (2018). Synergistic interactions of sulfamethoxazole and azole antifungal drugs against emerging multidrug-resistant *Candida auris*. *Int. J. Antimicrob. Agents.* 6, 754-761. doi:S0924-8579(18)30242-5 [pii]

Elefanti, A., Mouton, J. W., Krompa, K., Al-Saigh, R., Verweij, P. E., Zerva, L. and Meletiadis, J. (2013). Inhibitory and fungicidal effects of antifungal drugs against *Aspergillus* species in the presence of serum. *Antimicrob. Agents Chemother.* 4, 1625-1631. doi:10.1128/AAC.01573-12 [doi]

Elefanti, A., Mouton, J. W., Verweij, P. E., Zerva, L. and Meletiadis, J. (2014). Susceptibility breakpoints for amphotericin B and *Aspergillus* species in an in vitro pharmacokinetic-pharmacodynamic model simulating free-drug concentrations in human serum. *Antimicrob. Agents Chemother.* 4, 2356-2362. doi:10.1128/AAC.02661-13 [doi]

Ellepola, A. N. (2012). Amphotericin B-induced in vitro postantifungal effect on *Candida* species of oral origin. *Med. Princ. Pract.* 5, 442-446. doi:10.1159/000339080 [doi]

Ellsworth, M. and Ostrosky-Zeichner, L. (2020). Isavuconazole: Mechanism of action, clinical efficacy, and resistance. *J. Fungi (Basel).* 4, 10.3390/jof6040324. doi:E324 [pii]

Eriksson, U., Seifert, B. and Schaffner, A. (2001). Comparison of effects of amphotericin B deoxycholate infused over 4 or 24 hours: Randomised controlled trial. *Bmj.* 7286, 579-582. doi:10.1136/bmj.322.7286.579 [doi]

Ernst, E. J., Klepser, M. E. and Pfaller, M. A. (2000). Postantifungal effects of echinocandin, azole, and polyene antifungal agents against *Candida albicans* and *Cryptococcus neoformans*. *Antimicrob. Agents Chemother.* 4, 1108-1111. doi:10.1128/aac.44.4.1108-1111.2000 [doi]

Ervens, J., Ghannoum, M., Graf, B. and Schwartz, S. (2014). Successful isavuconazole salvage therapy in a patient with invasive mucormycosis. *Infection.* 2, 429-432. doi:10.1007/s15010-013-0552-6 [doi]

Espinel-Ingroff, A., Arendrup, M. C., Pfaller, M. A., Bonfietti, L. X., Bustamante, B., Canton, E. et al. (2013). Interlaboratory variability of caspofungin MICs for *Candida* spp. using CLSI and EUCAST methods: Should the clinical laboratory be testing this agent? *Antimicrob. Agents Chemother.* 12, 5836-5842. doi:10.1128/AAC.01519-13 [doi]

Espinel-Ingroff, A. and Canton, E. (2011). In vitro activity of echinocandins against non-*Candida albicans*: Is echinocandin antifungal activity the same? *Enferm. Infecc .Microbiol. Clin.*, 3-9. doi:10.1016/S0213-005X(11)70002-7 [doi]

Espinel-Ingroff, A. and Turnidge, J. (2016). The role of epidemiological cutoff values (ECVs/ECOFFs) in antifungal susceptibility testing and interpretation for uncommon yeasts and moulds. *Rev. Iberoam. Micol.* 2, 63-75. doi:10.1016/j.riam.2016.04.001 [doi]

Ette, I.E and Williams, J.P. (Eds). (2007). Pharmacometrics. the science of quantitative pharmacology. John Wiley and Sons.

EUCAST. (2020a). Amphotericin B: Rationale for the clinical breakpoints, version 2.0, 2020. https://eucast.org/astoffungi/rationale_documents_for_antifungals/

EUCAST. (2020b). EUCAST definitive document 7.3.2. Method for the determination of broth dilution minimum inhibitory concentrations of antifungal agents for yeasts. https://www.eucast.org/astoffungi/methodsinantifungalsusceptibilitytesting/susceptibility_testing_of_yeasts/

Fakhim, H., Chowdhary, A., Prakash, A., Vaezi, A., Dannaoui, E., Meis, J. F. and Badali, H. (2017). In vitro interactions of echinocandins with triazoles against multidrug-resistant *Candida auris*. *Antimicrob. Agents Chemother.* 11, 10.1128/AAC.01056-17. Print 2017 Nov. doi:e01056-17 [pii]

Forgacs, L., Borman, A. M., Prepost, E., Toth, Z., Kardos, G., Kovács, R. et al. (2020). Comparison of in vivo pathogenicity of four *Candida auris* clades in a neutropenic bloodstream infection murine model. *Emerg. Microbes Infect.* 1, 1160-1169. doi:10.1080/22221751.2020.1771218 [doi]

Furfaro, E., Signori, A., Di Grazia, C., Dominietto, A., Raiola, A. M., Aquino, S. et al. (2019). Serial monitoring of isavuconazole blood levels during prolonged antifungal therapy. *J. Antimicrob. Chemother.* 8, 2341-2346. doi:10.1093/jac/dkz188 [doi]

García-Effron, G. (2020). Rezafungin-mechanisms of action, susceptibility and resistance: Similarities and differences with the other echinocandins. *J. Fungi (Basel).* 4, 10.3390/jof6040262. doi:E262 [pii]

Ghannoum, M., Arendrup, M. C., Chaturvedi, V. P., Lockhart, S. R., McCormick, T. S., Chaturvedi, S. et al. (2020). Ibrexafungerp: A novel oral triterpenoid antifungal in development for the treatment of *Candida auris* infections. *Antibiotics (Basel).* 9, 10.3390/antibiotics9090539. doi:E539 [pii]

Giacobbe, D. R., Maraolo, A. E., Simeon, V., Magne, F., Pace, M. C., Gentile, I. et al. (2020). Changes in the relative prevalence of candidaemia due to non-albicans candida species in adult in-patients: A systematic review, meta-analysis and meta-regression. *Mycoses.* 4, 334-342. doi:10.1111/myc.13054 [doi]

Gil-Alonso, S., Jauregizar, N., Canton, E., Eraso, E. and Quindos, G. (2015a). In vitro fungicidal activities of anidulafungin, caspofungin, and micafungin against *Candida glabrata, Candida bracarensis*, and *Candida nivariensis* evaluated by time-kill studies. *Antimicrob.Agents Chemother.* 6, 3615-3618. doi:10.1128/AAC.04474-14 [doi]

Gil-Alonso, S., Jauregizar, N., Eraso, E. and Quindós, G. (2015b). Postantifungal effect of micafungin against the species complexes of *Candida albicans* and *Candida parapsilosis. PLoS One.* 7, e0132730. doi:10.1371/journal.pone.0132730 [doi]

Gil-Alonso, S., Jauregizar, N., Eraso, E. and Quindós, G. (2016a). Postantifungal effect of caspofungin against the *Candida albicans* and *Candida parapsilosis* clades. *Diagn. Microbiol. Infect. Dis.* 2, 172-177. doi:10.1016/j.diagmicrobio.2016.07.011 [doi]

Gil-Alonso, S., Jauregizar, N., Ortega, I., Eraso, E., Suarez, E. and Quindós, G. (2016b). In vitro pharmacodynamic modelling of anidulafungin against *Candida* spp. *Int.J.Antimicrob.Agents.* 3, 178-183. doi:10.1016/j.ijantimicag.2015.12.011 [doi]

González, D., Schmidt, S. and Derendorf, H. (2013). Importance of relating efficacy measures to unbound drug concentrations for anti-infective agents. *Clin. Microbiol. Rev.* 2, 274-288. doi:10.1128/CMR.00092-12 [doi]

Gray, K. C., Palacios, D. S., Dailey, I., Endo, M. M., Uno, B. E., Wilcock, B. C. and Burke, M. D. (2012). Amphotericin primarily kills yeast by simply binding ergosterol. *Proc. Natl. Acad. Sci. U.S.A.* 7, 2234-2239. doi:10.1073/pnas.1117280109 [doi]

Greco, W. R., Bravo, G. and Parsons, J. C. (1995). The search for synergy: A critical review from a response surface perspective. *Pharmacol. Rev.* 2, 331-385.

Greco, W. R., Faessel, H. and Levasseur, L. (1996). The search for cytotoxic synergy between anticancer agents: A case of Dorothy and the ruby slippers? *J. Natl. Cancer Inst.* 11, 699-700. doi:10.1093/jnci/88.11.699 [doi]

Grégoire, N., Raherison, S., Grignon, C., Comets, E., Marliat, M., Ploy, M. C. and Couet, W. (2010). Semimechanistic pharmacokinetic-pharmacodynamic model with adaptation development for time-kill experiments of ciprofloxacin against *Pseudomonas aeruginosa*. *Antimicrob. Agents Chemother.* 6, 2379-2384. doi:10.1128/AAC.01478-08 [doi]

Groll, A. H., Desai, A., Han, D., Howieson, C., Kato, K., Akhtar, S. et al. (2017). Pharmacokinetic assessment of drug-drug interactions of isavuconazole with the immunosuppressants cyclosporine, mycophenolic acid, prednisolone, sirolimus, and tacrolimus in healthy adults. *Clin. Pharmacol. Drug Dev.* 1, 76-85. doi:10.1002/cpdd.284 [doi]

Groll, A. H., Rijnders, B. J. A., Walsh, T. J., Adler-Moore, J., Lewis, R. E. and Bruggemann, R. J. M. (2019). Clinical pharmacokinetics, pharmacodynamics, safety and efficacy of liposomal amphotericin B. *Clin. Infect. Dis.* Suppl 4, S260-S274. doi:10.1093/cid/ciz076 [doi]

Guinea, J., Pelaez, T., Recio, S., Torres-Narbona, M. and Bouza, E. (2008). In vitro antifungal activities of isavuconazole (BAL4815), voriconazole, and fluconazole against 1,007 isolates of *Zygomycete, Candida, Aspergillus, Fusarium*, and *Scedosporium* species. *Antimicrob. Agents Chemother.* 4, 1396-1400. doi:10.1128/AAC.01512-07 [doi]

Gumbo, T., Drusano, G. L., Liu, W., Kulawy, R. W., Fregeau, C., Hsu, V. and Louie, A. (2007). Once-weekly micafungin therapy is as effective as daily therapy for disseminated candidiasis in mice with persistent neutropenia. *Antimicrob. Agents Chemother.* 3, 968-974. doi:AAC.01337-06 [pii]

Hiemenz, J., Cagnoni, P., Simpson, D., Devine, S., Chao, N., Keirns, J. et al. (2005). Pharmacokinetic and maximum tolerated dose study of micafungin in combination with fluconazole versus fluconazole alone for prophylaxis of fungal infections in adult patients

undergoing a bone marrow or peripheral stem cell transplant. *Antimicrob. Agents Chemother.* 4, 1331-1336. doi:49/4/1331 [pii]

Hooker, A. C., Staatz, C. E. and Karlsson, M. O. (2007). Conditional weighted residuals (CWRES): A model diagnostic for the FOCE method. *Pharm. Res.* 12, 2187-2197. doi:10.1007/s11095-007-9361-x [doi]

Hossain, M. A., Reyes, G. H., Long, L. A., Mukherjee, P. K. and Ghannoum, M. A. (2003). Efficacy of caspofungin combined with amphotericin B against azole-resistant *Candida albicans*. *J. Antimicrob. Chemother.* 6, 1427-1429. doi:10.1093/jac/dkg230 [doi]

Ishikawa, J., Maeda, T., Matsumura, I., Yasumi, M., Ujiie, H., Masaie, H. et al. (2009). Antifungal activity of micafungin in serum. *Antimicrob. Agents Chemother.* 10, 4559-4562. doi:10.1128/AAC.01404-08 [doi]

Jarque, I., Tormo, M., Bello, J. L., Rovira, M., Batlle, M., Julia, A. et al. (2013). Caspofungin for the treatment of invasive fungal disease in hematological patients (ProCAS study). *Med.Mycol.* 2, 150-154. doi:10.3109/13693786.2012.693213 [doi]

Kapralos, I., Mainas, E., Apostolopoulou, O., Siopi, M., Neroutsos, E., Apostolidi, S. et al. (2021). Population pharmacokinetics of anidulafungin in ICU patients assessing inter- and intrasubject variability. *Br. J. Clin. Pharmacol.* 3, 1024-1032. doi:10.1111/bcp.14457 [doi]

Kardos, T., Kovács, R., Kardos, G., Varga, I., Bozo, A., Tóth, Z. et al. (2018). Poor in vivo efficacy of caspofungin, micafungin and amphotericin B against wild-type *Candida krusei* clinical isolates does not correlate with in vitro susceptibility results. *J. Chemother.* 4, 233-239. doi:10.1080/1120009X.2018.1487150 [doi]

Karlsson, M. O. and Savic, R. M. (2007). Diagnosing model diagnostics. *Clin. Pharmacol. Ther.* 1, 17-20. doi:6100241 [pii]

Karlsson, M. O. and Sheiner, L. B. (1993). The importance of modeling interoccasion variability in population pharmacokinetic analyses. *J. Pharmacokinet. Biopharm.* 6, 735-750. doi:10.1007/BF01113502 [doi]

Katiyar, S. K., Alastruey-Izquierdo, A., Healey, K. R., Johnson, M. E., Perlin, D. S. and Edlind, T. D. (2012). *Fks1* and *Fks2* are functionally redundant but differentially regulated in *Candida glabrata*: Implications for echinocandin resistance. *Antimicrob. Agents Chemother.* 12, 6304-6309. doi:10.1128/AAC.00813-12 [doi]

Katragkou, A., McCarthy, M., Meletiadis, J., Hussain, K., Moradi, P. W., Strauss, G. E. et al. (2017). In vitro combination therapy with isavuconazole against *Candida* spp. *Med. Mycol.* 8, 859-868. doi:10.1093/mmy/myx006 [doi]

Katragkou, A., McCarthy, M., Meletiadis, J., Petraitis, V., Moradi, P. W., Strauss, G. E. et al. (2014). In vitro combination of isavuconazole with micafungin or amphotericin B deoxycholate against medically important molds. *Antimicrob. Agents Chemother.* 11, 6934-6937. doi:10.1128/AAC.03261-14 [doi]

Khan, D. D., Friberg, L. E. and Nielsen, E. I. (2016). A pharmacokinetic-pharmacodynamic (PKPD) model based on in vitro time-kill data predicts the in vivo PK/PD index of colistin. *J. Antimicrob. Chemother.* 7, 1881-1884. doi:10.1093/jac/dkw057 [doi]

Kim, J. H., Cheng, L. W., Chan, K. L., Tam, C. C., Mahoney, N., Friedman, M. et al. (2020). Antifungal drug repurposing. *Antibiotics (Basel).* 11, 10.3390/antibiotics9110812. doi:E812 [pii]

Kim, M. N., Shin, J. H., Sung, H., Lee, K., Kim, E. C., Ryoo, N. et al. (2009). *Candida haemulonii* and closely related species at 5 university hospitals in Korea: Identification, antifungal susceptibility, and clinical features. *Clin. Infect. Dis.* 6, e57-61. doi:10.1086/597108 [doi]

Kiraz, N., Dag, I., Yamac, M., Kiremitci, A., Kasifoglu, N. and Akgun, Y. (2009). Antifungal activity of caspofungin in combination with amphotericin B against candida glabrata: Comparison of disk diffusion, etest, and time-kill methods. *Antimicrob.Agents Chemother.* 2, 788-790. doi:10.1128/AAC.01131-08 [doi]

Kiraz, N., Dag, I., Yamac, M., Kiremitci, A., Kasifoglu, N. and Oz, Y. (2010). Synergistic activities of three triazoles with caspofungin against *Candida glabrata* isolates determined by time-kill, E-test, and disk diffusion methods. *Antimicrob. Agents Chemother.* 5, 2244-2247. doi:10.1128/AAC.01527-09 [doi]

Klepser, M. E., Wolfe, E. J., Jones, R. N., Nightingale, C. H. and Pfaller, M. A. (1997). Antifungal pharmacodynamic characteristics of fluconazole and amphotericin B tested against *Candida albicans*. *Antimicrob. Agents Chemother.* 6, 1392-1395. doi:10.1128/AAC.41.6.1392 [doi]

Kovács, R., Tóth, Z., Locke, J. B., Forgács, L., Kardos, G., Nagy, F. et al. (2021). Comparison of in vitro killing activity of rezafungin, anidulafungin, caspofungin, and micafungin against four *Candida auris* clades in RPMI-1640 in the absence and presence of human serum. *Microorganisms.* 4, 10.3390/microorganisms9040863. doi:863 [pii]

Kullberg, B. J. and Arendrup, M. C. (2015). Invasive candidiasis. *N. Engl. J. Med.* 15, 1445-1456. doi:10.1056/NEJMra1315399 [doi]

Kullberg, B. J., Viscoli, C., Pappas, P. G., Vázquez, J., Ostrosky-Zeichner, L., Rotstein, C. et al. (2019). Isavuconazole versus caspofungin in the treatment of candidemia and other invasive *Candida* infections: The ACTIVE trial. *Clin. Infect. Dis.* 12, 1981-1989. doi:10.1093/cid/ciy827 [doi]

Kuse, E. R., Chetchotisakd, P., da Cunha, C. A., Ruhnke, M., Barrios, C., Raghunadharao, D. et al. (2007). Micafungin versus liposomal amphotericin B for candidaemia and invasive candidosis: A phase III randomised double-blind trial. *Lancet.* 9572, 1519-1527. doi:S0140-6736(07)60605-9 [pii]

Laniado-Laborín, R. and Cabrales-Vargas, M. N. (2009). Amphotericin B: Side effects and toxicity. *Rev. Iberoam. Micol.* 4, 223-227. doi:10.1016/j.riam.2009.06.003 [doi]

Larkin, E., Hager, C., Chandra, J., Mukherjee, P. K., Retuerto, M., Salem, I. et al. (2017). The emerging pathogen *Candida auris*: Growth phenotype, virulence factors, activity of antifungals, and effect of SCY-078, a novel glucan synthesis inhibitor, on growth morphology and biofilm formation. *Antimicrob. Agents Chemother.* 5, 10.1128/AAC.02396-16. Print 2017 May. doi:e02396-16 [pii]

Lepak, A. J., Marchillo, K., VanHecker, J., Diekema, D. and Andes, D. R. (2013). Isavuconazole pharmacodynamic target determination for *Candida* species in an in vivo murine disseminated candidiasis model. *Antimicrob. Agents Chemother.* 11, 5642-5648. doi:10.1128/AAC.01354-13 [doi]

Lepak, A. J., Zhao, M., Berkow, E. L., Lockhart, S. R. and Andes, D. R. (2017). Pharmacodynamic optimization for treatment of invasive *Candida auris* infection. *Antimicrob. Agents Chemother.* 8, 10.1128/AAC.00791-17. Print 2017 Aug. doi:e00791-17 [pii]

Lepak, A. J., Zhao, M., VanScoy, B., Ambrose, P. G. and Andes, D. R. (2018). Pharmacodynamics of a long-acting echinocandin, CD101, in a neutropenic invasive-candidiasis murine model using an extended-interval dosing design. *Antimicrob.Agents Chemother.* 2, 10.1128/AAC.02154-17. Print 2018 Feb. doi:e02154-17 [pii]

Lewis, R. E., Diekema, D. J., Messer, S. A., Pfaller, M. A. and Klepser, M. E. (2002). Comparison of E-test, chequerboard dilution and time-kill studies for the detection of synergy or antagonism between antifungal agents tested against *Candida* species. *J. Antimicrob. Chemother.* 2, 345-351. doi:10.1093/jac/49.2.345 [doi]

Li, Y., Nguyen, M. H., Cheng, S., Schmidt, S., Zhong, L., Derendorf, H. and Clancy, C. J. (2008). A pharmacokinetic/pharmacodynamic mathematical model accurately describes the activity of voriconazole against *Candida* spp. in vitro. *Int. J. Antimicrob.Agents.* 4, 369-374. doi:10.1016/j.ijantimicag.2007.11.015 [doi]

Lignell, A., Johansson, A., Lowdin, E., Cars, O. and Sjolin, J. (2007). A new in-vitro kinetic model to study the pharmacodynamics of antifungal agents: Inhibition of the fungicidal activity of amphotericin B against *Candida albicans* by voriconazole. *Clin. Microbiol. Infect.* 6, 613-619. doi:S1198-743X(14)62228-X [pii]

Lockhart, S. R. (2019). *Candida auris* and multidrug resistance: Defining the new normal. *Fungal Genet. Biol.*, 103243. doi:S1087-1845(19)30150-1 [pii]

Lockhart, S. R., Etienne, K. A., Vallabhaneni, S., Farooqi, J., Chowdhary, A., Govender, N. P. et al. (2017). Simultaneous emergence of multidrug-resistant *Candida auris* on 3 continents confirmed by whole-genome sequencing and epidemiological analyses. *Clin. Infect. Dis.* 2, 134-140. doi:10.1093/cid/ciw691 [doi]

Louie, A., Deziel, M., Liu, W., Drusano, M. F., Gumbo, T. and Drusano, G. L. (2005). Pharmacodynamics of caspofungin in a murine model of systemic candidiasis: Importance

of persistence of caspofungin in tissues to understanding drug activity. *Antimicrob. Agents Chemother.* 12, 5058-5068. doi:49/12/5058 [pii]

Maharom, P. and Thamlikitkul, V. (2006). Implementation of clinical practice policy on the continuous intravenous administration of amphotericin B deoxycholate. *J. Med. Assoc. Thai.*, S118-24.

Manavathu, E. K., Ramesh, M. S., Baskaran, I., Ganesan, L. T. and Chandrasekar, P. H. (2004). A comparative study of the post-antifungal effect (PAFE) of amphotericin B, triazoles and echinocandins on *Aspergillus fumigatus* and *Candida albicans*. *J. Antimicrob. Chemother.* 2, 386-389. doi:10.1093/jac/dkh066 [doi]

Mangal, N., Hamadeh, I. S., Arwood, M. J., Cavallari, L. H., Samant, T. S., Klinker, K. P. et al. (2018). Optimization of voriconazole therapy for the treatment of invasive fungal infections in adults. *Clin. Pharmacol. Ther.* 5, 957-965. doi:10.1002/cpt.1012 [doi]

Marcos-Zambrano, L. J., Escribano, P., Sánchez-Carrillo, C., Bouza, E. and Guinea, J. (2016). Scope and frequency of fluconazole trailing assessed using EUCAST in invasive *Candida* spp. isolates. *Med. Mycol.* 7, 733-739. doi:10.1093/mmy/myw033 [doi]

Mariné, M., Espada, R., Torrado, J., Pastor, F. J. and Guarro, J. (2009). Efficacy of a new formulation of amphotericin B in murine disseminated infections by *Candida glabrata* or *Candida tropicalis*. *Int. J. Antimicrob. Agents.* 6, 566-569. doi:10.1016/j.ijantimicag.2009.07.005 [doi]

Martial, L. C., Bruggemann, R. J., Schouten, J. A., van Leeuwen, H. J., van Zanten, A. R., de Lange, D. W. et al. (2016). Dose reduction of caspofungin in intensive care unit patients with Child-Pugh B will result in suboptimal exposure. *Clin. Pharmacokinet.* 6, 723-733. doi:10.1007/s40262-015-0347-2 [doi]

Martial, L. C., Ter Heine, R., Schouten, J. A., Hunfeld, N. G., van Leeuwen, H. J., Verweij, P. E. et al. (2017). Population pharmacokinetic model and pharmacokinetic target attainment of micafungin in intensive care unit patients. *Clin. Pharmacokinet.* 10, 1197-1206. doi:10.1007/s40262-017-0509-5 [doi]

Mediavilla, A., Peralta, G. and Flórez, J. (2014). Fármacos antifúngicos. In J. Flórez, J. A. Armijo and A. Mediavilla (Eds.), *Farmacología humana* (6th ed., pp. 1055-1067). Elsevier.

Meletiadis, J., Verweij, P. E., TeDorsthorst, D. T., Meis, J. F. and Mouton, J. W. (2005). Assessing in vitro combinations of antifungal drugs against yeasts and filamentous fungi: Comparison of different drug interaction models. *Med. Mycol.* 2, 133-152. doi:10.1080/13693780410001731547 [doi]

Mohamed, A. F., Kristoffersson, A. N., Karvanen, M., Nielsen, E. I., Cars, O. and Friberg, L. E. (2016). Dynamic interaction of colistin and meropenem on a WT and a resistant strain of *Pseudomonas aeruginosa* as quantified in a PK/PD model. *J. Antimicrob. Chemother.* 5, 1279-1290. doi:10.1093/jac/dkv488 [doi]

Mohr, J. F., Hall, A. C., Ericsson, C. D. and Ostrosky-Zeichner, L. (2005). Fatal amphotericin B overdose due to administration of nonlipid formulation instead of lipid formulation. *Pharmacotherapy.* 3, 426-428. doi:10.1592/phco.25.3.426.61603 [doi]

Morales-López, S. E., Parra-Giraldo, C. M., Ceballos-Garzón, A., Martínez, H. P., Rodríguez, G. J., Álvarez-Moreno, C. A. and Rodríguez, J. Y. (2017). Invasive infections with multidrug-resistant yeast *Candida auris*, Colombia. *Emerg. Infect. Dis.* 1, 162-164. doi:10.3201/eid2301.161497 [doi]

Mouton, J. W., Dudley, M. N., Cars, O., Derendorf, H. and Drusano, G. L. (2005). Standardization of pharmacokinetic/pharmacodynamic (PK/PD) terminology for anti-infective drugs: An update. *J. Antimicrob. Chemother.* 5, 601-607. doi:dki079 [pii]

Mpakosi, A., Siopi, M., Falaina, V., Siafakas, N., Roilides, E., Kimouli, M. et al. (2016). Successful therapy of *Candida pulcherrima* fungemia in a premature newborn with liposomal amphotericin B and micafungin. *Med. Mycol. Case Rep.*, 24-27. doi:10.1016/j.mmcr.2016.08.002 [doi]

Mueller, M., de la Peña, A. and Derendorf, H. (2004). Issues in pharmacokinetics and pharmacodynamics of anti-infective agents: Kill curves versus MIC. *Antimicrob. Agents Chemother.* 2, 369-377. doi:10.1128/aac.48.2.369-377.2004 [doi]

Mukherjee, P. K., Sheehan, D. J., Hitchcock, C. A. and Ghannoum, M. A. (2005). Combination treatment of invasive fungal infections. *Clin. Microbiol. Rev.* 1, 163-194. doi:18/1/163 [pii]

Muñoz, J. F., Gade, L., Chow, N. A., Loparev, V. N., Juieng, P., Berkow, E. L. et al. (2018). Genomic insights into multidrug-resistance, mating and virulence in *Candida auris* and related emerging species. *Nat. Commun.* 1, 5346-018-07779-6. doi:10.1038/s41467-018-07779-6 [doi]

Nguyen, K. T., Ta, P., Hoang, B. T., Cheng, S., Hao, B., Nguyen, M. H. and Clancy, C. J. (2009). Anidulafungin is fungicidal and exerts a variety of postantifungal effects against *Candida albicans, C. glabrata, C. parapsilosis,* and *C. krusei* isolates. *Antimicrob. Agents Chemother.* 8, 3347-3352. doi:10.1128/AAC.01480-08 [doi]

Nielsen, E. I., Cars, O. and Friberg, L. E. (2011). Pharmacokinetic/pharmacodynamic (PK/PD) indices of antibiotics predicted by a semimechanistic PKPD model: A step toward model-based dose optimization. *Antimicrob. Agents Chemother.* 10, 4619-4630. doi:10.1128/AAC.00182-11 [doi]

Nielsen, E. I. and Friberg, L. E. (2013). Pharmacokinetic-pharmacodynamic modeling of antibacterial drugs. *Pharmacol .Rev.* 3, 1053-1090. doi:10.1124/pr.111.005769 [doi]

Novak, A. R., Bradley, M. E., Kiser, T. H. and Mueller, S. W. (2020). Azole-resistant *Aspergillus* and echinocandin-resistant *Candida* - what are the treatment options? *Curr. Fungal Infect. Rep.* 2, 141-152. doi:10.1007/s12281-020-00379-2 [doi]

O'Brien, B., Chaturvedi, S. and Chaturvedi, V. (2020). In vitro evaluation of antifungal drug combinations against multidrug-resistant *Candida auris* isolates from New York outbreak. *Antimicrob. Agents Chemother.* 4, 10.1128/AAC.02195-19. Print 2020 Mar 24. doi:e02195-19 [pii]

Odabasi, Z., Paetznick, V., Rex, J. H. and Ostrosky-Zeichner, L. (2007). Effects of serum on in vitro susceptibility testing of echinocandins. *Antimicrob. Agents Chemother.* 11, 4214-4216. doi:AAC.01589-06 [pii]

Odds, F. C. (2003). Synergy, antagonism, and what the chequerboard puts between them. *J. Antimicrob. Chemother.* 1, 1. doi:10.1093/jac/dkg301 [doi]

Olson, J. A., Adler-Moore, J. P., Smith, P. J. and Proffitt, R. T. (2005). Treatment of *Candida glabrata* infection in immunosuppressed mice by using a combination of liposomal amphotericin B with caspofungin or micafungin. *Antimicrob. Agents Chemother.* 12, 4895-4902. doi:49/12/4895 [pii]

Ong, C. W., Chen, S. C., Clark, J. E., Halliday, C. L., Kidd, S. E., Marriott, D. J. et al. (2019). Diagnosis, management and prevention of *Candida auris* in hospitals: Position statement of the Australasian Society for Infectious Diseases. *Intern. Med. J.* 10, 1229-1243. doi:10.1111/imj.14612 [doi]

Ong, V., Hough, G., Schlosser, M., Bartizal, K., Balkovec, J. M., James, K. D. and Krishnan, B. R. (2016). Preclinical evaluation of the stability, safety, and efficacy of CD101, a novel echinocandin. *Antimicrob. Agents Chemother.* 11, 6872-6879. doi:10.1128/AAC.00701-16 [doi]

Osei Sekyere, J. (2019). *Candida auris*: A systematic review and meta-analysis of current updates on an emerging multidrug-resistant pathogen. *Microbiologyopen.* 8, e00901. doi:10.1002/mbo3.901 [doi]

Ostrosky-Zeichner, L., Kontoyiannis, D., Raffalli, J., Mullane, K. M., Vazquez, J., Anaissie, E. J. et al. (2005). International, open-label, non-comparative, clinical trial of micafungin alone and in combination for treatment of newly diagnosed and refractory candidemia. *Eur.J.Clin.Microbiol.Infect.Dis.* 10, 654-661. doi:10.1007/s10096-005-0024-8 [doi]

Otto, R. G., van Gorp, E., Kloezen, W., Meletiadis, J., van den Berg, S. and Mouton, J. W. (2019). An alternative strategy for combination therapy: Interactions between polymyxin B and non-antibiotics. *Int. J. Antimicrob. Agents.* 1, 34-39. doi:S0924-8579(18)30262-0 [pii]

Owen, J. S. and Fiedler-Kelly J. (2014). Introduction to Population Pharmacokinetic/Pharmacodynamic Analysis with Nonlinear Mixed Effects Models. John Wiley and Sons.

Oz, Y., Kiremitci, A., Dag, I., Metintas, S. and Kiraz, N. (2013). Postantifungal effect of the combination of caspofungin with voriconazole and amphotericin B against clinical *Candida krusei* isolates. *Med. Mycol.* 1, 60-65. doi:10.3109/13693786.2012.697198 [doi]

Palacios, D. S., Anderson, T. M. and Burke, M. D. (2007). A post-PKS oxidation of the amphotericin B skeleton predicted to be critical for channel formation is not required for potent antifungal activity. *J. Am. Chem. Soc.* 45, 13804-13805. doi:10.1021/ja075739o [doi]

Pappas, P. G., Kauffman, C. A., Andes, D. R., Clancy, C. J., Marr, K. A., Ostrosky-Zeichner, L. et al. (2016). Clinical practice guideline for the management of candidiasis: 2016 update by the Infectious Diseases Society of America. *Clin. Infect. Dis.* 4, e1-50. doi:10.1093/cid/civ933 [doi]

Pappas, P. G., Lionakis, M. S., Arendrup, M. C., Ostrosky-Zeichner, L. and Kullberg, B. J. (2018). Invasive candidiasis. *Nat. Rev. Dis. Primers.*, 18026. doi:10.1038/nrdp.2018.26 [doi]

Pea, F. (2020). From bench to bedside: Perspectives on the utility of pharmacokinetics/pharmacodynamics in predicting the efficacy of antifungals in invasive candidiasis. *Mycoses.* 8, 854-858. doi:10.1111/myc.13121 [doi]

Peleg, A. Y. and Woods, M. L. (2004). Continuous and 4 h infusion of amphotericin B: A comparative study involving high-risk haematology patients. *J. Antimicrob. Chemother.* 4, 803-808. doi:10.1093/jac/dkh403 [doi]

Peletier, L. A., Benson, N. and van der Graaf, P. H. (2009). Impact of plasma-protein binding on receptor occupancy: An analytical description. *J. Theor. Biol.* 2, 253-262. doi:10.1016/j.jtbi.2008.09.014 [doi]

Perlin, D. S. (2011). Current perspectives on echinocandin class drugs. *Future Microbiol.* 4, 441-457. doi:10.2217/fmb.11.19 [doi]

Pfaller, M. A. (2012). Antifungal drug resistance: Mechanisms, epidemiology, and consequences for treatment. *Am. J. Med.* 1 Suppl, S3-13. doi:10.1016/j.amjmed.2011.11.001 [doi]

Pfaller, M. A., Carvalhaes, C., Messer, S. A., Rhomberg, P. R. and Castanheira, M. (2020). Activity of a long-acting echinocandin, rezafungin, and comparator antifungal agents tested against contemporary invasive fungal isolates (SENTRY program, 2016 to 2018).

Antimicrob. Agents Chemother. 4, 10.1128/AAC.00099-20. Print 2020 Mar 24. doi:e00099-20 [pii]

Pfaller, M. A., Huband, M. D., Flamm, R. K., Bien, P. A. and Castanheira, M. (2019). In vitro activity of APX001A (manogepix) and comparator agents against 1,706 fungal isolates collected during an international surveillance program in 2017. *Antimicrob. Agents Chemother.* 8, 10.1128/AAC.00840-19. Print 2019 Aug. doi:e00840-19 [pii]

Pfaller, M. A., Messer, S. A., Deshpande, L. M., Rhomberg, P. R., Utt, E. A. and Castanheira, M. (2021). Evaluation of synergistic activity of isavuconazole or voriconazole plus anidulafungin and the occurrence and genetic characterization of *Candida auris* detected in a surveillance program. *Antimicrob. Agents Chemother.* 4, 10.1128/AAC.02031-20. Print 2021 Mar 18. doi:e02031-20 [pii]

Prichard, M. N., Prichard, L. E. and Shipman, C., Jr. (1993). Strategic design and three-dimensional analysis of antiviral drug combinations. *Antimicrob.Agents Chemother.* 3, 540-545. doi:10.1128/aac.37.3.540 [doi]

Quindós, G. (2015). Micología médica. Elsevier.

Quindós, G., Marcos-Arias, C., San-Millán, R., Mateo, E. and Eraso, E. (2018). The continuous changes in the aetiology and epidemiology of invasive candidiasis: From familiar *Candida albicans* to multiresistant *Candida auris*. *Int. Microbiol.* 3, 107-119. doi:10.1007/s10123-018-0014-1 [doi]

Raffetin, A., Courbin, V., Jullien, V. and Dannaoui, E. (2017). In vitro combination of isavuconazole with echinocandins against azole-susceptible and -resistant *Aspergillus* spp. *Antimicrob. Agents Chemother.* 1, 10.1128/AAC.01382-17. Print 2018 Jan. doi:e01382-17 [pii]

Rex, J. H., Pappas, P. G., Karchmer, A. W., Sobel, J., Edwards, J. E., Hadley, S. et al. (2003). A randomized and blinded multicenter trial of high-dose fluconazole plus placebo versus fluconazole plus amphotericin B as therapy for candidemia and its consequences in non-neutropenic subjects. *Clin. Infect. Dis.* 10, 1221-1228. doi:CID30440 [pii]

Roberts, J. A., Pea, F. and Lipman, J. (2013). The clinical relevance of plasma protein binding changes. *Clin. Pharmacokinet.* 1, 1-8. doi:10.1007/s40262-012-0018-5 [doi]

Roberts, J. A., Stove, V., De Waele, J. J., Sipinkoski, B., McWhinney, B., Ungerer, J. P. et al. (2014). Variability in protein binding of teicoplanin and achievement of therapeutic drug monitoring targets in critically ill patients: Lessons from the DALI study. *Int. J. Antimicrob. Agents.* 5, 423-430. doi:10.1016/j.ijantimicag.2014.01.023 [doi]

Roberts, S. C., Zembower, T. R., Bolon, M. K., Kadakia, A. R., Gilley, J. H., Ko, J. H. et al. (2019). Successful treatment of a candida auris intra-articular infection. *Emerg.Microbes Infect.* 1, 866-868. doi:10.1080/22221751.2019.1625287 [doi]

Rodriguez, M. M., Ruiz, M., Pastor, F. J., Quindos, G., Carrillo, A. and Guarro, J. (2007). In vitro interaction of micafungin and fluconazole against *Candida*. *J. Antimicrob. Chemother.* 1, 188-190. doi:dkm177 [pii]

Roell, K. R., Reif, D. M. and Motsinger-Reif, A. A. (2017). An introduction to terminology and methodology of chemical synergy-perspectives from across disciplines. *Front. Pharmacol.* 158. doi:10.3389/fphar.2017.00158 [doi]

Roling, E. E., Klepser, M. E., Wasson, A., Lewis, R. E., Ernst, E. J. and Pfaller, M. A. (2002). Antifungal activities of fluconazole, caspofungin (MK0991), and anidulafungin (LY 303366) alone and in combination against *Candida* spp. and *Crytococcus neoformans* via time-kill methods. *Diagn. Microbiol. Infect. Dis.* 1, 13-17. doi:S0732889302003619 [pii]

Rosenberg, A., Ene, I. V., Bibi, M., Zakin, S., Segal, E. S., Ziv, N. et al. (2018). Antifungal tolerance is a subpopulation effect distinct from resistance and is associated with persistent candidemia. *Nat. Commun.* 1, 2470-018-04926-x. doi:10.1038/s41467-018-04926-x [doi]

Ruiz-Gaitán, A., Moret, A. M., Tasias-Pitarch, M., Aleixandre-Lopez, A. I., Martinez-Morel, H., Calabuig, E. et al. (2018). An outbreak due to *Candida auris* with prolonged colonisation and candidaemia in a tertiary care European hospital. *Mycoses.* 7, 498-505. doi:10.1111/myc.12781 [doi]

Ruiz-Gaitán, A. C., Cantón, E., Fernández-Rivero, M. E., Ramírez, P. and Pemán, J. (2019). Outbreak of *Candida auris* in Spain: A comparison of antifungal activity by three methods

with published data. *Int. J. Antimicrob. Agents.* 5, 541-546. doi:S0924-8579(19)30028-7 [pii]

Saitoh, T., Matsushima, T., Shimizu, H., Osaki, Y., Yamane, A., Irisawa, H. et al. (2008). Successful treatment of azole-refractory *Candida guilliermondii* fungemia with a combination therapy of micafungin and liposomal amphotericin B. *Rinsho Ketsueki.* 2, 94-98.

Sandison, T., Ong, V., Lee, J. and Thye, D. (2017). Safety and pharmacokinetics of CD101 IV, a novel echinocandin, in healthy adults. *Antimicrob. Agents Chemother.* 2, 10.1128/AAC.01627-16. Print 2017 Feb. doi:e01627-16 [pii]

Sasse, C., Dunkel, N., Schafer, T., Schneider, S., Dierolf, F., Ohlsen, K. and Morschhauser, J. (2012). The stepwise acquisition of fluconazole resistance mutations causes a gradual loss of fitness in *Candida albicans. Mol. Microbiol.* 3, 539-556. doi:10.1111/j.1365-2958.2012.08210.x [doi]

Satoh, K., Makimura, K., Hasumi, Y., Nishiyama, Y., Uchida, K. and Yamaguchi, H. (2009). *Candida auris* sp. nov., a novel ascomycetous yeast isolated from the external ear canal of an inpatient in a Japanese hospital. *Microbiol. Immunol.* 1, 41-44. doi:10.1111/j.1348-0421.2008.00083.x [doi]

Schmidt, S., Barbour, A., Sahre, M., Rand, K. H. and Derendorf, H. (2008). PK/PD: New insights for antibacterial and antiviral applications. *Curr. Opin. Pharmacol.* 5, 549-556. doi:10.1016/j.coph.2008.06.010 [doi]

Schmidt, S., Sabarinath, S. N., Barbour, A., Abbanat, D., Manitpisitkul, P., Sha, S. and Derendorf, H. (2009). Pharmacokinetic-pharmacodynamic modeling of the in vitro activities of oxazolidinone antimicrobial agents against methicillin-resistant *Staphylococcus aureus*. *Antimicrob. Agents Chemother.* 12, 5039-5045. doi:10.1128/AAC.00633-09 [doi]

Schmidt, S., Schuck, E., Kumar, V., Burkhardt, O. and Derendorf, H. (2007). Integration of pharmacokinetic/pharmacodynamic modeling and simulation in the development of new anti-infective agents - minimum inhibitory concentration versus time-kill curves. *Expert Opin. Drug Discov.* 6, 849-860. doi:10.1517/17460441.2.6.849 [doi]

Schmitt-Hoffmann, A., Roos, B., Maares, J., Heep, M., Spickerman, J., Weidekamm, E. et al. (2006). Multiple-dose pharmacokinetics and safety of the new antifungal triazole BAL4815 after intravenous infusion and oral administration of its prodrug, BAL8557, in healthy volunteers. *Antimicrob. Agents Chemother.* 1, 286-293. doi:50/1/286 [pii]

Schwarz, P., Bidaud, A. L. and Dannaoui, E. (2020). In vitro synergy of isavuconazole in combination with colistin against *Candida auris*. *Sci. Rep.* 1, 21448-020-78588-5. doi:10.1038/s41598-020-78588-5 [doi]

Scorneaux, B., Angulo, D., Borroto-Esoda, K., Ghannoum, M., Peel, M. and Wring, S. (2017). SCY-078 is fungicidal against *Candida* species in time-kill studies. *Antimicrob. Agents Chemother.* 3, 10.1128/AAC.01961-16. Print 2017 Mar. doi:e01961-16 [pii]

Serena, C., Mariné, M., Quindós, G., Carrillo, A. J., Cano, J. F., Pastor, F. J. and Guarro, J. (2008). In vitro interactions of micafungin with amphotericin B against clinical isolates of *Candida* spp. *Antimicrob. Agents Chemother.* 4, 1529-1532. doi:10.1128/AAC.01097-07 [doi]

Shaw, K. J. and Ibrahim, A. S. (2020). Fosmanogepix: A review of the first-in-class broad spectrum agent for the treatment of invasive fungal infections. *J. Fungi (Basel).* 4, 10.3390/jof6040239. doi:E239 [pii]

Smith, R. P., Baltch, A., Bopp, L. H., Ritz, W. J. and Michelsen, P. P. (2011). Post-antifungal effects and time-kill studies of anidulafungin, caspofungin, and micafungin against *Candida glabrata* and *Candida parapsilosis*. *Diagn. Microbiol. Infect. Dis.* 2, 131-138. doi:10.1016/j.diagmicrobio.2011.06.018 [doi]

Soo Hoo, L. (2017). Fungal fatal attraction: A mechanistic review on targeting liposomal amphotericin B (AmBisome®) to the fungal membrane. *J. Liposome Res.* 3, 180-185. doi:10.1080/08982104.2017.1360345 [doi]

Stone, J. A., Holland, S. D., Wickersham, P. J., Sterrett, A., Schwartz, M., Bonfiglio, C. et al. (2002). Single- and multiple-dose pharmacokinetics of caspofungin in healthy men. *Antimicrob. Agents Chemother.* 3, 739-745. doi:10.1128/aac.46.3.739-745.2002 [doi]

Stone, J. A., Xu, X., Winchell, G. A., Deutsch, P. J., Pearson, P. G., Migoya, E. M. et al. (2004). Disposition of caspofungin: Role of distribution in determining pharmacokinetics in plasma. *Antimicrob. Agents Chemother.* 3, 815-823. doi:10.1128/aac.48.3.815-823.2004 [doi]

Sy, S., Zhuang, L., Xia, H., Beaudoin, M. E., Schuck, V. J. and Derendorf, H. (2017). Prediction of in vivo and in vitro infection model results using a semimechanistic model of avibactam and aztreonam combination against multidrug resistant organisms. *CPT Pharmacometrics Syst. Pharmacol.* 3, 197-207. doi:10.1002/psp4.12159 [doi]

Taori, S. K., Khonyongwa, K., Hayden, I., Athukorala, G. D. A., Letters, A., Fife, A. et al. (2019). *Candida auris* outbreak: Mortality, interventions and cost of sustaining control. *J. Infect.* 6, 601-611. doi:S0163-4453(19)30278-6 [pii]

Teixeira-Santos, R., Rocha, R., Moreira-Rosario, A., Monteiro-Soares, M., Cantón, E., Rodrigues, A. G. and Pina-Vaz, C. (2012). Novel method for evaluating in vitro activity of anidulafungin in combination with amphotericin B or azoles. *J. Clin. Microbiol.* 8, 2748-2754. doi:10.1128/JCM.00610-12 [doi]

Thai, H. T., Mentre, F., Holford, N. H., Veyrat-Follet, C. and Comets, E. (2014). Evaluation of bootstrap methods for estimating uncertainty of parameters in nonlinear mixed-effects models: A simulation study in population pharmacokinetics. *J. Pharmacokinet. Pharmacodyn.* 1, 15-33. doi:10.1007/s10928-013-9343-z [doi]

Thompson, G. R., Soriano, A., Skoutelis, A., Vazquez, J. A., Honore, P. M., Horcajada, J. P. et al. (2020). Rezafungin versus caspofungin in a phase 2, randomized, double-blind study for the treatment of candidemia and invasive candidiasis- the STRIVE trial. *Clin. Infect. Dis.* doi:ciaa1380 [pii]

Townsend, R., Dietz, A., Hale, C., Akhtar, S., Kowalski, D., Lademacher, C. et al. (2017). Pharmacokinetic evaluation of CYP3A4-mediated drug-drug interactions of isavuconazole with rifampin, ketoconazole, midazolam, and ethinyl estradiol/norethindrone in healthy adults. *Clin. Pharmacol. Drug Dev.* 1, 44-53. doi:10.1002/cpdd.285 [doi]

Trivedi, A., Lee, R. E. and Meibohm, B. (2013). Applications of pharmacometrics in the clinical development and pharmacotherapy of anti-infectives. *Expert Rev. Clin. Pharmacol.* 2, 159-170. doi:10.1586/ecp.13.6 [doi]

Ulldemolins, M., Roberts, J. A., Rello, J., Paterson, D. L. and Lipman, J. (2011). The effects of hypoalbuminaemia on optimizing antibacterial dosing in critically ill patients. *Clin. Pharmacokinet.* 2, 99-110. doi:10.2165/11539220-000000000-00000 [doi]

Valentín, A., Cantón, E., Pemán, J., Fernández-Rivero, M. E., Tormo-Mas, M. A. and Martínez, J. P. (2016). In vitro activity of anidulafungin in combination with amphotericin B or voriconazole against biofilms of five *Candida* species. *J. Antimicrob. Chemother.* 12, 3449-3452. doi:dkw316 [pii]

Varga, I., Soczo, G., Kardos, G. and Majoros, L. (2008). Time-kill studies investigating the killing activity of caspofungin against *Candida dubliniensis*: Comparing RPMI-1640 and antibiotic medium 3. *J.Antimicrob.Chemother.* 1, 149-152. doi:10.1093/jac/dkn144 [doi]

Venisse, N., Grégoire, N., Marliat, M. and Couet, W. (2008). Mechanism-based pharmacokinetic-pharmacodynamic models of in vitro fungistatic and fungicidal effects against *Candida albicans*. *Antimicrob.Agents Chemother.* 3, 937-943. doi:10.1128/AAC.01030-07 [doi]

Wall, G., Chaturvedi, A. K., Wormley, F. L.,Jr, Wiederhold, N. P., Patterson, H. P., Patterson, T. F. and López-Ribot, J. L. (2018). Screening a repurposing library for inhibitors of multidrug-resistant *Candida auris* identifies ebselen as a repositionable candidate for antifungal drug development. *Antimicrob. Agents Chemother.* 10, 10.1128/AAC.01084-18. Print 2018 Oct. doi:e01084-18 [pii]

Walsh, T. J., Finberg, R. W., Arndt, C., Hiemenz, J., Schwartz, C., Bodensteiner, D. et al. (1999). Liposomal amphotericin B for empirical therapy in patients with persistent fever and neutropenia. *N. Engl. J. Med.* 10, 764-771. doi:10.1056/NEJM199903113401004 [doi]

Wiederhold, N. P., Kovanda, L., Najvar, L. K., Bocanegra, R., Olivo, M., Kirkpatrick, W. R. and Patterson, T. F. (2016). Isavuconazole is effective for the treatment of experimental cryptococcal meningitis. *Antimicrob. Agents Chemother.* 9, 5600-5603. doi:10.1128/AAC.00229-16 [doi]

Wiederhold, N. P., Najvar, L. K., Jaramillo, R., Olivo, M., Pizzini, J., Catano, G. and Patterson, T. F. (2018). Oral glucan synthase inhibitor SCY-078 is effective in an experimental murine model of invasive candidiasis caused by WT and echinocandin-resistant *Candida glabrata*. *J. Antimicrob. Chemother.* 2, 448-451. doi:10.1093/jac/dkx422 [doi]

WHO. (2019). WHO model list of essential medicines- 21st list, 2019. https://www.who.int/publications/i/item/WHOMVPEMPIAU2019.06

WHO. (2020). First meeting of the WHO Antifungal Expert Group on Identifying Priority Fungal Pathogens: meeting report. https://www.who.int/publications/i/item/9789240006355

Wu, X., Venkataramanan, R., Rivosecchi, R. M., Tang, C., Marini, R. V., Shields, R. K. et al. (2020). Population pharmacokinetics of intravenous isavuconazole in solid-organ transplant recipients. *Antimicrob. Agents Chemother.* 2, 10.1128/AAC.01728-19. Print 2020 Jan 27. doi:e01728-19 [pii]

Wu, Y., Totten, M., Memon, W., Ying, C. and Zhang, S. X. (2020). In vitro antifungal susceptibility of the emerging multidrug-resistant pathogen *Candida auris* to miltefosine alone and in combination with amphotericin B. *Antimicrob. Agents Chemother.* 2, 10.1128/AAC.02063-19. Print 2020 Jan 27. doi:e02063-19 [pii]

Xie, R., McFadyen, L., Raber, S., Swanson, R., Tawadrous, M., Leister-Tebbe, H. et al. (2020). Population analysis of anidulafungin in infants to older adults with confirmed or suspected invasive candidiasis. *Clin. Pharmacol. Ther.* 2, 316-325. doi:10.1002/cpt.1831 [doi]

Yilmaz, D., Balkan, C., Ay, Y., Akin, M., Karapinar, B. and Kavakli, K. (2011). A rescue therapy with a combination of caspofungin and liposomal amphotericin B or voriconazole in children with haematological malignancy and refractory invasive fungal infections. *Mycoses.* 3, 234-242. doi:10.1111/j.1439-0507.2009.01808.x [doi]

Zhao, C., Wistrand-Yuen, P., Lagerback, P., Tangden, T., Nielsen, E. I. and Friberg, L. E. (2020). Combination of polymyxin B and minocycline against multidrug-resistant *Klebsiella pneumoniae*: Interaction quantified by pharmacokinetic/pharmacodynamic modelling from in vitro data. *Int.J.Antimicrob.Agents.* 6, 105941. doi:S0924-8579(20)30091-1 [pii]

ANNEX I

Annex I: In vitro time-kill curves for the combinations of amphotericin B plus anidulafungin/caspofungin (Complementary to section 2.1 of Results)

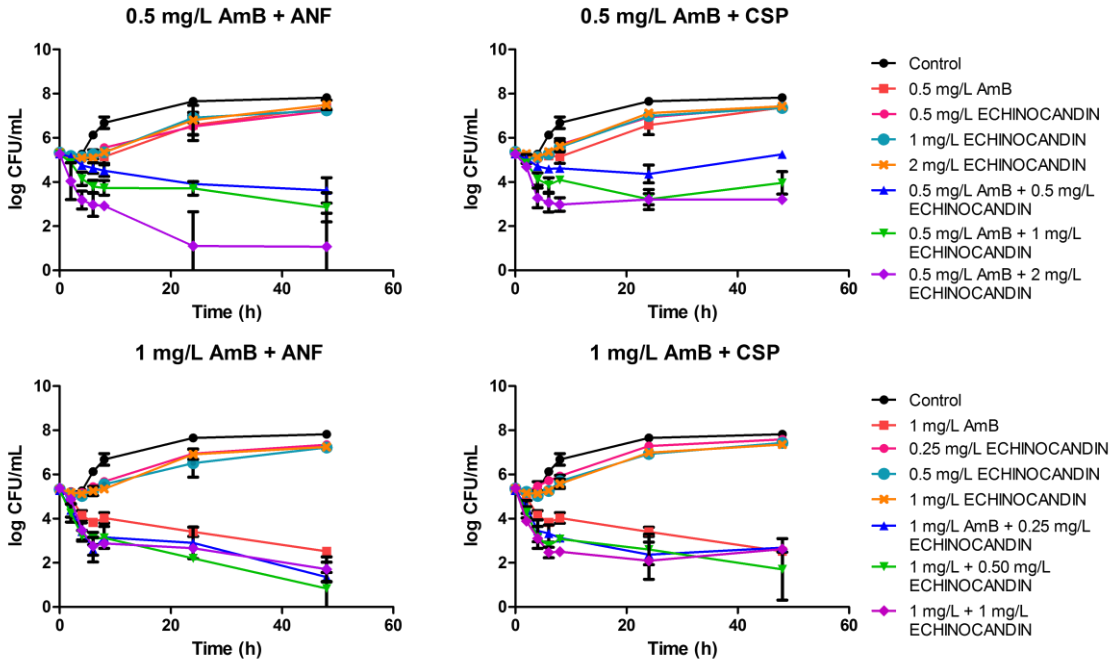

Figure AI-1. Mean time-kill curves for the combinations of amphotericin B + anidulafungin (top and bottom left) or caspofungin (top and bottom right) against *C. auris* 17-257. Each data point represents the mean result ± standard deviation (error bars) of all replicates.

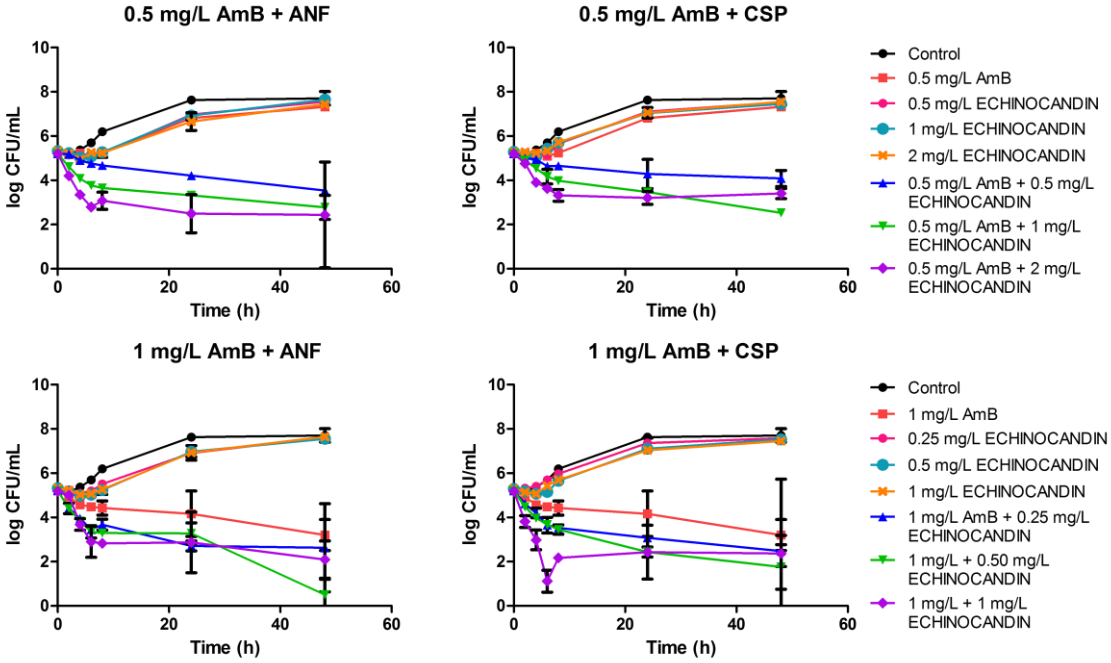

Figure AI-2. Mean time-kill curves for the combinations of amphotericin B + anidulafungin (top and bottom left) or caspofungin (top and bottom right) against *C. auris* 17-259. Each data point represents the mean result ± standard deviation (error bars) of all replicates.

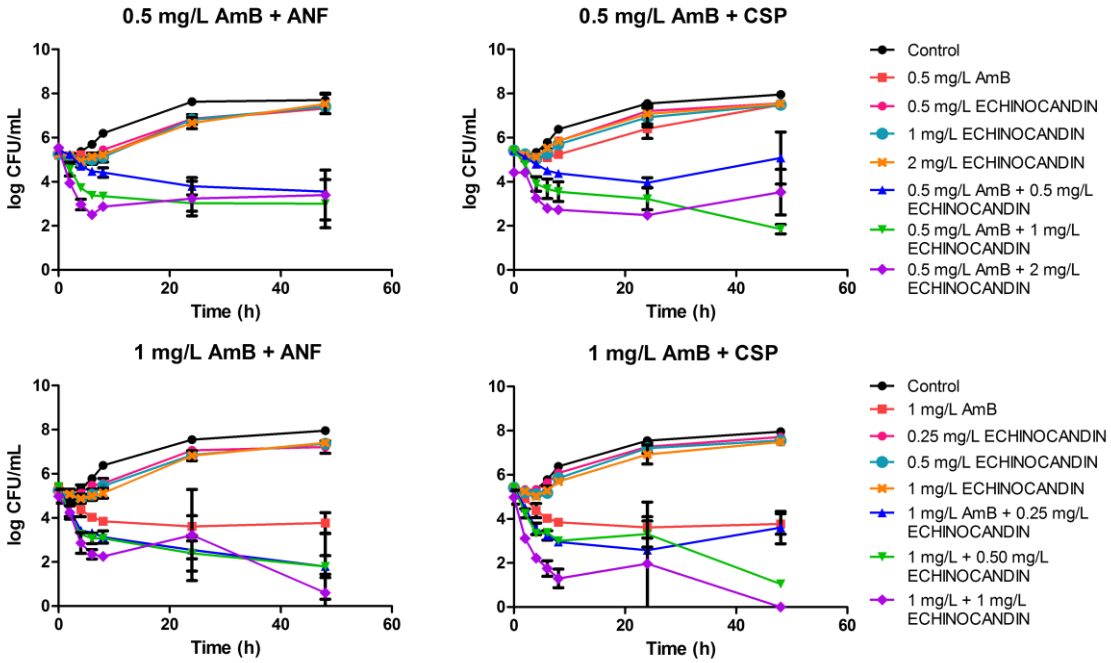

Figure AI-3. Mean time-kill curves for the combinations of amphotericin B + anidulafungin (top and bottom left) or caspofungin (top and bottom right) against *C. auris* 17-261. Each data point represents the mean result ± standard deviation (error bars) of all replicates.

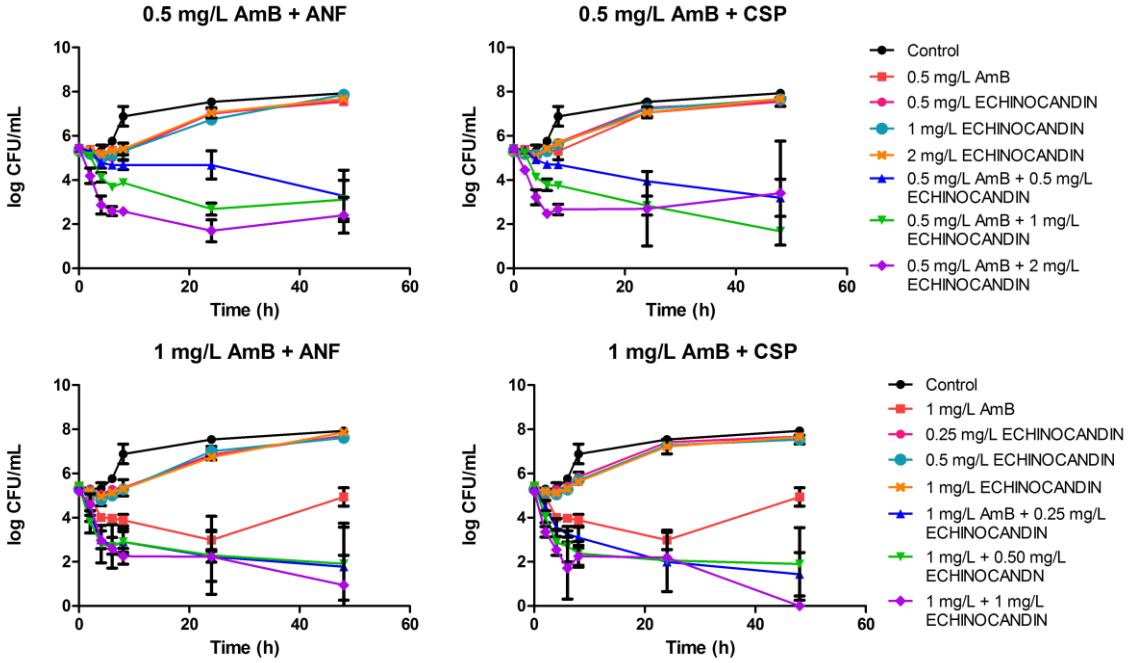

Figure AI-4. Mean time-kill curves for the combinations of amphotericin B + anidulafungin (top and bottom left) or caspofungin (top and bottom right) against *C. auris* 17-263. Each data point represents the mean result ± standard deviation (error bars) of all replicates.

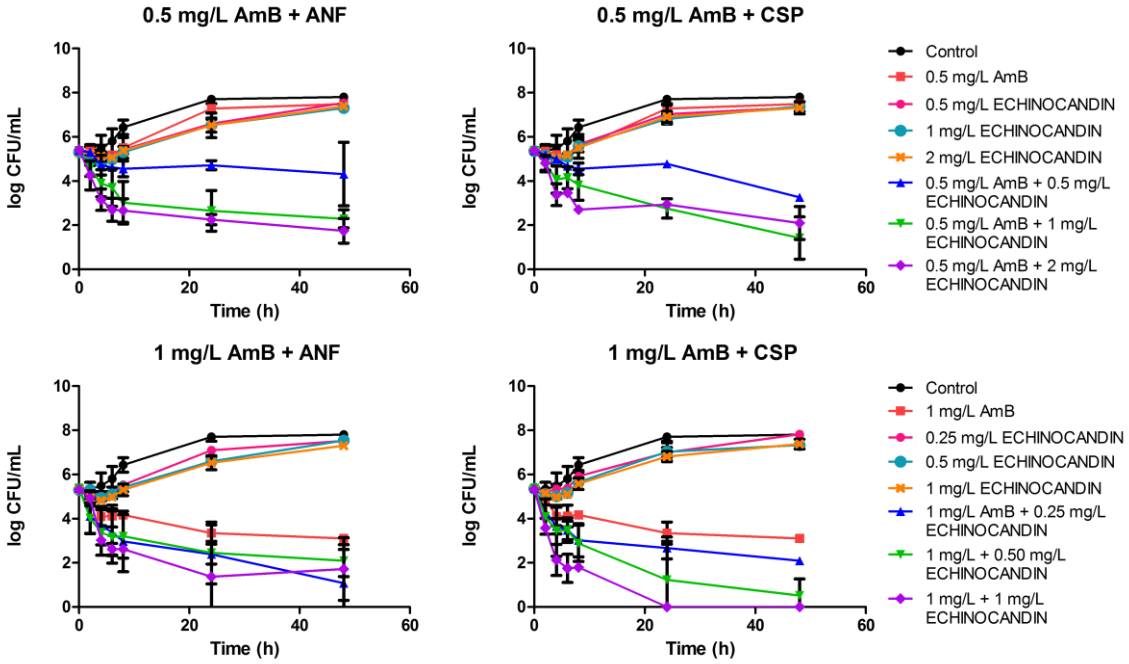

Figure AI-5. Mean time-kill curves for the combinations of amphotericin B + anidulafungin (top and bottom left) or caspofungin (top and bottom right) against *C. auris* 17-265. Each data point represents the mean result ± standard deviation (error bars) of all replicates.

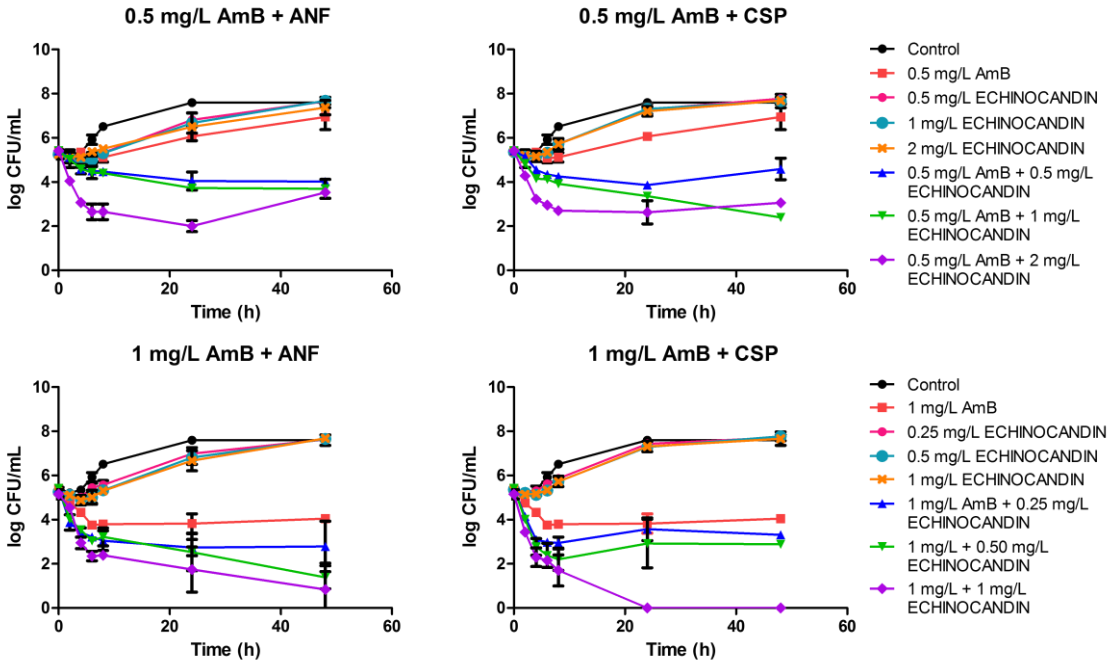

Figure AI-6. Mean time-kill curves for the combinations of amphotericin B + anidulafungin (top and bottom left) or caspofungin (top and bottom right) against *C. auris* 17-267. Each data point represents the mean result ± standard deviation (error bars) of all replicates.

ANNEX II

Annex II: Goodness-of-fit plots of the Greco model and synergy distributions for Bliss interaction (Complementary to section 2.2.1 of Results)

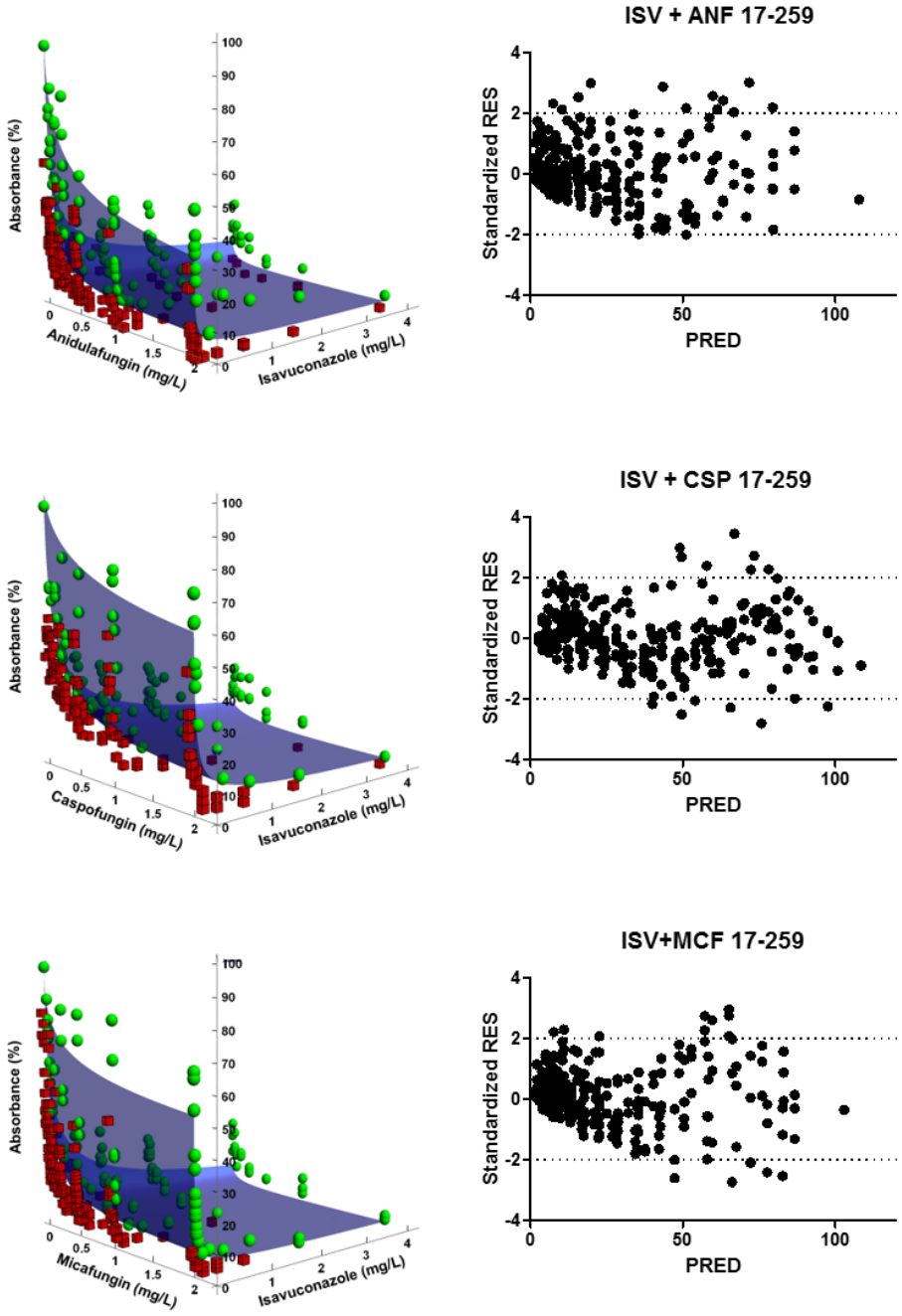

Figure AII-1. Goodness-of-fit plots of the Greco model for the combination of isavuconazole and anidulafungin, caspofungin or micafungin against *C. auris* 17-259. Left: The blue surface represents model predictions, the green spheres represent observations above the fitted surface and the red spheres represent observations below the fitted surface. Right: Standardized residuals (Standardized RES) versus predictions (PRED). ISV: isavuconazole. ANF: anidulafungin. CSP: caspofungin. MCF: micafungin.

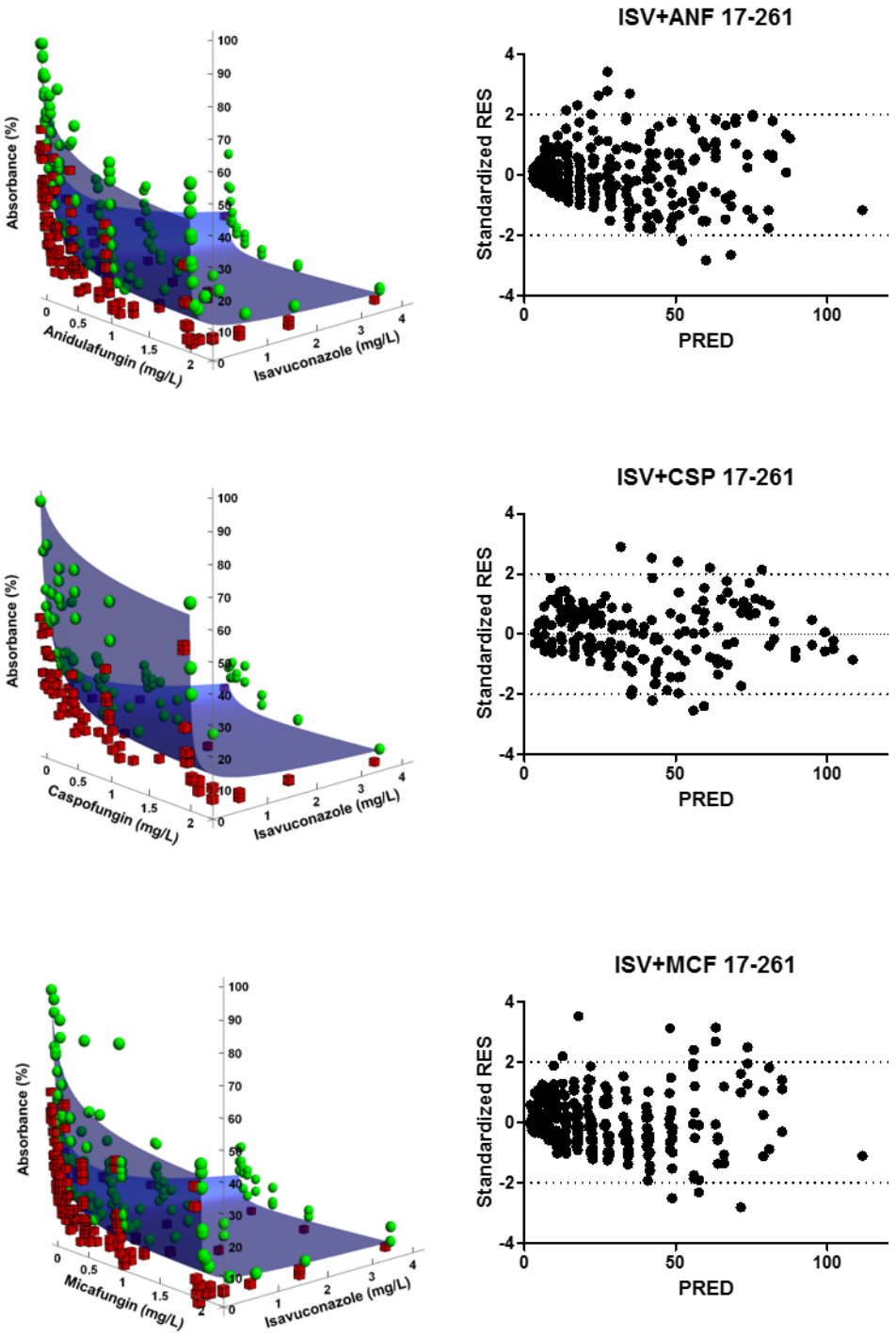

Figure AII-2. Goodness-of-fit plots of the Greco model for the combination of isavuconazole and anidulafungin, caspofungin or micafungin against *C. auris* 17-261. Left: The blue surface represents model predictions, the green spheres represent observations above the fitted surface and the red spheres represent observations below the fitted surface. Right: Standardized residuals (Standardized RES) versus predictions (PRED). ISV: isavuconazole. ANF: anidulafungin. CSP: caspofungin. MCF: micafungin.

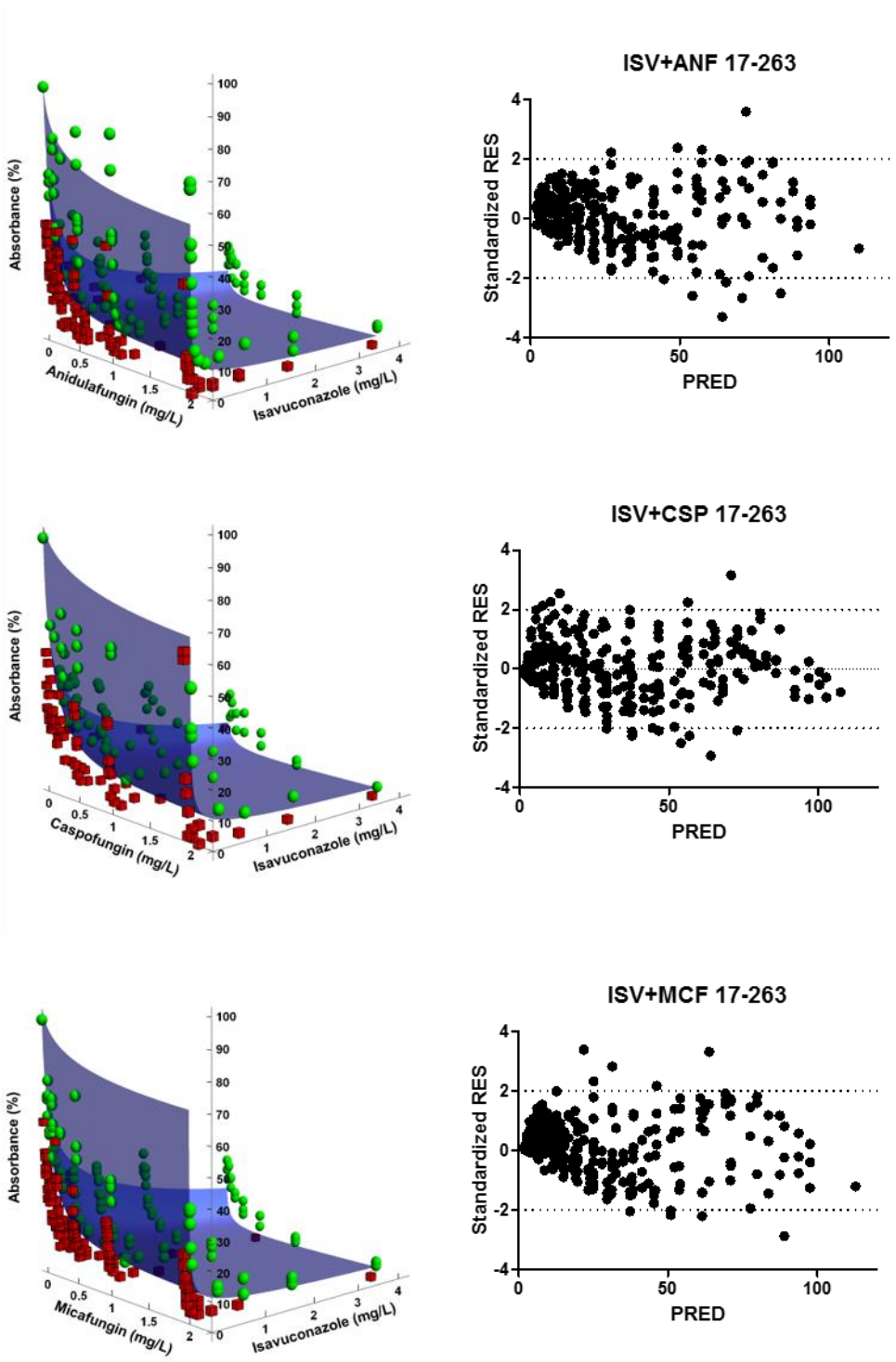

Figure AII-3. Goodness-of-fit plots of the Greco model for the combination of isavuconazole and anidulafungin, caspofungin or micafungin against *C. auris* 17-263. Left: The blue surface represents model predictions, the green spheres represent observations above the fitted surface and the red spheres represent observations below the fitted surface. Right: Standardized residuals (Standardized RES) versus predictions (PRED). ISV: isavuconazole. ANF: anidulafungin. CSP: caspofungin. MCF: micafungin.

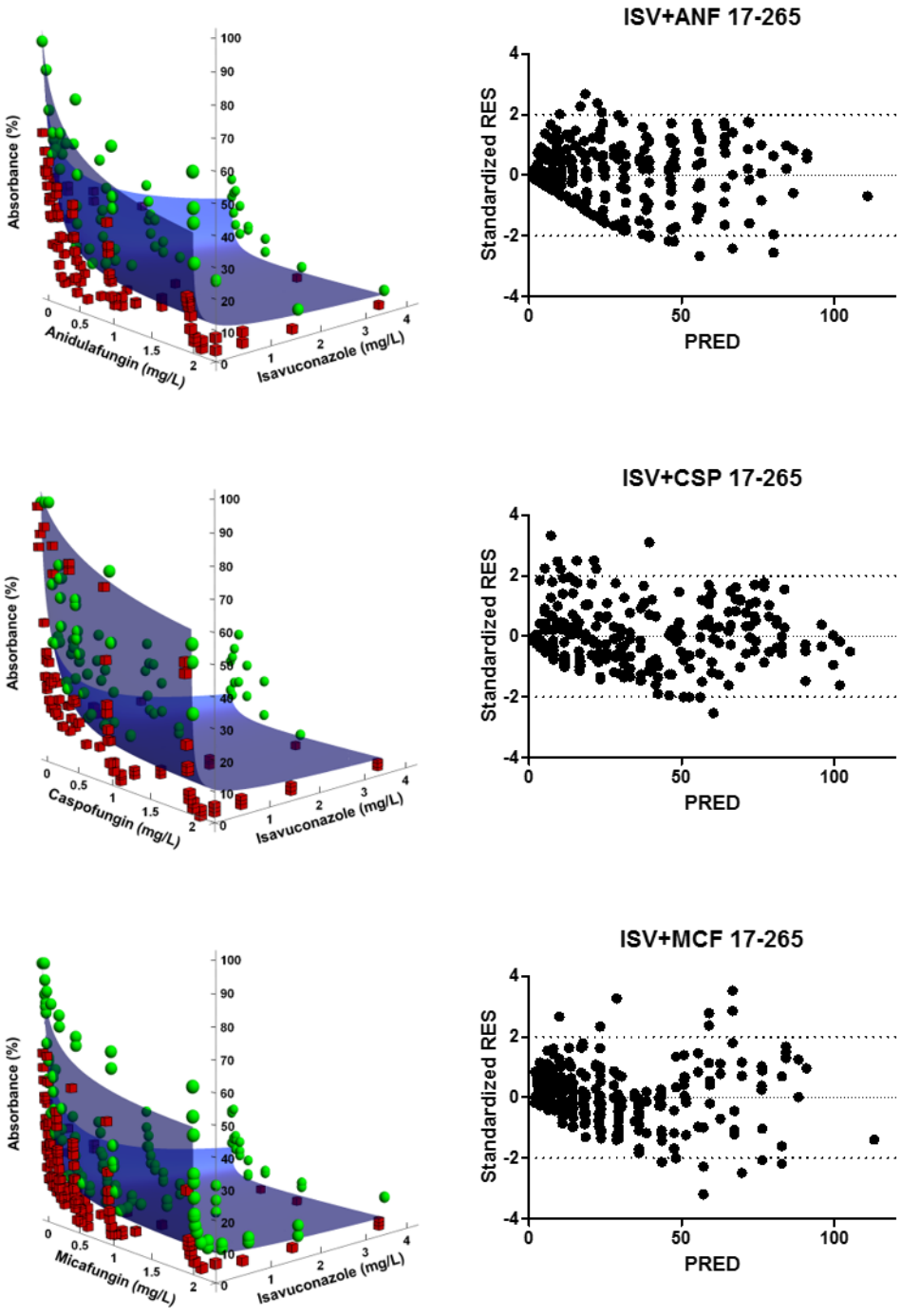

Figure AII-4. Goodness-of-fit plots of the Greco model for the combination of isavuconazole and anidulafungin, caspofungin or micafungin against *C. auris* 17-265. Left: The blue surface represents model predictions, the green spheres represent observations above the fitted surface and the red spheres represent observations below the fitted surface. Right: Standardized residuals (Standardized RES) versus predictions (PRED). ISV: isavuconazole. ANF: anidulafungin. CSP: caspofungin. MCF: micafungin.

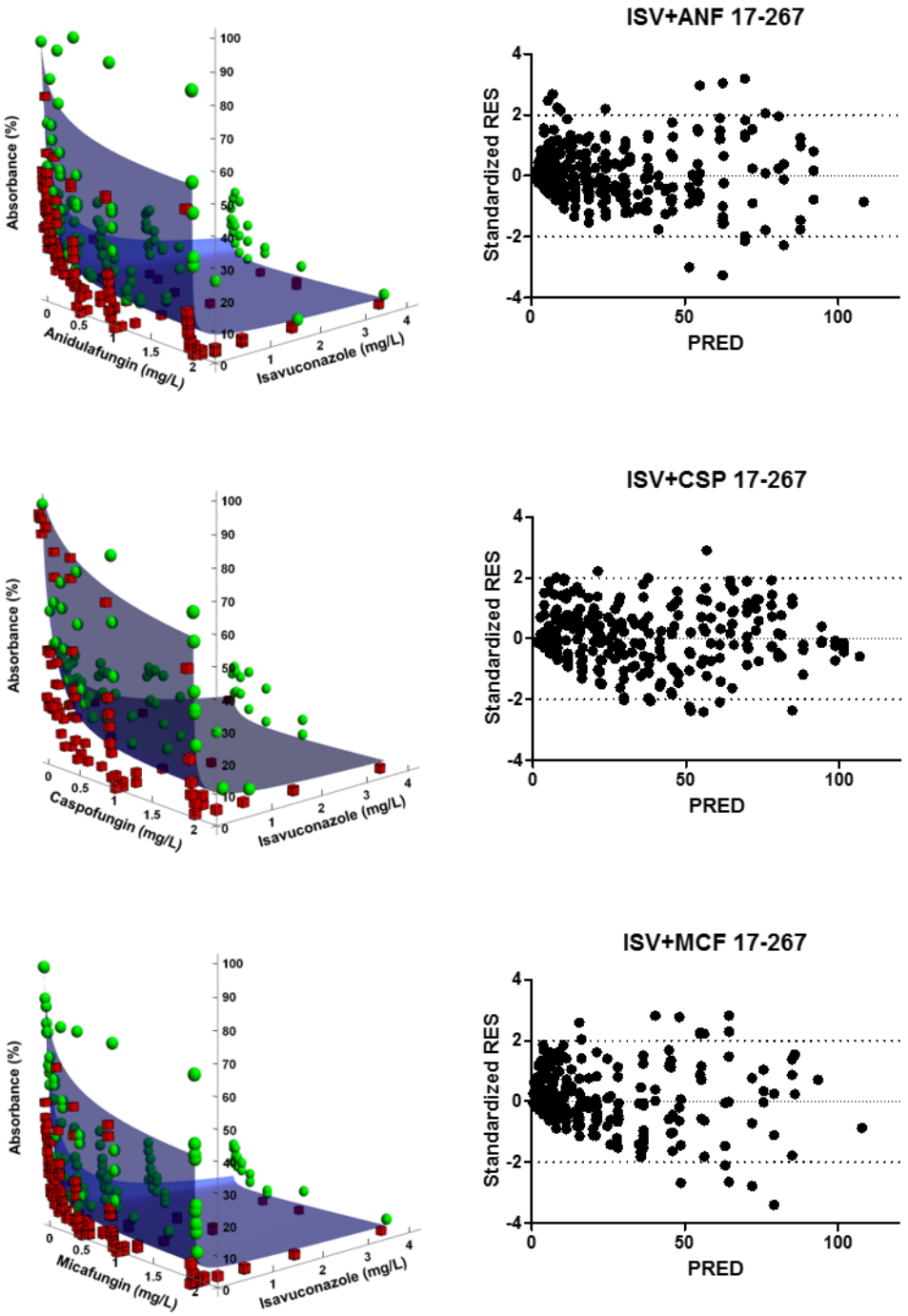

Figure AII-5. Goodness-of-fit plots of the Greco model for the combination of isavuconazole and anidulafungin, caspofungin or micafungin against *C. auris* 17-267. Left: The blue surface represents model predictions, the green spheres represent observations above the fitted surface and the red spheres represent observations below the fitted surface. Right: Standardized residuals (Standardized RES) versus predictions (PRED). ISV: isavuconazole. ANF: anidulafungin. CSP: caspofungin. MCF: micafungin.

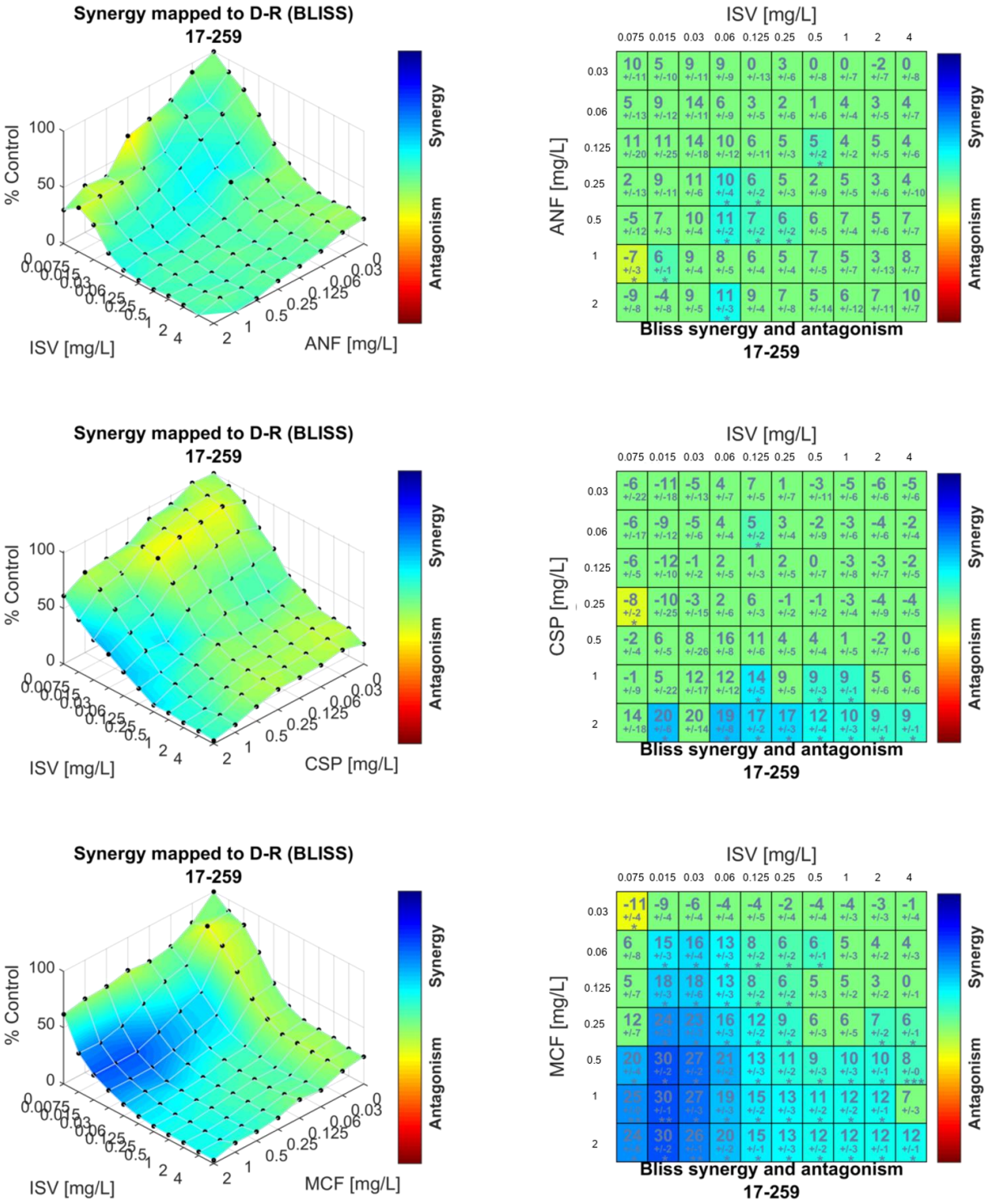

Figure AII-6. Synergy distribution determined by Bliss interaction model for the combination of isavuconazole (ISV) and anidulafungin (ANF), caspofungin (CSP) or micafungin (MFC) against *C. auris* 17-259. Left: Synergy distribution mapped to dose-response surface. Right: Matrix synergy plot with synergy scores for each combination.

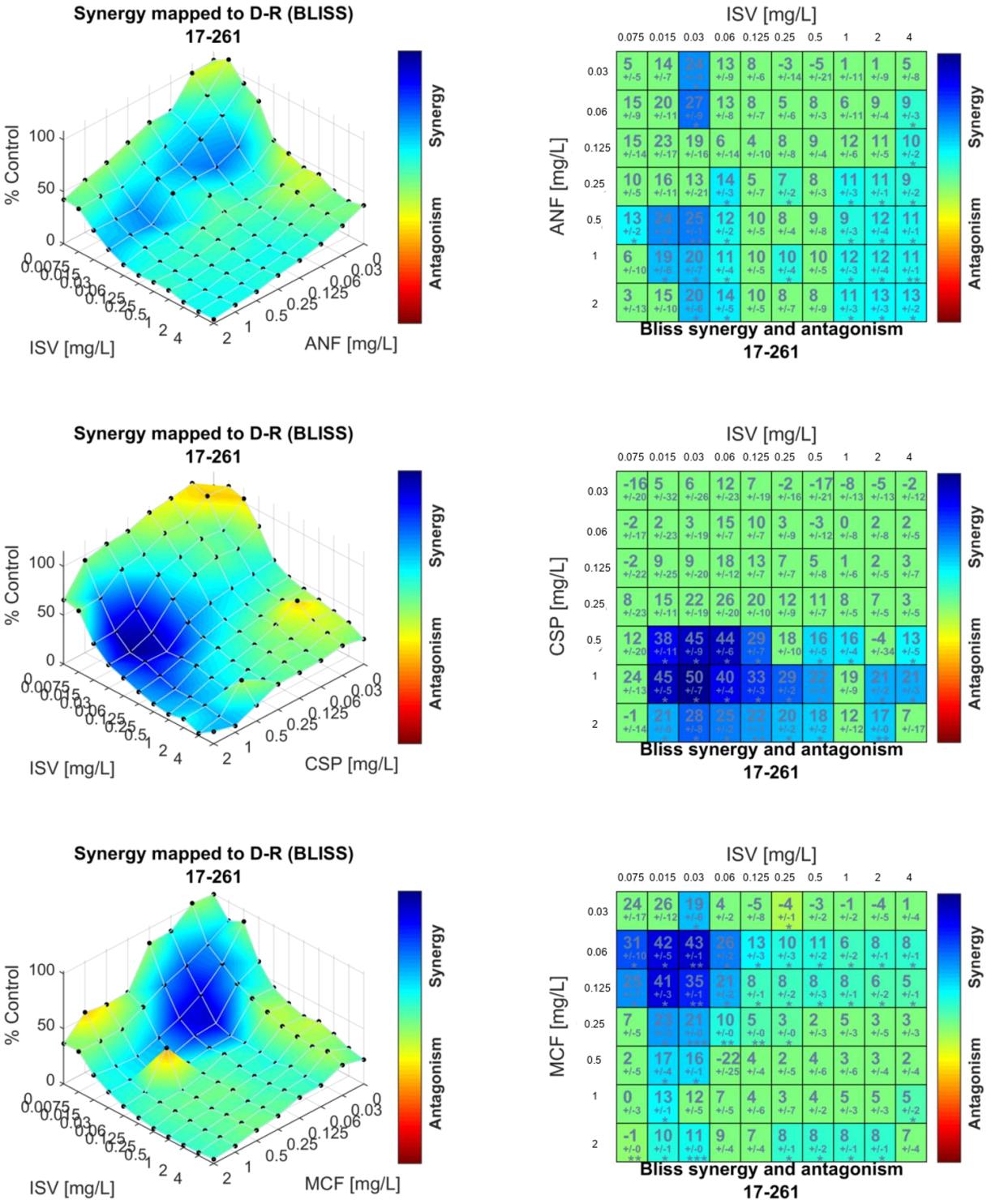

Figure AII-7. Synergy distribution determined by Bliss interaction model for the combination of isavuconazole (ISV) and anidulafungin (ANF), caspofungin (CSP) or micafungin (MFC) against *C. auris* 17-261. Left: Synergy distribution mapped to dose-response surface. Right: Matrix synergy plot with synergy scores for each combination.

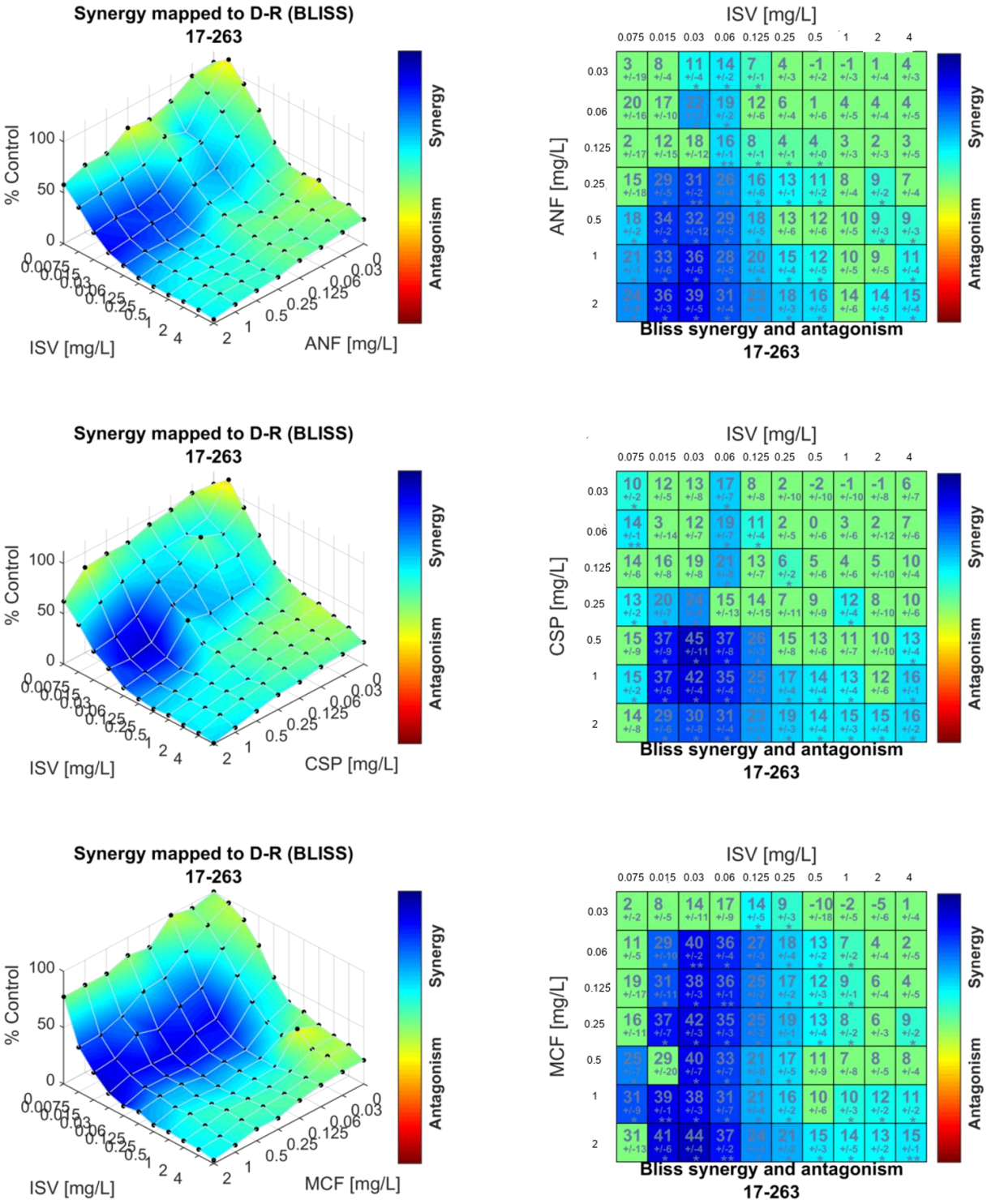

Figure AII-8. Synergy distribution determined by Bliss interaction model for the combination of isavuconazole (ISV) and anidulafungin (ANF), caspofungin (CSP) or micafungin (MFC) against *C. auris* 17-263. Left: Synergy distribution mapped to dose-response surface. Right: Matrix synergy plot with synergy scores for each combination.

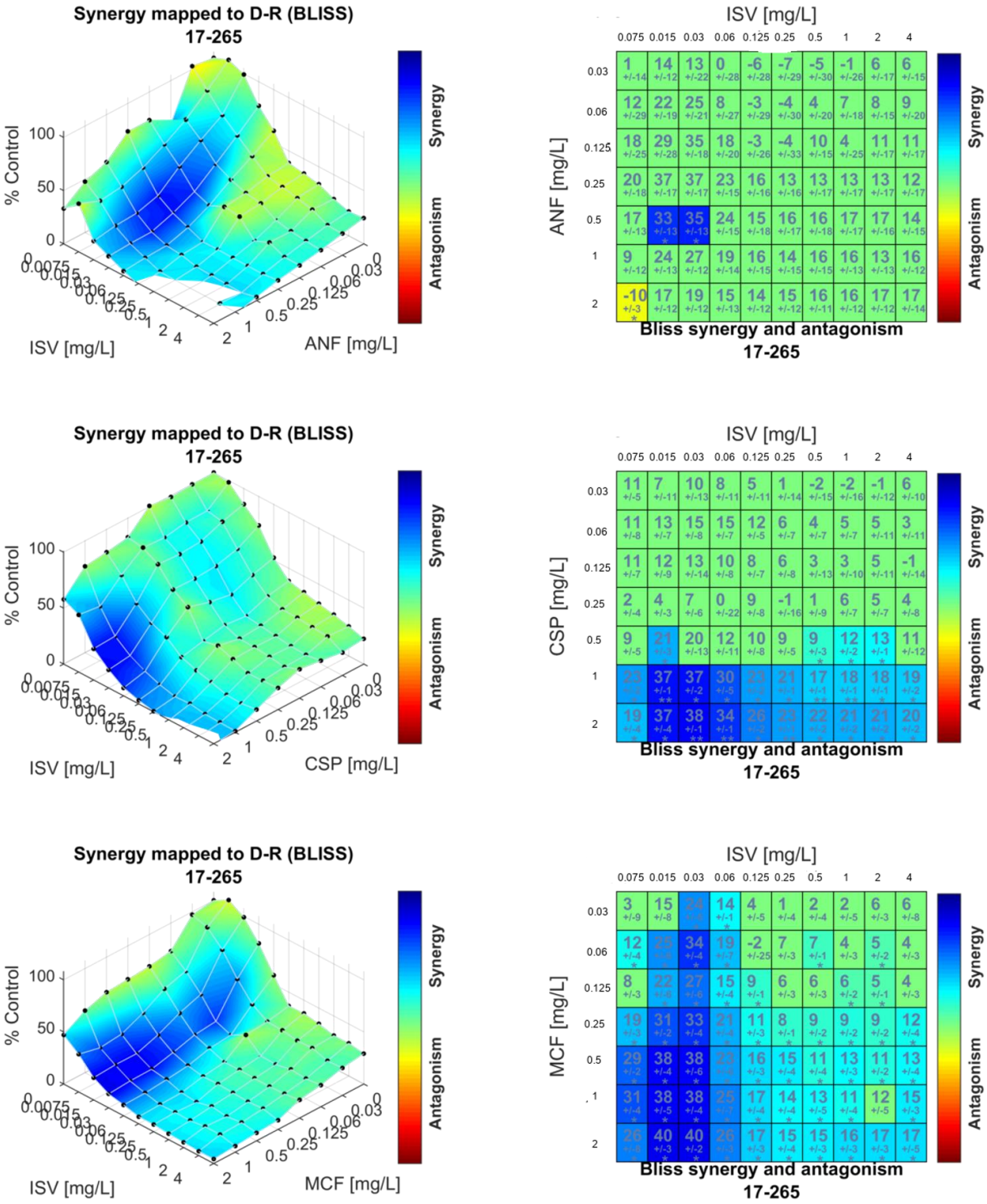

Figure AII-9. Synergy distribution determined by Bliss interaction model for the combination of isavuconazole (ISV) and anidulafungin (ANF), caspofungin (CSP) or micafungin (MFC) against *C. auris* 17-265. Left: Synergy distribution mapped to dose-response surface. Right: Matrix synergy plot with synergy scores for each combination.

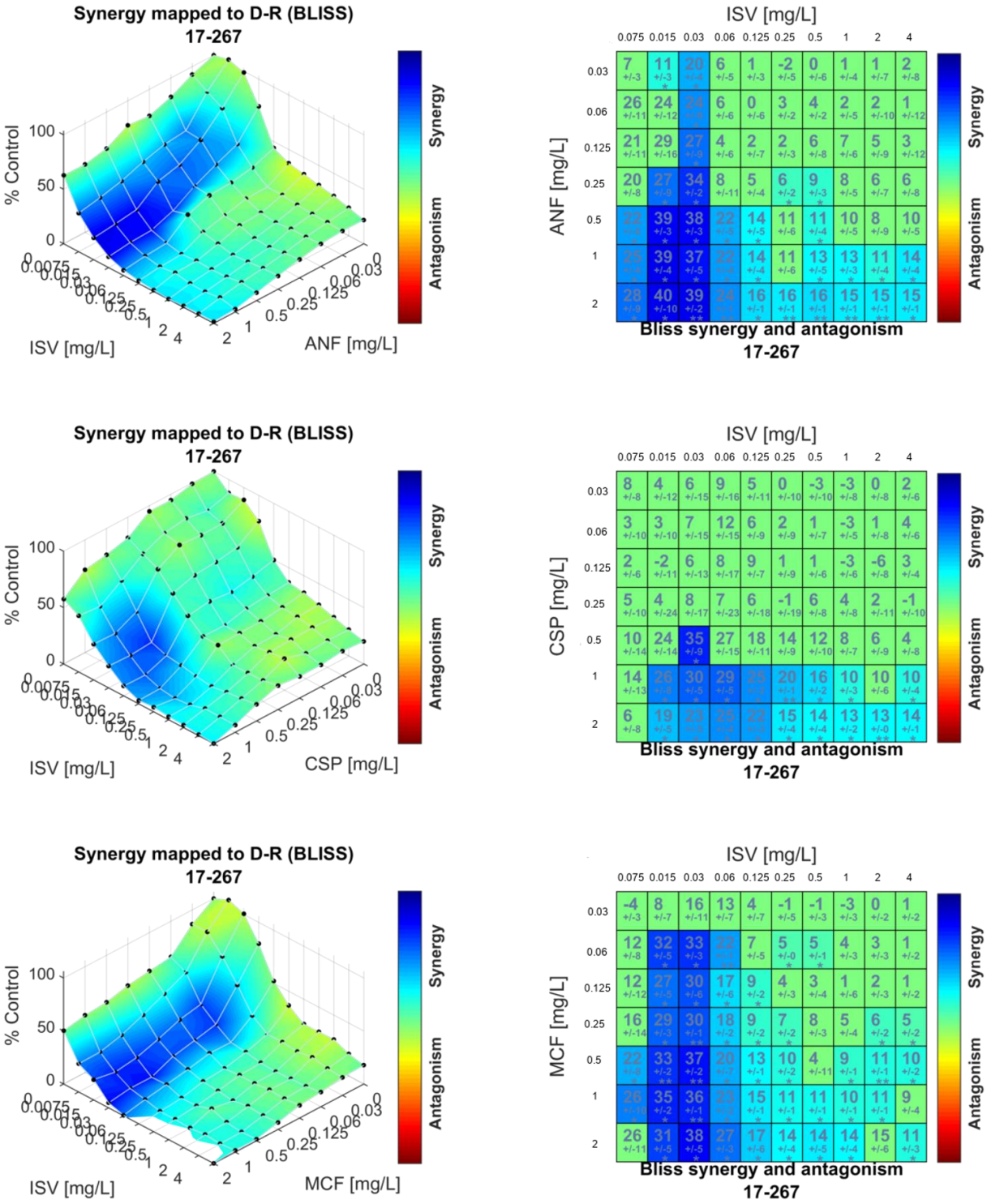

Figure AII-10. Synergy distribution determined by Bliss interaction model for the combination of isavuconazole (ISV) and anidulafungin (ANF), caspofungin (CSP) or micafungin (MFC) against *C. auris* 17-267. Left: Synergy distribution mapped to dose-response surface. Right: Matrix synergy plot with synergy scores for each combination.

ANNEX III

Annex III: Visual predictive checks of drugs in monotherapy (Complementary to section 3.2.1 of Results)

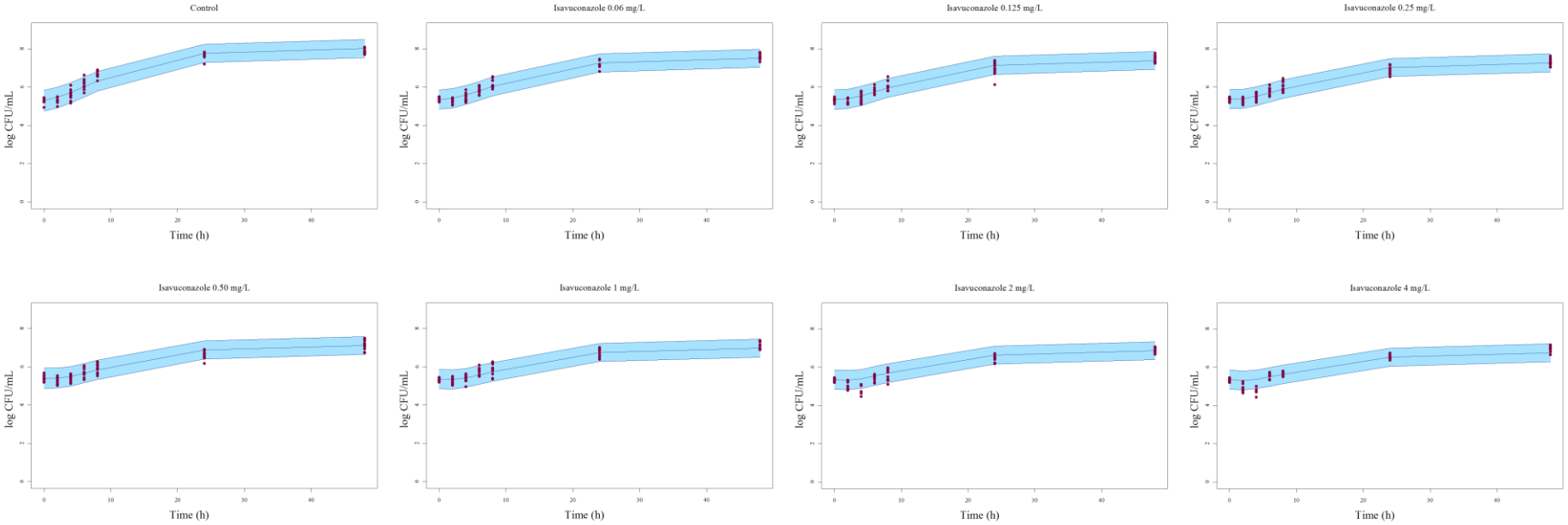

Figure AIII-1. Visual predictive check (VPC) for the final monotherapy model for isavuconazole, with the observed fungal counts (full circles), the mean prediction (solid line) and 95% model prediction interval (shaded area) of the simulations.

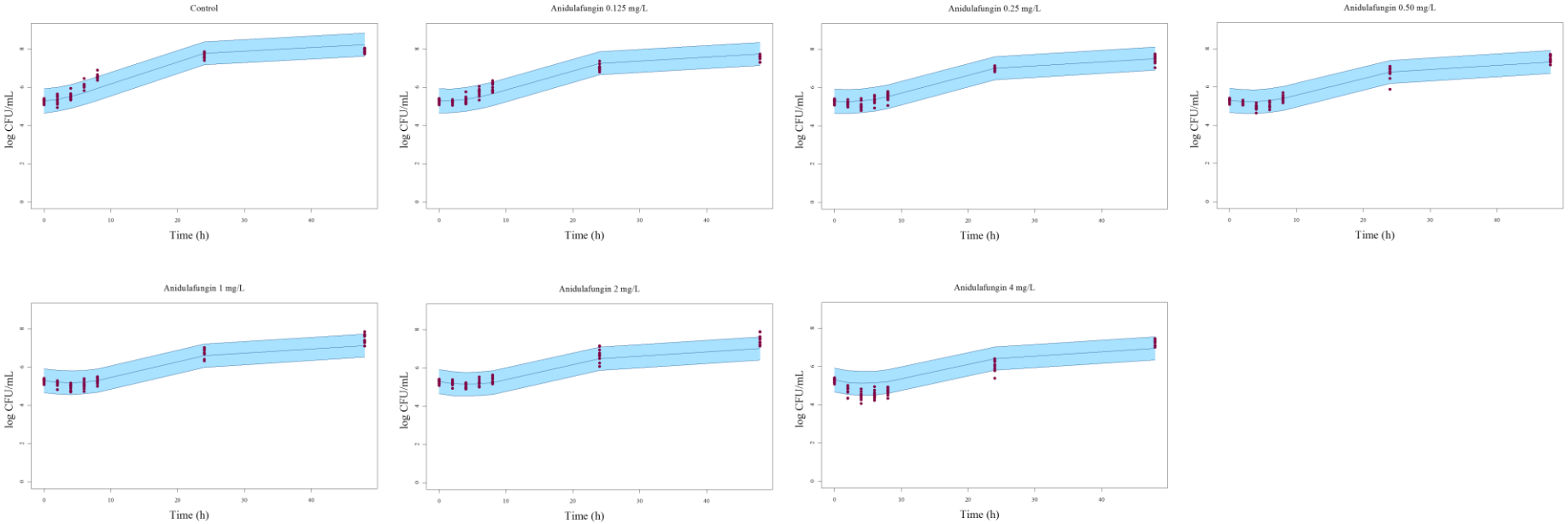

Figure AIII-2. Visual predictive check (VPC) for the final monotherapy model for anidulafungin, with the observed fungal counts (full circles), the mean prediction (solid line) and 95% model prediction interval (shaded area) of the simulations.

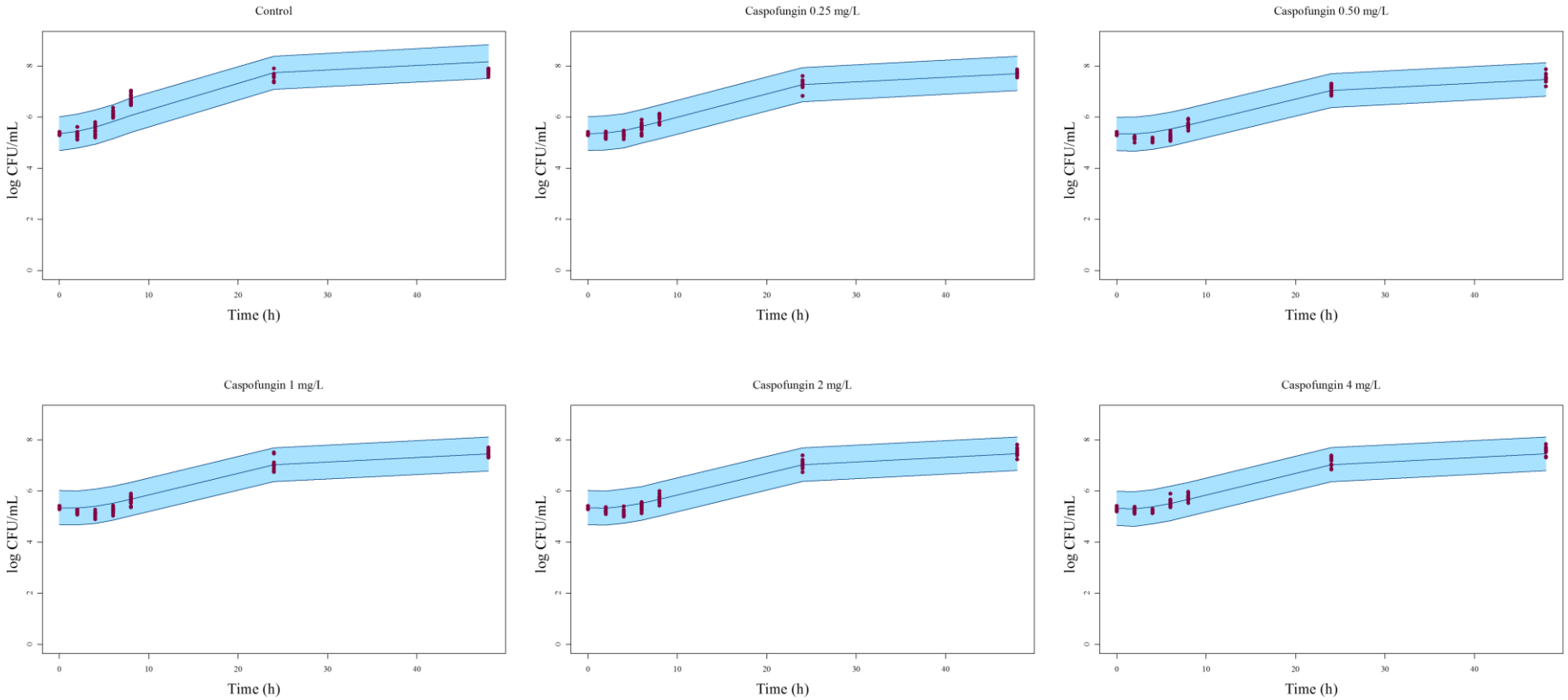

Figure AIII-3. Visual predictive check (VPC) for the final monotherapy model for caspofungin, with the observed fungal counts (full circles), the mean prediction (solid line) and 95% model prediction interval (shaded area) of the simulations.

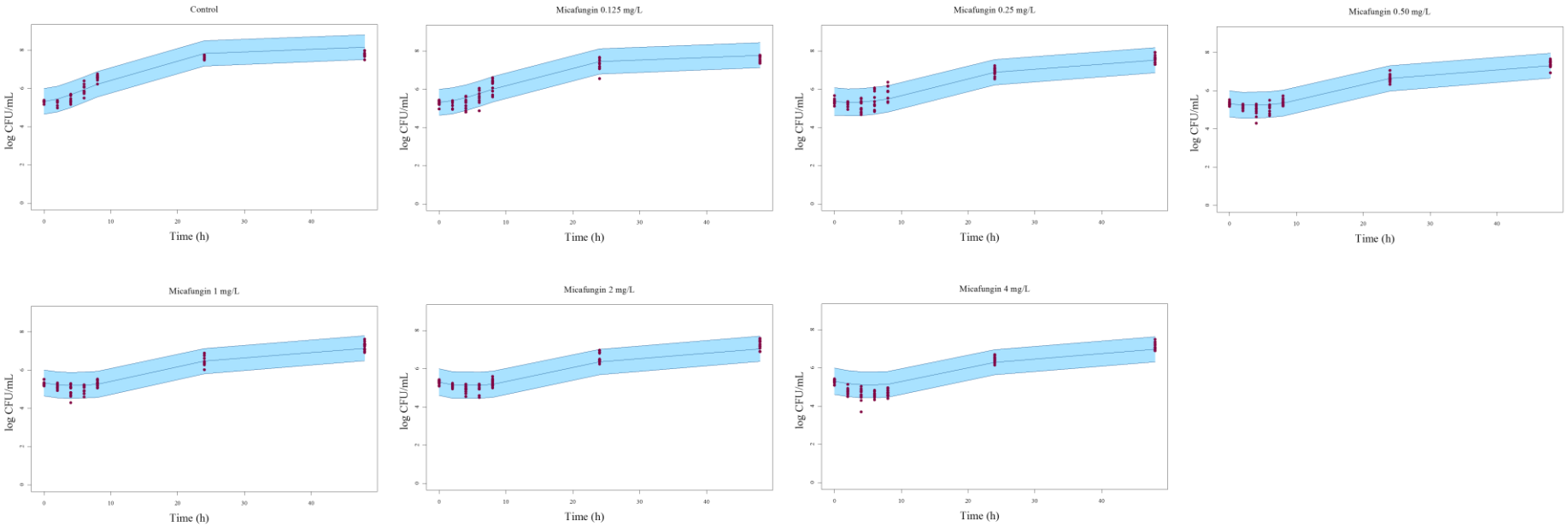

Figure AIII-4. Visual predictive check (VPC) for the final monotherapy model for micafungin, with the observed fungal counts (full circles), the mean prediction (solid line) and 95% model prediction interval (shaded area) of the simulations.

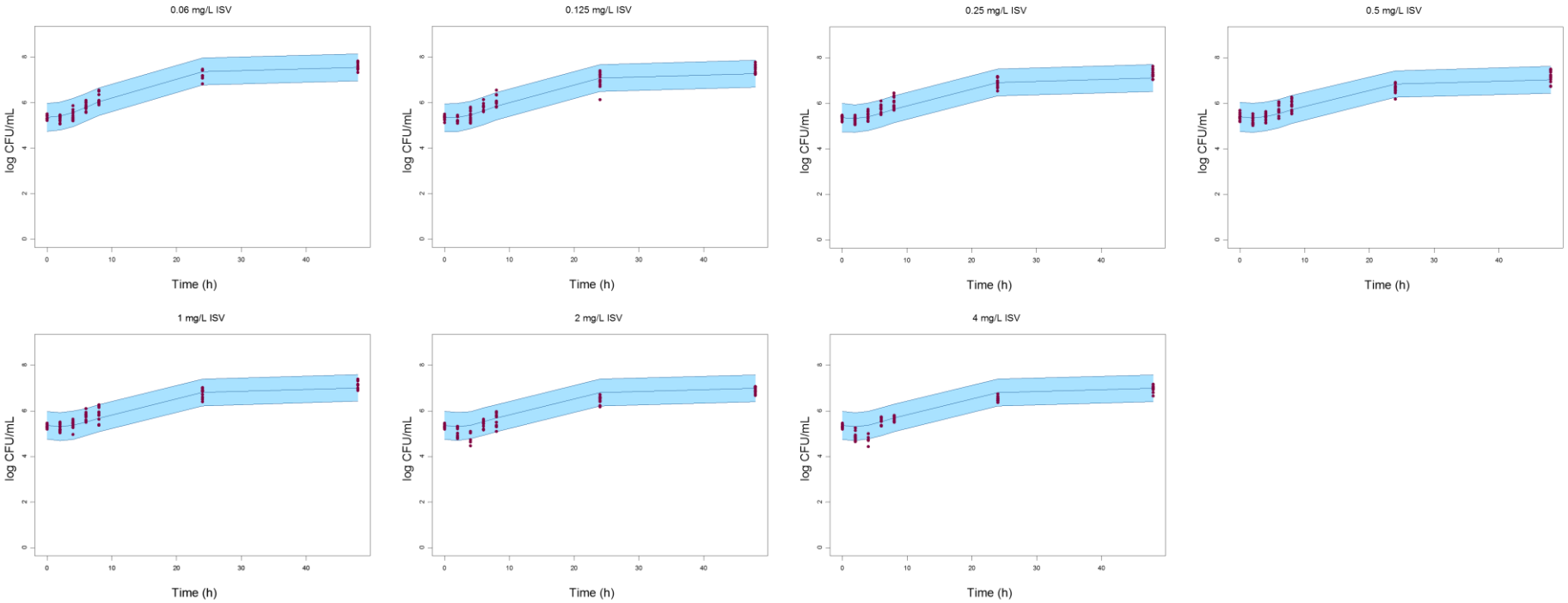

Figure AIII-5. Visual predictive check (VPC) for the final combination model of isavuconazole + anidulafungin, stratified by concentrations of isavuconazole (ISV) in monotherapy, with the observed fungal counts (full circles), the mean prediction (solid line) and 95% model prediction interval (shaded area) of the simulations. VPCs were identical for the combinations of isavuconazole with caspofungin or micafungin.

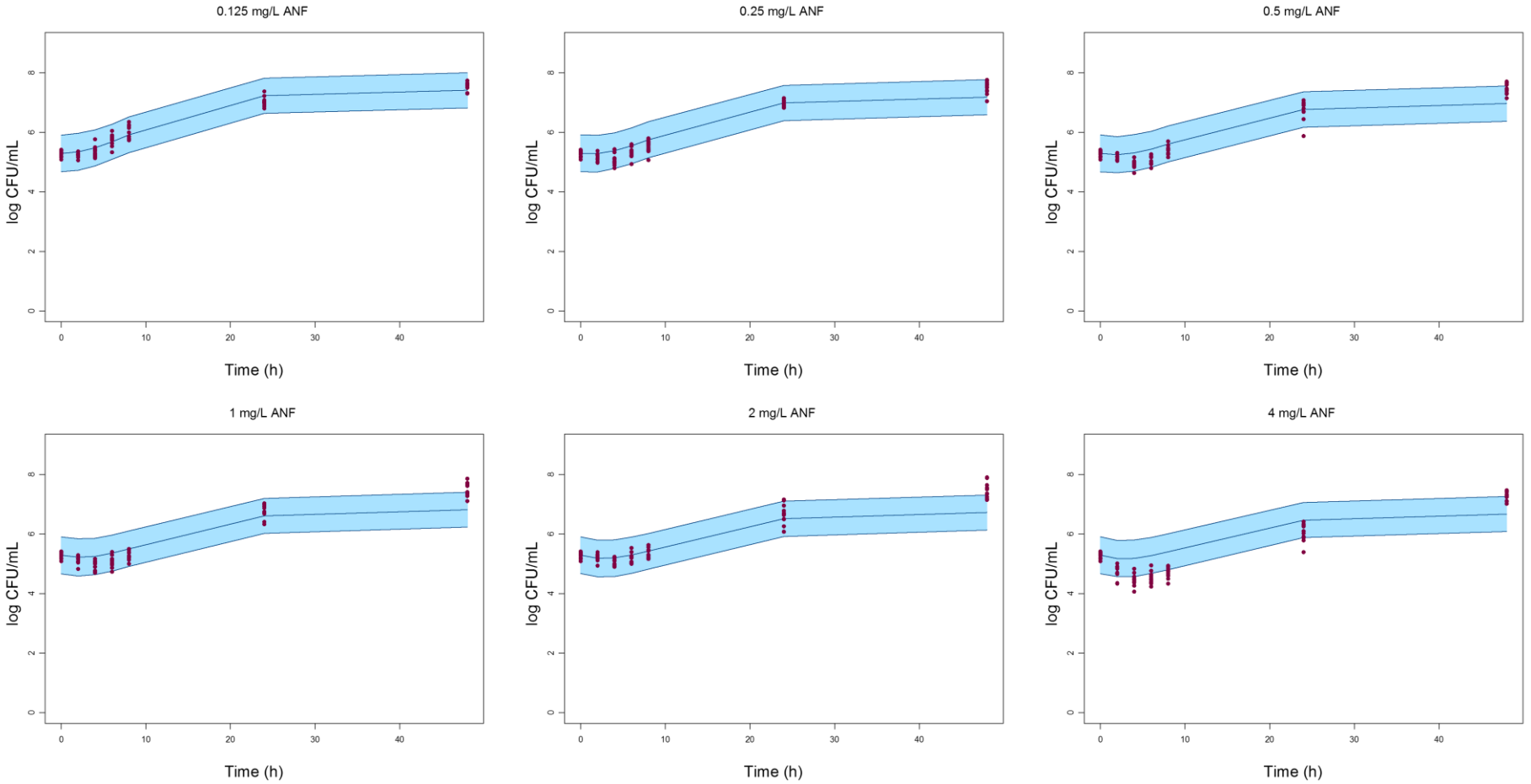

Figure AIII-6. Visual predictive check (VPC) for the final combination model of isavuconazole + anidulafungin, stratified by the concentrations of anidulafungin (ANF) in monotherapy, with the observed fungal counts (full circles), the mean prediction (solid line) and 95% model prediction interval (shaded area) of the simulations.

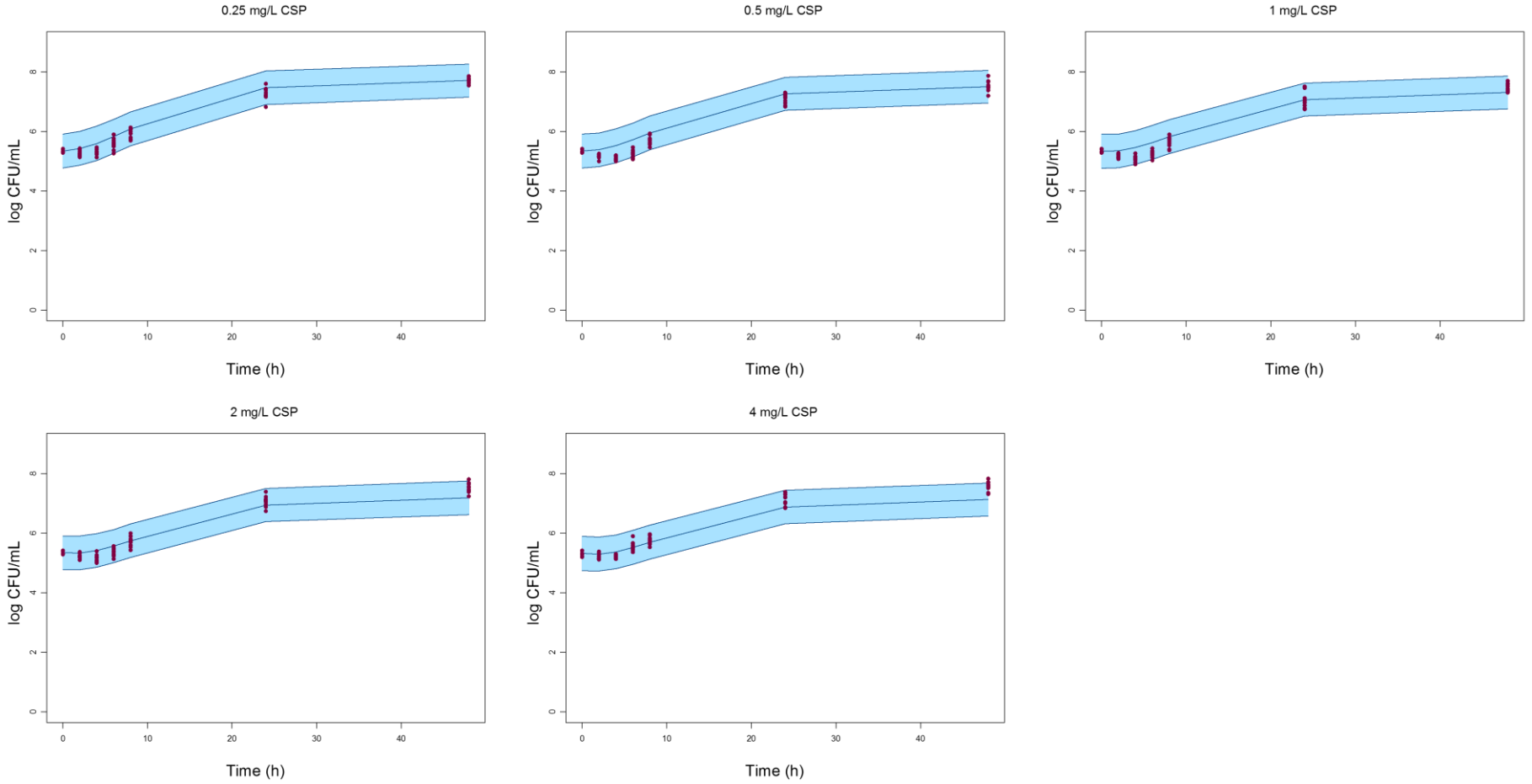

Figure AIII-7 Visual predictive check (VPC) for the final combination model of isavuconazole + caspofungin, stratified by the concentrations of caspofungin (CSP) in monotherapy, with the observed fungal counts (full circles), the mean prediction (solid line) and 95% model prediction interval (shaded area) of the simulations.

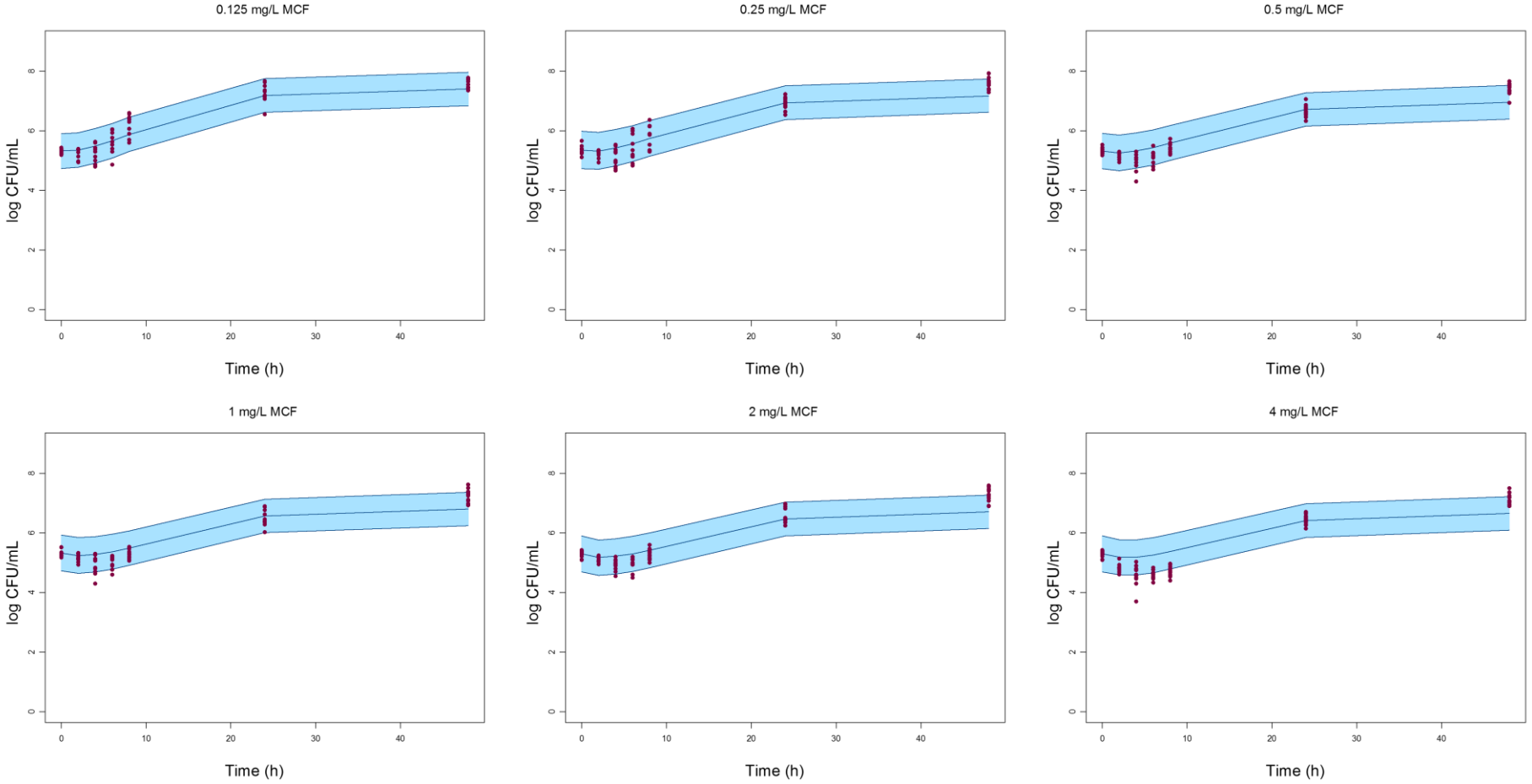

Figure AIII-8. Visual predictive check (VPC) for the final combination model of isavuconazole + micafungin, stratified by the concentration of micafungin (MCF) in monotherapy, with the observed fungal counts (full circles), the mean prediction (solid line) and 95% model prediction interval (shaded area) of the simulations.

ANNEX IV

ANNEX IV. Accompanying manuscript

antibiotics

MDPI

Article

In Vitro Synergistic Interactions of Isavuconazole and Echinocandins against *Candida auris*

Unai Caballero [1], Sarah Kim [2], Elena Eraso [3], Guillermo Quindós [3], Valvanera Vozmediano [2], Stephan Schmidt [2] and Nerea Jauregizar [1,*]

[1] Department of Pharmacology, Faculty of Medicine and Nursing, University of the Basque Country (UPV/EHU), 48940 Leioa, Spain; unai.caballero@ehu.eus
[2] Center for Pharmacometrics and Systems Pharmacology, Department of Pharmaceutics, College of Pharmacy, University of Florida, Orlando, FL 32827, USA; sarahkim@cop.ufl.edu (S.K.); valva@cop.ufl.edu (V.V.); SSchmidt@cop.ufl.edu (S.S.)
[3] Department of Immunology, Microbiology and Parasitology, Faculty of Medicine and Nursing, University of the Basque Country (UPV/EHU), 48940 Leioa, Spain; elena.eraso@ehu.eus (E.E.); guillermo.quindos@ehu.eus (G.Q.)
* Correspondence: nerea.jauregizar@ehu.eus

Abstract: *Candida auris* is an emergent fungal pathogen that causes severe infectious outbreaks globally. The public health concern when dealing with this pathogen is mainly due to reduced susceptibility to current antifungal drugs. A valuable alternative to overcome this problem is to investigate the efficacy of combination therapy. The aim of this study was to determine the in vitro interactions of isavuconazole with echinocandins against *C. auris*. Interactions were determined using a checkerboard method, and absorbance data were analyzed with different approaches: the fractional inhibitory concentration index (FICI), Greco universal response surface approach, and Bliss interaction model. All models were in accordance and showed that combinations of isavuconazole with echinocandins resulted in an overall synergistic interaction. A wide range of concentrations within the therapeutic range were selected to perform time-kill curves. These confirmed that isavuconazole–echinocandin combinations were more effective than monotherapy regimens. Synergism and fungistatic activity were achieved with combinations that included isavuconazole in low concentrations ($\geq$0.125 mg/L) and $\geq$1 mg/L of echinocandin. Time-kill curves revealed that once synergy was achieved, combinations of higher drug concentrations did not improve the antifungal activity. This work launches promising results regarding the combination of isavuconazole with echinocandins for the treatment of *C. auris* infections.

Keywords: *Candida auris*; checkerboard; combination; antifungal agents; isavuconazole; echinocandins; time-kill

Citation: Caballero, U.; Kim, S.; Eraso, E.; Quindós, G.; Vozmediano, V.; Schmidt, S.; Jauregizar, N. In Vitro Synergistic Interactions of Isavuconazole and Echinocandins against *Candida auris*. *Antibiotics* **2021**, *10*, 355. https://doi.org/10.3390/antibiotics10040355

Received: 22 February 2021
Accepted: 25 March 2021
Published: 28 March 2021

1. Introduction

Candida auris (*C. auris*) is a multidrug-resistant yeast pathogen responsible for numerous cases of fungemia globally since 2009 [1]. This non-*Candida albicans* fungus spreads rapidly in hospitals and nursing homes, and it has been classified as an "urgent threat" pathogen according to the United States Centers for Disease Control and Prevention's (CDC) 2019 Antibiotic Resistance Threats Report [2].

According to the first meeting of the WHO Antifungal Expert Group on Identifying Priority Fungal Pathogens, there is an overall consensus that *C. auris* is a pathogen of global public health interest and should be evaluated based on the limited existing therapeutic options due to resistance or other treatment issues [3].

Even though echinocandins are the recommended first-line treatment to fight *C. auris* infections [4], resistance to these drugs along with therapeutic failures have been reported [5]. Because of the limited available therapeutic options and the risk of treatment

failure, alternative strategies, such as combination therapies, are being investigated. Recent works have evaluated the in vitro interactions of antifungal drugs against *C. auris* [6–8], or the combination of antifungal drugs with other antimicrobial agents [9–12]. Considering the scarce number of studies on antifungal combinations against *C. auris*, we aimed to further characterize the in vitro activity of the azole–echinocandin pairing against blood isolates of *C. auris*. Combining isavuconazole and echinocadins may be an interesting approach to be further investigated, considering that, on one hand, echinocandins are nowadays the treatment of choice for infections caused by *C. auris*, and on the other hand, isavuconazole is the newest and safer addition to the triazole group. Although it is labeled for the treatment of aspergillosis and mucormycosis, its anti-*Candida* activity together with its biopharmaceutical properties make it an interesting alternative [13]. In addition, the synergistic interactions obtained from the combination of isavuconazole plus anidulafungin against *C. auris* by the fractional inhibitory concentration index (FICI) method [14], and from isavuconazole plus micafungin against other non-*auris Candida* by time-kill studies [15], supports the interest of further studying the isavuconazole–echinocandin combinations against *C. auris*.

Therefore, the aim of this study was to examine the in vitro interactions and potential synergy between isavuconazole and the three currently commercialized echinocandins (anidulafungin, caspofungin, and micafungin) against *C. auris* clinical isolates. Drug interactions were first assessed by analyzing checkerboard data with non-parametric (FICI) and parametric (Greco and Bliss) approaches. Then, interaction results were verified by time-kill curve assays.

2. Results

2.1. Checkerboard Assays and Analysis

Checkerboard experiments showed that none of the antifungal drugs in monotherapy at the concentrations tested were able to stop fungal growth completely, expressed as an absorbance value close to 0%. Isavuconazole had a higher potency than echinocandins, as it reached a 50% reduction in the absorbance value at concentrations 0.06–0.125 mg/L, whereas echinocandins needed the highest concentrations tested (1–2 mg/L) to reach that threshold. Conversely, absorbance values close to 0% were reached with combinations that included $\geq$0.125 mg/L of isavuconazole and $\geq$0.5 mg/L of echinocandins.

FICI results and the interaction parameters obtained from Greco and Bliss analysis for all *C. auris* isolates and drug combinations are summarized in Table 1. The determination of the FICI showed synergism for the three isavuconazole–echinocandin combinations against all isolates. On the other hand, synergistic interactions were found by the Greco model in 5 out of 6 clinical isolates for the combination of isavuconazole and micafungin, in 3 out of 6 for the combination of isavuconazole and anidulafungin, and in 2 out of 6 for the combination of isavuconazole and caspofungin. For the remaining isolates, the tested combinations were classified as additive, with a clear trend towards synergism, as shown by the 95% confidence interval (95% CI). Goodness-of-fit plots shown in Figure 1 for a representative isolate and drug combination revealed the concentrations for which the model-predicted effect (% absorbance) deviated from the experimental data. In general, the fitted response surface followed the same pattern as the experimental data, and no systematic deviation of the model was observed in the residual plots. However, the model deviated from the data at higher absorbance values, which corresponded to either echinocandin monotherapy or combinations with low concentrations of both drugs. As depicted in Figure 2, the IC_{50} obtained when fitting the Greco model to the experimental data was significantly higher for caspofungin than for anidulafungin or micafungin ($p < 0.001$).

Table 1. Fractional inhibitory concentration index (FICI) and interaction parameters determined by Greco model (α) and Bliss model (ΣSYN_ANT) [a].

C. auris Isolate	ISA + AFG [b]			ISA + CAS [b]			ISA + MFG [b]		
	FICI	Greco	Bliss	FICI	Greco	Bliss	FICI	Greco	Bliss
	Median (Range)	α (95% CI)	ΣSYN_ANT (ΣSYN; ΣANT)	Median (Range)	α (95% CI)	ΣSYN_ANT (ΣSYN; ΣANT)	Median (Range)	α (95% CI)	ΣSYN_ANT (ΣSYN; ΣANT)
CJ94	0.27 (0.24–0.30)	151 (16.53–285.5)	86.91 (87.22; −0.31)	0.26 (0.25–0.52)	38.59 (−8.106–85.28)	36.56 (41.22; −4.66)	0.24 (0.15–0.38)	112.8 (22.70–202.9)	66.01 (66.79; −0.78)
CJ97	0.36 (0.25–0.49)	21.70 (5.105–38.38)	29.24 (30.27; −1.03)	0.37 (0.36–1.25)	22.23 (1.016–43.44)	11.44 (20.75; −8.56)	0.15 (0.13–0.25)	216.7 (11.37–422.0)	57.59 (59.49; −1.90)
CJ98	0.19 (0.015–0.19)	102.1 (4.056–200.1)	57.38 (57.73; −0.35)	0.25 (0.08–0.5)	42.64 (−14.72–100.00)	40.67 (45.46; −4.79)	0.37 (0.15–0.49)	57.88 (0.85–114.9)	50.88 (53.70; −2.82)
CJ99	0.18 (0.09–0.18)	186.9 (−3.962–377.8)	73.23 (73.32; −0.09)	0.25 (0.18–0.37)	114.4 (−1.911–230.6)	75.71 (75.89; −0.18)	0.16 (0.08–0.38)	674.4 (−138.3–1487)	111.56 (112.09; −0.53)
CJ100	0.18 (0.15–0.37)	48.71 (−15.71–113.1)	72.80 (75.17; −2.37)	0.38 (0.25–0.49)	37.12 (2.344–71.90)	60.31 (60.64; −0.33)	0.14 (0.12–0.15)	175.1 (14.32–335.8)	80.14 (80.37; −0.23)
CJ102	0.25 (0.14–0.36)	204.1 (−5.106–413.9)	69.61 (69.63; −0.02)	0.36 (0.25–0.38)	41.85 (−1.016–84.71)	46.37 (48.08; −1.71)	0.25 (0.13–0.49)	95.66 (24.84–166.5)	71.35 (71.72; −0.37)
Median	0.22	–	71.205	0.31	–	43.52	0.20	–	68.68

[a] Synergic interactions according to FICI and Greco model are underlined. ΣSYN_ANT: total sum of synergic and antagonistic interactions. ΣSYN: sum of synergic interactions. ΣANT: sum of antagonistic interactions. [b] ISA, isavuconazole; AFG, anidulafungin; CAS, caspofungin; MFG, micafungin.

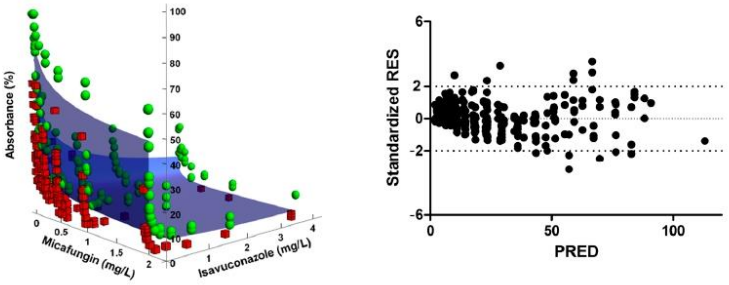

Figure 1. Goodness-of-fit plots of the Greco model for the combination of isavuconazole and micafungin against *C. auris* CJ100. (**a**) The blue surface represents model predictions, the green spheres represent observations above the fitted surface, and the red squares represent observations below the fitted surface. (**b**) Standardized residuals (Standardized RES) versus predictions (PRED).

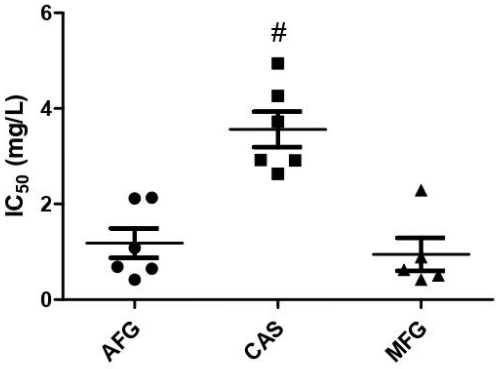

Figure 2. IC_{50} values determined by Greco model for each echinocandin and clinical strain. Mean and standard errors are plotted (#, $p < 0.001$ compared to anidulafungin (AFG) and micafungin (MFG)).

The summary parameter values of the Bliss independence–based model, ΣSYN_ANT, showed weak synergistic interactions (values below 100%) for all combinations and isolates, except for isavuconazole and micafungin against *C. auris* CJ99 (Table 1). Both response surface methods, Greco and Bliss, were in concordance. An exception was isolate CJ97, as the combination of isavuconazole with anidulafungin or caspofungin was classified as synergistic with Greco model, but ΣSYN_ANT values were low (29.44 and 11.44%, respectively), and the distribution matrix showed a scarce number of synergic combinations. The median ΣSYN_ANT for combinations with caspofungin was lower than the ones for anidulafungin and micafungin (Table 1), but the difference was not statistically significant. Checkerboard results and Bliss analysis also revealed that both synergy and a low absorbance value effect were achieved with the combination consisting of low isavuconazole concentration (0.125 mg/L) and higher echinocandins (≥0.5 mg/L). The surface response according to the Bliss method of a representative isolate and drug combination in an 8 × 12 checkerboard design is depicted in Figure 3. A synergistic distribution and the degree of synergism are represented by the colored area.

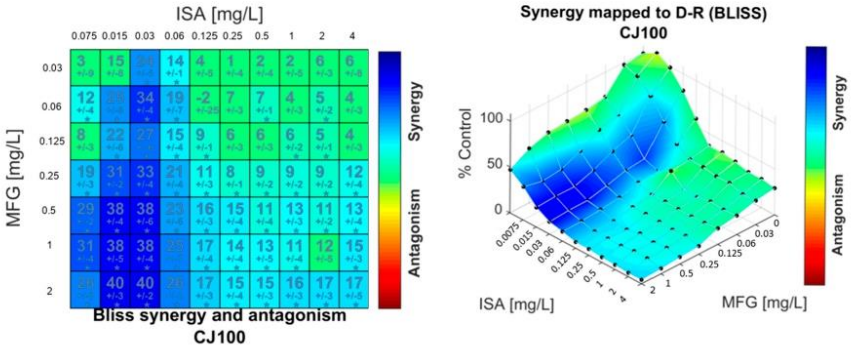

(**a**) (**b**)

Figure 3. Synergy distribution determined by Bliss interaction model for the combination of isavuconazole (ISA) and micafungin (MFG) against *C. auris* CJ100. (**a**) Matrix synergy plot with synergy scores for each combination. (**b**) Synergy distribution mapped to dose–response surface.

2.2. Time-Kill Procedures

Mean time-kill curves for isavuconazole and echinocandins, alone and in combination, are shown in Figure 4. Drug monotherapies did not achieve significant antifungal activity, as observed in the figure and demonstrated by the positive k values (0.01–0.05 h^{-1}). Conversely, synergism and fungistatic activity were achieved with combinations that included concentrations of isavuconazole $\geq$0.125 mg/L and echinocandin $\geq$1 mg/L, showing similar profiles of antifungal activity over time for all three azole–echinocandin combinations.

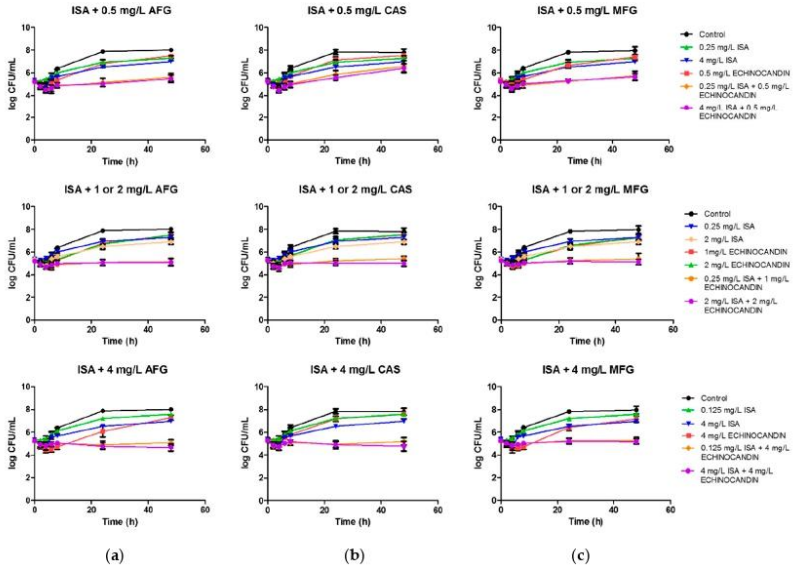

(**a**) (**b**) (**c**)

Figure 4. Mean time-kill curves for isavuconazole (ISA) in combination with echinocandins against *C. auris*. Each data point represents the mean result ± standard deviation (error bars) of the six isolates and replicates. (**a**) Mean time-kill curves for isavuconazole (ISA) in combination with anidulafungin (AFG). (**b**) Mean time-kill curves for isavuconazole (ISA) in combination with caspofungin (CAS). (**c**) Mean time-kill curves for isavuconazole (ISA) in combination with micafungin (MFG).

Although the activity of isavuconazole plus 0.5 mg/L of anidulafungin or micafungin was not fungistatic according to the established definition, the regression analysis of the curves revealed that the killing-rate constant of those drug combinations was not significantly different from a zero slope, indicating a lack of fungal growth through 48 h. That was not the case for the combinations with 0.5 mg/L of caspofungin, as it did not result in a significant reduction in fungal growth (positive k value of 0.02 h^{-1}). This result correlates with the aforementioned Greco analysis that pointed out a lower potency for this echinocandin. Combinations that included concentrations of echinocandin $\geq$1 mg/L also yielded curves with a killing-rate constant non-different from zero, indicating that once the fungistatic effect was achieved, increasing drug concentrations for both agents did not result in a significant reduction in fungal count over time (see also Table S1, Supplementary Materials).

3. Discussion

Among the different strategies to fight and overcome antimicrobial resistance, combination therapy is an attractive approach. This alternative strategy is increasingly interesting for the treatment of candidiasis caused by *C. auris*, recently classified as an "urgent threat" pathogen and with limited treatment choices [2].

In the present study, isavuconazole and echinocandin combinations showed promising results, as they were deemed mainly synergistic by different analytical approaches and were able to halt fungal growth for 48 h in time-kill experiments. Furthermore, the synergism resulting from this combination therapy is particularly relevant if we consider the lack of efficacy shown by the studied drugs in monotherapy. We found similarities between our monotherapy results and those reported by Dudiuk et al. [16] for *C. auris*, as no fungicidal activity was achieved with the echinocandins against the tested *C. auris* strains while similar time-kill curve patterns were observed. The in vitro evidence of non-fungicidal activity of the drugs in monotherapy supports the interest to study drug combinations. Up to now, there are only seven published studies that have evaluated the in vitro activity of antifungal drug combinations against *C. auris*. In a recent study, Pfaller et al. [14] used the FICI analysis to examine the in vitro activity of voriconazole or isavuconazole in combination with anidulafungin against *C. auris* isolates. They observed synergism or partial synergism against most isolates, greater for the combination of isavuconazole plus anidulafungin compared to voriconazole plus anidulafungin. In a previous study, Fakhim et al. [6] reported that voriconazole and micafungin exhibited synergism against *C. auris* determined by the FICI, whereas the combinations of voriconazole with caspofungin or echinocandins with fluconazole resulted indifferent. Therefore, the synergy results of our study are consistent with these two aforementioned reports. Furthermore, we validated the checkerboard results with time-kill experiments.

O'Brian et al. [8] studied *C. auris* isolates from a New York outbreak and found synergism for the combination of flucytosine with the rest of antifungal classes, but not for the combination of azoles with echinocandins. Conversely, flucytosine showed no interaction with other antifungal drugs against Indian *C. auris* isolates [7]. This highlights the fact that the antimicrobial activity of drug–drug interactions may be not only species specific but also strain specific. Other works have focused on the combination of antifungal drugs with non-antifungal agents as an approach to enhance the therapeutic arsenal against *C. auris* [9–12]. To date, the only published in vivo combination study, a model of *Caenorhabditis elegans* infected with *C. auris*, supported the combination of sulfamethoxazole and voriconazole [9]. However, there is no in vivo or clinical evidence regarding the combination of echinocandins plus azoles against *C. auris*. Additionally, *C. auris* is able to form biofilms on the skin, on implanted medical devices or in the hospital environment [17]. As these biofilms are even more resistant to antifungal agents compared to planktonic cells [17,18], the possible benefits of the aforementioned synergy should also be assessed in fighting such a biofilm community.

Synergism applied to drug–drug combinations can be defined in a simple way as the interaction between two or more compounds that exerts a greater effect than the additive

sum of the effects of each drug when acting alone [19]. Nevertheless, determination of synergism or antagonism is far from simple. There are many factors that have to be taken into account, such as the experimental setting to obtain the empirical data or the mathematical methods chosen for the analysis [20]. Widely accepted and employed theories for the determination of drug interactions are Loewe's additivity and Bliss independence [21]. When analyzing checkerboard data of antimicrobial drugs, Loewe's additivity is usually determined by the non-parametric approach of the FICI, obtained by comparing the MIC of the compounds alone and in combination [22]. On one hand, the FICI method is well established and straightforward; on the other, it ignores all the concentration–response data that do not correspond to MICs, and variable results and interpretations may be expected depending on the MIC endpoints [23]. Parametric approaches, such as the Greco universal response surface approach (URSA) and the Bliss interaction model, overcome this drawback, as the whole drug-concentration range is analyzed [24]. It also allows the estimation of parameters (such as IC_{50}) and the associated confidence intervals based on more robust mathematical and statistical methods [25]. The results obtained with the parametric and non-parametric approaches showed synergistic interactions for the isavuconazole–echinocandin combinations. Furthermore, this agreement between approaches and the sensitivity of the models in detecting even weak interactions is concordant with other reports that have compared different drug interaction models [10,23,26].

It is important to take into consideration that a lack of synergism of a drug combination does not necessarily mean that the effectiveness of the combination is negligible. After all, when antimicrobial agents are combined, the goal is to reduce the microbial density [27], regardless of the nature of the interaction. Additionally, for the interpretation of a synergism result, it should be considered whether it has been observed under clinically relevant conditions, whether the observed synergism has been obtained at concentrations that are clinically achievable, and the extent of the effect. Bliss independence model based surface analysis allowed us to identify the concentration range of each combined drug where synergism was claimed. In summary, synergism was detected for the combination of low concentrations (<0.125 mg/L) of both isavuconazole and echinocandins. The antifungal effect was further examined by time-kill experiments in which we selected the concentrations that showed zero absorbance value in the checkerboard assays, as that reflects an antifungal effect of interest. It was observed that fungal growth was reduced over 48 h by all the combinations tested, but none of them achieved fungicidal activity. Furthermore, the time-kill curve analysis revealed that once the fungistatic effect and synergism were achieved with the echinocandin–azole combinations, higher concentrations did not result in a higher reduction in fungal burden. These threshold concentrations were isavuconazole $\geq$0.125 mg/L and echinocandin $\geq$1 mg/L. Time-kill curve experiments also supported that an additive effect can be of interest, as none of the drugs in monotherapy showed fungistatic activity, while the interaction of all combinations at 24 h was additive but also fungistatic. To our knowledge, this is the first study that has determined the in vitro interactions of a triazole with echinocandins against *C. auris* by use of both checkerboard and time-kill assays.

The main limitation of the present study is the limited number of isolates tested. This limitation has also been recognized in previous studies of antifungal drug interactions against *C. auris* [14]. Moreover, our study only included bloodstream isolates of *C. auris*, collected from the main *C. auris* outbreak in a Spanish hospital, first detected in 2016.

It is worth noting that the antifungal effect and the synergy observed with the studied combinations were observed at clinically achievable and safe drug concentrations related to standard dosing [28]. Nevertheless, any in vitro system, no matter how sophisticated, is a simplification of the much more complex in vivo situation [29], and proper in vitro–in vivo correlations have not been established for azole–echinocandin combinations. In fact, in vivo and clinical studies on antifungal combination therapy in *C. auris* infections are lacking. The results of this work could assist in the design of further in vivo and clinical studies to better asses the therapeutic use of isavuconazole–echinocandin combination.

4. Materials and Methods

4.1. Fungal Strains

Six *C. auris* clinical blood isolates (CJ94, CJ97, CJ98, CJ99, CJ100, and CJ102) from an outbreak in the Hospital Universitario y Politécnico La Fe (Valencia, Spain) [30] were included in this study. Fungal strains were stored in vials with sterile distilled water at room temperature for up to 1 year, while commercially prepared cryogenic Microbank vials (Pro-Lab Diagnostics, USA) maintained at −70 °C were used for prolonged storage. Strains were cultivated in Sabouraud dextrose agar (SDA) for 24 h before every experiment. MIC determination at 24 h was performed following EUCAST guidelines [31]. MICs for isavuconazole, anidulafungin, caspofungin, and micafungin were 0.06, 0.125, 0.125, and 0.25 mg/L, respectively, for all isolates.

4.2. Antifungal Agents

Isavuconazole (Basilea Pharmaceutica International, Basel, Switzerland), anidulafungin (Pfizer SLU, Madrid, Spain), caspofungin (Merck Sharp & Dohme, Madrid, Spain), and micafungin (Astellas Pharma, Madrid, Spain) were obtained in powder form and were prepared and preserved according to their respective manufacturer's recommendations. The drugs were dissolved in dimethyl sulfoxide (DMSO) to obtain stock solutions of 3200 mg/L and stored at −80 °C until use.

4.3. Checkerboard Assay

Interactions between isavuconazole and echinocandins were first studied by a checkerboard microdilution method (8 × 12 design) in 96-well flat-bottom microtiter plates, in RPMI 1640 medium, following EUCAST guidelines and modified for drug combinations [7,10]. Isavuconazole was added to columns 2–11, with concentrations ranging from 0.0075 to 4 mg/L. Aliquots of anidulafungin, caspofungin, or micafungin were added to rows A–G, with a range of 0.03–2 mg/L. Thus, concentrations of the drug combinations ranged from 0.0075 mg/L of isavuconazole + 0.03 mg/L of echinocandin to 4 mg/L of isavuconazole + 2 mg/L of echinocandin. Wells from column 12 were left for growth control, and wells H1 and H12 were used as sterility control. On the day of the experiment, *C. auris* isolates, previously incubated at 37 °C overnight, were suspended in distilled water to obtain a starting inoculum of 0.5–2.5 × 10^5 CFU/mL and were added to the microtiter plates. Those plates were then incubated at 37 °C for 48 h, and the absorbance of each well was measured on an Infinite F50 spectrophotometer (Tecan, Switzerland) at a wavelength of 450 nm. *Candida parapsilosis* ATCC 22019 and *Candida krusei* ATCC 6258 were used as quality controls. Experiments were conducted in triplicate on different days.

4.4. Data Analysis

Absorbance data were transformed into percentages, with the mean value of the growth control absorbance set to 100%. The data were analyzed by FICI [22] and surface response models: Loewe's additivity–based Greco model and Bliss independence [23,24].

4.4.1. FICI

The determination of the FICI of a drug combination is based on Loewe's additivity and is calculated as follows:

$$\mathrm{FICI} = \frac{\mathrm{MIC_{A+B}}}{\mathrm{MIC_A}} + \frac{\mathrm{MIC_{A+B}}}{\mathrm{MIC_B}} \quad (1)$$

where $\mathrm{MIC_{A+B}}$ is the MIC of the drugs A and B in combination, $\mathrm{MIC_A}$ the MIC of drug A alone, and $\mathrm{MIC_B}$ the MIC of drug B alone. Drug interactions were defined as synergistic if FICI $\leq$ 0.5, no interaction if FICI > 0.5 $\leq$ 4, and antagonistic if FICI > 4 [22].

4.4.2. Greco Model

The parametric surface approach described in the Greco model is defined in the following equation:

$$1 = \frac{\text{Drug}_1}{\text{IC}_{50,1} \times \left(\frac{E}{E_{con}-E}\right)^{\left(\frac{1}{m1}\right)}} + \frac{\text{Drug}_2}{\text{IC}_{50,2} \times \left(\frac{E}{E_{con}-E}\right)^{\left(\frac{1}{m2}\right)}} + \frac{\alpha \times \text{Drug}_1 \times \text{Drug}_2}{\text{IC}_{50,1} \times \text{IC}_{50,2} \times \left(\frac{E}{E_{con}-E}\right)^{\left(\frac{1}{2m1}+\frac{1}{2m2}\right)}} \quad (2)$$

where $Drug_1$ and $Drug_2$ are the concentrations of isavuconazole and echinocandin, respectively, $IC_{50,1}$ and $IC_{50,2}$ are the concentrations of each drug that achieve 50% of the maximum activity, m1 and m2 are the slopes of the concentration–effect curves or Hill's coefficient, E_{con} is the effect in the absence of drug, E is the fractional effect, and α is the interaction parameter that describes the nature of the interaction. When the value of α was positive and its 95% confidence interval (95% CI) was also positive, the interaction was defined as synergistic. A positive α with 95% CI including zero described an additive interaction. When α was negative without its 95% CI overlapping zero, an antagonistic interaction was claimed. The analysis was run in ADAPT 5 [32], with weighted least-squares method and three-dimensional goodness-of-fit plots generated by Mathematica (v 12.1; Wolfram Research Inc., Champaign, IL, USA). The parameters obtained for the different combinations were then compared by one-way ANOVA and Tukey's multiple comparison test using GraphPad Prism 5.01 (GraphPad Software, San Diego, CA, USA).

4.4.3. Bliss Independence Model

The Bliss independence model, which assumes that the relative effect of a drug at a particular concentration is independent of the other drug, is defined by the following equation:

$$\Delta E = E_{ind} - E_{obs} \quad (3)$$

where ΔE is the difference between the predicted percentage of growth (E_{ind}) and the observed percentage of growth (E_{obs}). E_{ind} is calculated, in turn, as follows:

$$E_{ind} = E_A \times E_B \quad (4)$$

where E_A and E_B are the observed percentage of growth in the presence of drug A and drug B, respectively.

When the ΔE of each specific combination of *x* mg/L of isavuconazole and *y* mg/L of echinocandin was positive and its 95% CI did not include zero, the interaction was defined as synergistic. When the ΔE was negative and its 95% CI did not include zero, the interaction was defined as antagonistic. Any other case was considered indifferent.

The sum of all statistically significant synergistic and antagonistic interactions (ΣSYN_ANT) was considered as the main parameter that summarized the whole interaction surface for the studied three combinations [15,26]. Additionally, when the ΣSYN_ANT value obtained for each checkerboard analysis was below 100%, weak interaction was defined, between 100% and 200% was considered moderate, and those higher than 200% were considered as strong [15,23]. Combenefit was the software used to perform the Bliss analysis [33].

4.5. Time-Kill Procedures

Static time-kill assays were performed as previously described [34] and adapted with minor modifications for antifungal combinations. The concentrations of the drugs selected for the study were based on the checkerboard results. Isavuconazole concentrations were 0.125, 0.25, 2, and 4 mg/L, and anidulafungin, caspofungin, or micafungin concentrations ranged from 0.5 to 4 mg/L. Inoculum preparation was carried out as in the checkerboard assay previously described, but with a final fungal density of 1–5 × 10^5 CFU/mL. Samples for viable counts were taken at 0, 2, 4, 6, 8, 24, and 48 h, diluted in PBS, plated in triplicate onto Sabouraud dextrose agar (SDA), and incubated for 24–48 h at 37 °C to determine the number of CFU/mL. Fungistatic activity was defined as a reduction <3 log CFU/mL compared to the starting inoculum. Synergism was declared when the difference between

the drug with highest effect in monotherapy and the combination was >2 log CFU/mL [35]. Experiments were performed in duplicate on different days. Time-kill curves were analyzed by fitting the observations to the following exponential equation, as previously described [34]:

$$N_t = N_0 \times e^{kt} \quad (5)$$

where N_t is the number of CFU/mL at time t, N_0 is the starting inoculum, k is the growing or killing-rate constant, and t is the incubation time. Positive k values show growth, and negative values indicate killing. Goodness-of-fit for each combination was assessed by the r^2 value (>0.8). Significant differences in killing kinetics among combinations and concentrations were determined by the analysis of variance. A p value < 0.05 was considered significant.

5. Conclusions

In conclusion, in the present in vitro study, the combinations of isavuconazole with anidulafungin, caspofungin, or micafungin against *C. auris* were mostly synergistic and fungistatic, providing evidence that combination therapy is a promising approach to be further investigated, especially when the drugs alone show reduced activity against *C. auris*.

Supplementary Materials: The following are available online at https://www.mdpi.com/article/10.3390/antibiotics10040355/s1, Table S1: Average killing rate constant (k) values for the monotherapies and drug combinations against *Candida auris*.

Author Contributions: Conceptualization, U.C., E.E., G.Q. and N.J.; methodology, U.C., E.E., V.V. and S.S.; software, U.C., S.K., V.V. and S.S.; validation, U.C., S.K. and N.J.; formal analysis, U.C., S.K., V.V. and S.S.; investigation, U.C., E.E., G.Q. and N.J.; resources, N.J., G.Q. and E.E.; data curation, U.C. and S.K.; writing—original draft preparation, U.C.; writing—review and editing, N.J., E.E. and G.Q.; visualization, U.C., N.J. and G.Q.; supervision, N.J., G.Q. and S.S.; project administration, N.J., E.E. and G.Q.; funding acquisition, G.Q., E.E. and N.J. All authors have read and agreed to the published version of the manuscript.

Funding: This research was funded by Consejería de Educación, Universidades e Investigación of Gobierno Vasco-Eusko Jaurlaritza, GIC15/78 IT-990-16 and by FIS, Spain, PI17/01538. UC was funded by a Ph.D. grant from the University of the Basque Country UPV/EHU, PIF 17/266.

Institutional Review Board Statement: Not applicable.

Informed Consent Statement: Not applicable.

Data Availability Statement: Not applicable.

Acknowledgments: The authors wish to thank Javier Pemán and Alba Ruiz Gaitán (Hospital Universitario y Politécnico La Fe, Valencia, Spain) for kindly providing clinical isolates.

Conflicts of Interest: The authors declare no conflict of interest.

References

1. Bidaud, A.L.; Chowdhary, A.; Dannaoui, E. *Candida auris*: An emerging drug resistant yeast—A mini-review. *J. Mycol. Med.* **2018**, *28*, 568–573. [CrossRef] [PubMed]
2. CDC. *Antibiotic Resistance Threats in the United States*; U.S. Department of Health and Human Services, CDC: Atlanta, GA, USA, 2019. [CrossRef]
3. WHO. First Meeting of the WHO Antifungal Expert Group on Identifying Priority Fungal Pathogens: Meeting Report. Geneva: World Health Organization; 2020. Licence: CC BY-NC-SA 3.0 IGO. Available online: https://www.who.int/publications/i/item/9789240006355 (accessed on 8 February 2021).
4. Kenters, N.; Kiernan, M.; Chowdhary, A.; Denning, D.W.; Peman, J.; Saris, K.; Schelenz, S.; Tartari, E.; Widmer, A.; Meis, J.F.; et al. Control of *Candida auris* in healthcare institutions: Outcome of an International Society for Antimicrobial Chemotherapy expert meeting. *Int. J. Antimicrob. Agents* **2019**, *54*, 400–406. [CrossRef]
5. Biagi, M.J.; Wiederhold, N.P.; Gibas, C.; Wickes, B.L.; Lozano, V.; Bleasdale, S.C.; Danziger, L. Development of high-level echinocandin resistance in a patient with recurrent *Candida auris* candidemia secondary to chronic candiduria. *Open Forum. Infect. Dis.* **2019**, *6*, ofz262. [CrossRef] [PubMed]

6. Fakhim, H.; Chowdhary, A.; Prakash, A.; Vaezi, A.; Dannaoui, E.; Meis, J.F.; Badali, H. In vitro interactions of echinocandins with triazoles against multidrug-resistant *Candida auris*. *Antimicrob. Agents Chemother.* **2017**, *61*. [CrossRef] [PubMed]
7. Bidaud, A.L.; Botterel, F.; Chowdhary, A.; Dannaoui, E. In vitro antifungal combination of flucytosine with amphotericin B, voriconazole, or micafungin against *Candida auris* shows no antagonism. *Antimicrob. Agents Chemother.* **2019**. [CrossRef]
8. O'Brien, B.; Chaturvedi, S.; Chaturvedi, V. In vitro evaluation of antifungal drug combinations against multidrug-resistant *Candida auris* isolates from New York outbreak. *Antimicrob. Agents Chemother.* **2020**, *64*. [CrossRef]
9. Eldesouky, H.E.; Li, X.; Abutaleb, N.S.; Mohammad, H.; Seleem, M.N. Synergistic interactions of sulfamethoxazole and azole antifungal drugs against emerging multidrug-resistant *Candida auris*. *Int. J. Antimicrob. Agents* **2018**, *52*, 754–761. [CrossRef]
10. Bidaud, A.L.; Djenontin, E.; Botterel, F.; Chowdhary, A.; Dannaoui, E. Colistin interacts synergistically with echinocandins against *Candida auris*. *Int. J. Antimicrob. Agents* **2020**, *55*, 105901. [CrossRef] [PubMed]
11. Wu, Y.; Totten, M.; Memon, W.; Ying, C.; Zhang, S.X. In vitro antifungal susceptibility of the emerging multidrug-resistant pathogen *Candida auris* to miltefosine alone and in combination with amphotericin B. *Antimicrob. Agents Chemother.* **2020**, *64*. [CrossRef]
12. Schwarz, P.; Bidaud, A.L.; Dannaoui, E. In vitro synergy of isavuconazole in combination with colistin against *Candida auris*. *Sci. Rep.* **2020**, *10*. [CrossRef]
13. Warn, P.A.; Sharp, A.; Parmar, A.; Majithiya, J.; Denning, D.W.; Hope, W.W. Pharmacokinetics and pharmacodynamics of a novel triazole, isavuconazole: Mathematical modeling, importance of tissue concentrations, and impact of immune status on antifungal effect. *Antimicrob. Agents Chemother.* **2009**, *53*, 3453–3461. [CrossRef] [PubMed]
14. Pfaller, M.A.; Messer, S.S.; Deshpande, L.M.; Rhomberg, P.R.; Utt, E.A.; Castanheira, M. Evaluation of synergistic activity of isavuconazole or voriconazole plus anidulafungin and the occurrence and genetic characterisation of *Candida auris* detected in a surveillance program. *Antimicrob. Agents Chemother.* **2021**, in press. [CrossRef]
15. Katragkou, A.; McCarthy, M.; Meletiadis, J.; Hussain, K.; Moradi, P.W.; Strauss, G.E.; Myint, K.L.; Zaw, M.H.; Kovanda, L.L.; Petraitiene, R.; et al. In vitro combination therapy with isavuconazole against *Candida* spp. *Med. Mycol.* **2017**, *55*, 859–868. [CrossRef] [PubMed]
16. Dudiuk, C.; Berrio, I.; Leonardelli, F.; Morales-Lopez, S.; Theill, L.; Macedo, D.; Yesid-Rodriguez, J.; Salcedo, S.; Marin, A.; Gamarra, S.; et al. Antifungal activity and killing kinetics of anidulafungin, caspofungin and amphotericin B against *Candida auris*. *J. Antimicrob. Chemother.* **2019**, *74*, 2295–2302. [CrossRef] [PubMed]
17. Sherry, L.; Ramage, G.; Kean, R.; Borman, A.; Johnson, E.M.; Richardson, M.D.; Rautemaa-Richardson, R. Biofilm-Forming capability of highly virulent, multidrug-resistant *Candida auris*. *Emerg. Infect. Dis.* **2017**, *23*, 328–331. [CrossRef]
18. Du, H.; Bing, J.; Hu, T.; Ennis, C.L.; Nobile, C.J.; Huang, G. *Candida auris*: Epidemiology, biology, antifungal resistance, and virulence. *PLoS Pathog.* **2020**, *16*, e1008921. [CrossRef] [PubMed]
19. Greco, W.R.; Faessel, H.; Levasseur, L. The search for cytotoxic synergy between anticancer agents: A case of Dorothy and the ruby slippers? *J. Natl. Cancer Inst.* **1996**, *88*, 699–700. [CrossRef]
20. Chou, T.C. Theoretical basis, experimental design, and computerized simulation of synergism and antagonism in drug combination studies. *Pharmacol. Rev.* **2006**, *58*, 621–681. [CrossRef]
21. Roell, K.R.; Reif, D.M.; Motsinger-Reif, A.A. An introduction to terminology and methodology of chemical synergy-perspectives from across disciplines. *Front. Pharmacol.* **2017**, *8*, 158. [CrossRef]
22. Odds, F.C. Synergy, antagonism, and what the chequerboard puts between them. *J. Antimicrob. Chemother.* **2003**, *52*, 1. [CrossRef]
23. Meletiadis, J.; Verweij, P.E.; TeDorsthorst, D.T.; Meis, J.F.; Mouton, J.W. Assessing in vitro combinations of antifungal drugs against yeasts and filamentous fungi: Comparison of different drug interaction models. *Med. Mycol.* **2005**, *43*, 133–152. [CrossRef]
24. Greco, W.R.; Bravo, G.; Parsons, J.C. The search for synergy: A critical review from a response surface perspective. *Pharmacol. Rev.* **1995**, *47*, 331–385.
25. de Miranda Silva, C.; Hajihosseini, A.; Myrick, J.; Nole, J.; Louie, A.; Schmidt, S.; Drusano, G.L. Effect of linezolid plus bedaquiline against *Mycobacterium tuberculosis* in log phase, acid phase, and nonreplicating-persister phase in an in vitro assay. *Antimicrob. Agents Chemother.* **2018**, *62*. [CrossRef]
26. Otto, R.G.; van Gorp, E.; Kloezen, W.; Meletiadis, J.; van den Berg, S.; Mouton, J.W. An alternative strategy for combination therapy: Interactions between polymyxin B and non-antibiotics. *Int. J. Antimicrob. Agents* **2019**, *53*, 34–39. [CrossRef]
27. Brill, M.J.E.; Kristoffersson, A.N.; Zhao, C.; Nielsen, E.I.; Friberg, L.E. Semi-Mechanistic pharmacokinetic-pharmacodynamic modelling of antibiotic drug combinations. *Clin. Microbiol. Infect.* **2018**, *24*, 697–706. [CrossRef]
28. Bellmann, R.; Smuszkiewicz, P. Pharmacokinetics of antifungal drugs: Practical implications for optimized treatment of patients. *Infection* **2017**, *45*, 737–779. [CrossRef] [PubMed]
29. de la Pena, A.; Grabe, A.; Rand, K.H.; Rehak, E.; Gross, J.; Thyroff-Friesinger, U.; Muller, M.; Derendorf, H. PK-PD modelling of the effect of cefaclor on four different bacterial strains. *Int. J. Antimicrob. Agents* **2004**, *23*, 218–225. [CrossRef] [PubMed]
30. Ruiz-Gaitan, A.; Moret, A.M.; Tasias-Pitarch, M.; Aleixandre-Lopez, A.I.; Martinez-Morel, H.; Calabuig, E.; Salavert-Lleti, M.; Ramirez, P.; Lopez-Hontangas, J.L.; Hagen, F.; et al. An outbreak due to *Candida auris* with prolonged colonisation and candidaemia in a tertiary care European hospital. *Mycoses* **2018**, *61*, 498–505. [CrossRef] [PubMed]

31. EUCAST. The European Committee for Antimicrobial Susceptibility Testing. Method for the Determination of Broth Dilution Minimum Inhibitory Concentrations of Antifungal Agents for Yeasts. EUCAST Definitive Document E.def 7.3.2. 2020. Available online: https://www.eucast.org/fileadmin/src/media/PDFs/EUCAST_files/AFST/Files/EUCAST_E_Def_7.3.2_Yeast_testing_definitive_revised_2020.pdf (accessed on 8 February 2021).
32. D'Argenio, D.Z.; Schumitzky, A.; Wang, X. *ADAPT 5 User's Guide: Pharmacokinetic/Pharmacodynamic Systems Analysis Software*; Biomedical Simulations Resource: Los Angeles, CA, USA, 2009.
33. Di Veroli, G.Y.; Fornari, C.; Wang, D.; Mollard, S.; Bramhall, J.L.; Richards, F.M.; Jodrell, D.I. Combenefit: An interactive platform for the analysis and visualization of drug combinations. *Bioinformatics* **2016**, *32*, 2866–2868. [CrossRef]
34. Gil-Alonso, S.; Jauregizar, N.; Canton, E.; Eraso, E.; Quindos, G. In vitro fungicidal activities of anidulafungin, caspofungin, and micafungin against *Candida glabrata*, *Candida bracarensis*, and *Candida nivariensis* evaluated by time-kill studies. *Antimicrob. Agents Chemother.* **2015**, *59*, 3615–3618. [CrossRef] [PubMed]
35. Mukherjee, P.K.; Sheehan, D.J.; Hitchcock, C.A.; Ghannoum, M.A. Combination treatment of invasive fungal infections. *Clin. Microbiol. Rev.* **2005**, *18*, 163–194. [CrossRef] [PubMed]